UNIVERSITÀ DEGLI STUDI DI MILANO

Scuola di Dottorato in Scienze Biologiche e Molecolari

XXVII Ciclo

Oxidative stress response of model biofilm systems under different environmental cues

Michela Gambino

PhD Thesis

Scientific tutor: prof. Paolo Landini

Co-tutor: prof. Francesca Cappitelli

Academic year: 2013-2014

SSD: BIO/18; BIO/19

Thesis performed at Department of Biosciences, Università degli Studi di Milano, at Department of Food, Environmental and Nutrition Sciences, Università degli Studi di Milano, and at Costerton Biofilm Center, Department of International Health, Immunology, and Microbiology, University of Copenhagen.

Cover

Burkholderia thailandensis colony biofilm.

Contents

PART II

PUBLISHED PAPER_1:

"EFFECTS OF CHRONIC SUB-LETHAL OXIDATIVE STRESS ON BIOFILM FORMATION BY *AZOTOBACTER VINELANDII*."

PUBLISHED PAPER_2:

"EFFECTS OF SUB-LETHAL DOSES OF SILVER NANOPARTICLES ON *BACILLUS SUBTILIS* PLANKTONIC AND SESSILE CELLS."

PUBLISHED PAPER_3:

"A GATEWAY-COMPATIBLE ALLELIC EXCHANGE SYSTEM FOR GENERATION OF IN-FRAME AND UNMARKED GENE DELETIONS IN *BURKHOLDERIA CENOCEPACIA*"

PART III

UNPUBLISHED RESULTS:

"RESPONSE TO OXIDATIVE STRESS OF *BURKHOLDERIA THAILANDENSIS* BIOFILM"

Abstract

During my PhD, I focused on three important environmental bacteria, namely, *Azotobacter vinelandii*, *Bacillus subtilis* and *Burkholderia thailandensis*. In each model, I studied different mechanisms of oxidative stress, related to their role in the environment or, in the case of *B. thailandensis*, related to its condition of opportunistic pathogen of invertebrates and model for the human pathogen *B. pseudomallei*. In *A. vinelandii*, inactivation of the rhodanese-like protein RhdA resulted in continuous generation of endogenous oxidative stress, promoting biofilm genesis, stimulating the activity of scavenging systems and triggering a switch between swarming and biofilm-like phenotypes. Furthermore, the oxidative stress affected the composition of the exopolymeric substances (EPS), resulting in the production of a polysaccharide-rich extracellular polymeric matrix in mutant (part II, chapter 1). In *B. subtilis*, the antimicrobial mechanism of silver nanoparticles (Ag-NPs) involve the production of reactive oxygen species (ROS), with possible consequences on soil bacteria. Sub-lethal doses of Ag-NPs increased the ROS formation in *B. subtilis* planktonic cells, but not in sessile cells, suggesting the presence of scavenging systems in biofilms. Consistently, proteomic analysis in Ag-NPs-treated biofilms showed increased production of proteins related to redox , quorum sensing and to stress response, thus suggesting a coordinated regulation of biofilm and stress response genes. Extracellular polysaccharide production and inorganic phosphate solubilization were also increased, possibly as part of a coordinated response to oxidative stress (part II, chapter 2). Finally we challenged *B. thailandensis* with phenazine methosulphate (PMS) to simulate the oxidative stress encountered in the soil and in the infected host. A new molecular approach to create mutants in *Burkholderia* spp. has been developed as part of this work (part II, chapter 3). In *B. thailandensis* biofilm, oxidative stress decreased as the biofilm reached the mature phase. The presence of PMS affected the biofilm morphology, triggering the production of more EPS. Interestingly , the deletion of the periplasmic superoxide dismutase, *sodC*, triggered polysaccharide production in biofilm cells (part III, chapter 1). My results demonstrate how the matrix production plays a pivotal role in protection from oxidative injuries in bacterial biofilm, both in Gram-negative and Gram-positive bacteria. The protection mechanisms activated by biofilm in response to oxidative stress can have important consequences on environmental biodiversity and in the balance between planktonic and biofilm cells.

PART I

1. Soil microbial community

Soil systems host a complex network of interactions between microorganisms and plants. Plants acquire nutrients from inorganic sources that are supplied primarily by decomposers, whereas decomposers, mostly soil microorganisms, acquire carbon from organic resources that are supplied primarily by plants (Eisenhauer et al., 2010). In soil ecosystems, microorganisms are a driving force several processes: nutrient acquisition (Sprent et al., 2000), nitrogen cycling (Kowalchuk et al., 2001), carbon cycling (Hogberg et al. 2001), soil structure and transport processes (Feeney et al., 2006), thus contributing to establish specific microbial ecological niches in plant-based systems (Vacheron et al., 2013). The rhizosphere, defined as the portion of soil where microorganism-mediated processes are under the influence of the plant root (Hiltner, 1904), is one of the most important niches (Berg et al., 2009). Roots provide plant anchorage in soil, absorption of water and ions, nutrient storage and plant vegetative growth, but the rhizosphere is above all the place where plants get in close contact with a wide range of soil microbial populations (Vacheron et al., 2013). Plant roots exude a huge diversity of organic nutrients (organic acids, phytosiderophores, sugars, vitamins, amino acids, nucleosides, mucilage), making the rhizosphere a very selective environment with a rich microbial community (Van Der Heijden et al., 2008), differentiated from the surrounding soil biome (Bulgarelli et al., 2013). Root exudates also contain signalling molecules to change microbial community, according to type of compound detected in the rhizosphere (Badri et al., 2009). On the other hand, microorganisms are able to produce canonical plant growth-regulating substances such as auxins or cytokinins to colonize rhizosphere. This molecular dialogue will determine the outcome of the relationship, ranging from pathogenesis to symbiosis, through highly coordinated cellular processes (Ortiz-Castro et al., 2009). Within the microbial community of rhizosphere, some microorganisms establish beneficial cooperation, in which the plants and the microorganisms share costs and benefits (Bulgarelli et al., 2013). These microorganisms, defined as plant growth-promoting rhizobacteria (PGPR), promote plant growth through several indirect or direct mechanisms. In turn, plants supply through the roots the sugars that can be metabolized for bacterial growth. Direct

growth promotion mechanisms include the root development through the production of phytohormones or enzymatic activities (such as as 1-aminocyclopropane-1-carboxylate deaminase) able to modulate the level of plant hormones; this allows a higher uptake of minerals and water and thus the growth of the whole plant (Vacheron et al., 2013). Other direct PGPR mechanisms are nitrogen fixation and solubilization of inorganic phosphate. As nutrient availability in soil is often poor, nitrogen-fixing bacteria contribute consistently to the plant growth, enriching the soil with appreciable amounts of nitrogen from the atmospheric reservoir (Saharan et al., 2011). The reduction of nitrogen gas to ammonia by the nitrogenase enzyme complex is well known in rhizobia-legume symbiosis, but has also been demonstrated for rhizosphere bacteria, as in the case of *A. vinelandii* (part I, chapter 1). In soil, a large proportion of phosphorous is not available for plants, being present in insoluble complexes. Phosphate-solubilizing bacteria mobilize insoluble inorganic phosphates from their mineral matrix to the bulk soil where they can be absorbed by plant roots (Sashidhar et al., 2010). The main mechanisms are associated with the release of low molecular weight organic acids for the mineral phosphate solubilization and the release of acid phosphatases for the organic phosphate solubilization, to chelate the phosphate-bound cations thereby converting it into soluble forms (Rodriguez et al., 1999; Bulgarelli et al., 2013). *Bacillus subtilis* is among bacteria having this useful ability (part I, chapter 2). Indirect growth promotion is the decrease or prevention of deleterious effect of pathogenic microorganisms (Rodriguez et al., 1999). Siderophores and antibiotics are three of the most effective mechanisms employed to counteract phytopathogenic proliferation (Beneduzi et al., 2012). Siderophores are small molecules, secreted to solubilize iron from their surrounding environments, forming a complex ferric-siderophore that can move by diffusion to come back to the cell surface (Andrews et al., 2003). Siderophore production confers a competitive advantage in iron-limiting conditions, so that PGPR can exclude other microorganisms from this ecological niche (Beneduzi et al., 2012). A well-known example is pyoverdine, a siderophore produced by pseudomonads, very efficient in scavenging iron and antagonize some fungal plant pathogens (Duijff et al., 1999). Besides siderophore production, the mechanism most commonly associated with the ability of PGPR to act as antagonistic agents against phytopathogens is the production of compounds inhibiting microbial growth: bacteriocins, phenazines, phloroglucinols, pyoluteorin, pyrrolnitrin, cyclic lipopeptides, hydrogen cyanide and

lipopeptide biosurfactants are compounds with proved efficacy (Beneduzi et al., 2012). Especially, phenazines are of particular interest in our case as they are a well-known source of oxidative stress. In the presence of molecular oxygen and reducing agents, phenazines lead to the accumulation of reactive oxygen species (ROS) in organisms and tissues (Xie et al., 2013). Furthermore, phenazines are among those substances able to activate Induced Systemic Resistance (ISR) in plants (Pierson et al., 2010). ISR is the state of enhanced defensive ability developed by plants when appropriately stimulated (Van Loon et al., 1998) and depends on the expression of the plant ethylene and jasmonic acid pathways (Verhagen et al., 2004). Another indirect PGPR beneficial effect on plants is the increased tolerance to heavy metal contamination (Vacheron et al. 2013). At high concentrations, heavy metals greatly affect the quantity, the activity and the structure of microbial communities (Tak et al., 2011). For these reason, microorganisms developed resistance or tolerance mechanisms that can be advantageous also for plants. PGPR can improve heavy metal tolerance of plants and phytoextraction activities by altering the solubility, availability, and transport of heavy metals, by reducing soil pH and releasing chelators (Ma et al., 2011). PGPR interact with a large range of host plant species and encompass a huge taxonomic diversity, especially within the Firmicutes and Proteobacteria phyla (Bulgarelli et al., 2013). In this work, we focused on three bacteria that belong to these phyla: *A. vinelandii* (gamma-Proteobacteria) (chapter I), *B. subtilis* (firmicutes) (chapter II) and *B. thailandensis* (beta-Proteobacteria) (chapter III and IV). While *A. vinelandii* and *B. subtilis* are known as PGPR, *B. thailandensis* is a soil microorganism used as model for the pathogen *B. pseudomallei*.

2. Bacterial biofilms

Biofilms are heterogenic microbial communities embedded in a self- produced polymeric matrix attached to a surface (Hall-Stoodley et al., 2004). The biofilm formation is a nearly universal trait enabling bacteria to develop coordinated architectural and survival strategies (Vlamakis et al., 2013) and is now largely accepted that biofilms constitute the predominant microbial lifestyle in natural and engineered ecosystems (Mc Dougald et al., 2011). Bacteria growing as a biofilms are distinct from free- swimming planktonic bacteria in their physiology, in gene expression pattern and even morphology (Landini et al., 2010). While planktonic cells rapidly grow to disseminate and colonize new habitats, the sessile form allows bacteria to settle in that particular habitat. As the bacterial cells adapt to grow in these complex communities, they express phenotypic specific traits that confer to biofilm a higher resistance to adverse condition and adaptability to environmental changes (Stewart et al., 2008). Evidence from the fossil records (more than 3-billion-year-old) indicate that the ability to form biofilms is an ancient and integral characteristic of bacteria (Westall et al., 2001). In that time, bacteria suffered drastic and fluctuating conditions, with extreme high temperatures, pH and exposure to ultraviolet light (Hall-Stoodley et al., 2004). The biofilm lifestyle guaranteed the protection that bacteria needed for survival, providing homeostasis and facilitating the development of complex interactions between individual cells. Biofilm represents an optimal solution to colonize and survive in niches despite the limited availability of nutrients, desiccation, low pH and predation (Rinaudi et al., 2010). The biofilm structure, the adhesion to a surface and the polymeric matrix offer to cells a suitable environment for signalling pathways, for the exchange of genetic material, of metabolites and enzymes, and with a high nutrient and water concentration (Davey et al., 2000). In addition, the heterogeneity of a biofilm offers a gradient of physicochemical conditions (Stoodley et al., 2002; Flemming et al., 2007), allowing the formation of stable consortia of different microbial species in different compartments of the biofilm. Indeed, although much has been learned through the study of single-species biofilms grown in laboratory conditions, natural biofilms are mostly polymicrobial communities with unique characteristics originating from the combination of bacterial

species and extracellular condition in which it develops (Vlamakis et al., 2013). A good example is the spatial distribution of microorganisms according to oxygen gradient inside the biofilm. Oxygen-profile measurements in biofilms reveal that oxygen concentrations decrease from the external aerated fluid into the biofilm depths, until is completely depleted. Oxygen is actively respired by aerobic cells in the upper layers of the biofilm, forming anaerobic niches suitable for anaerobic bacteria, deeply in the biofilm (Schramm et al., 1996). Therefore, the chemical and physical heterogeneity of biofilm lead to the heterogeneity in the bacterial species distribution in natural multi-species biofilms. In mono-species biofilm, the same heterogeneity can be find at a different level: gene expression, activated pathways and produced proteins respond to the local and unique conditions (Stewart et al., 2008). Within the biofilm, genetically identical cells express different genes and produce subpopulations of functionally distinct, coexisting cell types (Vlamakis et al., 2013).

2.1 Biofilm development

Microscope observations of sub-aquatic biofilm (i.e., biofilm growing on a solid surface in contact with a liquid) revealed complex spatial organization with pillars, mushroom-like and tree-like structures with water channels that allow an efficient exchange of nutrients, waste products, and signalling molecules (Stoodley et al., 2002). Biofilm development from a single cell to a complex 3D structure has been often compared to multi-cellular organisms and cellular communities. Because of this similarity, Asally et al. (2012) suggested that the two processes guiding tissue development could govern biofilm formation: a genetic program to rule cellular processes (growth, death, and differentiation) and a macroscopic movement of cell populations, determined by mechanical properties and physical forces. This is particularly interesting if applied to the available models of biofilm formation: the developmental model (O'Toole et al., 2000) and the individualist model (Mods et al., 2009). The largely accepted **developmental model** mainly arise from imaging techniques, microbiological observations of biofilm morphology and isolation of mutants, considering the biofilm from a macroscopic point of view. According to this model, biofilm formation occurs because of a sequence of events, where different stages can be identified (O'Toole et al., 2000) (Fig. 1). The formation of microbial biofilms begins with the reversible adhesion

of a small number of cells to a surface. On the abiotic surface, the balance between non-specific interactions, such as electrostatic, hydrophobic, and van der Waals forces, drive the initial attachment between bacteria and the surface (van Merode et al., 2008). Upon sensing the contact with the surface, bacteria undergo a cascade of metabolic changes and the alteration in structural components such as membrane proteins and transporters, allowing a transient attachment to the surface (Sauer et al., 2001). Environmental signals can activate cellular mechanisms to strengthen the adhesion, make it irreversible, and cells proliferate in clusters forming a monolayer called microcolony (Hinsa et al., 2003; Ono et al., 2014). Monolayer cells keep dividing by active binary division and recruiting cells to accumulate as multilayered cell clusters. This cell accumulation requires coordinated efforts from the microbial community to produce a well-organized structure. A multilayer biofilm develops when bacteria are able to adhere to a surface and to each other. Intercellular adhesions require an outer adhesive bacterial surface, requirement that can be satisfied by the synthesis of an adhesive matrix (Karatan et al., 2009). The matrix is composed of extracellular polymeric substances (EPS), i.e. a mixture of polysaccharides, proteins, and nucleic acids that surrounds the bacterial colony, allowing strong cell-to-cell and cell-to-surface interactions towards the differentiation of a mature biofilm (Karatan et al., 2009). EPS are essential in building the 3D biofilm structure, in retaining nutrients for cell growth, and in protecting cells from dehydration and other cellular stresses (Flemming et al., 2007). Biofilm commonly develops to form a differentiated, vertical structure with variable thickness and cell-free channels for the transport of nutrients and oxygen from the interface to the inner parts of the biofilm, and for the removal of metabolic wastes. At this point, different microenvironments are present, characterized by specific physicochemical conditions that can support the growth of heterogeneous bacterial species or bacteria with different physiological states (Stoodley et al., 2002). The last step of biofilm development is the dispersal. Bacterial cells detached from the biofilm re-enter the planktonic state, and may start a new biofilm formation cycle. Signalling molecules in response to environmental changes (e.g. nutrients availability, oxygen concentration, oxidative stress) or inner accumulation of waste products cause the disruption of the biofilm, through the production of lytic enzymes, the return of motility, surfactant production, and cell lysis (Mc Dougald et al., 2011). In this way, bacteria detect and respond to the unfavorable environmental conditions by returning to the

planktonic mode of existence (Karatan et al., 2009). This first model entails the evolution of dedicated, hierarchically ordered pathways for regulation of biofilm formation. Nevertheless, little evidence from molecular studies supports the idea that biofilm formation relies on an independent and dedicated gene network (Ghigo, 2003; Monds et al., 2009). Recently, Monds and O'Toole (2009) propose an alternative model, called **individualist model**, more consistent with the involvement of genetic modules from different pathways to regulate biofilm formation. In this model, biofilm formation occur following the same steps of the previous model, except that individual bacteria – not the multicellular community- sense and respond to its specific surrounding environment. The process leads to cooperation between bacteria and to biofilm formation as a highly adaptive measure. Indeed, some of the apparently cooperative traits are advantageous for the individual bacterium (Klausen et al., 2006). According to this model, each cell reacts individually and constantly adjust to being part of a microbial community (Monds and O'Toole, 2009) (Fig. 2). Data in support of both models have been published. The complexity of the biofilm formation analysed is probably better described merging the two models. In the early stages of biofilm formation, the individualist model fit well as the contribute of the genetic program to rule cellular processes is evident; on the other hand, in the late stages of biofilm formation the coordination and the macroscopic movement of cell populations are the main actors and are better described by the developmental model.

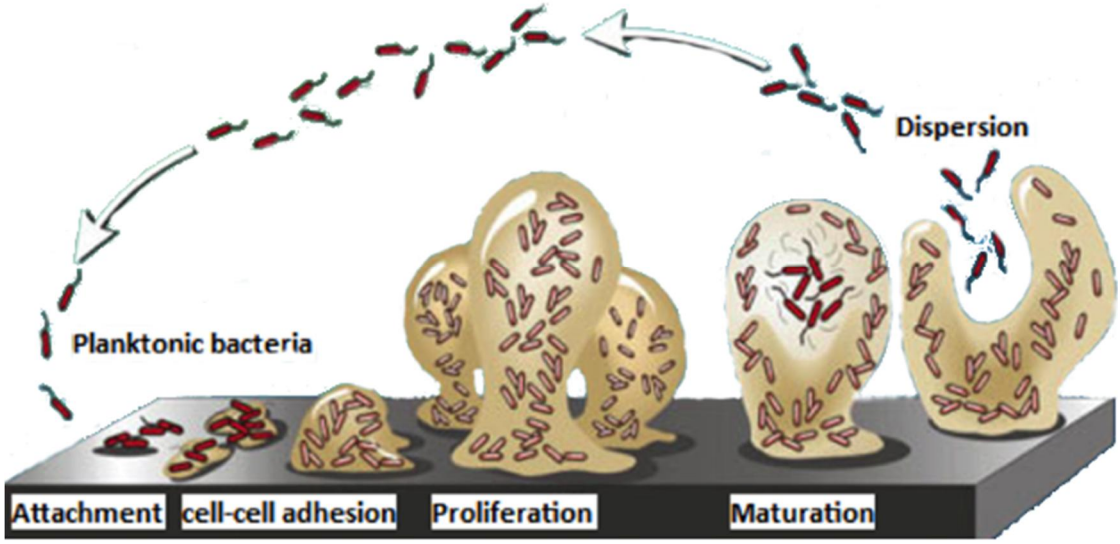

Figure 1. Biofilm formation according to the developmental model. Image retrieved from CBE Image Library, Center for Biofilm Engineering Montana State University-Bozeman.

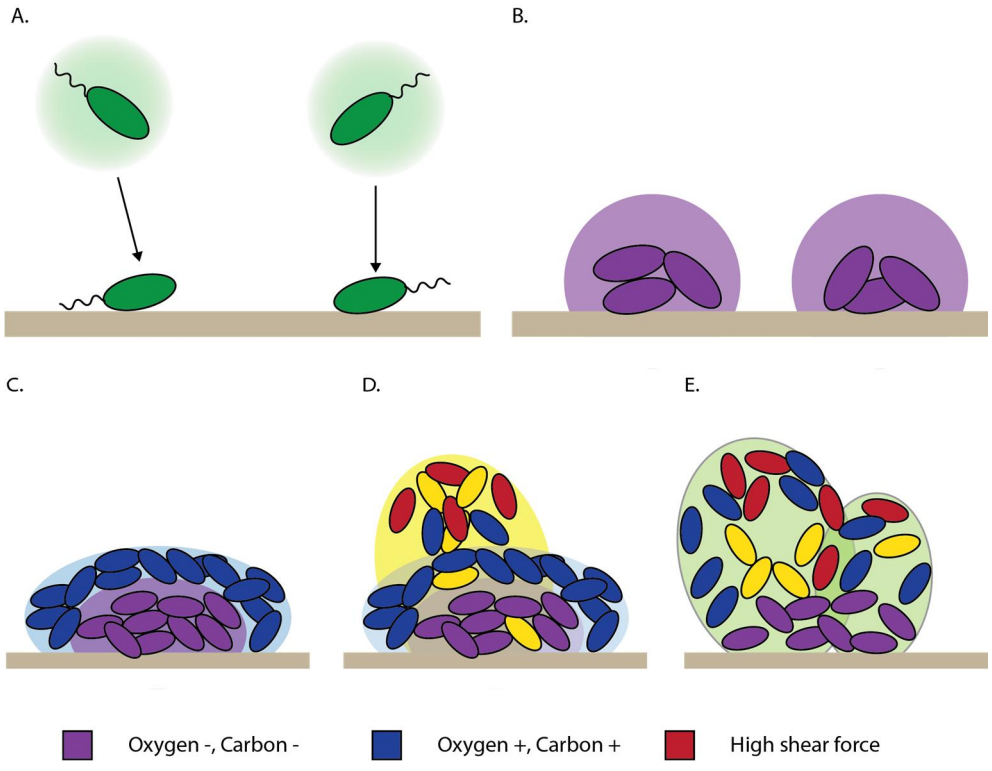

Figure 2. Biofilm formation according to the individual model. Adapted from Monds et al., 2009. A. Independent cells attachment to a surface. B. Oxygen and carbon favours cell division. C. Microcolony: active metabolism of cells on top pushes the bottom cells to adapt, creating heterogeneity. D. Macrocolonies: stochastic production of EPS (yellow cells) promotes biofilm maturation. Higher shear forces (yellow zone) make top cells adapt, increasing heterogeneity. E. Mature biofilm.

2.2 Biofilms impact

Biofilms can colonize different surfaces, either biotic or abiotic, causing a beneficial or detrimental effect on environment, industry and human health (Costerton et al., 1987). Biofilm characteristics are beneficially exploited in the wastewater treatment plants (Nicolella, 2000), for bioremediation (Wu et al., 2015; Dash et al., 2013), for the production of biomaterials, or enhance the effect of plant growth promoting rhizobacteria in soil (Rinaudi et al., 2010). Indeed, in rhizosphere, many microbial species adopt a sessile lifestyle to colonize roots. The biofilm allows them to overcome common environmental stresses, such as desiccation and nutrient limitation, and to establish with plants complex and advantageous interactions, which modulate gene expression in both the plant and the associated bacteria (Rudrappa et al., 2008). This interaction is favourable for plants too. Indeed, EPS produced by bacteria in the rhizosphere also enhance soil aggregation, which in turn improves water stability, critical to the survival of the plant (Davey et al., 2000). Nevertheless, biofilm can also be destructive, causing chronic infections (Bjarnsholt et al., 2013), parasitism phenomena in animals and plants (Rinaudi et al., 2010), biodeterioration of engineered systems and artworks (Cappitelli et al., 2006), fouling of food-processing equipment (Villa et al., 2012a). Indeed, biofilms adhesion to metal surfaces promotes corrosion, clogging of pipelines in food processing plants and reduction of heat transfer efficiency, resulting in important economic losses and high risks for health because of the possible food contamination by pathogens, such as *Listeria*, *Pseudomonads*, *Bacillus* and *Salmonella* spp. (Tan et al., 2014). In addition, the presence of biofilms on artificial surfaces instigates biofouling, stimulating the subsequent attachment of macro-foulers, like plants and animals, through biochemical signals and changes of physical surface properties (Zardus et al., 2008). Biofilm removal is carried out using either biocides or mechanical methods (i.e. grinding, wash-out with high-pressure water), but the complete and efficient eradication is often difficult (Bruellhoff et al., 2010). In the sanitary field, biofilm-associated diseases are more difficult to treat and require a considerable amount of time and higher antibiotics doses before they can be completely eradicated (Donlan et al., 2002; Gilbert et al., 2002). Eradication problems arise because cells living in a biofilm are less sensitive to antimicrobial agents compared to planktonic bacteria (Mah et al., 2003). Various different mechanisms have been proposed to explain

the reduced susceptibility to antibiotics shown by bacterial biofilms. The barrier properties of the extracellular matrix, the presence of niches of starved and stationary phase bacteria (Anderl et al., 2003; Walters et al., 2003), the existence of sub-populations called persisters (Percival et al., 2011) and the spreading of antimicrobial resistance by gene transfer are the main mechanisms ensuring a higher tolerance of biofilm to biocides and other stress. The eradication of biofilm results even more difficult because killed cells might provide nutrients for subsequent colonization, but, above all, a small surviving population of persistent bacteria can repopulate the surface immediately, becoming more resistant to further biocide treatment (Pace et al., 2006). A possible solution is a combined approach of conventional biocides with additional treatments (e.g., permeabilisers, exopolysaccharide inhibitors, DNase; Vaara et al., 1992; Huang et al., 1999) to increase the vulnerability of organisms, though reducing the biocide concentrations and the health hazard for operators and environment (Young et al., 2008). Furthermore, effforts have been addressed towards the development of preventive strategies that can be used to disarm microorganisms without killing them. Possible target to inhibit biofilm formation are: the early adhesion phase, interacting with the surface sensing process to repel pioneering cells keeping them in a planktonic form; the reversible-to-irreversible adhesion phase, interfering with cell-to-cell communication. Villa et al. (2010; 2011) described a recent biocide-free approach, aimed at interfering with the adhesion phase of biofilm genesis: zosteric acid significantly reduced, at sub-lethal concentrations, both bacterial and fungal adhesion. Furthermore, zosteric acid has been recently successfully tested to inhibit the biofouling in membrane bioreactor systems used in wastewater treatment plants (Polo et al., 2014).

2.3 Biofilm composition

Matrix is the main component of biofilms, sometimes accounting for over 90% of the dry mass (Flemming et al., 2010) and, as mentioned before, forms the scaffold for the 3D architecture of the biofilm. Cells themselves produce and extrude the exopolymeric substances (EPS) composing the matrix, necessary to ease cell adhesion onto solid surfaces overcoming the electrostatic interaction that would repulse cells from the surface (Tsuneda et al., 2003). EPS supply the physicochemical conditions apt for the

development and growth of sessile cells, because it affects charge, porosity, water content, hydrophobicity, and viscoelasticity of the environment surrounding cells (Flemming et al., 2007). Furthermore, EPS protects cells against abiotic and biotic stress (e.g. desiccation, antibiotics, biocides, metals, ultraviolet radiation, host immune defences), allowing the colonization of niches not suitable for planktonic cells (Davey et al., 2000; Flemming et al., 2010). Despite the structural and defensive functions, biofilm is a fluid and dynamic system that allows the movement of cells, nutrients and gases (Sutherland, 2001). While matrix from *in vitro* and mono-specie biofilm is principally composed by polysaccharides, EPS from natural biofilm account also proteins, DNA, lipids, humic substances (Vu et al. 2009) and other extracellular structures, i.e. outer membrane proteins (Wu et al., 2014), lipopolysaccharides (Chatterjee et al., 2006), fimbriae, pili, and flagella (Klausen et al., 2003), which are involved in cell-to-cell and cell-to-surface adhesion (Pamp et al., 2007). Molecular mechanisms for polysaccharides production vary from species to species, as well as the type of polysaccharides produced. Here I focused my attention on those polysaccharides known as matrix components of biofilm studied during my PhD: *A. vinelandii*, *B. thailandensis* and *B. subtilis*.

2.3.1 Polysaccharides

Capsular polysaccharides (CPS) are highly hydrated molecules, often linked to the cell surface of the bacterium via covalent attachments to either phospholipid or lipolysaccahride (Whitfield et al., 1993). They can be either homo- or heteropolymers composed of repeating monosaccharides joined by glycosidic linkages in a high number of configurations, which leads to large structural diversity among CPS types (Roberts, 1996). They promote adherence of bacteria to both surfaces and other bacterial cells, which may facilitate colonization and persistence in a particular niche through the formation of biofilms (Costerton et al., 1987). CPS are well-known virulence factors in many bacteria, e.g. *Escherichia coli*, *Acinetobacter calcoaceticus*, *Erwinia stewartii* and *Neisseria meningitides* (Reckseidler, 2012). CPS can help bacteria to escape phagocytosis, as deposition of complement factor C3b on the bacterial cell surface is lower in the presence of capsule (Reckseidler et al., 2005). The genes necessary for the biosynthesis and the export of CPS are generally clustered at a single chromosomal locus, which genetic organization is conserved in most bacterial species (Roberts, 1996). This is true

also for the so-called *Bptm* group, including three species from *Burkholderia* genus *B. pseudomallei*, *B. thailandensis* and *B. mallei* (Majerczyk et al., 2014). *B. pseudomallei* is the etiological agent of melioidosis, a serious disease endemic in South-East Asia, while *B. thailandensis* rarely causes disease and it is often used as model organism for *B. pseudomallei* (Wiersinga et al., 2006). *B. pseudomallei* produces a CPS with the structure -3)-2-O-acetyl-6-deoxy- β-d-manno-heptopyranose-(1- that is required for *B. pseudomallei* virulence in experimental animal models (Reckseidler et al., 2001). The genes involved in the production of this capsule demonstrated strong homology to the genes involved in the production of capsular polysaccharides in many organisms, including *N. meningitidis*, *H. influenzae*, and *E. coli* (Reckseidler, 2012). The relation between CPS production and virulence in *Bptm* group is still controversial. Indeed, some *B. thailandensis* strains also produce the capsule as *B. pseudomallei*, despite being avirulent in mouse infection models (Sim et al., 2010). On the contrary, some *B. thailandensis* clinical isolates such as *B. thailandensis* CDC2721121 (part III, chapter 1), are virulent despite the absence of the capsule; instead, they produce an exopolysaccharide more typical of environmental strains (Peano et al., 2104).

Exopolysaccharides, are long, thin molecular chains with high molecular weight (10 to 30 kDa) (Kumar et al., 2007), whose properties can vary depending on the type of monomer units, the kind of glycosidic linkages and the presence of different organic and inorganic substitutions. Exopolysaccharides can form various types of structures within a biofilm and interact with other molecules to form a very complex network structure (Sutherland, 2001). The role of these polysaccharides includes maintaining structural integrity of cell envelope, preventing cellular desiccation (Whitney and Howell, 2013), as well as promoting the correct shaping and maturation of biofilm (Branda et al., 2006) and contributing to the protection of bacteria from environmental stresses and bactericidals (Hall-Stoodley et al., 2004). The majority of exopolysaccharides (alginate, pel, psl, cellulose, PNAG) is synthetized at the cell membrane and exported out of the cytoplasmic membrane, as it happens for cell wall polymer, peptidoglycan and lipopolysaccharide (Kumar et al., 2007; Baker et al., 2014). In Gram-negative bacteria, such as *A. vinelandii* and *B. thailandensis*, three molecular mechanisms describe the construction and the export of these biopolymers. The first is the Wzx/Wzy-transporter-dependent pathway, which uses a lipid as an acceptor; examples of this mechanism are the *E. coli* group 1 capsular polysaccharides, O-antigen and cepacian production in *B.*

cenocepacia. The second system, which relies upon ATP-binding cassette (ABC) transporters, assembles the entire polysaccharide on a lipid acceptor and is used, for example, in the production of *E. coli* group 2 capsular polysaccharides and lipopolysaccharides common antigen. The synthase-dependent pathway, a third mechanism of assembly, for which the requirement for a lipid acceptor depends on the polysaccharide, is typical of complex polymers such as alginate, cellulose, acetylated cellulose and poly-N-acetylglucosamine (PNAG) (Whitney and Howell, 2013). **Alginate** is an anionic linear polymer composed of β-1,4-linked mannuronic acids and its epimer, α-L-guluronic acid. Alginate attracted great attention because of its role in the pathogenesis of the opportunistic human pathogen *Pseudomonas aeruginosa* (Govan et al., 1996), but also because of its use in the food and pharmaceutical industries. An alternative source of this polymer can be the rhizobacterium *A. vinelandii* (Rehm, 2010) (part II, chapter 1), that require alginate for the formation of a dormant desiccation-resistant cyst (Campos et al., 1996). Alginate maintain the hydration of the cells and is required for survival and biofilm formation under desiccating conditions. It can protect the bacteria from common bactericides used in plants (Hodges et al., 1991) and from host defence mechanisms, including scavenge reactive oxygen species (ROS), which are used by macrophages and neutrophils for pathogen killing and released during the hypersensitive response plant defence system (Simpson et al., 1989). As for *P. aeruginosa*, all but one of the core genes involved in alginate biosynthesis are contained within a single 12-gene operon: *algD*, *alg8*, *alg44*, *algK*, *algJ*, *algG*, *algX*, *algL*, *algI*, *algV*, *algF* and *algA*. Its regulation is slightly different as *A. vinelandii* alginate gene cluster has two promoters upstream of *algD*, one AlgU-dependent and one RpoS (σs)-dependent (Castaneda et al., 2001), and three additional internal promoters regulating the level of polymer modification (Hay et al., 2014). The master regulator of alginate biosynthesis is the alternate sigma factor AlgU, a homologue of the stress response regulator RpoE from *E. coli*. AlgU is classified as an extra cytoplasmic function (ECF) sigma factor, a family of sigma factors that confer resistance to envelope stress caused by antimicrobial and oxidizing agents, elevated temperatures, and osmotic imbalances. Under uninduced conditions, the activity of AlgU is sequestered, but various environmental cues can lead to the release of AlgU, allowing activation of AlgU-dependent promoters. AlgU is encoded in an operon containing four other genes, *mucA*, *mucB*, *mucC* and *mucD*, which modulate its activity. AlgU promotes the expression of its own operon, along with

several other genes involved in alginate biosynthesis and regulation: *algR*, *algB*, *algD*, *algC* and *amrZ*. In addition, AlgU has been determined to be involved in the regulation of motility, quorum sensing and virulence (Hay et al., 2009). In response to envelope stress, AlgU is released from their anti-sigma factor (MucA and MucB) complexes through a well-conserved signal transduction pathway known as a regulated intramembrane proteolysis (RIP) cascade, involving several proteases (Hay et al., 2014). The proteases action allows the degradation of the repressor MucA and let AlgU free to interact with RNA polymerase to drive expression of its regulon, including the alginate operon (Qiu et al., 2008). Under unstressed conditions, cleavage sites on repressors are not available, thus the RIP cascade cannot be initiated (Qiu et al., 2007). RIP cascade can also be activated by the accumulation of misfolded and/or mislocalized components of outer membrane proteins (OMP) and lipopolysaccharides (LPS), caused by envelope stress (Lima et al., 2013). On the other hand, MucD, a periplasmic serine protease and chaperone-like protein, negatively regulates the RIP cascade by chaperoning and/or degrading misfolded OMPs, forming the first line of defence from envelope stress (Qiu et al., 2007). Once AlgU is released, several other steps take place to allow it to bind to the RNA polymerase and activate the *algD* promoter. Transcription from the *algD* promoter is regulated by the coordination with two other sigma factors, RpoD and RpoN (Yin et al., 2013; Boucher et al., 2000) and a range of other DNA-binding proteins, which promote algD operon expression by latching onto its promoter region (Baynham et al., 2006). These DNA binding proteins are also involved in other pathways, such as the biosynthesis of other polysaccharides, the control of flagella production and virulence (Jones et al., 2013). The KinB-AlgB and FimS-AlgR two-component signal transduction systems also control the expression of alginate production genes in response to unknown environmental cue. Both the response regulators, AlgB and AlgR, bind to the *algD* promoter, activating the expression of alginate biosynthesis genes (Leech et al., 2008). In *A. vinelandii*, noncoding small RNAs (sRNA) have an emerging role in the regulation of alginate. They can bind RsmA, a translational regulatory protein, able to repress translation of the *algD* mRNA transcripts. The disruption of the two-component system producing these sRNAs leads to reduction in alginate production that can be restored through the constitutive expression of several sRNAs (Manzo et al., 2011). Alginate biosynthesis is also regulated posttranslationally by bis-(3′-5′)-cyclic dimeric guanosine monophosphate (c-di-GMP) binding to the PilZ domain of Alg44, the putative

co-polymerase of the alginate biosynthesis machinery (Hay et al., 2009). c-di- GMP is a generic secondary messenger molecule utilized by bacteria for regulation of motility, exopolysaccharide production and virulence (Roemling et al., 2005). Together with alginate, **psl** and **pel** are polysaccharides composing *P. aeruginosa* biofilm matrix, particularly in the non-mucoid strains (Ghafoor et al., 2011; Karatan et al., 2009). Psl is rich in mannose and galactose and is involved both in initial attachment and in biofilm maturation where it is mostly localized at the caps of the mushroom-like structures (Ma et al., 2009). Pel is a cellulose-like, glucose-rich polymer, essential for the formation of a pellicle at the air-liquid interface and associated with the wrinkled colony phenotype (Friedman et al., 2004). **Cellulose**, a polysaccharide consisting of a linear chain of several hundreds ß-1,4-linked D- glucose monomers, is the most abundant polysaccharide in nature and is produced by both plants and bacteria. Its production has been described in *E. coli*, *Salmonella* strains, *Vibrio fischeri*, *Gluconacteobacter xylinus*, *Sarcina ventriculi*, *Agrobacterium tumefaciens*, *Rhizobium leguminosarum*, and in different *Pseudomonas* environmental isolates (Ausmees et al., 1999; Matthysse et al., 1995; Ross et. al., 1991; Zogaj et al., 2001; Jonas et al., 2008; Bassis et al., 2010; Ude et al., 2006). However, comparative sequence analyses indicate that many other bacteria, including *Yersinia* and *Burkholderia cepacia* complex species, can synthesize cellulose (Cuzzi et al., 2014). In *E. coli*, *Salmonella sp*. and *G. xylinus*, pathways for cellulose production are regulated by intracellular levels of the second messenger c-di-GMP levels (Gualdi et al., 2008). **Cepacian** is the major exopolysaccharide produced by a large percentage of clinical isolates of the *Burkholderia cepacia* complex, i.e. a group of bacterial species, including some opportunistic pathogens in patients immunocompromised and affected by cystic fibrosis (Zlosnik et al., 2008). Cepacian has been recognized as a virulence factor, inhibiting neutrophil chemotaxis and the production of reactive oxygen species, both essential components of the innate host defenses (Bylund et al., 2006). Cepacian is composed of a branched acetylated heptasaccharide repeat-unit with D-4 glucose, D-rhamnose, D-mannose, three unities of D-galactose and D-glucuronic acid (Cescutti et al., 2000). Two gene clusters have been identified as responsible for the production of cepacian, namely *bce-I* and *bce-II* (Moreira et al., 2003; Ferreira et al., 2010). With the exception of some genes involved also in metabolic processes such as, the biosynthesis of lipopolysaccharide and other cell polysaccharides, most of the enzymes required for cepacian synthesis are encoded by

bce genes. These two clusters include genes encoding proteins for the nucleotide sugar precursor biosynthesis (BceA, BceC), the assembly of the heptasaccharide repeat-unit of cepacian (BceB, BceG, BceH, BceJ, BceK, BceR), the cytosolic acetylation (BceO, BceS, BceU) and the export of the repeat-units to the periplasmic side of the inner membrane, their polymerization, and export of the nascent polymer (BceQ, BceI). All evidence indicates that cepacian biosynthesis proceeds via the Wzx/Wzy-transporter-dependent pathway (Ferreira et al., 2010). *In silico* analysis reported the presence of *bce-I* and *bce-II* clusters also in *B. thailandensis*, suggesting the possible partecipation of cepacian to its matrix composition (Ferreira et al., 2010) (part II, chapter 3 and part III, chapter 1). The EPS produced by *B. thailandensis* biofilm have not been identified yet, but it has been reported that anoxic conditions strongly increased expression of genes involved in EPS production, suggesting a linkage between polysaccharides production and limited oxygen conditions (Peano et al., 2014). The genes responsible for the synthesis of another polysaccharide, poly-N-acetylglucosamine (**PNAG**), are present in a large number of both Gram-negative bacteria, including *E. coli*, *Yersinia pestis*, *Actinobacillus pleuropneumonea*, *Bordetella bronchiseptica* (Whitney et al., 2013), and Gram-positive bacteria, such as *Staphylococcus epidermidis* and *S. aureus* (Maira-Litran et al., 2002). PNAG is a homopolymer of ß-1,6-linked N-acetyl-D-glucosamine molecules and functions as an important component of the matrix of these bacteria, contributing to biofilm formation and persistence during infections (Maira-Litran et al., 2002; Darby et al., 2002). Three different loci are involved in β-1,6-N-acetyl-D-glucosamine biosynthesis: *icaADBC* (in staphylococcal species), *pgaABCD* (in *E. coli* and other Gram-negative bacteria), or *hmsHFRS* (in *Yersinia* species). In these loci it has been possible recognize a glycosyltransferase necessary for catalyzing the synthesis of the N-acetylglucosamine polymers (*pgaC*/ *hmsR*/ *icaA*), enzymes for deacetylation of the N-acetylglucosamine polymer (*pgaB*/ *hmsF*/ *icaB*), proteins for appropriate polymer length and transport of the polymer to the cell surface, a porin-like protein for PNAG secretion (Vuong et al., 2004; Itoh et al., 2008). In *E. coli*, PNAG is involved in both surface attachment and formation of multilayer biofilms, suggesting that this polysaccharide mediates cell-cell adhesion in addition to cell-surface adhesion (Vuong et al.,2004; Karatan et al., 2009). Despite the EPS composition in *B. subtilis* biofilm (part II, chapter 2) can vary greatly depending on growth conditions, **EpsA-O polysaccharide** is essential for biofilm formation (Dogsa et al., 2013) Indeed, it is known that *eps*-defective

mutants are still able to grow in cell chains, but develop flat colonies and extremely fragile pellicles (Branda et al., 2006). This polysaccharide is composed of glucose, galactose and N-acetyl- galactosamine and is produced under the direction of the 15-gene operon *epsA-O* (Branda et al., 2006; Chai et al., 2012). In addition, *B. subtilis* secretes the 31-kDa TasA protein, which assembles in amyloid fibers essential for biofilm structure (Branda et al., 2006; part I, chapter 2.2.2). Activation of both operons are under the control of the repressor SinR and its antagonist SinI (Kearns et al., 2005; Chu et al., 2006). In turn, *sinI* is under the control of Spo0A, i.e. the master regulator for entry into sporulation, suggesting a tight link between matrix production and spore formation (Chai et al., 2008). Furthermore, in a *B. subtilis* biofilm, matrix operons are derepressed only in a sub-population of the cells; it has been recently proposed that when a high enough proportion of the cell population express the *epsA-O* operon, the EpsAB kinase can be activated and polysaccharide stimulate their production (Elsholz et al., 2014). The γ-polyglutamic acid (**γ- PGA**) is another component that can play an important role in *B. subtilis* biofilm formation and has been linked to mucoid appearance of the *B. subtilis* colonies. Poly-DL-glutamic acid production require the two-component system ComPA (Tran et al., 2000), DegSU two- component system, DegQ and SwrA. The effects of ComPA, DegSU and DegQ on γ -PGA production appear to be at the transcriptional level, while SwrA acts post-transcriptionally. Identification of these regulatory proteins suggest that γ –PGA should be produced in an environment with high cell density or high salinity and/or osmolarity (Stanley et al. 2005). In addition, PGA is one of the major virulence factors of *Bacillus anthracis* confers virulence to B. anthracis by its antiphagocytic activity (Leppla et al., 2002). Contrary to the polysaccharides described so far, **levans, alternans** and **dextrans** are synthetized extracellularly (Vanhooren et al., 1998). Dextran is a homopolysaccharide with varying molecular weight [15−20,000 kDa] produced by *Leuconostoc mesenteroides*, produced by dextransucrase, a glucosyltransferase, which transfers glucose from sucrose to the reducing end of a growing dextran chain. Formation of alternan by *L. mesenteroides* occurs by alternansucrase, probably a translation product of a mutant gene sequence originally coding for a dextransucrase. The alternansucrase synthesizes alternan by the enzyme levansucrase, a glucan containing alternating α-(1 → 6) and α-(1 → 3) glycosidic linkages. Levan is a β-2,6-fructan produced in *Bacillus*, *Erwinia*, *Gluconobacter* spp. and the phytopathogen *Pseudomonas syringae*, especially when grown on sucrose as a

carbon source (Vanhooren et al., 1998). In *B. subtilis*, the structural gene of levansucrase, *sacB*, is part of *sacB–yveB–yveA* operon and is activated in the presence of sucrose (Pereira et al., 2001). Recently, levan has been highlighted to strengthen *B. subtilis* biofilm (part II, chapter 2), although its presence is dependent on either protein TasA or EpsA-O polysaccharide that serve as a scaffold for levan entanglement. Considering that plants roots release sucrose in the soil, the ability to transform sucrose to levan may increase *B. subtilis* advantage in the rhizosphere, also providing an additional mechanism to sequester carbon in a highly competitive environment (Dogsa et al., 2013).

2.3.2 Proteins

EPS matrix of biofilms generally include large **multimeric cellular appendages**, such as flagella, fimbriae, and pili. They typically consist of numerous major structural protein components and several auxiliary proteins. **Flagella** are helicoidal rotary appendages driven from a motor at the base, with a filament acting as a propeller (Bardy et al., 2003). This complex structure is primarily involved in cellular motility and chemotaxis, but it also has a sensory function in detecting environmental wetness (Wang et al., 2005). The relation between flagellar activity and biofilm formation is not completely clear yet. A functional flagellar apparatus appears to be important in the initial stages of biofilm formation stabilizing the contact between the surface and the cell, helping bacteria to overcome the repulsive forces generated by electrostatic interactions (Pratt et al., 1998). During biofilm formation, the increase of the intracellular level of the second messenger c-di-GMP regulates the flagellum activity by a backstop brake mechanism (Paul et al., 2010) and by repression of the flagellar genes (Srivastava et al., 2013; Krasteva et al., 2010). In addition, c-di-GMP is able to inhibit motility with a coordinated action on the flagellum motor and on the rotation movement itself, promoting the biosynthesis of cellulose to obstruct the flagellum rotation (Zorraquino et al., 2013). In *P. aeruginosa* FleQ, the master regulator of flagellum biosynthesis, is a c-di-GMP-binding protein: the binding to c-di- GMP derepresses the pel operon, with the consequent polysaccharide production, and represses the expression of flagellum biosynthesis genes (Baraquet et al., 2013). The regulation of motility during biofilm formation can vary depending on the analysed bacterium. However, the molecular mechanisms addressing motility to biofilm formation in *Bacillus*, *Pseudomonas*, *Vibrio*,

and *Escherichia* spp. reveal a common trend. In the short term, motility is decreased either by inhibition of the flagellar rotation or by modulation of the basal flagellar reversal frequency; over the long term, flagellar gene transcription is inhibited or, in the absence of *de novo* synthesis, flagella are diluted out through growth (Guttenplan et al., 2013). **Pili** are long filamentous structures extending from bacteria surfaces. In Gram-negative bacteria, pilins, the major pilus subunit proteins, typically assemble by non-covalent homopolymerization. Additional pilins may be added to the fiber and often function as host cell adhesins. Some pili are also involved in biofilm formation, phage transduction, DNA uptake and twitching motility. In contrast, in Gram-positive bacteria, pilins polymerize covalently to form pili, through a process that requires a dedicated and specialized transpeptidase. Minor pilins are added to the fiber and play a major role in host cell colonization (Proft et al., 2009). There are different types of pili, with different composition and biosynthesis, depending on the bacterial species. In *E. coli*, conjugative F-pili are used to establish tight cell-cell connections, promoting genetic material transfer between donor and recipient cells. Even minor changes of the conjugative pili structure resulted in either the formation of biofilms with altered spatial structure, or in a decrease in biofilm formation (Reisner et al., 2003). Type F pili are encoded by natural conjugative plasmids, which thus direct the expression of biofilm factors as a part of a coordinated strategy aimed to their propagation (Ghigo, 2001). In *P. aeruginosa*, type IV pili are important to mediate adhesion to both abiotic and biotic surfaces and for biofilm formation; strains defective for their production are unable to form microcolonies and cannot progress beyond the initial adhesion step (Giltner et al., 2006). In addition, type IV pili bind extracellular DNA (eDNA) with high affinity, and might thus act as crosslinkers between the cells and the eDNA matrix (van Schaik et al., 2005). **Fimbriae** are generally shorter than pili and have been associated with attachment to host tissues or abiotic surfaces in several pathogenic *E. coli* strains. The most common adhesins found in *E. coli* isolates as well as in other *Enterobacteriaceae* are Type 1 fimbriae (Van Houdt et al., 2005). Type 1 fimbriae consist primarily of the structural protein FimA, but several auxiliary proteins are necessary for transport and assembly of the structural proteins. Furthermore, the expression of the encoding operon, the *fim* operons, is phase variable due to a DNA switch in the promoter region that depends on the activity of the two recombinases FimB and FimE (Gally et al., 1996). A particular type of fimbriae, **curli** fibres, plays a pivotal role in cellular adhesion during

biofilm formation in *E. coli, Salmonella, Citrobacter* and *Enterobacter* species, in which they mediate surface adhesion and cell-to-cell aggregation (Prigent-Combart et al., 2001; Zogaj et al., 2001). More recently, similar structures have also been identified in the Gram-positive bacteria *Mycobacterium tuberculosis* and *B. subtilis* (Alteri et al., 2007; Romero et al., 2010) and in biofilm of several environmental isolates belonging to *Gammaproteobacteria*, *Bacteriodetes*, *Firmicutes* and *Actinobacteria* (Larsen et al., 2007). Curli are flexible amyloid-like structures protruding from the cell surface (Prigent-Combart et al., 2001) made up of a primary structural component (CsgA) and a minor structural unit (CsgB). Genes involved in curli biosynthesis are clustered in the *csgBAC* operon, encoding curli structural components, and the *csgDEFG* operon, encoding the CsgD transcription regulator and proteins involved in curli assembly and transport (Hammar et al., 1995). The CsgD protein activates transcription of the *csgBAC* operon and of AdrA production via c-di-GMP synthesis (Simm et al., 2004). Regulation of *csgD* is extraordinarily complex and responds to a combination of environmental cues (i.e., low growth temperature, low osmolarity, slow growth and oxygen availability) (Tagliabue et al., 2010; Roemling et al., 2000), but also to the intracellular levels of the signal molecules cAMP and c-di-GMP, and to the concentration of pyrimidine nucleotides (Garavaglia et al., 2012). Surface proteins are regularly present in the biofilm matrix of many microorganisms, such as species from the genera *Streptococcus*, *Staphylococcus*, *Enterococcus*, *Lactobacillus*, *Pseudomonas*, *Bordetella*, *Burkholderia*, *Escherichia* and *Salmonella.* Their presence has been mainly related to the initial attachment of microbial cells to surfaces, but they are also important for the intercellular adhesion and for the accumulation in multilayered cell clusters. A group of surface proteins with sequence similarities to the biofilm-associated protein (Bap) of *Staphylococcus aureus*, known as **Bap-related proteins**, are able to induce biofilm formation in the absence of exopolysaccharides. These proteins are generally large (up to 8800 aminoacids) and have a signal sequence at their N terminus followed by domains containing a number of tandem repeats that play a role in cellular adhesion. The production of such large proteins entail a considerable metabolic effort by the bacteria, which therefore strictly regulate their production in coordination with other elements of the biofilm matrix (Lasa et al., 2006). Most of these proteins are anchored to the surface of the cells, loosely associated with the surface of the cells, or secreted into the medium. Thus, they hold cells in the biofilm together possibly by interacting with similar proteins on the surface

or on the neighbour cells. In addition, Bap-related proteins may also be involved in the virulence and the development of chronic infections (Karatan et al., 2009). Bap-related proteins includes the biofilm-associated protein (Bap) of *Staphylococcus aureus*, the large adhesion protein (LapA) of *P. fluorescens* and *P. putida*, the biofilm associated protein (BapA) of *Salmonella enterica*, the enterococcal surface protein (Esp) of *Enterococcus faecalis* and the AdhA adhesin of *Burkholderia cenocepacia* (Pamp et al., 2007). **Bap** was identified during the screening of a library of mutants in the bovine mastitis *S. aureus* strain V329 as a protein that is essential for biofilm formation (Cucarella et al., 2001). It promotes both primary attachment to abiotic surfaces and intercellular adhesion through a mechanism of biofilm development alternative to the regular PIA/PNAG-dependent mechanism (Lasa et al., 2006). Close homologs of Bap have been found in numerous other staphylococcal species among these *S. epidermidis* (Tormo et al., 2005). The Bap- like protein **Esp** is required for biofilm formation by *Enterococcus faecalis*, although some strains can form biofilms in the absence of this protein, suggesting the existence of a mechanisms of biofilm development alternative to Esp (Kristich et al., 2004). A study showed that the N-terminal domain of Esp is sufficient for Esp-mediated biofilm enhancement in *E. faecalis* and that Esp enhance the cell surface hydrophobicity (Tendolkar et al., 2005), a unexpected phenomenon, also observed for other members of the Bap family and apparently related to an interaction of Bap-like proteins with other matrix components such as polysaccharides. The secreted Bap-like protein **LapA** is required for biofilm formation in *Pseudomonas fluorescens*, *Pseudomonas putida* and environmental pseudomonads, suggesting that the involvement of LapA in adhesion to both abiotic and biotic surfaces is a general mechanism. The *lapA* mutants are unable to promote stable adhesion (irreversible attachment) to a surface (Hinsa et al., 2003). LapA is transported to the bacterial surface via an ABC transport system which is encoded by the *lapEBC* genes, and is analogous to the type 1 transporter associated with transport of the BapA protein of *S. enterica*. (Hinsa et al., 2006). Also in *S. enteritidis*, the Bap-like protein **BapA** is required for biofilm formation. Moreover, expression of *bapA* is coordinated with production of cellulose and curli fimbriae in connecting cells, either by strengthening fimbriae-mediated interactions or by allowing the interconnection of bacteria separated by long distances. To promote cell–cell interactions, BapA might interact with itself through homophilic interactions, thus acting both as a receptor and as a ligand between two

bacterial clusters (Lasa et al., 2006). The Bap-type protein of *B. cenocepacia* **AdhA** is able to bind to filaments on the apical surface of injured tracheobronchial epithelial cells and is necessary for migration across the epithelium surface (Urban et al., 2005). In Gram-positive bacteria a large group of proteins termed **MSCRAMM** proteins (microbial surface components that recognize adhesive matrix molecules) share many of the characteristics of the Bap-type protein family, although the functions have mostly been demonstrated in relation to adhesion to host factors such as fibronectin-, fibrinogen-, collagen-, and heparin-related polysaccharides (Pamp et al., 2007). **Lectins** are characterized by affinity towards carbohydrate residues on host cell surfaces, but they can also recognize carbohydrates in extracellular biofilm matrices and thereby promote cell-to-cell interconnection. For example, in *P. aeruginosa*, expression profiling of P.aeruginosa biofilm revealed the involvement of the two lectins LecA and LecB (Waite et al., 2006). LecA is specific for D-galactose and its derivatives (Diggle et al., 2006), while LecB is specific for L-fucose and its derivatives. LecB is exported and bound to the outer-membrane through interaction with fucose containing ligands, suggesting that it promotes cell-cell interactions (Tielker et al., 2005). **Autotransporters** are proteins that are able to transport themselves to the cell surface without the need for other transport systems (Girard et al., 2006). The self-associating autotransporter sub-family of these proteins are capable of interacting with themselves or with other members of the family, thus mediating cell-cell interactions and leading to cell aggregation. Three glycoproteins in this family, Ag43, AIDA, and TibA, promote biofilm formation in *E. coli* strains (Sherlock et al., 2005; Klemm et al., 2006). These proteins could potentially serve to maintain close- range interactions between some cells of the biofilm. Interestingly, the presence of fimbriae on the cell surface abolishes the intercellular interactions mediated by these proteins, suggesting that bacterial adhesins may function in mutually exclusive manners (Sherlock et al., 2005; Karatan et al., 2009). In *B. substilis* (part II, chapter 2), two secreted proteins provide structural integrity to the matrix: **TasA** and **TapA** are encoded by the three-gene operon *tapA-sipW-tasA* (Branda et al., 2006). TasA is an amyloid protein, secreted into the extracellular space with the help of SipW, where it self- assembles into fibers that are anchored to the cell wall by TapA (Romero et al., 2011). A *tasA*-defective mutant produce cell chains that are not held together (Branda et al., 2006). As previously stated, in addition to the TasA protein, biofilm formation requires the EpsA-O polysaccharide, but the inactivation of either TasA protein or EpsA-

O can be compensated by other mechanisms resulting in a residual biofilm matrix (Branda et al., 2006; Pamp et al., 2007). **BslA** is secreted during the final stages of biofilm maturation and self-assembles into a hydrophobic layer on top of the biofilm where it serves as a water-repellent barrier for the community (Hobley et al., 2013). (Mielich-Suess et al., 2014). Finally, natural biofilm offer a more complex variety of proteins in EPS, including cold shock proteins (CspC), superoxide dismutase (SOD), chaperones and peroxidase (Park et al., 2008), probably as a defence mechanism to extreme conditions. In addition, Jiao et al. (2011) identified histone-like DNA binding proteins in the EPS of an acid mine drainage biofilm, possibly as part of the extracellular DNA scaffold to support and organize biofilm structure.

2.3.3 Extracellular DNA

Extracellular DNA (eDNA) is an important constituent of the biofilm matrix in a number of bacterial species (Karatan et al., 2009). eDNA is indistinguishable from chromosomal DNA in its primary sequence (Boeckelmann et al., 2006), thus, it is supposed to accumulate in the biofilm matrix through lysis of a fraction of cells in bacterial populations. However, according to data collected from different microorganisms (e.g. *P. aeruginosa*, *Neisseria meningitidis*, *Shewanella oneidensis*, *Enterococcus faecalis*, *Staphylococcus epidermidis, Staphylococcus aureus*), active eDNA release is mediated by both quorum-sensing (QS)-independent (early and late exponential growth phase) and QS-dependent mechanisms (early stationary growth phase) (Das et al., 2013b). The biofilm matrix in *P. aeruginosa* contains significant amounts of DNA, which are necessary for biofilm integrity (Whitchurch, et al., 2002; Allesen-Holm et al., 2006). Indeed, DNase treatment of *P. aeruginosa* prevents biofilm formation and dissolves preformed biofilms, in both laboratory and clinical conditions (Whitchurch, et al., 2002; Nemoto et al., 2003). The treatment is so efficient that aerosolized DNase I is used as a therapeutic to reduce the viscosity of the sputum in cystic fibrosys patients (Bakker et al., 2007). The distribution of eDNA on the *P. aeruginosa* biofilm substratum in grid-like patterns, developed throughout the biofilm maturation, led to speculate that DNA could serve as sort of scaffold on which bacteria can climb and move using type IV pili (van Schaik et al., 2005). eDNA release mechanism in *P. aeruginosa* has been widely studied and appears to be mediated by both QS-dependent and QS-independent mechanisms (Allesen-Holm et al., 2006). QS-independent mechanisms are responsible for basal levels

of eDNA release, occurring via prophage- induced cell lysis controlled through flagella and type IV pili, while QS-dependent mechanisms elevate cell lysis and concurrently generate elevated amounts of eDNA release (Allesen-Holm et al., 2006). QS molecules, such as acylated homoserine lactones (AHLs) and *Pseudomonas* quinolone signal (PQS), controls the production of cell lysis factors such as prophage and phenazine that induce cell lysis and triggers eDNArelease (Allesen-Holm et al., 2006; Das et al., 2013a). In Gram-positive bacteria, eDNA release is triggered via QS-dependent lysis of bacterial cells mostly mediated by autolysins. In *Staphylococcus epidermidis*, eDNA release is mediated by the autolysin AtlE, the major autolysin involved in cell wall turnover, cell division, and cell lysis in this organism (Qin et al., 2007). Likewise, eDNA is released through the activity of CidA murein hydrolase in *S. aureus* biofilms and contributes to the strength of the biofilm matrix (Rice et al., 2007). Therefore, cell lysis and subsequent release of genomic DNA may be a common mechanism for introduction of DNA into biofilm matrices (Karatan et al., 2009). In oral bacterial strains developing dental plaque, eDNA release is mediated through QS-dependent autolysins (*Streptococcus intermedius* and *Streptococcus mutans;* Petersen et al.; 2005), hydrogen peroxide generation or bacteriophages (*Streptococcus pneumoniae* and *Streptococcus sanguinis*; Regev-Yochay et al., 2006; Carrolo et al., 2010; Zheng et al., 2011).

2.4 Regulation of biofilm development

The biofilm lifestyle is the result of very complex interactions among cells, involving physiological and metabolic changes in response to adverse or changed environmental conditions. Survival in adverse niche is energetically expensive: cells involved in biofilm formation need to coordinate and activate many different pathways, integrating environmental and physiological stimuli. This section summarizes the common mechanisms that regulate the biofilm formation process, focusing on the known pathways regulation biofilm formation in the three microorganisms studied in this thesis.

2.4.1 Environmental signals

Several different environmental signals influence biofilm formation, both directly and indirectly. The **nutrient** availability is one of the more important cues for biofilm

formation. Both scarcity (e.g., *Staphylococcus epidermidis*, Dobinsky et al., 2003) and abundance (e.g., *Vibrio cholera*, Yildiz et al., 2004) can trigger biofilm formation, depending on the bacteria studied and its adaptation strategies to the environment. It seems that, in nutrient starvation conditions, some bacteria find convenient to settle and to minimize metabolism, waiting for better times, whereas other species self-inhibit the biofilm formation to enable cell dispersion (Nagar et al., 2014). Both in *B.thailandensis* and *B. subtilis* biofilms, nutrient exhaustion respectively affects polyhydroxyalkanoate (PHA) and polysaccharides accumulation (Peano et al., 2014; Dogsa et al., 2013). In particular, in *B. subtilis* biofilms grown in sucrose-rich medium, EPS is rich in the polysaccharide levan. Levan concurs to the stability and thickness of the biofilm and it can be used as carbon storage, increasing *B. subtilis* competitive advantage in the rhizosphere (Dogsa et al., 2013). **Oxygen** is another cue that influences cellular adhesion and biofilm formation. In oxygen-limiting condition *P. aeruginosa* forms more biofilm, and shows increased antibiotic tolerance and alginate biosynthesis (Schobert et al., 2010). EPS production is also enhanced in anoxic condition in *B. thailandensis* (Peano et al., 2014) and in *B. cepacia* (Pessi et al., 2013).On the contrary, a microaerophilic environment negatively affects *E. coli* adherence capacity on hydrophilic substrates (Landini et al., 2002). Moreover, in the model organism *E. coli* K-12 str. MG1655 curli fibres and PNAG are regulated by the oxygen sensory system DosP/DosC, which probably adjust levels of the second messenger c-di-GMP in response to oxygen availability (Tagliabue et al., 2010). **Temperature** is another recognized environmental signal. In pathogens or commensal bacteria, temperature changes correspond to the entrance in the host, where temperature is higher and more stable. In *B. thailandensis*, temperature plays a major role in flagellar production and cellular motility, through a mechanism involving down-regulation of *fliC* gene expression at the mRNA stability level (Peano et al., 2014). Down-regulation of flagellar expression at 37°C has been observed in human pathogens, like in *Listeria monocytogenes* (Kamp et al., 2011) and *B. pseudomallei* (Ooi et al., 2013) and it is considered a strategy to prevent recognition of the highly antigenic flagellar structure by the host immune system. Osmolarity, iron, phosphate and zinc availability, compounds resealed by host/other organisms are other important environmental signals, which trigger different responses depending on the bacterium analysed (Nagar et al., 2014). Furthermore, many environmental signals, e.g. the immune response, biocides, antibiotics and toxic compound (Albesa et al., 2004;

Lushchak, 2011), involve the formation of reactive oxygen species (ROS), causing oxidative stress in the cells. Oxidative stress itself is a signal connected with biofilm: this relation will be examined in the chapter 2.5.

2.4.2 Metabolic cues

Products of primary or secondary metabolism may function as intracellular signals molecules that influence extracellular structures formation. **D-amino acids** are important in regulating peptidoglycan composition, amount, and strength, both via their incorporation into the polymer and by regulation of enzymes that synthetize and modify it (Lam et al., 2009). The amino acid valine is secreted by Gram-negative bacteria biofilms and inhibits the growth of *E. coli* (Valle et al., 2008). In *B. subtilis*, incorporation of D-amino acids in the cell wall promotes the release from the peptidoglycan of the protein TasA, required for the structural maintenance of the bacterial community, thus leading to biofilm disassembly (Kolodkin- Gal et al., 2010). An adaptor protein, TapA, forms D-amino acid- sensitive foci in the cell wall to allow this release (Romero et al., 2011). D-amino acids inhibit biofilm formation also in *S. aureus* and *P. aeruginosa* (Hochbaum et al., 2011; Kolod- kin-Gal et al., 2010). In *B. subtilis* biofilm dispersal is also achieved through norspermidine, a **polyamine**, i.e. organic polycations with at least two amine groups (Wortam et al., 2007). Norspermidine directly interact with the negatively- charged extracellular polysaccharides network promoting its collapse and the release of polymers, thus leading to biofilm dispersal (Kolodkin-Gal et al., 2012). Also in the case of metabolic cues, **oxidative stress** can be evoke as metabolic product able to regulate the biofilm formation. For example, in *A.vinelandii*, the inactivation of the rhodanese-like protein RhdA, involved in oxidative stress response, act as continuous endogenous oxidative stress generator that promotes the biofilm genesis, the activity of ROS-scavenging systems and the switch between swarming and biofilm-like phenotypes (Villa et al., 2012b).

2.4.3 Global regulators and signal molecules

The global regulators allow bacteria to rapidly modulate the expression of a large variety of unrelated genes or operons scattered over the genome through non-coding RNAs and signalling molecules that can act at transcriptional, post-transcriptional and post-translational level. **Quorum-sensing** (QS) is a mechanism that enable bacteria to monitor their cell population density through the production and release of chemical

signal molecules called autoinducers. Autoinducers interact with specific receptors on themselves and in neighbouring cells and, once reached a minimal threshold concentration, they induce a response that alters gene expression patterns and modulates bacteria behaviour (Miller et al., 2001). Using these signal-response systems, bacteria take collective decisions, synchronize with the rest of the population and thus function as multicellular organisms (Waters et al., 2005). QS is phylogenetically widespread, which suggests an early origin in bacterial evolution (Lerat et al., 2004) and the importance of cell-to-cell counication among bacteria. Nevertheless, each system (types of signals, receptors, mechanisms of signal transduction, target outputs) reflects the environmental conditions in which a particular species of bacteria resides (Water et al., 2005). QS regulate various traits as surface attachment (Dunne, 2002), extracellular polymer production (Davies et al., 1998), biosurfactant synthesis (Schuster et al., 2006), motility (Daniels et al. 2004), sporulation (Ren et al., 2004), competence (Zafra et al., 2012), bioluminescence (Wilson et al., 1998), the secretion of antibiotic and virulence factors (Williams et al., 2000). QS is often linked to biofilm formation (Nadell et al., 2008), mediating the transition from microcolony to mature biofilm (He et al., 2015; Ueda et al., 2009). Studies carried out in *P. aeruginosa* show that, although biofilm is not completely impaired, mutants lacking the autoinducer form a thinner and less structured biofilm, which is more susceptible to antibiotic (Davies et al., 1998). In Gram-negative bacteria, all the quorum-sensing systems characterized so far, with the sole exceptions of *V. harveyi* and *M. xanthus*, resemble the first identified quorum sensing circuit of the symbiotic bacterium *V. fischeri*. (Manefield et al., 2002). The system relies on two proteins: an autoinducer synthase and a receptor, usually belonging to the LuxI and LuxR protein families, respectively. LuxI-like proteins are responsible for the biosynthesis of a specific N-Acyl homoserine lactones signalling molecule (AHL), while LuxR-like proteins bind the cognate autoinducer once it reaches a critical threshold concentration, and activate the transcription of target genes (Wilson et al., 1998). AHL QS is common to many *Burkholderia* species, including the so-called *Bptm* group (see part I, chapter 2.3.1) (Majerczyk et al., 2014). Members of this group have homologous QS systems. *B. thailandensis* and *B. pseudomallei* contain three complete QS circuits, QS-1, QS-2, and QS-3. *B. mallei* has retained QS-1 and QS-3, but not QS-2. The *B. thailandensis* QS-1 circuit consists of the BtaI1-BtaR1 pair and the signal N-octanoyl homoserine lactone (C8-HSL), QS-2 consists of BtaI2-BtaR2 and N-3-hydroxy-decanoyl homoserine

lactone (3OHC10-HSL), and QS-3 consists of BtaI3-BtaR3 and N-3-hydroxy-octanoyl homoserine lactone(3OHC8-HSL) (Chandler et al., 2009; Ulrich et al., 2004). Additionally, each member of the *Bptm* group contains two LuxR homologs without a cognate LuxI homolog, called BtaR4 and BtaR5. The *B. thailandensis* QS-1 system favour biofilm formation, CPS, EPS and oxalate production, while inhibiting cell motility; QS-2 controls synthesis of the broad-spectrum bactobolin antibiotics, apparently necessary for saprophyte survival, not for host colonization; QS-3 seems to control some chitin-binding proteins and chitinases that contribute to virulence in insects (Ulrich et al., 2004). In Gram-positive QS circuits, the signal molecules is commonly constituted by short peptides (5 – 50 amino acids) synthesized directly by ribosomes and often subjected to extensive post-translational modifications (Miller et al., 2001). The major *B. subtilis* quorum sensing mechanism is *comQXPA* locus that operates through the signaling peptide ComX (Dogsa et al., 2014). *comQXPA* plays a key role in the differentiation of competent cells, surfactin producer cells and in their physiological systems when cells enter the stationary growth phase (Tran et al., 2000). The *comX* gene encodes a precursor of competence pheromone, which is processed and secreted into the medium with a modification at a tryptophan residue, probably by the ComQ function (Lazazzera et al., 1999). ComP is a sensor protein kinase of the ComP-ComA two-component system; its N-terminal sensor domain interact with the ComX pheromone (Piazza et al., 1999). The interaction with the extracellular pheromone generate a signal, which allows the phosphorylation of the cognate ComA. Once phosphorylated, ComA activate the transcription of a set of genes that include *srfA* and *degQ* (Lazazzera et al., 1999). The *srf* operon encodes surfactin synthetases and the *comS* gene, encoding ComS, which liberates ComK. At this point, ComK can activate the transcription of its own gene and the late competence genes (Morikawa, 2006). Surfactin is a QS molecule too; it induces the phosphorylation of Spo0A, which, in turn, induces the expression of SinI, the antagonist of SinR, causing the derepression of genes involved in biofilm matrix synthesis (Lopez et al., 2009). The *degQ* gene encodes DegQ, a small protein that activate by phosphorylation DegU, one of the three main master regulators of *B. subtilis*. Once phosphorylated, DegU leads to expression of the machinery responsible for the production and secretion of proteases in a sub-population of the biofilm, called miners (Verhamme et al., 2007). Miners degrade extracellular proteins into small peptides that serve as food for the entire community (Veening et al., 2008). An important class of

signal molecules affecting biofilm formation is represented by modified nucleotides. Cyclic nucleotides such as cyclic dimeric guanosine 3',5'-monophosphate (**c-di-GMP**), cyclic dimeric adenosine 3',5'- monophosphate (c-di-AMP), cyclic guanosine 3',5'-monophosphate (cGMP), cyclic adenosine 3',5'-monophosphate (cAMP) as well as linear nucleotides such as guanosine 3',5'-bispyrophosphate (ppGpp) and guanosine 3'-diphosphate, 5'-triphosphate (pppGpp) emerged as important second messengers involved in the regulation of virulence factor and biofilm formation (reviewed in Kalia et al., 2012). In particular, a rise in c-di-GMP levels results in an increase in expression of various factors necessary for the establishment and maintenance of biofilm communities, whereas decrease in the production of the cyclic dinucleotide or its cleavage usually leads to enhanced expression of virulence and motility factors. c-di-GMP levels are regulated by the opposing activities of diguanylate cyclases (DGCs), that synthesize the molecule, and phosphodiesterases (PDEs) that degrade it (Paul et al., 2010; Ryan et al., 2006). These enzymes are characterized respectively by the conserved GGDEF and EAL motifs respectively (Galperin et al., 2001). Specific domains within the N-terminal region of the DGC sense external environmental stimuli, including sensing of oxygen (Sawai et al., 2010), nitric oxide (Plate et al., 2012), redox potential (Qi et al., 2009) and light (Cao et al., 2010; Savakis et al., 2012; Tarutina et al., 2006). Studies in many bacteria have demonstrated the reciprocal relationship of DGC and PDE activities (Lee et al., 2007). In *B. pseudomallei*, the inactivation of *cdpA*, encoding a protein with PDE activity, resulted in increased intracellular levels of c-di-GMP, which promoted exopolysaccharide production, cell-to- cell aggregation and biofilm formation, and inhibited flagellum biosynthesis and swimming motility (Lee et al., 2010). In *B. cenocepacia*, c-di-GMP play the same role, in cooperation with QS systems (Fazli et al., 2014). A c-di-GMP signaling pathways was also identified in *B. subtilis*. The increase of c-di-GMP levels led to transient inhibition of swarm motility, but biofilm formation was unaffected (Gao et al., 2013).

3. Reactive Oxygen Species (ROS)

Reactive oxygen species (ROS) are chemically reactive molecules produced in aerobic conditions as by-products of several metabolic processes. Molecular oxygen (O_2) is small, nonpolar and it diffuses easily across biological membranes (Ligeza et al., 1998). Nevertheless, O_2 poorly reacts with cellular biomolecules. Its toxicity derives from the formation of ROS (Gerschman et al., 1954) which result from the addition of consecutive electrons to O_2, generating superoxide (O_2^-), hydrogen peroxide (H_2O_2) and the hydroxyl radical (•OH), and the formation of singlet oxygen ($^1O_2$) (Fig. 3). **O_2** is stable diradical, which can accept one electron at a time with low affinity, having two unpaired electrons in its π antibonding orbitals and a slightly negative reduction potential (– 0.16 V) (Bielski et al., 1985; Imlay., 2003). O_2 is harmless against biomolecules, but its unpaired electrons can easily interact with the unpaired electrons of transition metals and organic radicals, flavins and respiratory quinones. The other ROS (O_2^-, H_2O_2, and •OH) have higher reduction potential, thus they are stronger oxidants than O_2. **O_2^-** is a free radical.

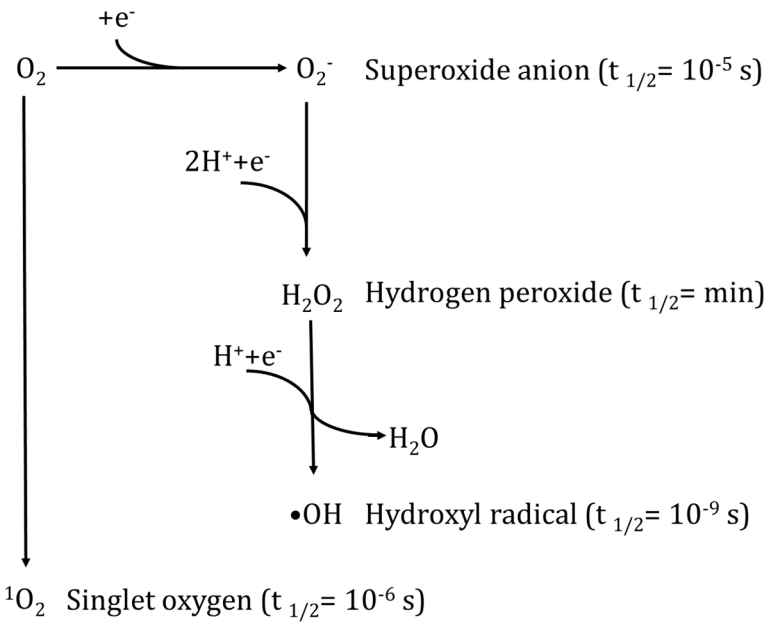

Figure 3. Generation of reactive oxygen species (ROS) and their half-life. Adapted from Imlay (2003).

It is not very reactive because it is negatively charged, so that it cannot oxidize electron-rich molecules and its lifetime is just a few seconds. O_2^- rapidly reacts with another molecule of O_2^- (self-dismutation reaction) to form H_2O_2 or it reacts with nitric oxide (radical–radical reaction) to form a very potent oxidant and reactive nitrogen species, peroxynitrite (NO_3^- with half-life of seconds) (Pacher et al., 2007). **H_2O_2** is a precursor of free radicals as UV radiation causes the cleavage of the oxygen–oxygen bond to form •OH. H_2O_2 is stable, it has a half-life of months, when protected against light and trace metal contamination because of the stability of its oxygen-oxygen bond. As the cell is not free from trace metal or UV radiations, antioxidant enzymes (catalase, glutathione peroxidase) rapidly destroy H_2O_2. **•OH** originates from the Fenton reaction between redox metal ions (Fe^{2+} or Fe^{3+} or Cu^+) and H_2O_2:

$H_2O_2 + Fe^{2+} \rightarrow OH^- + FeO^{2+} + H^+ \rightarrow Fe^{3+} + OH^- + \bullet OH$

•OH is the most reactive and less selective species, reacting with most biomolecules at the same time it diffuse in the cell. Its lifetime is extremely short (10^{-9} s) (Bokare et al., 2014). **$^1O_2$** is a photoexcited form of O_2, in which the π antibonding electrons are spin-paired. Excited molecules, readily produced upon UV–visible light absorption, can transfer their energy to O_2 generating $^1O_2$ (Ogilby, 2010). This happens often in photosynthetic systems with high risk for the biomolecules, as $^1O_2$ reacts rapidly with cysteine, histidine, methionine, tyrosine and tryptophan residues present in proteins, unsaturated lipids and some nucleic acids (Briviba et al, 1997). Typically, this species exhibits a half-life time in water of 3.5 μs (Ogilby, 2010). As microbial life first evolved in a world devoid of O_2 and rich in reduced iron, microorganisms evolved strategies to maintain a reducing environment and to prevent damage to essential macromolecules (Anbar, 2008). Bacteria have evolved sensitive and specific sensors to monitor different redox signals such as the presence or absence of O_2, cellular redox state or ROS. The sensing mechanisms can involve redox-active cofactors such as haem, flavins, pyridine nucleotides and iron–sulphur clusters, or redox-sensitive amino acid side chains such as cysteine thiols (Green et al 2004). The sensor signal is converted in the activation of pathways linked to the oxidative stress response to allow bacteria to face the changed redox environment. Enzymatic and non-enzymatic scavenger systems control the cellular concentration of ROS in order to maintain steady-state intracellular concentrations. When the balance between ROS and scavenger systems is disturbed, the accumulation of ROS inside the cell lead to a condition called **oxidative stress** (Groves

et al., 2010; Green et al., 2004; Cabiscol et al. 2000). In this condition, the ROS concentration is so high that they can damage proteins, DNA, and lipids, leading to an increased rate of mutagenesis and cell death. In humans, oxidative stress is involved in many diseases, such as atherosclerosis, Parkinson's disease, heart failure, myocardial infarction and Alzheimer's disease. On the other hand, ROS are essential for the immune system to attack and kill pathogens (Groves et al., 2010).

3.1 Sources of oxidative stress.

3.1.1 Endogenous sources.

Microorganisms routinely generate ROS when they grow in aerobic environments. The endogenous ROS production has been widely investigated in *E. coli*. To understand which mechanisms are involved in scavenging and ROS formation, the O_2^- and H_2O_2 formation rate was calculated measuring the H_2O_2 produced in mutants devoid of scavenging system. A rate of 10-15 μm/s have been observed for cells grown in air-saturated glucose medium (Seaver et al., 2004). The accidental autoxidation of flavoenzymes is the main responsible for O_2^- and H_2O_2 production (Seaver et al., 2004). *In vitro* analysis identified several flavoproteins releasing ROS (Grinblat et al., 1991; Messner et al., 2002; Kussmaul et al., 2006), but the same role in *in vivo* experiment was confirmed for a few of them (Korshunov et al., 2011). The adventitious electron transfer of one or both electron from O_2 to the flavoprotein generate O_2^- and/or H_2O_2. The rate of H_2O_2 production is proportional to the intracellular O_2 concentration, as higher the O_2 cellular concentration, most probable the collision frequency with a flavoenzyme and its oxidation (Seaver et al., 2004). The degree of flavin exposure, the flavin redox potential and the residence time of electrons on it condition the autoxidation rates of flavoproteins (Messner et al., 2002). Thus, it seems that the ROS level in a cell depends on the state of its flavoenzymes, the most autoxidizable enzymes. *In vitro* studies suggested NADH dehydrogenase II as the most autoxidizable component of the electron transport chain, but it turned out that is only a minor source of cellular H_2O_2 (Seaver et al., 2004). More recently, *in vivo* studies identified two fumarate-reducing flavoenzymes as generators of H_2O_2 in *E. coli*. One of these enzymes is **fumarate reductase**, an anaerobic respiratory enzyme that forms substantial O_2^- and H_2O_2 when anaerobic

bacteria enter aerobic habitats. Its detrimental activity is suppressed through its interaction with the respiratory chain, with cytochrome oxidase acting as an ultimate electron sink (Korshunov et al., 2011). This strategy seems to be widespread among all the bacteria to enable the organisms to survive transient oxygen exposure. Furthermore, cytochrome d oxidase activity may help to re-establish local anaerobiosis when oxygenated fluids invade self-contained microhabitats such as biofilms (Korshunov et al., 2011). Another flavoenzyme was identified as a significant H_2O_2 source *in vivo* in *E.coli*: **NadB** is a dehydrogenase, which desaturates aspartate, using fumarate as electron acceptor (Mortarino et al., 1996). In aerobic conditions, NadB quantitatively uses molecular oxygen, rather than fumarate, as its electron acceptor. Indeed, the aerobic metabolism consumes NADH, reverses the flux through the fumarate-generating branch of the anaerobic TCA cycle, fumarate levels drop and reduced NadB turn over by the less efficient transfer of electrons to oxygen (Korshunov et al., 2011). **Menaquinone** autoxidation also concur to the endogenous ROS production, accounting for another 5-10% (Korshunov et al., 2006). The sources of ROS identified so far, justify just a part of the H_2O_2 measuered in vivo. Evidences suggest that the remaining ROS arises from adventitious reactions.

3.1.1 Exogenous sources.

In both anthropic and natural systems, bacteria experience environmental stress factors known to be sources of a cascade of ROS and of oxidative injuries (Dwyer et al., 2007; Kohanski et al., 2007). Thus, many lethal stressors act through a common biochemical mechanism that is reminiscent of ROS involvement in eukaryotic apoptosis (Jung et al., 2001; Mates et al., 2000; Simizu et al., 1998). Different bacteria may experience different amounts of oxidative stress in the same environment, depending on the efficacy of its scavenging resources (Imlay, 2003). It is well established that the exposure of microorganisms to ionizing (γ) and non-ionizing **irradiation** (UV) leads to the intracellular formation of ROS from ionization of intracellular water (Sies, 1997). According to the induction of antioxidant defence in bacteria exposed to UV-B, oxidative stress could be the responsible for UV-B- induced damage to the biomolecules. (Matallana-Surget et al., 2009). High **temperatures** result in more oxidative stress with consequent DNA double-strand breaks and of damage to proteins at high temperature in *E. coli* (Murata et al., 2011) and in heat-induced cell death in *Saccharomyces cerevisiae*

(Davidson et al., 1996). It has been shown that, in *Lactococcus lactis* grown in aerobiosis, high temperatures correspond to riboflavin starvation due to reduced activity of flavoprotein disulfide reductase (glutathione and thioredoxin reductase), causing a less reduced cytoplasm and thus oxidative stress (Chen et al., 2013). Also cold temperatures cause oxidative stress: cells of the Antarctic bacterium *Pseudomonas fluorescens*, grown at 4°C, suffer an increasing amount of free radicals and the enhanced activity of two antioxidant enzymes (Chattopadhyay et al., 2011). Another source of oxidative stress, mainly for pathogenic bacteria, is the interaction with host **immune system**. In presence of pathogens, plants and animals immune system rapidly releases ROS as a first-line defence mechanism, generating the so-called "oxidative burst" (Apel et al., 2004). In addition, animals' macrophages recognize and import bacteria into phagosomes, compartments that mature into phagolysosomes, containing ROS and reactive nitrogen species (RNS) (Garin et al., 2001). The multi-subunit NADPH-dependent phagocytic oxidase is assembled on the phagolysosome membrane and pumps electrons into the compartment to reduce oxygen to superoxide anion (O_2^-). The inducible nitric oxide synthase uses arginine and oxygen as substrates to produce nitric oxide (Fang, 2004). Nevertheless, a number of the more successful human pathogens can survive this defense strategy, as in the case of *Salmonella* (Slauch, 2011) and *B. pseudomallei* (Chieng et al., 2012). ROS signalling in **plants** is well established (reviewed in Apel et al., 2004). ROS are used for stomata closing (Pei et al. 2000), programmed cell death (Gechev et al., 2005) and response to abiotic stress (Laloi et al. 2007; Miller et al. 2007). In the rhizosphere, ROS are important for roots development (Mori et al., 2004), for interactions between roots and microorganisms (Jamet et al., 2003), the regulation of symbiosis (Shaw et al., 2003; Rubio et al. 2004), and the establishment of mycorrhiza (Fester et al., 2005). During the early stages of plant-microorganism interactions, plants use ROS subject microorganisms in the rhizosphere to high oxidative stress, both to prevent pathogens infection and to establish advantageous symbiotic interactions. In return, microorganisms produce ROS scavenging enzymes in order to successfully infect the plant or down-regulate the plant ROS producing systems (Nanda et al., 2010). In a natural habitat, microorganisms also face the release of ROS-producing compounds produced by other neighbour microorganisms. This is the case of natural **phenazines**, a large group of nitrogen-containing heterocyclic compounds with different chemical and physical properties depending on the functional groups present (Mavrodi et al. 2010).

Phenazines are mainly studied in pseudomonads because of their role in cystic fibrosis (Lau et al., 2004) and in plant disease management (Saharan et al., 2011), but they are produced by both Gram-negative and Gram-positive species, including *Burkholderia* spp. (Mavrodi et al. 2010). The majority of phenazine generate ROS accumulation in other cells, assisting the producing bacterium in competitive survival, although this is probably not their primary function (Pierson et al., 2010). For example, pyocyanin, the most studied pseudomonads phenazine, serves as an alternate electron acceptor that reoxidizes NADH to NAD+ to balance intracellular redox in the absence of other electron acceptors (Price-Whelan et al. 2007). Furthermore, phenazines in pseudomonads have been proposed as signalling molecules, involved in QS regulated pathways and various stages of biofilm formation (Pierson et al., 2010). In addition to natural sources of ROS, soil collect environmental **pollutants**, such as xenobiotics, metals and chemicals, able to cause oxidative stress in microorganisms (Kang et al., 2007; Pérez-Pantoja et al., 2013). This effect can greatly impair the degradation capacity of microorganisms used for the bioremediation of polluted sites (Kang et al., 2007). **Nanoparticles** (NPs) are among the emerging soil pollutants causing oxidative stress in microorganisms (Fabrega et al. 2009). In particular, silver NPs (Ag-NPs) are widely used for medical and industrial applications (Levan et al., 2012; Duncan, 2011, Banejeree et al., 2011), as they are effective against a broad spectrum of bacterial and fungal species (Sotiriou et al., 2011), including antibiotic-resistant strains (Schacht et al., 2013). The growing diffusion of Ag-NPs in commercially available products used daily (Benn et al., 2008) and the application of treated sewage from wastewater treatment plants as soil fertilizer (Schlich et al. 2013) leads to an NP dispersal in the soil difficult to track (Mueller et al., 2009), by causing oxidative stress. Another exogenous source of ROS are the **disinfectants and cleaning agents**. They contain peroxides, chloramines or hypochlorites (Van Houdt et al., 2010) and are increasingly used in a number of medical, food and industrial applications due to their broad spectrum activities, the lack of environmental toxicity following their complete degradation and their lower cost (Linley et al. 2012). Their usage raises concern about the raising of resistance mechanisms among pathogenic bacteria (Van Houdt et al., 2010) and the exposure of beneficial soil microbial community to oxidative stress (Ortiz de Orué Lucana et al., 2012). A wide and still open question is whether **antibiotics** generate ROS to kill

bacteria. Two excellent and recent reviews resume data published so far and deal with this issue (Imlay, 2015; Dwyer et al., 2015).

3.4 Damage caused by oxidative stress

Proteins are the first target of oxidative stress. ROS cause protein modifications, such as oxidation of sulfur-containing side chains, chlorination of side-chain amines, oxidation of histidines and tryptophans and dityrosine formation (Cai et al., 2013), thus causing fragmentation, destabilization, aggregation and degradation of proteins (Dahl et al., 2015). **O_2^-** stress results in growth defects in *E. coli*. Specifically, O_2^- destroy the catalytic [4Fe-4S] cluster of the dihydroxyacid dehydratase, the penultimate step in the pathway for the formation of branched-chain (Leu, Ile, Val) aminoacids, thus cells lose the ability to grow without supplements of branched-chain and sulphur-containing amino acids (Kuo et al., 1987). In addition, other members of this enzyme family are equally sensitive to O_2^-: aconitase B and fumarases A and B (Gardner et al., 1991; Liochev et al., 1993) are inactivated by O_2^-. Thus, the tricarboxylic acid cycle lose function and the non-fermentable substrates (e.g., succinate and acetate) can no longer support growth (Imlay, 2003). In addition to the branched-chain auxotrophy, O_2^- stress causes auxotrophies for aromatic amino acids (Tyr, Trp, Phe), as it oxidize the 1,2-dihydroxyethyl thiamine pyrophosphate intermediate of transketolase, inactivating this enzyme and inhibiting the production of erythrose-4-phosphate, which is essential for the first step of the aromatic biosynthetic pathway (Benov et al., 1999). The basis of the sulfur auxotrophy (Cys, Met) seem to lie in the damages caused by O_2^- to the cell envelope. A damaged membrane allows leakage of sulphite, which limits the synthesis of sulfide by the action of sulfite reductase, and that in turn limits the synthesis of cysteine via the action of the O-acetylserine sulfhydrylases. Lacking the cysteine, cell also run out of methionine (Benov et al., 1996). O_2^- also causes a high rate of DNA mutations (Farr et al., 1986), which is proportional to the concentration of free iron in the cell. Indeed, O_2^- causes an increase in the internal pool of free iron, released from the [4Fe-4S] clusters of damaged dehydratases (Keyer et al., 1996). To limit DNA damage, the intracellular iron pool can vary freely in response to environmental availability only during anaerobiosis in *E. coli*. On the contrary, in aerobiosis, iron levels and the sysnthesis of O_2^- sensitive enzymes (aconitase, fumarase, and 6-phosphogluconate dehydratase) are tighly

regulated (Keyer et al., 1996). **H_2O_2** oxidizes protein cysteinyl residues, creates sulfenic acid adducts which form disulfide cross-links with other cysteines, with consequent protein inactivation (Kim et al., 2000). In addition, H_2O_2 can directly oxidize the same dehydratase iron-sulfur clusters that O_2^-, directly oxidizing the catalytic iron atom of dehydratase clusters, precipitating iron loss and enzyme inactivation. However, the enzyme inactivation is just temporal, as defence mechanisms are activated to limit the damage to a repairable $[3Fe\text{-}4S]^+$, without the production of the more dangerous •OH. This damage mechanism is typical of dehydratases, while most iron-sulphur proteins protect their clusters from oxidants (Imlay, 2013). H_2O_2 is particularly dangerous because of the production of **•OH** by the Fenton reaction in presence of free iron. •OH mediate the oxidation catalysed by metals that create protein carbonyls *in vitro*. The amino acid radicals generated by •OH can be propagated to secondary sites, causing further modifications in proteins sites far from the first site of attack. This propagation mechanism endangers the protein active site, even if shielded by other amino acids in surface (Hawkins et al., 2001). DNA is seriously damaged by HO•. HO• can extract electrons from either sugar or base moieties, as well as add to the unsaturated bases. The resultant DNA radicals are resolved in a variety of ways, thereby producing a broad spectrum of lesions. The low reduction potential of guanine facilitates electron hop to electron holes in nearby oxidized base radicals, thereby leaving guanine with an unpaired electron (Giese, 2002). This produces 8-hydroxyguanine, which is highly mutagenic because it can to base pair with adenine, eluding the mispair detection system of DNA polymerases (Candeias et al., 1993). By contrast, thymine blocks polymerase progression and is thus lethal (Demple et al., 1986). ROS also cause the lipid peroxidation of polyunsaturated fatty acids in membranes with the decrease of membrane fluidity, the alteration of membrane properties and the disruption of membrane-bound proteins (Cabiscol et al., 2000). The propagation of this effect causes the degradation of polyunsaturated fatty acids and the production of long-living and reactive products, such as aldehydes, able to damage proteins (Humpries et al., 1998; Esterbauer et al., 1991). Thus, ROS cause direct oxidative modification on bacterial unsaturated lipids, and indirect modifications through reactive products of lipid peroxidation (Stark, 2005). Recently lipid peroxidation was associated to oxidative stress caused by nanoparticles and nanowires (Premanathan et al., 2011; Krishnamoorthy et al., 2012) and porphyrinic photosensitizers (Lopes et al., 2014). A

further target for ROS are the polyunsaturated fatty acids within the thylakoid membranes of photosynthetic bacteria (Imlay, 2003).

3.5 Pathways activated in response to oxidative stress

3.5.1 Scavenging systems

To avoid oxidative stress damages, bacteria produce both enzymatic and non-enzymatic scavenging systems, regulated by a dense network of pathways, as described in section 3.5.2. A first strategy to defend cell components from oxidative stress is the maintenance of an intracellular reducing environment. For this purpose, some non-enzymatic antioxidants such as NADPH/NADH pools, β-carotene, ascorbic acid, α-tocopherol, and glutathione (GSH) are constantly present in the cell (Cabiscol et al., 2000). **GSH** is the major low-molecular-weight thiol cofactor in eukaryotes and most Gram-negative bacteria (Masip et al., 2006). In the cell, it is present at high concentrations as it plays a critical role in toxicity and oxidative stress management, maintaining a strong reducing environment. Glutathione reductase maintains GSH in its reduced form using NADPH as a source of reducing power (Sharma et al., 2013). Contrary to eukaryotes, in bacteria only a few proteins undergo protein glutathionylation, i.e. the reversible formation of GS-S-protein disulfides (Masip et al., 2006). This is a way to regulate protein function post-translationally and to protect exposed cysteine residues (Dalle Donne et al., 2007). In addition, GSH takes part in the glutaredoxin pathway, which reduces ribonucleotides to deoxyribonucleotides to provide the precursors needed for DNA synthesis (Leeper et al., 2011). All GSH functions are detailed in Masip et al. (2006). Other low molecular thiols are present in microorganisms devoid of GSH: anaerobic sulfur bacteria use glutathione amide, aerobic phototrophic halobacteria use γ-glutamylcysteine (Masip et al., 2006), actinobacteria use mycothiol (described in Jothivasan et al., 2008) and Gram-positive bacteria use coenzyme A and bacillithiol (Newton et al., 2009). **Coenzyme A** is a suitable protective thiol for an aerobic organism, but it cannot function as a protected reservoir of cysteine (Newton et al., 2009). On the contrary, **bacillithiol** functions as a thiol redox buffer in the detoxification of ROS and toxins and it is used for S-thiolation to protects critical cysteine residues against oxidation, exactly as it happens for GSH in Gram-negative bacteria (Chi et al., 2013). In the same way, protein S-bacillithiolation is

emerging as an important thiol redox mechanism for the regulation of protein function (e.g., the redox-sensitive peroxiredoxin transcription regulator OhrR and the methionine synthase MetE) during oxidative stress (Sharma et al., 2013; Gaballa et al., 2014). In bacteria devoid of GSH (e.g., *B. subtilis*), the **thioredoxin** system is particularly important (Lu et al., 2013). It includes thioredoxin reductase and thioredoxin, and it provides electrons to many enzymes, being involved in DNA synthesis and in the defence against oxidative stress (Boronat et al., 2014). In bacteria with GSH, the thioredoxin system is not essential to scavenge oxidative stress, but is critical to control the ratio between disulphide and dithiols of cellular proteins (Lu et al., 2013). H_2O_2 is removed by **catalases**, which promote H_2O_2 dismutation ($2\ H_2O_2 \rightarrow 2H_2O+O_2$) and contain dimanganese (MnCats) or heme groups (KatEs), and **peroxidases**, which use H_2O_2 to oxidize a number of compounds according to the reaction: $H_2O_2 + 2A + 2H^+ \rightarrow 2\ H_2O + 2A^{\bullet+}$, where A is an organic or metal ion electron donors (A). In *E. coli*, two catalases remove H_2O_2, encoded by *katG* that is induced by OxyR, and *katE*, induced by *rpoS* gene, thus activated in stationary-phase or upon various types of starvation (Gonzalez-Flecha et al., 1997). KatG is metal catalase-peroxidase, able to catalyse both reactions albeit the catalase reaction is more efficient than the peroxidase reaction (Ivancich et al., 2013). KatG from *Mycobacterium tuberculosis* plays an essential role in the survival to the phagocyte oxidative burst (Zhang et al., 1992) and is responsible for the activation of the antitubercular drug isoniazid (Bertrand et al., 2004). In *A. vinelandii*, catalase activity is essential since *A. vinelandii* maintains a very high respiratory rate to protect its nitrogenases from oxygen (Robson et al., 1980; Kelly et al., 1990) with consequent formation of large quantities of ROS. As in *E. coli*, the efficient scavenging system relies on two catalases: the first one is a KatG homologue, and the second catalase is a stationary-phase inducible, thermostable and protease resistant enzyme (Sandercock et al., 2008). A further defence against oxidative stress in *A. vinelandii* is the rhodanese-like protein RhdA. Its important role has been demonstrated in both planktonic cells (Remelli et al., 2010) and biofilm (Villa et al., 2012b; part II, chapter 1). **Superoxide dismutases** (SOD) convert the dangerous ROS O_2^- to H_2O_2 and O_2. In the cytoplasm, two main SOD scavenge O_2^-: an iron-containing enzyme, encoded by *sodB* and whose expression is modulated by intracellular iron levels (Niederhoffer et al., 1990), and a manganese- containing SOD, the predominant enzyme during aerobic growth, encoded by *sodA* and whose expression is transcriptionally regulated by six control systems

(Compan et al., 1993). *E. coli* strains that lack both SODs grow normally in anaerobic cultures, but they have evident growth defects in aerobic media (Carlioz et al., 1986). In many Gram-negative bacteria, copper and zinc SODs are present in the periplasm (Kroll et al., 1995). Since O_2^- cannot cross membranes, periplasmic SOD defend cells from O_2^- produced in the periplasm, likely from the bc1 complex (Han et al., 2001), or exogenously (Hassan et al., 1979). For this reason, periplasmic SOD play a major role in protecting bacteria from toxic free radicals produced by the host immune system; thus, they are often suggested as virulence and pathogenicity factors (Sanjay et al., 2011). In *B. pseudomallei*, *sodC* encodes for a periplasmic SOD, which plays a key role in its virulence and survival in the host cells (Vanaporn et al., 2011). A**lkylhydroperoxide reductases** (Ahp) are members of the peroxiredoxin family of enzymes, which have activity against H_2O_2, organic peroxides, and peroxynitrite (Poole, 2005). AhpC and AhpF were initially identified in *Salmonella enterica* serovar typhimurium (*S.* typhimurium) (Jacobson et al., 1989), but they are widespread in all organisms (Mishra et al., 2012). AhpC contains two redox-active cysteines that can be oxidised to a sulfenic acid by the peroxide substrate. Usually, AhpF, a flavoprotein with NADH:disulfide oxidoreductase activity, restores the disulfide in AhpC to its reduced form (Jacobson et al., 1989; Poole, 2005). It has been demonstrated that AhpC is the main scavenger of endogenous H_2O_2, as its efficiency is higher than catalase for low H_2O_2 concentrations (Scherman et al., 1996; Seaver et al., 2001). Indeed, if H_2O_2 concentration exceed 20 μM, AhpC is saturated, whereas catalase is not, thus a division in the role of the two enzymes can be hypothesized (Mishra et al., 2012). In addition to the first line of defense, the regulation of **iron solubilization** and metabolism through specific membrane-bound receptors that regulate iron entrance, and through the ferroxidase activity of bacterioferritin and ferritin (Cabiscol et al., 2000). A first evidence of this link was the induction of Dps, a ferritin-like protein that has been demonstrated to be a scavenger of free iron, in response to H_2O_2 (Imlay, 1995). In addition, **DNA and protein repair systems** concur to limit cellular damages. DNA repair enzymes include endonuclease IV, induced by oxidative stress, and exonuclease III, induced in the stationary phase and in starving cells (Demple et al., 1994). Bacteria can repair directly some covalent modifications to the primary structure of proteins, such as the oxidized disulfide bonds with thioredoxin reductase, with glutaredoxin or protein disulfide isomerase (Cabiscol et al., 2000).

3.5.2 Regulators of oxidative stress response

Bacteria sense and adapt to oxidative stress by activating two main systems, which can be activated through the oxidation of sensor molecules by H_2O_2 or O_2^-. The genes responsible for such responses are usually grouped in regulons: in *E. coli*, for example, OxyR responds to the stress induced by H_2O_2, while SoxRS responds to the O_2^--induced one. **OxyR** is a protein of the LysR family, which senses H_2O_2 and activates the transcription of several genes involved in the antioxidative defence, e.g. peroxide scavengers, thiol redox buffers, enzymes to repair iron-sulfur centres and to repress iron uptake genes (Storz et al., 1999; Zheng et al., 2001). OxyR is a tetramer that binds to DNA both in the reduced/inactive form and in the oxidized/active form. Low micromolar concentrations of H_2O_2 (e.g. 5 μM) fully activate OxyR by the formation of an intramolecular disulfide bond (S-S) between two cysteine residues (Cys 199 and Cys 208) (Zheng et al., 1998). The S-S formation causes a major structural change in OxyR tetramer. In this form, OxyR is able to recruit RNA polymerase to promoters of oxidative stress genes through protein-protein interaction with the carboxy-terminal domain of the α-subunit of RNA polymerase (Storz et al., 1999; Lushchak, 2001; Choi et al., 2001). Oxidized OxyR binds all OxyR-regulated promoters, among which genes for catalase KatG, the alkylhydoperoxide reductase AhpC and the GSH system (glutaredoxin and glutathione reductase) (Zheng et al. 2001). Alternative models have been proposed, where oxidant compound agents active OxyR through the S-nitrosylation (Hausladen et al., 1996; Seth et al., 2012) or the S-glutathionylation (Kim et al., 2002). The oxidation is only transient, as OxyR is reduced back to the inactive conformation by disulfide reduction by glutaredoxin 1, using GSH as the electron donor (Zheng et al., 1998). The reduced form of the OxyR protein can bind the *oxyR* promoter, but not the *katG* and *ahpC* promoters, suggesting that the reduced form of OxyR maintain a different function from the antioxidative one (Lushchak, 2011). OxyR has been retrieved also in *S.* Typhimurium (Christman et al., 1985), *P. aeruginosa* (Vinckx et al., 2008) and *Neisseria meningitides* (Ieva et al., 2008) and *Streptomyces coelicolor* A3 (Baltz, 2006). The **SoxRS** regulon is a two-component system, part of the inducible protection against oxidant compounds (Wu et al., 2012), nitric oxide radical (Nunoshiba et al., 1993) and hypochlorous acid (Dukan et al., 1996). SoxR is a homodimer containing two [2Fe–2S] clusters responsible

for the regulation of its activity as a transcriptional factor (Hidalgo et al., 1996; Hidalgo et al., 1997). SoxR is the specific switch regulated by redox signals that enhance the expression of *soxS* gene, resulting in increased levels of the small regulatory protein SoxS (Hidalgo et al., 1997). SoxS regulates its transcription and the transcription of nine superoxide-activated proteins, included manganese-SOD, endonuclease IV and glucose-6-phosphate dehydrogenase, and down-regulates the outer membrane protein OmpF (Storz et al., 1999). Evidence indicates OxyR/SoxRS interplay in the response to oxidative stress (Lushchak, 2011; Semchyshyn, 2009), in addition, both proteins are involved in more complex pathways with RpoS, the alternative σ factor of RNA polymerase essential during stationary phase and in response to various stresses, including oxidative stress (Hengge-Aronis, 2002). Although with some differences, the regulatory system of *B. pseudomallei* also relies on both OxyR and RpoS for transcription of oxidative stress response genes, included *katG* and *dpsA* (Chutoam et al., 2013; Jangiam et al., 2010). In *Streptomyces reticuli*, another regulator, **FurS**, represses the transcription of the catalase-peroxidase *cpeB* gene (Ortiz de Orué Lucana et al., 2000). Under oxidative stress, FurS undergoes a conformational change because of the formation of an internal S-S bridge. In this form, FurS loses the ability to block the transcription of *furS-cpeB*, leading to a high production of CpeB under oxidative stress conditions (Ortiz de Orué Lucana et al., 2003). FurS contains motifs common to a number of redox-active proteins, including thioredoxin, glutaredoxins and thiol-disulfide oxidoreductases (Groves et al., 2010). In *B. pseudomallei* the gene *fur*, homolog of the ferric uptake regulator gene of *E. coli*, positively regulates the activity of FeSOD and peroxidase (Loprasert et al., 2000). In *B. subtilis*, **PerR** is the homologus of FurS and it controls the induction of specific stress proteins in response to H_2O_2 (Chen et al., 1995; Bsat et al., 1998). The metal cofactor of PerR, necessary for DNA binding, can be oxidized by H_2O_2, impairing its binding ability (Herbig et al., 2001). The removal of PerR increases the synthesis of the catalase KatA, the alkyl hydroperoxide reductase AhpC/AhpF, the DNA- protecting protein MrgA, the haem biosynthesis proteins (HemA, HemX,HemC, HemD, HemB and HemL), the iron-uptake regulator Fur, the zinc-uptake system ZosA and PerR itself (Bsat et al., 1996; Helmann et al., 2003). **OhrR** repressor, instead, is involved in the resistance against organic peroxides (Fuangthong et al., 2001) and no specific regulator for O_2^- has been found in *B. subtilis*. O_2^- response partially overlaps to the H_2O_2 one, although an additional induction of genes for sulfur

assimilation and the biosynthesis of cysteine and methionine has been observed (Mostertz et al., 2004).

3.5.3 Hormetic behaviour of ROS

As many toxins and compounds with a hormetic behaviour, ROS can have either a detrimental or a beneficial effect depending on the concentration (Lewis, 2008; Pan., 2011). According to the hormetic concept, represented as an inverted U-shaped dose response (Fig. 4), low doses of toxin correspond to a stimulation, whereas high doses of toxin correspond to an inhibition (Southam et al., 1943; Calabrese et al., 2011). This is possible as exposure to low levels of toxin or stress can induce adaptive responses protecting the organism (Cap et al., 2012). In bacteria, ROS typically have a hormetic behaviour, with important consequences in the sanitary and industrial fields for the resistance to antimicrobials (Marathe et al., 2013), as well as for the possible environmental repercussions on the water and soil microflora exposed to low (sub-lethal) concentrations of oxidizing agents (Villa et al., 2012b). Despite the fact that biocides are generally used at high concentrations to exert their killing action, downstream of the treated area there is likely to be a continuum of biocide concentration ranging from the treatment concentration to nil (Gilbert et al., 2003).

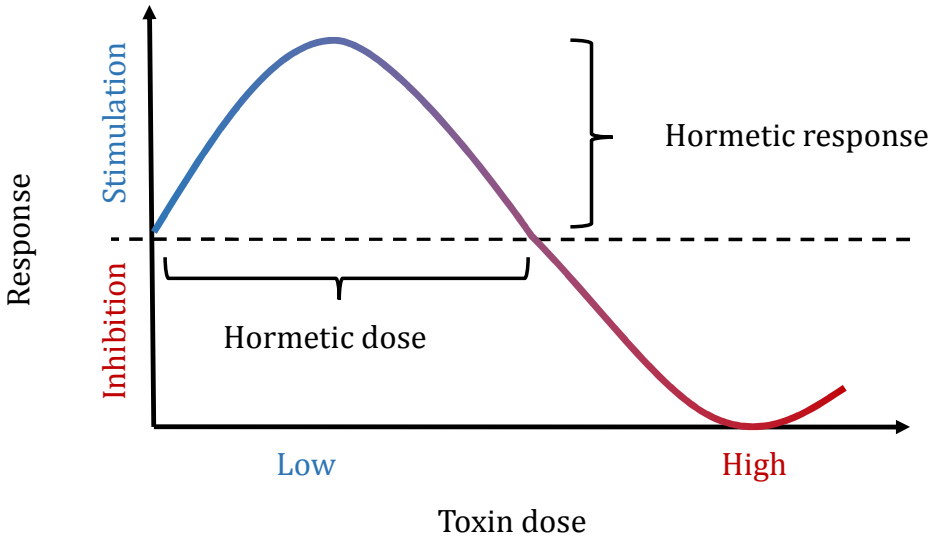

Figure 4. Dose-response curve of a toxin with a hormetic behaviour. At high concentration the response is inhibitory, while at low concentration the response is stimulatory.

Thus, there will be sub-inhibitory levels of biocide along this concentration gradient in all domestic, health care, industrial systems (Mc Cay et al. 2009), as well as in soil and water compartments, the major sink for toxic compounds. Here, the hormetic response of bacteria can trigger the activation of effective defence mechanisms or the activation of programmed cell death. Indeed, some stress factors can act in different ways, activating opposite pathways, according to the level of oxidative stress. **Moderate levels** of stress trigger the activation of protective mechanisms through a complex pathway involving various regulators (Zhao et al., 2014). In *E. coli*, the very first lesions are transmitted to the ROS-generating system by MazE/MazF, a toxin /antitoxin system: MazF cleaves many cellular RNAs (Gerdes et al., 2005), which thus are translated into truncated proteins, in turn activating the Cpx envelope protein stress system (Kohanski et al., 2008; Dorsey-Oresto et al., 2013). Cpx allows either the refolding or the degradation of misfolded proteins in the periplasm (Raivio et al., 2001) and triggers the expression of YihE (Pogliano et al., 1997). YihE keeps MazF at low levels, thus reducing the degradation of *katG* mRNA by MazF and inhibiting the MazF-mediated •OH accumulation. Low levels of stress lead to the activation of protective pathways (Fig. 5, blue arrows). On the other hand, stress could be so high and persistent to exceed a **point of no return** (Amitai et al., 2004). The accumulation of misfolded proteins MazF action forces Cpx to interact with the Arc two-component system. The Arc system perturbs electron transfer complexes, such as cytochrome bd oxidase (Green et al., 2004), increasing ROS levels up to a condition of lethal oxidative stress (Fig. 5, red arrows).

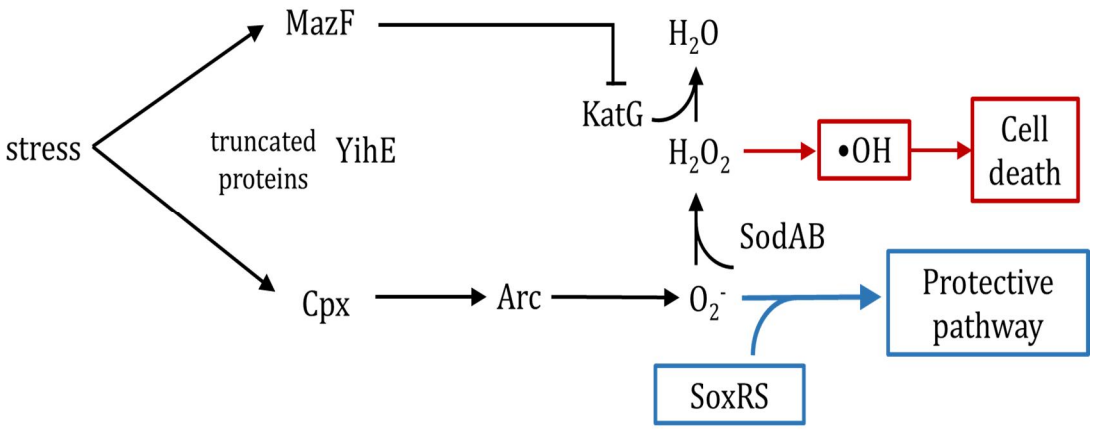

Figure 5. Different levels of stress trigger opposite responses, the MazE/MazF system. Adapted from Dorsey-Oresto et al. (2013).

Thus, in the case of extreme stress, the same proteins used to trigger ROS scavenging systems, contribute to a cascade of ROS and activate a programmed cell death pathways, essential to reduce the risk of hypermutation and loss of genetic integrity (Zhao et al., 2014). In *B. subtilis*, NdoA plays the same role as the *E. coli* MazE/MazF (Wu et al., 2011).

4. Biofilm and oxidative stress

A tight connection between biofilm and oxidative stress is evident, as biofilm is an effective defence strategy from various stresses, included oxidative stress (Landini, 2009). Though the mechanisms connecting ROS scavenging and biofilm still need to be clarified (Arce Miranda et al., 2011), data suggest that three main topic are central: the existence of common regulators, the production of polysaccharides and the biofilm heterogeneity.

4. 1 Common regulators and pathways

A first evidence of the tight connection between oxidative stress and biofilm formation is the involvement, in both processes, of the general stress response regulator **RpoS**. This protein up-regulates cellular stress-related genes in response to slow growth, both in stationary phase and stress conditions (Hengge-Aronis, 1999). In *E. coli*, RpoS is activated also in response to oxidative stress, collaborating in scavenging ROS with OxyR and SoxRS and inducing the transcription of genes involved in protection from oxidative damage (i.e. *dspA*, *katE* and *sodC*) (Patten et al., 2004; Schellhorn et al., 1992). In addition, RpoS has an essential role during the biofilm growth, as it controls the expression of almost 50% of genes specifically induced by growth as a biofilm (Collet et al., 2008). Recent studies highlight a more complex picture where RpoS triggers the production of extracellular structures and biofilm formation only under conditions of limited nutrient availability (Sheldon et al. 2012; Corona-Izquierdo et al., 2002). **OxyR** plays the opposite role, as *oxyR* mutants exhibit increased autoaggregation and ability to form biofilms in minimal

medium, both in *E. coli, B. pseudomallei* (Loprasert et al., 2002) and *P. chlororaphis* (Xie et al., 2013). In *E.coli* the process is mediated by the de-repression of *agn43*, which encodes the autotransporter protein Ag43 and stimulates bacterial biofilm formation at the microcolony stage (Danese et al., 2000). In *P. aeruginosa*, OxyR probably promotes the dispersion of biofilm bacteria under oxidative stress, as the oxidized regulator can bind the promoter region of the bacteriophage Pf4 operon and *bdlA*, a biofilm dispersion locus (Wei et al., 2012). In addition, *P. aeruginosa* OxyR is also involved in the expression of the QS transcriptional regulators *rsaL* and *mvfR* (Wei et al., 2012). Indeed, **QS systems** also connect biofilm formation and oxidative stress response. In *P. aeruginosa*, QS-deficient mutants (*lasI*, *rhlI* and *lasI rhlI*) are more sensitive to oxidative stress because of the lower expression of *katA* and *sodA* (Hassett et al., 1999). As QS enhance the oxidative stress response, triggering the production of scavenging enzymes, cells with an active QS system are more protected from oxidative damage and will be selected by the oxidative stress pressure (García-Contreras et al., 2014). In *B. pseudomallei*, **DpsA** has this double role (Lumjiaktase et al., 2006). DpsA is a protein that both bind DNA and sequester iron (Martinez et al., 1997) to protect DNA from damage by both acid and oxidative stress (Loprasert et al., 2004). At the same time, *bpsRI* mutants, unable to produce the quorum sensing molecules N-octanoylhomoserine lactone (C8-HSL) and N-(3-oxooctanoyl) homoserine lactone (3-oxo- C8-HSL), show a reduced *dpsA* expression, thus a higher sensitivity to organic hydroperoxides (Lumjiaktase et al., 2006). Lumjiaktase et al. (2006) also hypothesized that the control of the oxidative stress response through QS could be useful in high-density cultures, e.g. biofilm or stationary phase cultures, to protect DNA from oxidative damage. Another pathway regulated by QS is the production of phenazine, which generate ROS in other organisms and tissues, work as electron shuttle and are essential for long term survival under anaerobic conditions, e.g. in the inner part of biofilms (Drago, 2009). Phenazines are themselves signals capable of altering patterns of gene expression (Pierson et al., 2010; Dietrich et al. 2008), as it has been observed that *P. chloraphis* mutant strains defective of phenazine cannot form biofilm (Maddula et al., 2006). Moreover, *P. chlororaphis* produces different ratios of various phenazine derivatives, according to the needs of the population, as each derivative has particular characteristics. For example, it has been supposed that 2-hydroxy-phenazine-1-carboxylic acid (2OHPCA) may facilitate cellular adhesion, whereas phenazine-1-carboxylic acid (PCA) may allow biofilm growth, as an electron shuttle within the

microaerophilic community (Pierson et al., 2010). The pseudomonas quinolone signal (**PQS**) is a very active QS signal molecule of *P. aeruginosa* (Pesci et al., 1999), which, in iron-rich media, induces many genes associated with oxidative stress (Bredenbruch et al., 2006). Interestingly, PQS has both beneficial and deleterious effects. On the one hand, PQS acts as a pro- oxidant that sensitizes bacteria towards oxidative stresses; on the other hand, it efficiently induces a protective anti-oxidative stress response, reducing the intracellular levels of ROS. This could be a strategy to better respond to environmental stress (Häussler et al., 2008). Also PQS promotes the autolysis at high cell population densities under stressful conditions (Allesen-Holm et al., 2006), balancing viability and cell death to better utilize available resources (e.g., eDNA for matrix) (Williams et al., 2009).

4.2 Polysaccharides production

EPS production is very expensive in terms of metabolic energy (Landini, 2009). Nevertheless, the presence of a matrix is so advantageous for bacteria to be the trait that marks bench and environmental biofilms. EPS production pathway is inevitably connected to the environmental stress sensors, to be activated with a perfect timing and according to the external conditions. Among EPS components, polysaccharides seem to be often involved in the oxidative stress response. Indeed, chitosan and alginate are able to scavenge the hydroxyl radicals (•OH), inhibiting the lipid and protein peroxidation (Tomida et al., 2010). *P. aeruginosa* produces **alginate** in response to H_2O_2 (Mathee et al., 1999), produced by macrophages and neutrophils for pathogen killing and also released during the hypersensitive response plant defence system (Hay et al., 2014). The network regulating its production (also studied in *A.vinelandii*, part I, chapter 2.3.1) is controlled through the cross-talk between different regulators, but the mechanisms behind the specific environmental cues that induce alginate production remain unclear (Hay et al., 2014). Another relevant example is the production of **colanic acid** of *E. coli* biofilm, promoted by the GGDEF protein YddV, under the regulation of *rpoS*. YddV induce genes for this polysaccharide synthesis and membrane-associated genes, thus promoting cell aggregation and EPS production via its diguanylate cyclase activity (Méndez-Ortiz et al., 2006), but also genes in response to oxidative and nutritional stresses (Landini, 2009). Another aspect to consider is that cells subjected to exogenous

oxidative stress try to decrease their metabolism to limit ROS production. This is the case of *B. pseudomallei* succinyl-coA:3-ketoacid-coenzyme A transferase (SCOT) enzyme, which is down-regulated upon oxidative stress to avoid ROS production and, instead, leads to the accumulation of poly-hydroxybutyrate (PHB) inside cells as storage molecule (Chutoam et al., 2013).

4.3 Biofilm heterogeneity

Biofilm represents a very heterogeneous environment both spatially and temporally, enclosing many microenvironments with different characteristics, in a continuous changing flux of chemical gradients, influenced by the metabolism of resident bacteria, by the transport limitation (Teal et al., 2006) and by the aging of the biofilm (Saint-Ruf et al., 2014). According to the individualist model (part I, chapter 2.1), every single cell forming a biofilm responds in an individual and unique way to environmental changes (Monds et al., 2009; part I, chapter 2.1). Thus, in every microenvironment, the local conditions trigger a dishomogeneous response in bacteria and select for more favorable phenotypes variants. Thus, phenotypes variants would arise from both stochastic gene expression and genetic variation (mutation and genetic rearrangements) (Stewart et al., 2008). Oxidative stress is one of the main sources of heterogeneity in many bacterial species (Saint-Ruf et al., 2014). In *E. coli*, preincubation of cells with paraquat, a redox cycling agent (i.e. a compound able to produce ROS changing its oxidative state), induces SoxRS, which in turn determines the occurrence of several phenotypic variants able to survive to fluoroquinolone antibiotics (Wu et al., 2012). Exposure of *Staphylococcus aureus* to sub-lethal concentrations of hydrogen peroxide leads to the adaptations to oxidative stress of a sub-population of small-colony variants with enhanced catalase production via a mutagenic DNA repair pathway that included DNA double-strand break (DSBs) repair system (Painter et al., 2015). In *P. aeruginosa* biofilm, oxidative stress triggers the activation of DNA repair system, included the mutagenic double strand breaks (DSBs), resulting in higher phenotypic diversity (Boles et al., 2008). Thus, the presence of subpopulations within a bacterial community, distinctive at phenotypic level, appears to be a quite common occurrence and might even be considered as an evolutionary strategy to withstand environmental stresses.

5. Aim of the project and main results

The role of oxidative stress in bacterial biofilms is a topic of outstanding importance as it has consequences in sanitary, industrial and environmental fields. The comprehension of mechanisms regulating biofilm in response to oxidative stress may shed light on the determinants required by bacteria to colonize hostile habitats and on the molecular strategies to sense environmental cues and adapt accordingly. My PhD thesis has aimed to study the planktonic and the biofilm responses to exogenously (e.g. nanoparticles and phenazine methosulfate) and endogenously (interruption of genes coding for proteins involved in maintaining the redox homeostasis) induced oxidative stress in term of dynamic of growth, biofilm architecture, EPS composition, extracellular and intracellular reactive oxygen species (ROS) level and expressed proteins.

In the manuscript by **Villa et al. (2012)** (part II, chapter I), the biofilm of the rhizosphere bacterium *A. vinelandii* was challenged with endogenous sub-lethal oxidative stress. To this aim, we used the mutant strain MV474, which has a deletion in the gene encoding for the rhodanese-like protein RhdA involved in the redox balance in planktonic *A. vinelandii* cells (Remelli et al., 2011). During biofilm growth, chronic endogenous oxidative events in the MV474 strain generated a stress condition to which the bacterium responded by adopting the biofilm lifestyle more efficiently than the wild type strain. The same effect resulted from the addition of an exogenous source of oxidative stress, e.g. the superoxide generator phenazine methosulhate (PMS). Collected data suggested a sensitive growth stage in biofilm development, corresponding to the early stage of biofilm formation. Likely, the elevated oxidative stress level observed in the most vulnerable biofilm growth step, the early stage, might provide the selective pressure to increase the biofilm forming capacity of MV474. As the biofilm reached the mature phase, a reduced metabolic activity and enhanced redox buffering properties may avoid stress inducers, providing an explanation for the low level of ROS and the higher activity of scavenging enzymes detected in the MV474 biofilm. In addition, oxidative stress triggered both swimming and swarming motility and affected the

composition of the EPS, producing a polysaccharide- rich extracellular polymeric matrix in MV474, which was more resistant to H_2O_2 than the wild type. Thus, the inactivation of rhodanese RhdA acted as continuous endogenous oxidative stress generator that promoted the social behaviour orchestrating biofilm genesis, the activity of ROS-scavenging systems and the switch between swarming and biofilm-like phenotypes.
In the attached manuscript by **Gambino et al. (2015)** (part II, chapter II), silver nanoparticles (Ag-NPs) were chosen as a source of exogenous oxidative stress to challenge *A. vinelandii* and *B. subtilis*, used as representatives of rhizosphere bacteria With the constantly growing utilization of Ag-NPs in commercially available products, NP dispersal raises concern about the possible repercussion on the environment. Ag-NPs, already at 0.1 mg/l, i.e., at a concentration close to the proposed "no effect concentration", affected the planktonic growth of *A. vinelandii*, reducing both its growth rate and the amount of culture biomass. In contrast, growth of the Gram-positive *B. subtilis* was only affected at 10 mg/l. Our observation suggested that, already at concentrations thought to be devoid of biological activity, Ag-NPs could have consequences on the composition of rhizosphere microbial community by affecting growth of specific bacteria. At higher, yet sub-lethal, concentrations (i.e. 10 mg/l), Ag-NPs entered *B. subtilis* cells grown in liquid cultures and accumulate in their cytoplasm, triggering ROS formation. However, a more complex picture emerges from exposure to Ag-NPs of *B. subtilis* colony biofilms, a condition more likely to resemble bacterial growth and physiology in the soil environment. Despite showing some reduction in initial growth rate, fully overcome in the later stages of biofilm development, 10 mg/l Ag-NPs failed to trigger ROS formation, either in the biofilm matrix or inside the biofilm cells. However, exposure to 10 mg/l Ag-NPs strongly induced polysaccharide production in the biofilm matrix, suggesting that the ATP consumption required by this process might be responsible for reduced growth rate in the presence of Ag-NPs in the earlier stages of biofilm formation. In addition to the buffering effect of the polysaccharide matrix, reduction in ROS levels in biofilm cells might suggest that, at the concentrations tested, Ag-NPs might trigger an adaptive response to oxidation stress. To verify this hypothesis, we carried out a proteomic analysis in *B. subtilis* biofilm either in the presence or in the absence of 10 mg/l Ag-NPs. Our proteomic analysis allowed us to identify cellular processes induced in response to Ag-NP treatment of *B. subtilis* biofilm, namely, stress responses (included oxidative stress) and quorum sensing, leading to a

more efficient detoxification and removal of ROS, as observed, and maybe to the induction of quorum sensing, thus affecting gene expression at large in *B. subtilis* biofilms. Finally, our results seemed to suggest that sub-lethal doses of Ag-NPs might exert a positive effect on PGP activity by *B. subtilis*. Altogether, we showed that Ag-NPs at sub-inhibitory concentrations affects pivotal cellular processes such as stress responses, quorum sensing and PGP activities. This is a good example of how exogenous sources of oxidative stress could re-direct cellular processes and gene expression, but also be toxic in a selective way on some bacterial species, thus exerting a strong impact on soil bacterial communities.

The results are summarized in the part III, chapter I are still unpublished, and focus on the response to oxidative stress in biofilms of *B. thailandensis*, a soil bacterium and a pathogen of invertebrates. We challenged *B. thailandensis* biofilms with PMS and evaluated oxidative stress using a set of microbiological and biochemical assays. Monitoring of ROS revealed that the early stages of biofilm formation are characterized by strong induction of oxidative stress, which decreases as the biofilm reaches the mature phase. Surprisingly, in the presence of PMS, we observed reduced production of ROS and lower oxidative stress than in its absence. However, PMS affected biofilm morphology and triggered the production of a matrix richer in polysaccharides. To investigate which enzymes might be involved in buffering oxidative stress, we deleted *sodC*, encoding for the periplasmic superoxide dismutase, possibly involved in defense against exogenous sources of oxidative stress. To this aim, a Gateway compatible allelic exchange system based on the counter-selectable *pheS* gene was used. Deletion of *sodC* led to the higher accumulation of polysaccharides in the EPS, confirming that oxidative stress, both exogenous and endogenous, triggers the production of polysaccharides in the matrix, as already observed in *A. vinelandii* and *B. subtilis*. Interestingly, however, the exposure of the mutant strain to PMS did not cause a further accumulation of polysaccharides in the matrix. In conclusion, the connection between polysaccharides production and sub-lethal oxidative stress, both endogenously and exogenously induced, is strong, though the mechanism remain unidentified. We have planned transcriptomic experiments to gather more information on the response mechanisms to oxidative stress in *B. thailandensis*.

The deletion method utilized in my study was partly developed with my contribution during my stay at the Costerton Biofilm Center of the University of Copenhagen (03/02 –

10/04/2014). The method was set up in *B. cenocepacia* and is applicable to other *Burkholderia* species, and its description has recently been published in a manuscript with me as co-author (part II, chapter III).

6. Conclusions and future prospects

All the data presented in this thesis clearly highlight and reiterate the importance of the biofilm matrix production as a common mechanism of defence to oxidative stress, triggered both by sub-lethal doses of exogenous and endogenous sources. Pathways leading to EPS production are likely to be connected with the main regulators of the oxidative stress response. The explanation of this pathway could be the key to understanding which mechanisms lead to the colonization of certain habitats of ecological end economic interest. In the future, it could also be possible to use oxidative stress in a controlled way to trigger biofilm formation and dispersal.

7. References

Albesa, I., Becerra, M. C., Battán, P. C., Páez, P. L. (2004) Oxidative stress involved in the antibacterial action of different antibiotics. Biochem Biophys Res Comm 317: 605-609.
Allesen-Holm, M., Barken, K.B., Yang, L., Klausen, M., Webb, J.S., et al. (2006) A characterization of DNA-release in *Pseudomonas aeruginosa* cultures and biofilms. Mol Microbiol 59: 1114-1128.
Alteri, C. J., Xicohténcatl-Cortes, J., Hess, S., et al. (2007) *Mycobacterium tuberculosis* produces pili during human infection. PNAS USA104: 5145-5150.
Amitai, S., Yassin, Y., Engelberg-Kulka, H. (2004) MazF-mediated cell death in *Escherichia coli*: a point of no return. J Bacteriol 186: 8295-8300.
Anbar, A. D. (2008) Elements and evolution. Science 322: 1481-1483.
Andrews, S.C, Robinson, A. K., Rodríguez-Quiñones, F. (2003) Bacterial iron homeostasis. FEMS Microbiol Rev 27: 215- 237.
Apel, K., Hirt, H. (2004) Reactive oxygen species: metabolism, oxidative stress, and signal transduction. Annual Review of Plant Biology, 55, 373-399.
Arce Miranda, J. E., Sotomayor, C. E., Albesa, I., Paraje, M. G. (2011) Oxidative and nitrosative stress in *Staphylococcus aureus* biofilm. FEMS Microbiol Letters 315: 23-29.
Asally, M., Kittisopikul, M., Rué, P., Du, Y., Hu, Z., et al. (2012) Localized cell death focuses mechanical forces during 3D patterning in a biofilm. PNAS USA 109: 18891-18896.
Aslund, F., Zheng, M., Beckwith, J., Storz, G. (1999) Regulation of the OxyR transcriptional factor by hydrogen peroxide and the cellular thiol-disulfide status. PNAS 96: 6161-6165.
Ausmees, N., Jonsson, H., Hoglund, S., Ljunggren, H., Lindberg M. (1999) Structural and putative regulatory genes involved in cellulose synthesis in *Rhizobium leguminosarum* bv. *trifolii.* Microbiology 145: 1253-1262.
Badri, D. V., Weir, T. L., van der Lelie, D., Vivanco, J. M. (2009) Rhizosphere chemical dialogues: plant-microbe interactions. Curr Opin Biotechnol 20: 642-650.
Baker, P., Ricer, T., Moynihan, P. J., Kitova, E. N., Walvoort, M. T. C., et al. (2014) *P. aeruginosa* SGNH Hydrolase-like proteins AlgJ and AlgX have similar topology but separate and distinct roles in alginate acetylation. PLoS Pathogens 10: 1004334.
Bakker, E. M., Tiddens, H. A. W. M. (2007) Pharmacology, clinical efficacy and safety of recombinant human DNase in cystic fibrosis. Expert Rev Respir Med 1: 317-329.
Baltz, R. H. (2006) Molecular engineering approaches to peptide, polyketide and other antibiotics. Nat Biotechnol 24: 1533-1540.
Banejeree, I., Pangule, R. C., Kane, R. S. (2011) Antifouling coatings: Recent developments in the design of surfaces that prevent fouling by proteins, bacteria, and marine organisms. Adv Mater 23: 690-718.

Baraquet, C., Harwood, C.S. (2013) Cyclic diguanosine monophosphate represses bacterial flagella synthesis by interacting with the Walker A motif of the enhancer-binding protein FleQ. PNAS USA 110: 18478–18483.
Bardy, S. L., Ng, S. Y. M., Jarrell, K. F. (2003) Prokaryotic motility structures. Microbiology 149: 295–304.
Bassis, C. M., Visick, K. L. (2010) The cyclic-di-GMP phosphodiesterase BinA negatively regulates cellulose- containing biofilms in *Vibrio fischeri*. J Bacteriol 192: 1269-1278.
Baynham, P. J., Wozniak, D. J. (1996) Identification and characterization of AlgZ, an AlgT-dependent DNA-binding protein required for *Pseudomonas aeruginosa algD* transcription. Mol Microbiol 22: 97-108.
Beneduzi, A., Ambrosini, A., Passaglia, L. M. P. (2012) Plant growth-promoting rhizobacteria (PGPR): their potential as antagonists and biocontrol agents. Genet Mol Biol 35: 1044–1051.
Benn, T. M., Westerhoff, P. (2008) Nanoparticle silver released into water from commercially available sock fabrics. Environ Sci Technol 42: 4133-4139.
Benov, L., Fridovich, I. (1999) Why superoxide imposes an aromatic amino acid auxotrophy in *Escherichia coli*. J Biol Chem 274: 4202-4206.
Benov, L, Kredich, N. M., Fridovich, I. (1996) The mechanism of the auxotrophy for sulfur-containing amino acids imposed upon *Escherichia coli* by superoxide. J Biol Chem 271: 21037-21040.
Berg, G., Smalla, K. (2009) Plant species and soil type cooperatively shape the structure and function of microbial communities in the rhizosphere. FEMS Microbiol Ecol 68: 1-13.
Bertrand, T., Eady, N. J., Jones, J. N., Jesmin, Nagy, J. M., et al. (2004) Crystal structure of *Mycobacterium tuberculosis* catalase-peroxidase. J Biol Chem 279: 38991–38999.
Bielski, B. H. J., Cabelli, D. E., Arudi, R. L. (1985) Reactivity of HO_2/O_2^- radicals in aqueous solution. J Phys Chem Ref Data 14: 1041-1062.
Bjarnsholt, T., Alhede, M., Alhede, M., Eickhardt-Sørensen, S. R., Moser, C., et al. (2013) The *in vivo* biofilm. Trends Microbiol 21: 466-474.
Boeckelmann, U., Janke, A., Kuhn, R., Neu, T. R., et al. (2006) Bacterial extracellular DNA forming a defined network-like structure. FEMS Microbiol Letters 262: 31-38.
Bokare, A. D., Choi, W. (2014) Review of iron-free Fenton-like systems for activating H_2O_2 in advanced oxidation processes. J Hazard Mat 275: 121-135.
Boles, B. R., Singh, P. K. (2008) Endogenous oxidative stress produces diversity and adaptability in biofilm communities. PNAS USA 105: 12503-12508.
Boronat, S., Domènech, A., Paulo, E., Calvo, I. a., García-Santamarina, S., et al. (2014) Thiol-based H_2O_2 signalling in microbial systems. Redox Biology 2: 395-399.
Boucher, J. C., Schurr, M. J., Deretic, V. (2000) Dual regulation of mucoidy in *Pseudomonas aeruginosa* and sigma factor antagonism. Mol Microbiol 36: 341-351.
Branda, S., Chu, F., Kearns, D. B, Losick, R., Kolter, R. (2006) A major protein component of the *Bacillus subtilis* biofilm matrix. Mol Microbiol 59: 1229–1238.
Bredenbruch, F., Geffers, R., Nimtz, M., Buer, J., et al. (2006) The *Pseudomonas aeruginosa* quinolone signal (PQS) has an iron-chelating activity. Environ Microbiol 8: 1318-1329.

Briviba, K., Klotz, L. O., Sies, H. (1997) Toxic and signaling effects of photochemically or chemically generated singletoxygenin biological systems. Biol Chem 378: 1259-1265.
Bruellhoff, K., Fiedler, J., Möller, M., Groll, J., et al. (2010) Surface coating strategies to prevent biofilm formation on implant surfaces. Int J Artificial Organs 33: 646-653.
Bsat, N., Herbig, A., Casillas-Martinez, L., Setlow, P., Helmann, J. D. (1998) *Bacillus subtilis* contains multiple Fur homologues: identification of the iron uptake (Fur) and peroxide regulon (PerR) repressors. Mol Microbiol 29: 189-198.
Bsat, N., Chen, L. Helmann, J. D. (1996) Mutation of the *Bacillus subtilis* alkyl hydroperoxide reductase (*ahpCF*) operon reveals compensatory interactions among hydrogen peroxide stress genes. J Bacteriol 178: 6579-6586.
Bulgarelli, D., Schlaeppi, K., Spaepen, S., Ver Loren, E., Schulze-Lefert, P. (2013) Structure and functions of the bacterial microbiota of plants. Annu Rev Plant Biol 64: 807-838.
Bylund, J., Burgess, L. A., Cescutti, P., Ernst, R. K., Speert, D. P. (2006) Exopolysaccharides from *Burkholderia cenocepacia* inhibit neutrophil chemotaxis and scavenge reactive oxygen species. J Biol Chem 281: 2526-2532.
Cabiscol, E., Tamarit, J., Ros, J. (2000) Oxidative stress in bacteria and protein damage by reactive oxygen species. Intern Microbiol 3: 3-8.
Cai, Z., Yan, L-J. (2013) Protein oxidative modifications: beneficial roles in disease and health. J Biochem Pharmacol Res 1: 15-26.
Calabrese, V., Cornelius, C., Cuzzocrea, S., Iavicoli, I., Rizzarelli, E., Calabrese, E. J. (2011) Hormesis, cellular stress response and vitagenes as critical determinants in aging and longevity. Molec Aspects Med 32: 279-304.
Campos, M., Martinez-Salazar, J.M., Lloret, L., Moreno, S., Nunez, C., et al. (1996) Characterization of the gene coding for GDP-mannose dehydrogenase (*algD*) from *Azotobacter vinelandii*. J Bacteriol 178: 1793-1799.
Candeias, L. P., Steenken, S. (1993) Electron transfer in di(deoxy)nucleoside phosphates in aqueous solution. Rapid migration of oxidative damage (via adenine) to guanine. J Am Chem Soc 115: 2437-2440.
Cao, Z., Livoti, E., Losi, A., Gartner, W. (2010) A blue light-inducible phosphodiesterase activity in the cyanobacterium *Synechococcus elongatus*. Photoch Photobiol 86: 606-611.
Cáp, M., Váchová, L., Palková, Z. (2012) Reactive oxygen species in the signaling and adaptation of multicellular microbial communities. Oxid Med Cell Longevity: 976753.
Cappitelli, F., Principi, P. Sorlini, C. (2006) Biodeterioration of modern materials in contemporary collections: can biotechnology help? Trends in Biotechnol 24: 350-354.
Carlioz, A., Touati, D. (1986) Isolation of superoxide dismutase mutants in *Escherichia coli*: is superoxide dismutase necessary for aerobic life? EMBO J 5: 623-630.
Carrolo, M., Frias, M.J., Pinto, F.R., MeloCristino, J., Ramirez, M. (2010) Prophage spontaneous activation promotes DNA release enhancing biofilm formation in *Streptococcus pneumoniae*. PLoS ONE 5: 1-10.

Castañeda, M., Sánchez, J., Moreno, S., Núñez, C., Espín, G. (2001) The global regulators GacA and σS form part of a cascade that controls alginate production in *Azotobacter vinelandii*. J Bacteriol 183: 6787-6793.
Cescutti, P., M., Bosco, F., Picotti, G., Impallomeni, J., Leitão, H., et al. (2000) Structural study of the exopolysaccharide produced by a clinical isolate of *Burkholderia cepacia*. Biochem Biophys Res Commun 273: 1088-1094.
Chai, Y., Beauregard, P. B., Vlamakis, H., Losick, R., Kolter, R. (2012) Galactose metabolism plays a crucial role in biofilm formation by *Bacillus subtilis*. mBio 3: 184-12.
Chandler, J. R., Duerkop, B. A., Hinz, A., West, T. E., Herman, J.P., et al. (2009) Mutational analysis of *Burkholderia thailandensis* quorum sensing and self-aggregation. J Bacteriol 191: 5901-5909.
Chatterjee, S. N., Chaudhuri, K. (2006) Lipopolysaccharides of *Vibrio cholerae*. Biological functions. Biochim Biophys Acta 1762: 1-16.
Chattopadhyay, M. K., Raghu, G., Sharma, Y. V., Biju, A. R., Rajasekharan, M. V., et al. (2011) Increase in oxidative stress at low temperature in an antarctic bacterium. Curr Microbiol 62: 544-546.
Chen, J., Shen, J., Solem, C., Jensen, P. R. (2013) Oxidative stress at high temperatures in *Lactococcus lactis* due to an insufficient supply of riboflavin. App Environ Microbiol 79: 6140-6147.
Chen, L., Keramati, L. Helmann, J. D. (1995) Coordinate regulation of *Bacillus subtilis* peroxide stress genes by hydrogen peroxide and metal ions. PNAS 92: 8190-8194.
Chi, B. K., Roberts, A. A., Huyen, T. T., Basell, K., Becher, D., et al. (2013) S-bacillithiolation protects conserved and essential proteins against hypochlorite stress in *Firmicutes* bacteria. Antioxid Redox Signal 18: 1273-1295.
Chieng, S., Carreto, L., Nathan, S. (2012) *Burkholderia pseudomallei* transcriptional adaptation in macrophages. BMC Genomics 13: 1-13.
Choi, H. J, Kim, S. J., Mukhopadhyay, P., Cho, S., Woo, J. R., et al. (2001) Structural basis of the redox switch in the OxyR transcription factor. Cell 105: 103-113.
Chu, F., Kearns, D. B., Branda, S. S., Kolter, R., Losick, R. (2006) Targets of the master regulator of biofilm formation in *Bacillus subtilis*. Mol Microbiol 59: 1216-1228.
Chutoam, P., Charoensawan, V., Wongtrakoongate, P., Kumarth, A., Buphamalai, P., et al. (2013) RpoS and oxidative stress conditions regulate succinyl-CoA: 3-ketoacid-coenzyme A transferase (SCOT) expression in *Burkholderia pseudomallei*. Microbiol Immunol 57: 605-615.
Christman, M.F., Morgan, R.W., Jacobson, F.S., Ames, B.N. (1985) Positive control of a regulon for defenses against oxidative stress and some heat-shock proteins in *Salmonella typhimurium*. Cell 41: 753-762.
Collet, A., Cosette, P., Beloin, C., Ghigo, J.M., Rihouey, C., et al. (2008) Impact of *rpoS* deletion on the proteome of *Escherichia coli* grown planktonically and as biofilm. J Proteome Res 7: 4659-4669.
Compan, I., Touati, D. (1993) Interaction of six global transcription regulators in expression of manganese superoxide dismutase in *Escherichia coli* K-12. J Bacteriol 175: 1687-1696.

Corona-Izquierdo, F. P., J. Membrillo-Hernández (2002) A mutation in *rpoS* enhances biofilm formation in *Escherichia coli* during exponential phase of growth. FEMS Microbiol Lett 211: 105-110.
Costerton, J. W., Cheng, K-J., Geesy, G. G., Ladd, T. I., Nickel, J. C., et al. (1987) Bacterial biofilms in nature and disease. Annu Rev Microbiol 41: 435-464.
Cucarella, C., Solano, C., Valle, J., Amorena, B. et al. (2001) Bap, a *Staphylococcus aureus* surface protein involved in biofilm formation. J Bacteriol 183: 2888-2896.
Cuzzi, B., Herasimenka, Y., Silipo, A., Lanzetta, R., Liut, G., Rizzo, R., Cescutti, P. (2014) Versatility of the *Burkholderia cepacia* complex for the biosynthesis of exopolysaccharides: a comparative structural investigation. PloS One 9: e94372.
Dahl, J.-U., Gray, M. J., Jakob, U. (2015) Protein quality control under oxidative stress conditions. J Molec Biol 427: 1549-1563.
Danese, P. N., Pratt, L., Dove, S. L., Kolter, R. (2000) The outer membrane protein, Antigen 43, mediates cell-to-cell interactions within *Escherichia coli* biofilms. Mol Microbiol 37: 424-432.
Daniels, R., Vanderleyden, J., Michiels, J. (2004) Quorum sensing and swarming migration in bacteria. FEMS Microbiol Rev 28: 261-289.
Darby, C., Hsu, J. W., Ghori, N., Falkow, S. (2002) *Caenorhabditis elegans*: plague bacteria biofilm blocks food intake. Nature 417: 243-244.
Das, T., Manefield, M. (2013a) Phenazine production enhances extracellular DNA release via hydrogen peroxide generation in *Pseudomonas aeruginosa*. Comm Int Biol 6: 23570.
Das, T., Sehar, S., Manefield, M. (2013b) The roles of extracellular DNA in the structural integrity of extracellular polymeric substance and bacterial biofilm development. Environ Microbiol Rep 5: 778-786.
Dash, H. R., Mangwani, N., Chakraborty, J., Kumari, S., Das S. (2013) Marine bacteria: potential candidates for enhanced bioremediation. Appl Microb Biotechnol 97: 561-571.
Davey, M. E., O'toole, G. (2000) Microbial biofilms: from ecology to molecular genetics. MMBR, 64: 847-867.
Davidson, J. F., Whyte, B., Bissinger, P. H., Schiestl, R. H. (1996) Oxidative stress is involved in heat-induced cell death in *Saccharomyces cerevisiae*. PNAS 93: 5116-5121.
Davies, D. G., Parsek, M. R., Pearson, J. P., Iglewski, B. H. et al. (1998) The involvement of cell-to-cell signals in the development of a bacterial biofilm. Science 280: 295-298.
Demple, B., Harrison, L. (1994) Repair of oxidative damage to DNA: enzymology and biology. Annu Rev Biochem 63: 915-948.
Demple, B., Johnson, A., Fung, D. (1986) Exonuclease III and endonuclease IV remove 3' blocks from DNA synthesis primers in H_2O_2-damaged *Escherichia coli*. PNAS USA 83: 7731–7735.
Dietrich, L. E. P., Teal, T. K., Price-Whelan, A., Newman, D. K. (2008) Redox-active antibiotics control gene expression and community behavior in divergent bacteria. Science 321: 1203-1206.

Diggle, S.P., Stacey, R.E., Dodd, C., Cámara, M., Williams, P., Winzer, K. (2006) The galactophilic lectin, LecA, contributes to biofilm development in *Pseudomonas aeruginosa*. Environ Microbiol 8: 1095-1104.
Dobinsky,S., Kiel, K., Rohde, H., Bartscht, K., Knobloch, J. K., et al. (2003) Glucose-related dissociation between icaADBC transcription and biofilm expression by *Staphylococcus epidermidis*: evidence for an additional factor required for polysaccharide intercellular adhesin synthesis. J Bacteriol 185: 2879-2886.
Dogsa, I., Brloznik, M., Stopar, D., Mandic-Mulec, I. (2013). Exopolymer diversity and the role of levan in *Bacillus subtilis* biofilms. PloS One 8: e62044.
Donlan, R.M., Costerton, J.W. (2002) Biofilms: survival mechanisms of clinically relevant microorganisms. Clin Microbiol Rev 15: 167-193.
Dorsey-Oresto, A., Lu, T., Mosel, M., Wang, X., Salz, T., et al. (2013) YihE Kinase is a central regulator of programmed cell death in bacteria. Cell Reports 3: 528-537.
Drago, L. (2009) Bacteria and biofilm in respiratory tract infections. Infect Med 17: 3-9.
Duijff, B. J., Recorbet, G., Bakker, P. A. H. M., Loper, J. E., Lemanceau, P. (1999) Microbial antagonism at the root level is involved in the suppression of *Fusarium* wilt by the combination of nonpathogenic *Fusarium oxysporum* Fo47 and *Pseudomonas putida* WCS358. Phytopathology 89: 1073-1079.
Dukan, S., Touati, D. (1996) Hypochlorous acid stress in *Escherichia coli*: resistance, DNA damage, and comparison with hydrogen peroxide stress. J Bacteriol 178: 6145-6150.
Duncan, T. V. (2011) Applications of nanotechnology in food packaging and food safety: Barrier materials, antimicrobials and sensors. J Colloid Interface Sci 363: 1-24.
Dunne, M. (2002) Bacterial adhesion: seen any good biofilms lately? Clin Microbiol Rev 15: 155-166.
Dwyer, D. J., Collins, J. J., Walker, G. C. (2015) Unraveling the physiological complexities of antibiotic lethality. Annu Rev Pharmacol Toxicol 55: 313-332.
Dwyer, D.J., Kohanski, M.A., Hayete, B., Collins, J.J. (2007) Gyrase inhibitors induce an oxidative damage cellular death pathway in *Escherichia coli*. Mol Syst Biol 3: 91.
Eisenhauer, N., Bessler, H., Engels, C., Gleixner, G. et al. (2010) Plant diversity effects on soil microorganisms support the singular hypothesis. Ecology 91: 485-496.
Elsholz, A. K. W., Wacker, S., Losick, R. (2014) Self-regulation of exopolysaccharide production in *Bacillus subtilis* by a tyrosine kinase. Genes Develop 28: 1710-1720.
Esterbauer, H., Schaur, R. J., Zollner, H. (1991) Chemistry and biochemistry of 4-hydroxynonenal, malonaldehyde and related aldehydes. Free Rad Biol Med 11: 81-128.
Fabrega, J., Fawcett, S.R., Renshaw, J.C., Lead, J.R. (2009) Silver nanoparticle impact on bacterial growth: effect of pH, concentration, and organic matter. Environ Sci Technol 43: 7285-7290.
Fang, F.C. (2004) Antimicrobial reactive oxygen and nitrogen species: concepts and controversies. Nat Rev Microbiol 2: 820-832.
Farr, S. B., D'Ari, R., Touati, D. (1986) Oxygen- dependent mutagenesis in *Escherichia coli* lacking superoxide dismutase. PNAS USA 83: 8268-8272.

Fazli, M., Almblad, H., Rybtke, M. L., Givskov, M., Eberl, L., Tolker-Nielsen, T. (2014) Regulation of biofilm formation in *Pseudomonas* and *Burkholderia* species. Environ Microbiol 16: 1961-1981.
Fester, T., Hause, G. (2005) Accumulation of reactive oxygen species in arbuscular mycorrhizal roots. Mycorrhiza 15, 373–379.
Flemming, H., Wingender, J. (2010) The biofilm matrix. Nature Rev Microbiol 8: 623-633.
Flemming, H. C., Neu, T. R., Wozniak, D. J. (2007) The EPS matrix: the "house of biofilm cells". J Bacteriol 189: 7945-7947.
Friedman, L., Kolter, R. (2004) Two genetic loci produce distinct carbohydrate-rich structural components of the *Pseudomonas aeruginosa* biofilm matrix. J Bacteriol 186: 4457-65.
Fuangthong, M., Herbig, A. F., Bsat, N., Helmann, J. D. (2002). Regulation of the *Bacillus subtilis fur* and *perR* genes by PerR: not all members of the PerR regulon are peroxide inducible. J Bacteriol 184: 3276-3286.
Gaballa, A., Chi, B. K., Roberts, A., Becher, D., Hamilton, C., et al. (2014) Redox regulation in *Bacillus subtilis*: the bacilliredoxins BrxA (YphP) and BrxB (YqiW) function in de-bacillithiolation of S-Bacillithiolated OhrR and MetE. Antiox Redox Signal 21: 357-367.
Gally, D. L., Leathart, J., Blomfield, I. C. (1996) Interaction of FimB and FimE with the fim switch that controls the phase variation of type 1 fimbriae in *Escherichia coli* K-12. Mol Microbiol 21: 725-738.
Galperin, M. Y., Nikolskaya, A. N., Koonin, E. V. (2001) Novel domains of the prokaryotic two-component signal transduction systems. FEMS Microbiol Lett 203: 11-21.
Gao, X., Mukherjee, S., Matthews, P. M., Hammad, L., Kearns, D. B., et al. (2013) Functional characterization of core components of the *Bacillus subtilis* cyclic-Di-GMP signaling pathway. J Bacteriol 195: 4782-4792.
Garavaglia, M., Rossi., E., Landini, P. (2012) The pyrimidine nucleotide biosynthetic pathway modulates production of biofilm determinants in *Escherichia coli*. PLOS ONE 2: e31252.
Gardner, P. R., Fridovich, I. (1991) Superoxide sensitivity of the *Escherichia coli* aconitase. J. Biol Chem 266: 19328-19333.
Garin, J., Diez, R., Kieffer, S., Dermine, J.F., Duclos, S., et al. (2001) The phagosome proteome: insight into phagosome functions. J Cell Biol 152: 165-180.
Gechev, T. S., Hille, J. (2005) Hydrogen peroxide as a signal controlling plant programmed cell death. J Cell Biol 168: 17-20.
Gerdes, K., Christensen, S. K., Lobner-Olesen, A. (2005) Prokaryotic toxin–antitoxin stress response loci. Nat Rev Microbiol 3: 371-382.
Gerschman, R., Gilbert, D. L., Nye, S. W., Dwyer, P., Fenn, W. O. (1954) Oxygen poisoning and X-irradiation: a mechanism in common. Science 119: 623-626.
Ghafoor, A., Hay, I. D., Rehm, B. H. (2011) Role of exopolysaccharides in *Pseudomonas aeruginosa* biofilm formation and architecture. Appl Environ Microbiol 77: 5238-5246.

Ghigo, J. M. (2003) Are there biofilm-specific physiological pathways beyond a reasonable doubt? Res Microbiol 154: 1-8.
Ghigo, J.M. (2001) Natural conjugative plasmids induce bacterial biofilm development. Nature 412: 442-445.
Giese, B. (2002) Electron transfer in DNA. Curr Opin Chem Biol 6: 612–618.
Gilbert, P., Mc Bain, A. J. (2003) Potential impact of increased use of biocides in consumer products on prevalence of antibiotic resistance. Clin Microbiol Rev 16: 189-208.
Gilbert, P., Allison, D.G., Mc Bain, A. J. (2002) Biofilms *in vitro* and *in vivo*: do singular mechanisms imply cross-resistance? Symp Ser Soc Appl Microbiol 31: 98-110.
Giltner, C. L., van Schaik, E. J., Audette, G. F., Kao, D., Hodges, R.S., et al. (2006) The *Pseudomonas aeruginosa* type IV pilin receptor binding domain functions as an adhesin for both biotic and abiotic surfaces. Mol Microbiol 59: 1083-1096.
Girard, V., Mourez, M. (2006) Adhesion mediated by autotransporters of Gram-negative bacteria: structural and functional features. Res Microbiol 157:407-416.
Gonzalez-Flecha, B., Demple, B. (1997) Homeostatic regulation of intracellular hydrogen peroxide concentration in aerobically growing *Escherichia coli*. J Bacteriol 179: 382-388.
Govan, J.R., Deretic, V. (1996) Microbial pathogenesis in cystic fibrosis, mucoid *Pseudomonas aeruginosa* and *Burkholderia cepacia*. Microbiol Rev 60: 539–74.
Green, J., Paget, M. S. (2004) Bacterial redox sensors. Nature Rev Microbiol 2: 954–66.
Grinblat, L, Sreider, C. M., Stoppani, A.O. (1991) Superoxide anion production by lipoamide dehydrogenase redox-cycling: effect of enzyme modifiers. Biochem 23: 83-92.
Groves, M., Lucana, D. (2010). Adaptation to oxidative stress by Gram-positive bacteria: the redox sensing system HbpS-SenS-SenR from *Streptomyces reticuli*. Appl Microbiol Microb Biotechnol: 33–42.
Gualdi, L., Tagliabue, L., Bertagnoli, S., Ieranò, T., De Castro, C., et al. (2008). Cellulose modulates biofilm formation by counteracting curli-mediated colonization of solid surfaces in *Escherichia coli*. Microbiology 154: 2017-2024.
Guttenplan, S. B., Kearns,D. B. (2013) Regulation of flagellar motility during biofilm formation. FEMS Microbiol Rev 37: 849–71.
Hall-Stoodley, L., Costerton, J. W., Stoodley, P. (2004) Bacterial biofilms: from the natural environment to infectious diseases. Nature Rev Microbiol 2: 95-108.
Hammar, M., Arnqvist, A., Bian, Z., Olsen, A., Normark, S. (1995) Expression of two *csg* operons is required for production of fibronectin- and congo red-binding curli polymers in *Escherichia coli* K-12. Mol Microbiol 18: 661–670.
Han, D., Williams, E., Cadenas, E. (2001) Mitochondrial respiratory chain-dependent generation of superoxide anion and its release into the intermembrane space. Biochem J 353: 411-416.
Hassan, H. M., Fridovich, I. (1979) Paraquat and *Escherichia coli*. Mechanism of production of extracellular superoxide radical. J Biol Chem 254: 10846-10852.
Hassett, D. J., Ma J.-S., Elkins J. G., McDermott T., Ochsner U. A., et al. (1999) Quorum sensing in *Pseudomonas aeruginosa* controls expression of catalase and superoxide

dismutase genes and mediates biofilm susceptibility to hydrogen peroxide. Mol Microbiol 34: 1082-1093.
Hausladen, A., Privalle, C. T., Keng, T., DeAngelo, J., Stamler, J. S. (1996) Nitrosative stress: activation of the transcription factor OxyR. Cell 86: 719-729.
Häussler, S., Becker, T. (2008) The pseudomonas quinolone signal (PQS) balances life and death in *Pseudomonas aeruginosa* populations. PLoS Pathogens 4: e1000166.
Hawkins, C. L., Davies, M. J. (2001) Generation and propagation of radical reactions on proteins. Biochim Biophys Acta 1504: 196-219.
Hay, I. D., Wang, Y., Moradali, M. F., Rehman, Z. U., Rehm, B. H. (2014) Genetics and regulation of bacterial alginate production. Environ Microbiol 16: 2997-3011.
Hay, I.D., Remminghorst, U., Rehm, B.H. (2009) MucR, a novel membrane-associated regulator of alginate biosynthesis in *Pseudomonas aeruginosa*. Appl Environ Microbiol 75: 1110-1120.
He, Z., Liang, J., Tang, Z., Ma, R., Peng, et al. (2015) Role of the *luxS* gene in initial biofilm formation by *Streptococcus mutans*. J Mol Microbiol Biotechnol 25: 60-68.
Helmann, J. D., Wu, M. F., Gaballa, A., Kobel, P. A., Morshedi, M. M., et al. (2003) The global transcriptional response of *Bacillus subtilis* to peroxide stress is coordinated by three transcription factors. J Bacteriol 185: 243–253.
Hengge-Aronis, R. (2002) Signal transduction and regulatory mechanisms involved in control of the sigma (RpoS) subunit of RNA polymerase. Microbiol Mol Biol 66: 373–395.
Hengge-Aronis, R. (1999) Interplay of global regulators and cell physiology in the general stress response of *Escherichia coli*. Curr Opin Microbiol 2: 148-152.
Herbig, A. F. Helmann, J. D. (2001) Roles of metal ions and hydrogen peroxide in modulating the interaction of the *Bacillus subtilis* PerR peroxide regulon repressor with operator DNA. Mol Microbiol 41: 849–859.
Hidalgo, E., Ding, H., Demple, B. (1997) Redox signal transduction: mutations shifting [2Fe–2S] centers of the SoxR sensor-regulator to the oxidized form. Cell 88: 121–129.
Hidalgo, E., Demple, B. (1996) The redox state of the [2Fe–2S] clusters in SoxR protein regulates its activity as a transcription factor. J Biol Chem 271: 33173–33175.
Hiltner, L. (1904) Über neuere Erfahrungen und Probleme auf dem Gebiete der Bodenbakteriologie unter besonderer Berücksichtigung der Gründüngung und Brache. Arb DLG 98: 59–78.
Hinsa, S. M., O'Toole, G. A. (2006) Biofilm formation by *Pseudomonas fluorescens* WCS365: a role for LapD. Microbiology 152: 1375–1383.
Hinsa, S. M., Espinosa-Urgel, M., Ramos, J. L., O'Toole, G. (2003) Transition from reversible to irreversible attachment during biofilm formation by *Pseudomonas fluorescens* WCS365 requires an ABC transporter and a large secreted protein. Mol Microbiol 49: 905–918.
Hobley, L., Ostrowski, A., Rao, F.V., Bromley, K.M., et al. (2013) BslA is a self-assembling bacterial hydrophobin that coats the *Bacillus subtilis* biofilm. PNAS 110: 13600-13605.

Hochbaum, A. I., Kolodkin-Gal, I., Foulston, L., Kolter, R., Aizenberg, J., Losick, R. (2011). Inhibitory effects of D-amino acids on *Staphylococcus aureus* biofilm development. J Bacteriol 193: 5616–5622.
Hodges, N. A., Gordon, C. A. (1991) Protection of *Pseudomonas aeruginosa* against ciprofloxacin and betalactams by homologous alginate. Antimicrob Agents Chemother 35: 2450–2452.
Hogberg, P., Nordgren, A., Buchmann, N., Taylor, A. F. S., Ekblad, A., et al. (2001) Large-scale forest girdling shows that current photosynthesis drives soil respiration. Nature 411: 789–792.
Huang, C. T., Stewart, P. S. (1999) Reduction of polysaccharide production in *Pseudomonas aeruginosa* biofilms by bismuth dimercaprol (BISBAL) treatment. J Antimicrob Chemother 44: 601–605.
Humpries, K. M., Sweda, L. I. (1998) Selective inactivation of α-ketoglutarate dehydrogenase: reaction of lipoic acid with 4-hydroxy-2-nonenal. Biochem 37: 15835–15841.
Ieva, R., Roncarati, D., Metruccio, M.M., Seib, K.L., Scarlato, V., et al. (2008) OxyR tightly regulates catalase expression in *Neisseria meningitidis* through both repression and activation mechanisms. Mol Microbiol 70: 1152–1165.
Imlay, J. (2015) Diagnosing oxidative stress in bacteria: not as easy as you might think. Curr Op Microbiol 24: 124–131.
Imlay, J. (2013) The molecular mechanisms and physiological consequences of oxidative stress: lessons from a model bacterium. Nat rev Microbiol 11: 443-454.
Imlay, J. (2003) Pathways of oxidative damage. Annual Rev Microbiol 57: 395–418.
Imlay, J. (1995) A metabolic enzyme that rapidly produces superoxide, fumarate reductase of *Escherichia coli*. J Biol Chem 270: 19767–19777.
Itoh, Y., Rice, J. D., Goller, C., Pannuri, A., Taylor, J. et al. (2008) Roles of *pgaABCD* genes in synthesis, modification, and export of the *Escherichia coli* biofilm adhesin poly-beta-1,6-N-acetyl-D-glucosamine. J Bacteriol 190: 3670–3680.
Ivancich, A., Donald, L. J., Villanueva, J., Wiseman, B., Fita, I., et al. (2013) Spectroscopic and kinetic investigation of the reactions of peroxyacetic acid with *Burkholderia pseudomallei* catalase-peroxidase, KatG. Biochemistry 52: 7271–7282.
Jacobson, F. S., Morgan, R. W., Christman, M. F., Ames, B. N. (1989) An alkyl hydroperoxide reductase from *Salmonella* Typhimurium involved in the defense of DNA against oxidative damage. J Biol Chem 264: 1488–1496.
Jamet, A., Siguad, S., Van de Sype, G., Puppo, A., D. Herouart (2003) Expression of the bacterial catalase genes during *Sinorhizobium meliloti- Medicago sativa* symbiosis and their crucial role during the infection process. Mol Plant Microbe Interact 16: .217–225
Jangiam, W., Loprasert, S., Smith, D. R., Tungpradabkul, S. (2010) *Burkholderia pseudomallei* Rpos regulates OxyR and the *katG-dpsA* operon under conditions of oxidative stress. Microbiol Immunol 54: 389–397.
Jiao, Y., D'haeseleer, P., Dill, B. D., Shah, M., Verberkmoes, N. C., et al. (2011) Identification of biofilm matrix-associated proteins from an acid mine drainage microbial community. Appl Environ Microbiol 77: 5230–5237.

Jonas, K., Edwards, A. N., Simm, R., Romeo, T., Römling, U., Melefors, O. (2008) The RNA binding protein CsrA controls cyclic di-GMP metabolism by directly regulating the expression of GGDEF proteins. Mol Microbiol 70: 236–257.
Jones, C. J., Ryder, C. R., Mann, E. E., Wozniak, D.J. (2013) AmrZ modulates *Pseudomonas aeruginosa* biofilm architecture by directly repressing transcription of the *psl* operon. J Bacteriol 195: 1637–1644.
Jothivasan, V. K., Hamilton, C. J. (2008). Mycothiol: synthesis, biosynthesis and biological functions of the major low molecular weight thiol in actinomycetes. Nat Prod Reports 25: 1091–1117.
Kalia, D., Merey, G., Nakayama, S., Zheng, Y., Zhou, J., et al. (2012). Nucleotide, c-di-GMP, c-di-AMP, cGMP, cAMP, (p)ppGpp signaling in bacteria and implications in pathogenesis. Chem Society Rev 305–341.
Kamp, H. D., Higgins, D. E. (2011) A protein thermometer controls temperature-dependent transcription of flagellar motility genes in *Listeria monocytogenes*. PLoS Pathog 7: e1002153.
Kang, Y. S., Lee, Y., Jung, H., Jeon, C. O., Madsen, E. L., Park, W. (2007) Overexpressing antioxidant enzymes enhances naphthalene biodegradation in *Pseudomonas* sp. strain As1. Microbiology 153: 3246–3254.
Karatan, E., Watnick, P. (2009) Signals, regulatory networks, and materials that build and break bacterial biofilms. MMBR: 73: 310–347.
Kearns, D. B., Losick, R. (2005) Cell population heterogeneity during growth of *Bacillus subtilis*. Genes & Development 19: 3083–3094.
Kelly, M. J., R. K. Poole, M. G. Yates, C. Kennedy (1990) Cloning and mutagenesis of genes encoding the cytochrome bd terminal oxidase complex in *Azotobacter vinelandii*: mutants deficient in the cytochrome d complex are unable to fix nitrogen in air. J Bacteriol 172: 6010–6019.
Keyer, K., Imlay, J. A. (1996) Superoxide accelerates DNA damage by elevating free- iron levels. PNAS USA 93: 13635–13640.
Kim, S.O., Merchant, K., Nudelman, R., Beyer, W.F., Keng, T. et al. (2002) OxyR: a molecular code for redox-related signaling. Cell 109: 383–396.
Kim, J. R., Yoon, H. W., Kwon, K. S., Lee, S. R., Rhee, S. G. (2000) Identification of proteins containing cysteine residues that are sensitive to oxidation by hydrogen peroxide at neutral pH. Anal Biochem 283: 214–221.
Klausen, M., Gjermansen, M., Kreft, J. U., Tolker-Nielsen, T. (2006) Dynamics of development and dispersal in sessile microbial communities: Examples from *Pseudomonas aeruginosa* and *Pseudomonas putida* model biofilms. FEMS Microbiol Letters 261: 1–11.
Klemm, P., Vejborg, R. M., Sherlock, O. (2006) Self-associating autotransporters, SAATs: Functional and structural similarities. Int J Medical Microbiol 296: 187–195.
Kohanski, M. A., Dwyer, D. J., Wierzbowski, J., Cottarel, G., Collins, J. J. (2008) Mistranslation of membrane proteins and two-component system activation trigger antibiotic-mediated cell death. Cell 135: 679–690.

Kohanski, M. A., Dwyer, D. J., Hayete, B., Lawrence, C. A., Collins, J. J. (2007) A common mechanism of cellular death induced by bactericidal antibiotics. Cell 130: 797-810.
Kolodkin-Gal, I., Cao, S., Chai, L., Böttcher, T., Kolter, R., et al. (2012) A self-produced trigger for biofilm disassembly that targets exopolysaccharide. Cell 149: 684–92.
Kolodkin-Gal, I., Romero, D., Cao, S., Clardy, J., Kolter, R., and Losick, R. (2010) D-amino acids trigger biofilm disassembly. Science 328: 627–629.
Korshunov, S., Imlay, J. A. (2011) Two sources of endogenous hydrogen peroxide in *Escherichia coli*. Mol Microbiol 75: 1389–1401.
Korshunov, S., Imlay, J. A. (2006) Detection and quantification of superoxide formed within the periplasm of *Escherichia coli*. J Bacteriol 188: 6326–6334.
Kowalchuk, G.A., Stephen, J.R. (2001) Ammonia-oxidizing bacteria: a model for molecular microbial ecology. Ann Rev Microbiol 55: 485–529.
Krasteva, P. V., Fong, J. C., Shikuma, N. J., Beyhan, S., Navarro, M. V., et al. (2010) *Vibrio cholerae* VpsT regulates matrix production and motility by directly sensing cyclic di-GMP. Science 327: 866–868.
Krishnamoorthy, K., Veerapandian, M., Zhang, L., Yun, K. (2012) Antibacterial efficiency of graphene nanosheets against pathogenic bacteria via lipid peroxidation. J Physical Chem B 17280–17287.
Kristich, C. J., Li, Y. H., Cvitkovitch, D. G., Dunny, G. M. (2004) Esp-independent biofilm formation by *Enterococcus faecalis*. J Bacteriol 186: 154–163.
Kroll, J., Langford, P., Wilkes, K., Keil, A. (1995) Bacterial [Cu,Zn] superoxide dismutase: phylogenetically distinct from the eukaryotic enzyme, and not so rare after all! Microbiology 141: 2271–2279.
Kumar, A. S., Mody, K., Jha, B. (2007) Bacterial exopolysaccharides - A perception. J Microbiol 47: 103–117.
Kuo, C. F., Mashino, T., Fridovich, I. (1987) α,β-dihydroxyisovalerate dehydratase: a superoxide-sensitive enzyme. J Biol Chem 262: 4724–4727.
Kussmaul, L., Hirst, J. (2006) The mechanism of superoxide production by NADH:ubiquinone oxidoreductase (complex I) from bovine heart mitochondria. PNAS USA 103: 7607–7612.
Laloi, C., Stachowiak, M., Pers-Kamczyc, E., Warzych, E., Murgia, I., Apel, K. (2007). Cross-talk between singlet oxygen- and hydrogen peroxide-dependent signaling of stress responses in *Arabidopsis thaliana*. PNAS USA 104: 672–677.
Lam, H., Oh, D. C., Cava, F., Takacs, C. N., Clardy, J. et al. (2009) D-amino acids govern stationary phase cell wall remodeling in bacteria. Science 325: 1552–1555.
Landini, P., Antoniani, D., Burgess, J. G., Nijland, R. (2010) Molecular mechanisms of compounds affecting bacterial biofilm formation and dispersal. Appl Microbiol Biotechnol 86: 813–823.
Landini, P. (2009) Cross-talk mechanisms in biofilm formation and responses to environmental and physiological stress in *Escherichia coli*. Res Microbiol 160: 259-266.
Landini, P., Zehnder, A. J. B. (2002) The global regulatory *hns* negatively affects adhesion to solid surfaces by anaerobically grown *Escherichia coli* by modulating expression of flagellar genes and lipopolysaccharide production. J Bacteriol 184: 1522–1529.

Lasa, I., Penadés, J. R. (2006) Bap: A family of surface proteins involved in biofilm formation. Res Microbiol 157: 99–107.
Lau, G. W., Hassett, D. J., Ran, H., Kong, F. (2004) The role of pyocyanin in *Pseudomonas aeruginosa* infection. Trends Mol Med 10: 599–606.
Lazazzera, B. A., Kurtser, I. G., McQuade, R. S., Grossman, A. D. (1999) An autoregulatory circuit affecting peptide signaling in *Bacillus subtilis*. J Bacteriol 181: 5193–5200.
Lee, H. S., Gu, F., Ching, S. M., Lam, Y. et al. (2010) CdpA is a *Burkholderia pseudomallei* cyclic di-GMP phosphodiesterase involved in autoaggregation flagellum synthesis, motility, biofilm formation, cell invasion, and cytotoxicity. Infect Immun 78: 1832–1840.
Lee, V.T., Matewish, J.M., Kessler, J.L., Hyodo, M. et al. (2007) A cyclic-di-GMP receptor required for bacterial exopolysaccharide production. Mol Microbiol 65: 1474–1484.
Leech, A. J., Sprinkle, A., Wood, L., Wozniak, D.J., Ohman, D.E. (2008) The NtrC family regulator AlgB, which controls alginate biosynthesis in mucoid *Pseudomonas aeruginosa*, binds directly to the *algD* promoter. J Bacteriol 190: 581–589.
Leeper, T., Zhang, S., Van Voorhis, W. C., Myler, P. J., Varani, G. (2011) Comparative analysis of glutaredoxin domains from bacterial opportunistic pathogens. Acta Crystallographica F 67: 1141–1147.
Leppla, S. H., Robbins, J. B., Schneerson, R., Shiloach, J. (2002) Development of an improved vaccine for anthrax. J Clinical Investigation 110: 141–144.
Lerat, E., Moran, N. (2004) The evolutionary history of Quorum-Sensing systems in bacteria. Mol Biol Evol 21: 903–913.
Lewis, K. (2008) Multidrug tolerance of biofilms and persister cells. Curr Topics Microbiol Immunol 322: 107–131.
Ligeza, A., Tikhonov, A. N., Hyde, J. S. Subczynski, W. K. (1998) Oxygen permeability of thylakoid memranes: electron paramagnetic resonance spin labeling study. Biochim Biophys Acta 1365: 453–463.
Lima, S., Guo, M.S., Chaba, R., Gross, C.A., and Sauer, R.T. (2013) Dual molecular signals mediate the bacterial response to outer-membrane stress. Science 340: 837– 841.
Linley, E., Denyer, S. P., McDonnell G., Simons, C., Maillard, J-Y. (2012) Use of hydrogen peroxide as a biocide: new consideration of its mechanisms of biocidal action. J Antimicrob Chemother 67: 1589–1596.
Liochev, S. I., Fridovich, I. (1993) Modulation of the fumarases of *Escherichia coli* in response to oxidative stress. Arch Biochem Biophys 301: 379–384.
Lopes, D., Melo, T., Santos, N., Rosa, L., Alves, E., et al. (2014) Evaluation of the interplay among the charge of porphyrinic photosensitizers, lipid oxidation and photoinactivation efficiency in *Escherichia coli*. J Photochem Photobiol B 141: 145–153.
López, D., Vlamakis, H., Losick, R., Kolter, R. (2009) Paracrine signaling in a bacterium. Genes Develop 23: 1631–1638.
Loprasert, S., Sallabhan, R., Whangsuk, W. et al. (2002) The *Burkholderia pseudomallei oxyR* gene: expression analysis and mutant characterization. Gene 96:161-169.
Loprasert, S., Sallabhan, R., Whangsuk, W., Mongkolsuk, S. (2000) Characterization and mutagenesis of *fur* gene from *Burkholderia pseudomallei*. Gene 254: 129–137.

Lumjiaktase, P., Diggle, S. P., Loprasert, S., Tungpradabkul, S., Daykin, M., et al. (2006) Quorum sensing regulates *dpsA* and the oxidative stress response in *Burkholderia pseudomallei*. Microbiology 152: 3651–3659.
Lushchak, V. I. (2011) Adaptive response to oxidative stress: bacteria, fungi, plants and animals. Comparative Biochem Physiol 153: 175–190.
Ma, L., Conover, M., Lu, H., Parsek, M. R., Bayles, K., Wozniak, D. J. (2009) Assembly and development of the *Pseudomonas aeruginosa* biofilm matrix. PLoS Pathog 5:e1000354.
Maddula, V. S., Zhang, Z., Pierson, E. A., Pierson, L. S. (2006) Quorum sensing and phenazines are involved in biofilm formation by *Pseudomonas chlororaphis* (*aureofaciens*) strain 30-84. Microb Ecol 52: 289–301.
Mah, T. F., Pitts, B., Pellock, B., Walker, G. C., Stewart, P. S. (2003) A genetic basis for *Pseudomonas aeruginosa* biofilm antibiotic resistance. Nature 426: 306–310.
Maira-Litran, T., Kropec, A., Abeygunawardana, C., Joyce, J., Mark, G. et al. (2002) Immunochemical properties of the staphylococcal poly-N-acetylglucosamine surface polysaccharide. Infect Immun 70: 4433–4440.
Majerczyk, C., Brittnacher, M., Jacobs, M., Armour, C. D., Radey, M., et al. (2014). Global analysis of the *Burkholderia thailandensis* quorum sensing-controlled regulon. J Bacteriol 196: 1412–1424.
Manefield, M., Turner, S. L. (2002) Quorum sensing in context: out of molecular biology and into microbial ecology. Microbiology 148: 3762–3764.
Manchado, M., Micha, K., Pueyo, C. (2000). Hydrogen peroxide activates the SoxRS regulon *in vivo*. J Bacteriol 182: 6842–6844.
Manzo, J., Cocotl-Yanez, M., Tzontecomani, T., Martinez, V.M., Bustillos, R., et al. (2011) Post- transcriptional regulation of the alginate biosynthetic gene *algD* by the Gac/Rsm system in *Azotobacter vinelandii*. J Mol Microbiol Biotechnol 21: 147–159.
Marathe, S. A., Kumar, R., Ajitkumar, P., Nagaraja, V., Chakravortty, D (2013) Curcumin reduces the antimicrobial activity of ciprofloxacin against *Salmonella* typhimurium and *Salmonella* typhi. J Antimicrob Chemother 68: 139-152.
Martinez, A., Kolter, R. (1997) Protection of DNA during oxidative stress by the nonspecific DNA-binding protein Dps. J Bacteriol 179: 5188-5194.
Masip, L., Veeravalli, K., Georgiou, G. (2006) The many faces of glutathione in bacteria. Antiox Redox Signal 8: 753–762.
Massey, V., Strickland, S., Mayhew, S. G., Howell, L. G., Engel, P. C., et al. (1969) The production of superoxide anion radicals in the reaction of reduced flavins and flavoproteins with molecular oxygen. Biochem Biophys Res Commun 36: 891–897.
Massey, V. (1994) Activation of molecular oxygen by flavins and flavoproteins. J Biol Chem 36: 22459–22462.
Matallana-Surget, S., Joux, F., Raftery, M. J., Cavicchioli, R. (2009) The response of the marine bacterium *Sphingopyxis alaskensis* to solar radiation assessed by quantitative proteomics. Environ Microbiol 11: 2660–2675.
Mathee, K., Ciofu, O., Sternberg, C., Lindum, P. W., Campbell, J. I. (1999) Mucoid conversion of *Pseudomonas aeruginosa* by hydrogen peroxide: a mechanism for virulence activation in the cystic fibrosis lung. Microbiology 145: 1349–1357.

Matthysse, A. G., White, S., Lightfoot, R. (1995). Genes required for cellulose synthesis in *Agrobacterium tumefaciens*. J Bacteriol 177: 1069–1075.
Mavrodi, D. V, Peever, T. L., Mavrodi, O. V, Parejko, J., Raaijmakers, J. M. et al. (2010) Diversity and evolution of the phenazine biosynthesis pathway. Appl Environ Microbiol 76: 866–879.
Mc Cay, P. H., Ocampo-Sosa, A. A., Fleming, G. T. (2010) Effect of subinhibitory concentrations of benzalkonium chloride on the competitiveness of *Pseudomonas aeruginosa* grown in continuous culture. Microbiology 156: 30–38.
Mc Dougald, D., Rice, S. a., Barraud, N., Steinberg, P. D., Kjelleberg, S. (2011) Should we stay or should we go: mechanisms and ecological consequences for biofilm dispersal. Nat Rev Microbiol 10: 39–50.
Messner, K. R. , Imlay, J. A. (2002) Mechanism of superoxide and hydrogen peroxide formation by fumarate reductase, succinate dehydrogenase, and aspartate oxidase. J Biol Chem 277: 42563–42571.
Mielich-Suess, B., Lopez, D. (2014) Molecular mechanisms involved in *Bacillus subtilis* biofilm formation. Environ Microbiol 1–23.
Miller, G., Suzuki, N., Rizhsky, L., Hegie, A., Koussevitzky, S., Mittler, R. (2007) Double mutants deficient in cytosolic and thylakoid ascorbate peroxidase reveal a complex mode of interaction between reactive oxygen species, plant development, and response to abiotic stresses. Plant Physiol 144: 1777–1785.
Miller, M. B., Bassler, B. L. (2001) Quorum Sensing in bacteria. Ann Rev Microbiol 55: 165–199.
Mishra, S., Imlay, J. (2012) Why do bacteria use so many enzymes to scavenge hydrogen peroxide? Arch Biochem Biophys 525: 145–160.
Moreira, L. M., Videira, P., Sousa, S., Leitão, J. H., Cunha, M. V., et al. (2003) Identification and physical organization of the gene cluster involved in the biosynthesis of *Burkholderia cepacia* complex exopolysaccharide. Biochem Biophys Res C 312: 323–333.
Mori, I. C., J. I. Schroeder (2004) Reactive oxygen species activation of plant Ca^{2+} channels: a signaling mechanism in polar growth, hormone transduction, stress signaling, and hypothetically mechanotransduction. Plant Physiol 135: 702–708.
Morikawa, M. (2006) Beneficial biofilm formation by industrial bacteria *Bacillus subtilis* and related species. J Biosci Bioeng 101: 1–8.
Mortarino, M., Negri, A., Tedeschi, G., Simonic, T., Duga S, et al. (1996) L-aspartate oxidase from *Escherichia coli*. Characterization of coenzyme binding and product inhibition. Eur J Biochem 239: 418-426.
Mostertz, J., Scharf, C., Hecker, M., Homuth, G. (2004) Transcriptome and proteome analysis of *Bacillus subtilis* gene expression in response to superoxide and peroxide stress. Microbiology 150: 497–512.
Mueller, P., Jacobsen, N. R., Folkmann, J. K., Danielsen, P. H., Mikkelsen, L. et al. (2009) Role of oxidative damage in toxicity of particulates. Free Radic Res 44: 1–46.

Murata, M., Fujimoto, H., Nishimura, K., Charoensuk, K., Nagamitsu, H., et al. (2011) Molecular strategy for survival at a critical high temperature in *Escherichia coli*. PLoS ONE 6: e0020063.
Nadell, C. D., Xavier, J. B., Levin, S. a., Foster, K. R. (2008) The evolution of quorum sensing in bacterial biofilms. PLoS Biology 6: 0171–0179.
Nanda, A. K., Andrio, E., Marino, D., Pauly, N., Dunand, C. (2010) Reactive oxygen species during plant-microorganism early interactions. J Integrative Plant Biol 52: 195–204.
Nemoto, K., Hirota, K., Murakami, K. et al. (2003) Effect of Varidase (streptodornase) on biofilm formed by *Pseudomonas aeruginosa*. Chemother 49: 121-125.
Newton, G. L., Rawat, M., La Clair, J. J., Jothivasan, V. K. et al. (2009) Bacillithiol is an antioxidant thiol produced in Bacilli. Nat Chemical Biol 5: 625-627.
Nicolella, C. (2000) Wastewater treatment with particulate biofilm reactors. J Biotechnol 80: 1-33.
Niederhoffer, E. C., Naranjo, C. M., Bradley, K. L. (1990) Control of *Escherichia coli* superoxide dismutase (*sodA* and *sodB*) genes by the ferric uptake regulation (*fur*) locus. J Bacteriol 172: 1930-1938.
Nunoshiba, T., de Rojas-Walker, T., Wishnok, J.S., Tannenbaum, S.R., Demple, B. (1993) Activation by nitric oxide of an oxidative-stress response that defends *Escherichia coli* against activated macrophages. PNAS USA 90: 9993-9997.
Ogilby, P. R. (2010) Singlet oxygen: there is indeed something new under the sun. Chem Society Rev 39: 3181.
Ono, K., Oka, R., Toyofuku, M., Sakaguchi, A., Hamada, M., et al. (2014) cAMP signaling affects irreversible attachment during biofilm formation by *Pseudomonas aeruginosa* PAO1. Microbes Environments 29: 104-106.
Ooi, W. F., Ong, C., Nandi, T., Kreisberg, J. F., et al. (2013) The condition-dependent transcriptional landscape of *Burkholderia pseudomallei*. PLoS Genet 9: e1003795.
Ortiz-Castro, R., Contreras-Cornejo, H. A., Macías-Rodríguez, L., López-Bucio, J. (2009) The role of microbial signals in plant growth and development. Plant Signal Behavior 4: 701–712.
Ortiz de Orué Lucana, D., Wedderhoff, I., Groves, M. R. (2012) ROS-mediated signalling in bacteria: zinc-containing Cys-X-X-Cys redox centres and iron-based oxidative stress. J Signal Transd 605905.
Ortiz de Orué Lucana, D., Tröller, M., Schrempf, H. (2003) Amino acid residues involved in reversible thiol formation and zinc ion binding in the *Streptomyces reticuli* redox regulator FurS. Mol Genet Genomics 268: 618-627.
Ortiz de Orué Lucana, D., Schrempf, H. (2000) The DNA-binding characteristics of the *Streptomyces reticuli* regulator FurS depend on the redox state of its cysteine residues. Mol Gen Genet 264: 341-353.
Pace, J. L., Rupp, M.E., Finch, R.G. (2006) Biofilms, infection, and antimicrobial therapy. CRC Press Taylor & Francis Group.
Pacher, P., Beckman, J. S., Liaudet, L. (2007) Nitric oxide and peroxynitrite in health and disease. Physiol Rev 87: 315–424.

Painter, K. L., Strange, E., Parkhill, J., Bamford, K. B., Armstrong-James, D., et al. (2015) *Staphylococcus aureus* adapts to oxidative stress by producing H_2O_2-resistant small colony variants via the SOS response. Infection Immun 83: 1830-1844.
Pamp, S. J., Gjermansen, M., Tolker-Nielsen, T. (2007) The biofilm matrix: a sticky framework. In: The biofilm mode of life: mechanisms and adaptations. 37–69.
Pan, Y. (2011) Mitochondria, reactive oxygen species, and chronological aging: a message from yeast. Experimental Gerontology, 46: 847–852.
Park, C., Novak, J. T., Helm, R. F., Ahn, Y.-O., Esen, A. (2008) Evaluation of the extracellular proteins in full-scale activated sludges. Water Research 42: 3879–3889.
Patten, C. L., Kirchhof, M. G., Schertzberg, M. R., Morton, R., Schellhorn, H. E. (2004) Microarray analysis of RpoS-mediated gene expression in *Escherichia coli* K-12. Mol Genetics Genomics 272: 580-591.
Paul, K., Nieto, V., Carlquist, W. C., Blair, D. F., Harshey, R. M. (2010) The c-di-GMP binding protein YcgR controls flagellar motor direction and speed to affect chemotaxis by a "backstop brake" mechanism. Mol Cell 38: 128-139.
Peano, C., Chiaramonte, F., Motta, S., Pietrelli, A., Jaillon, S., et al. (2014) Gene and protein expression in response to different growth temperatures and oxygen availability in *Burkholderia thailandensis*. PLoS ONE 9: e93009.
Pei, Z. M., Murata, Y., Benning, G., Thomine, S., et al. (2000) Calcium channels activated by hydrogen peroxide mediate abscisic acid signalling in guard cells. Nature 406: 731.
Percival, S. L., Hill, K. E., Malic, S., Thomas, D. W., Williams, D. W. (2011) Antimicrobial tolerance and the significance of persister cells in recalcitrant chronic wound biofilms. Wound Repair Regen 19: 1-9.
Pereira, Y., Petit-Glatron, M. F., Chambert, R. (2001) *yveB*, encoding endolevanase LevB, is part of the *sacB–yveB–yveA* levansucrase tricistronic operon in *Bacillus subtilis*. Microbiology 147: 3413–3419.
Pérez-Pantoja, D., Nikel, P. I., Chavarría, M., de Lorenzo, V. (2013) Endogenous stress caused by faulty oxidation reactions fosters evolution of 2, 4-dinitrotoluene-degrading bacteria. PLoS Genetics 9: e1003764.
Pesci, E. C., Milbank, J. B., Pearson, J. P., Mc Knight, S., Kende, A. S. et al. (1999) Quinolone signaling in the cell-to-cell communication system of *Pseudomonas aeruginosa*. PNAS USA 96: 11229-11234.
Pessi, G., Braunwalder, R., Grunau, A., Omasits, U., Ahrens, C. H., Eberl, L. (2013) Response of *Burkholderia cenocepacia* H111 to micro-oxia. PLoS ONE 8: e72939.
Petersen, F. C., Tao, L., Scheie, A. A. (2005) DNAbinding-uptake system: a link between cell-to-cell communication and biofilm formation. J Bacteriol 187: 4392–4400.
Piazza, F., Tortosa, P., Dubnau, D. (1999) Mutational analysis and membrane topology of ComP, a quorum-sensing histidine kinase of *Bacillus subtilis* controlling competence development. J Bacteriol 181: 4540–4548.
Pierson, L. S., Pierson, E. A. (2010) Metabolism and function of phenazines in bacteria: impacts on the behavior of bacteria in the environment and biotechnological processes. Appl Microbiol Biotechnol 86:1659-1670.

Plate, L., Marletta, M. (2012) Nitric oxide modulates bacterial biofilm formation through a multicomponent cyclic-di-GMP signaling network. Molecular Cell 46: 449-460.
Pogliano, J., Lynch, A.S., Belin, D., Lin, E.C., Beckwith, J. (1997) Regulation of *Escherichia coli* cell envelope proteins involved in protein folding and degradation by the Cpx two-component system. Genes Dev 11: 1169-1182.
Polo, A., Foladori, P., Ponti, B., Bettinetti, R., Gambino, M., Villa, F., Cappitelli, F. (2014) Evaluation of zosteric acid for mitigating biofilm formation of *Pseudomonas putida* isolated from a membrane bioreactor system. Int J Mol Sci 15: 9497-9518.
Poole, R.K. (2005) Nitric oxide and nitrosative stress tolerance in bacteria. Biochem Soc Trans 33: 176-180.
Pratt, L. A., Kolter, R. (1998) Genetic analysis of *Escherichia coli* biofilm formation: roles of flagella, motility, chemotaxis and type I pili. Mol Microbiol 30: 285-293.
Premanathan, M., Karthikeyan, K., Jeyasubramanian, K., Manivannan, G. (2011) Selective toxicity of ZnO nanoparticles toward Gram-positive bacteria and cancer cells by apoptosis through lipid peroxidation. Nanomedicine 7: 184-192.
Price-Whelan, A., Dietrich, L. E., Newman, D. K. (2006) Rethinking 'secondary' metabolism: physiological roles for phenazine antibiotics. Nat Chem Biol 2: 71-78.
Prigent-Combaret, C., Brombacher, E., Vidal, O., Ambert, A., Lejeune, P. et al. (2001) Complex regulatory network controls initial adhesion and biofilm formation in *Escherichia coli* via regulation of the *csgD* gene. J Bacteriol 183: 7213-7223.
Proft, T., Baker, E. N. (2009) Pili in Gram-negative and Gram-positive bacteria - structure, assembly and their role in disease. Cell Mol Life Sci 66: 613-635.
Qi, Y., Rao, F., Luo, Z., Liang, Z. X. (2009) A flavin cofactor-binding PAS domain regulates c-di-GMP synthesis in AxDGC2 from *Acetobacter xylinum*. Biochemistry 48: 10275-84.
Qin, Z., Ou, Y., Yang, L., Zhu, Y., Tolker-Nielsen, T., et al. (2007) Role of autolysin-mediated DNArelease in biofilm formation of *Staphylococcus epidermidis*. Microbiology 153: 2083–2092.
Qiu, D., Eisinger, V.M., Head, N.E., Pier, G.B., Yu, H.D. (2008) ClpXP proteases positively regulate alginate overexpression and mucoid conversion in *Pseudomonas aeruginosa*. Microbiology 154: 2119-2130.
Qiu, D., Eisinger, V.M., Rowen, D.W., Yu, H.D. (2007) Regulated proteolysis controls mucoid conversion in Pseudomonas aeruginosa. PNAS USA 104: 8107-8112.
Raivio, T. L., Silhavy, T. J. (2001) Periplasmic stress and ECF sigma factors. Annu Rev Microbiol 55: 591-624.
Reckseidler, S. L., Deshazer, D., Sokol, P., Woods, D. E. et al. (2001) Detection of bacterial virulence genes by subtractive hybridization: identification of capsular polysaccharide of *Burkholderia pseudomallei* as a major virulence determinant detection of bacterial virulence genes by subtractive hybridization. Identificat Infection Immunity 69: 34-44.
Reckseidler, S. L., DeVinney, R., Woods, D. E. (2005) The capsular polysaccharide of *Burkholderia pseudomallei* contributes to survival in serum by reducing complement factor C3b deposition. Infect Immun 73: 1106-1115.
Reckseidler, S. L. (2012) Capsular polysaccharides produced by the bacterial pathogen *Burkholderia pseudomallei*. In: The complex world of polysaccharides. 128-152.

Regev-Yochay, G., Trzciński, K., Thompson, C. M., Malley, R., Lipsitch, M. (2006) Interference between *Streptococcus pneumoniae* and *Staphylococcus aureus*: *in vitro* hydrogen peroxide-mediated killing by *Streptococcus pneumoniae*. J Bacteriol 188: 4996.
Rehm, B.H. (2010) Bacterial polymers: biosynthesis, modifications and applications. Nat Rev Microbiol 8: 578-592.
Remelli, W., Cereda, A., Papenbrock, J., Forlani, F., Pagani, S. (2010) The rhodanese RhdA helps *Azotobacter vinelandii* in maintaining cellular redox balance. Biol Chem 391: 777.
Ren, D., Bedzyk, L., Setlow, P., Thomas, S. M., Ye, R. W., Wood, T. K. (2004) Gene expression in *Bacillus subtilis* surface biofilms with and without sporulation and the importance of *yveR* for biofilm maintenance. Biotechnol Bioengin 86: 344-364.
Reisner, A., Haagensen, J. A., Schembri, M. A., Zechner, E. L. et al. (2003) Development and maturation of *Escherichia coli* K-12 biofilms. Mol Microbiol 48: 933-946.
Rice, K. C., Mann, E. E., Endres, J. L., Weiss, E. C., Cassat J. E., et al. (2007) The *cidA* murein hydrolase regulator contributes to DNA release and biofilm development in *Staphylococcus aureus*. PNAS USA 104: 8113-8118.
Rinaudi, L. V, Giordano, W. (2010) An integrated view of biofilm formation in rhizobia. FEMS Microbiol Letters 304: 1-11.
Roberts, I. S. (1996) The biochemistry and genetics of capsular polysaccharide production in bacteria. Ann Rev Microbiol 50: 285-315.
Robson, R. L., Postgate, J. R. (1980) Oxygen and hydrogen in biological nitrogen fixation. Annu Rev Microbiol 34: 183-207.
Rodriguez, H., Fraga, R. (1999) Phosphate solubilizing bacteria and their role in plant growth promotion. Biotechnol Advances 17: 319-339.
Roemling, U., Gomelsky, M., Galperin, M. Y. (2005) C-di-GMP: the dawning of a novel bacterial signalling system. Mol Microbiol 57: 629-639.
Roemling, U., Rohde, M., Olsén, A., Normark, S., Reinköster, J. (2000) AgfD the checkpoint of multicellular and aggregative behaviour in *Salmonella* typhimurium regulates at least two independent pathways. Mol Microbiol 36: 10-23.
Romero, D., Vlamakis, H., Losick, R., Kolter, R. (2011) An accessory protein required for anchoring and assembly of amyloid fibres in *B. subtilis* biofilms. Mol Microbiol 80: 1155-1168.
Romero, D., Aguilar, C., Losick, R., Kolter, R. (2010) Amyloid fibers provide structural integrity to *Bacillus subtilis* biofilms. PNAS USA 107: 2230-2234.
Ross, P., Mayer, R., Benziman, M. (1991) Cellulose biosynthesis and function in bacteria. Microbiol Rev 55: 35-58.
Rubio, M. C., James, E. K., Clemente, M. R., Bucciarelli, B., Fedorova, M. et al. (2004) Localization of superoxide dismutases and hydrogen peroxide in legume root nodules. Mol Plant Microbe Interact 17: 1294-1305.
Rudrappa, T., Biedrzycki, M. L., Bais, H. P. (2008) Causes and consequences of plant-associated biofilms. FEMS Microbiol Ecol 64: 153-166.

Ryan, R. P., Fouhy, Y., Lucey, J. F., Crossman, L. C., Spiro S. et al. (2006) Cell-cell signaling in *Xanthomonas campestris* involves an HD-GYP domain protein that functions in cyclic di-GMP turnover. PNAS USA 103: 6702-6717.
Saharan, B., Nehra, V. (2011) Plant growth promoting rhizobacteria: a critical review. Life Sci Med Res 1-30.
Saint-Ruf, C., Garfa-Traoré, M., Collin, V., Cordier, C., Franceschi, C., Matic, I. (2014) Massive diversification in aging colonies of *Escherichia coli*. J Bacteriol 196: 3059-3073.
Sandercock, J. R., Page, W. J. (2008) Identification of two catalases in *Azotobacter vinelandii*: a KatG homologue and a novel bacterial cytochrome c catalase. J Bacteriol 190: 954-962.
Sanjay, M. K., Srideshikan, S. M., Vanishree, V. L., Usha, M. S., Raj, P. et al. (2011) Copper, Zinc-superoxide dismutase from clinically isolated *Escherichia coli*: cloning, analysis of *sodC* and its possible role in pathogenicity. Indian J Microbiol 51: 326-331.
Sashidhar, B., Podile, A. R. (2010) Mineral phosphate solubilization by rhizosphere bacteria and scope for manipulation of the direct oxidation pathway involving glucose dehydrogenase. J Appl Microbiol 109: 1-12.
Sauer, K., Camper, A. K. (2001) Characterization of phenotypic changes in *Pseudomonas putida* in response to surface-associated growth. J Bacteriol 183: 6579-6589.
Savakis, P., De Causmaecker, S., Angerer, V., Ruppert, U., Anders, K., et al. (2012) Light-induced alteration of c-di-GMP level controls motility of *Synechocystis* sp. PCC 6803. Mol Microbiol 85: 239-251.
Sawai, H., Yoshioka, S., Uchida, T., Hyodo, M., Hayakawa, Y., et al. (2010) Molecular oxygen regulates the enzymatic activity of a heme-containing diguanylate cyclase (HemDGC) for the synthesis of cyclic di-GMP. Biochim Biophys Acta 1804: 166-172.
Schacht, V. J., Neumann, L. V., Sandhi, S. K., Chen, L., Henning, T. et al. (2013) Effects of silver nanoparticles on microbial growth dynamics. J Appl Microbiol 114: 25-35.
Schellhorn, H. E., Stones, V. L. (1992) Regulation of katF and katE in *Escherichia coli* K-12 by weak acids. J Bacteriol 174: 4769-4776.
Schembri, M., Kjaergaard, K., Klemm, P. (2003) Global gene expression in *Escherichia coli* biofilms. Mol Microbiol 48: 253–267.
Schlich, K., Klawonn, T., Terytze, K., Hund-Rinke, K. (2013) Hazard assessment of a silver nanoparticle in soil applied via sewage sludge. Environ Sci Europe 25, 1-14.
Schobert, M., Tielen, P. (2010) Contribution of oxygen-limiting conditions to persistent infection of *Pseudomonas aeruginosa*. Future Microbiol 5: 603-621.
Schuster, M. P. (2006) A network of networks: quorum-sensing gene regulation in *Pseudomonas aeruginosa*. Int J Med Microbiol 296: 73–81.
Seaver, L. C., Imlay, J. A. (2004) Are respiratory enzymes the primary sources of intracellular hydrogen peroxide? J Biol Chem 279: 48742–48750.
Seaver, L. C., Imlay, J. A. (2001) Alkyl hydroperoxide reductase is the primary scavenger of endogenous hydrogen peroxide in *Escherichia coli*. J Bacteriol 183: 7173-7181.
Semchyshyn, H. (2009) Hydrogen peroxide-induced response in *E. coli* and *S. cerevisiae*: different stages of the flow of the genetic information. Cent Eur J Biol 4: 142-153.

Sharma, S. V., Arbach, M., Roberts, A., Macdonald, C. J., Groom, M., Hamilton, C. J. (2013) Biophysical features of bacillithiol, the glutathione surrogate of *Bacillus subtilis* and other firmicutes. ChemBioChem 14: 2160–2168.
Shaw, S. L., Long, S. R. (2003) Nod factor inhibition of reactive oxygen efflux in a host legume. Plant Physiol 132: 2196-2204.
Sherlock, O., Vejborg, R. M., Klemm, P. (2005) The TibA adhesin/ invasin from enterotoxigenic *Escherichia coli* is self recognizing and induces bacterial aggregation and biofilm formation. Infect Immun 73: 1954-1963.
Sheldon, J. R., Yim, M. S., Saliba, J. H., Chung, W. H., Wong, K. Y., Leung, K. T. (2012) Role of *rpoS* in *Escherichia coli* O157:H7 strain H32 biofilm development and survival. App Environ Microbiol 78: 8331-8339.
Sherman, D. R., Mdluli, K., Hickey, M. J., Arain, T. M., Morris, S. L., Barry, C. E. et al. (1996) Compensatory *ahpC* gene expression in isoniazid-resistant *Mycobacterium tuberculosis*. Science 272: 1641-1643.
Schramm, A., Larsen, L. H., Revsbech, N. P., Ramsing, N. B., Amann, R., Schleifer, K. H. (1996) Structure and function of a nitrifying biofilm as determined by *in situ* hybridization and the use of microelectrodes. App Environ Microbiol 62: 7.
Seth, D., Hausladen, A., Wang, Y.J., Stamler, J.S. (2012) Endogenous protein S-Nitrosylation in *E. coli*: regulation by OxyR. Science 336: 470-473.
Shatalin, K., Shatalina, E., Mironov, A., Nudler, E. (2011) H_2S: a universal defense against antibiotics in bacteria. Science 334: 986-990.
Sies, H. (1997) Oxidative stress: oxidants and antioxidants. Exp Physiol 82: 291–295.
Sim, B. M., Chantratita, N., Ooi, W. F., Nandi, T., Tewhey, R., et al. (2010) Genomic acquisition of a capsular polysaccharide virulence cluster by non-pathogenic *Burkholderia* isolates. Genome Biol 11: R89.
Simm, R., Morr, M., Kader, A., Nimtiz, M., Roemling, U. (2004) GGDEF and EAL domains inversely regulate cyclic di-GMP levels and transition from sessility to motility. Mol Microbiol 53: 1123-1134.
Simpson, J.A., Smith, S.E., Dean, R.T. (1989) Scavenging by alginate of free radicals released by macrophages. Free Radic Biol Med 6: 347–353.
Slauch, J. M. (2011) How does the oxidative burst of macrophages kill bacteria? Still an open question. Mol Microbiol 80: 580-583.
Sotiriou, G. A., Pratsinis, S. E. (2011) Engineering nanosilver as an antibacterial biosensor and bioimaging material. Curr Opin Chem 1: 3–10.
Southam, C.M., Ehrlich, J. (1943) Effects of extract of western red-cedar heartwood on certain wood-decaying fungi in culture. Phytopathol 33: 517-524.
Sprent, J. I., Parsons, R. (2000) Nitrogen fixation in legume and non-legume trees. Field Crops Res. 65: 183-196.
Srivastava, D., Hsieh, M.-L., Khataokar, A., Neiditch, M. B., Waters, C. M. (2013) Cyclic di-GMP inhibits *Vibrio cholerae* motility by repressing induction of transcription and inducing extracellular polysaccharide production. Mol Microbiol 90: 1262-1276.

Stanley, N. R., Lazazzera, B. (2005) Defining the genetic differences between wild and domestic strains of *Bacillus subtilis* that affect poly-γ-DL-glutamic acid production and biofilm formation. Mol Microbiol 1143–1158.
Stark, G. (2005) Functional consequences of oxidative membrane damage. J Membrane Biol 205: 1–16.
Stewart, P. S., Franklin, M. J. (2008) Physiological heterogeneity in biofilms. Nat Rev Microbiol 6: 199-210.
Stoodley, P., Sauer, K., Davies, D. G., Costerton, J. W. (2002) Biofilms as complex differentiated communities. Ann Rev Microbiol 56: 187-209.
Storz, G., Imlay, J.A. (1999) Oxidative stress. Curr Opin Microbiol 2: 188–194.
Tagliabue, L., Maciag, A., Antoniani, D., Landini, P. (2010) The *yddV-dos* operon controls biofilm formation through the regulation of genes encoding curli fibers' subunits in aerobically growing *Escherichia coli*. FEMS Immunol Med Microbiol 59: 477-484.
Tan, S. Y., Chew, S. C., Tan, S. Y.-Y., Givskov, M., Yang, L. (2014). Emerging frontiers in detection and control of bacterial biofilms. Curr Opin Biotechnol 26: 1-6.
Tarutina, M., Ryjenkov, D. A., Gomelsky, M. (2006) An unorthodox bacteriophytochrome from *Rhodobacter sphaeroides* involved in turnover of the second messenger c-di-GMP. J Biol Chem 281: 34751-34758.
Teal, T. K., Lies, D. P., Wold, B. J., Newman, D. K. (2006) Spatiometabolic stratification of *Shewanella oneidensis* biofilms. Appl Environ Microbiol 72: 7324–7330.
Tendolkar, PM, Baghdayan, A.S., Shankar, N. (2005) The N-terminal domain of enterococcal surface protein, Esp, is sufficient for Esp-mediated biofilm enhancement in *Enterococcus faecalis*. J Bacteriol 187: 6213–6222.
Tielker, D., Hacker, S., Loris, R., Strathmann, M., Wingender, J., et al. (2005) *Pseudomonas aeruginosa* lectin LecB is located in the outer membrane and is involved in biofilm formation. Microbiology 151: 1313-1323.
Tomida, H., Yasufuku, T., Fujii, T., Kondo, Y., Kai, T., Anraku, M. (2010) Polysaccharides as potential antioxidative compounds for extended-release matrix tablets. Carbohydrate Res 345: 82-86.
Tormo, M. A., Knecht, E., Götz, F., Lasa, I., Penades, J.R. (2005) Bap-dependent biofilm formation by pathogenic species of *Staphylococcus*, evidence of horizontal gene transfer? Microbiology 151: 2465-2475.
Tran, L. S., Nagai, T., Itoh, Y. (2000) Divergent structure of the ComQXPA quorum-sensing components: molecular basis of strain-specific communication mechanism in *Bacillus subtilis*. Mol Microbiol 37: 1159-1171.
Tsuneda, S., Aikawa, H., Hayashi, H., Yuasa, A., Hirata, A. (2003) Extracellular polymeric substances responsible for bacterial adhesion onto solid surface. FEMS Microbiol Letters 223: 287-292.
Ude, S., Arnold, D. L., Moon, C., D., Timms-Wilson, T., Spiers, A. J. (2006) Biofilm formation and cellulose expression among diverse environmental *Pseudomonas* isolates. Environ. Microbiol 8: 1997-2011.

Urban, T. A., Goldberg, J. B., Forstner, J. F., Sajjan, U. S. (2005). Cable pili and the 22-kilodalton adhesin are required for *Burkholderia cenocepacia* binding to and transmigration across the squamous epithelium. Infect Immun 73: 5426-5437.
Ulrich, R. L., Hines, H. B., Parthasarathy, N., Jeddeloh, J. A. (2004) Mutational analysis and biochemical characterization of the *Burkholderia thailandensis* DW503 quorum-sensing network. J Bacteriol 186: 4350-4360.
Vaara, M. (1992) Agents that increase the permeability of the outer membrane. Microbiol Mol Biol Rev 56: 395-411.
Valle, J., Da Re, S., Schmid, S., Skurnik, D., D'Ari, R., Ghigo, J. M. (2008) The amino acid valine is secreted in continuous-flow bacterial biofilms. J Bacteriol 190: 264-274.
Van Der Heijden, M. G., Bardgett, R. D., Van Straalen, N. M. (2008) The unseen majority: soil microbes as drivers of plant diversity and productivity in terrestrial ecosystems. Ecol Letters 11: 296-310.
Van Houdt, R., Michiels, C. W. (2010). Biofilm formation and the food industry, a focus on the bacterial outer surface. J App Microbiol 109: 1117-1131.
Van Houdt, R., Michiels, C.W. (2005) Role of bacterial cell surface structures in *Escherichia coli* biofilm formation. Res Microbiol 156: 626-633.
Van Loon, L. C., Bakker, P. A. H. M., Pieterse, C. M. J. (1998) Systemic resistance induced by rhizosphere bacteria. Annu Rev Phytopathol 36: 453-483.
Van Merode, A. E. J., Duval, J. F. L., van der Mei, H. C., Busscher, H. J., Krom, B. P. (2008) Increased adhesion of *Enterococcus faecalis* strains with bimodal electrophoretic mobility distributions. Colloids Surfaces B 64: 302-306.
Van Schaik, E. J., Giltner, C. L., Audette, G. F., Keizer, D. W. et al. (2005) DNA binding: a novel function of *Pseudomonas aeruginosa* type IV pili. J Bacteriol 187: 1455-1464.
Vanhooren, P., Vandamme, E. J. (1998) Biosynthesis, physiological role, use and fermentation process characteristics of bacterial exopolysaccharides. Recent Res Devel Fermen Bioeng 1: 253-299.
Veening, J. W., Igoshin, O. A., Eijlander, R. T., et al. (2008) Transient heterogeneity in extracellular protease production by *Bacillus subtilis*. Mol Syst Biol 4: 184.
Verhagen, B. W., Glazebrook, J., Zhu, T., Chang, H. S., van Loon, L. C., Pieterse, C. M. (2004) The transcriptome of rhizobacteria-induced systemic resistance in *Arabidopsis*. Mol Plant-Microbe Int 17: 895-908.
Verhamme, D. T., Kiley, T. B., Stanley-Wall, N. R. (2007) DegU coordinates multicellular behaviour exhibited by *Bacillus subtilis*. Mol Microbiol 65: 554-568.
Villa, F., Borgonovo, G., Cappitelli, F., Giussani, B. (2012a). Sub-lethal concentrations of *Muscari comosum* bulb extract suppress adhesion and induce detachment of sessile yeast cells Biofouling 28: 1107-1117.
Villa, F., Remelli, W., Forlani, F., Gambino, M., Landini, P., Cappitelli, F. (2012b) Effects of chronic sub-lethal oxidative stress on biofilm formation by *Azotobacter vinelandii*. Biofouling 28: 823-833.
Villa, F., Pitts, B., Stewart, P. S., Giussani, B. et al. (2011) Efficacy of zosteric acid sodium salt on the yeast biofilm model *Candida albicans*. Microb Ecol 62: 584 598.

Villa, F., Albanese, D., Giussani, B., Stewart, P. S., Daffonchio, D., Cappitelli, F. (2010) Hindering biofilm formation with zosteric acid. Biofouling 26: 739-752.
Vinckx, T., Matthijs, S., Cornelis, P. (2008) Loss of the oxidative stress regulator OxyR in *Pseudomonas aeruginosa* PAO1 impairs growth under iron-limited conditions. FEMS Microbiol Lett 288: 258-265.
Vlamakis, H., Chai, Y., Beauregard, P., Losick, R., Kolter, R. (2013) Sticking together: building a biofilm the *Bacillus subtilis* way. Nat Rev Microbiol 11: 157-168.
Vu, B., Chen, M., Crawford, R. J., Ivanova, E. P. (2009) Bacterial extracellular polysaccharides involved in biofilm formation. Molecules 14: 2535-2554.
Vuong, C., Kocianova, S., Voyich, J. M., Yao, Y., Fischer, E. R. et al. (2004) A crucial role for exopolysaccharide modification in bacterial biofilm formation, immune evasion, and virulence. J Biol Chem 279: 54881-54886.
Waite, R.D., Paccanaro, A., Papakonstantinopoulou, A. et al. (2006) Clustering of *Pseudomonas aeruginosa* transcriptomes from planktonic cultures, developing and mature biofilms reveals distinct expression profiles. BMC Genomics 7: 162.
Walters, M. C., Roe, F., Bugnicourt, A., Franklin, M. J., Stewart, P. S. (2003) Contributions of antibiotic penetration, oxygen limitation, and low metabolic activity to tolerance of *Pseudomonas aeruginosa* biofilms to ciprofloxacin and tobramycin. Antimicrob Agents Chemother 47: 317-323.
Wang, Q., Suzuki, A., Mariconda, S., Porwollik, S., Harshey, R. M. (2005) Sensing wetness: a new role for the bacterial flagellum. EMBO J 24: 2034-2042.
Waters, C. M., Bassler, B. L. (2005) Quorum sensing: cell-to-cell communication in bacteria. Ann Rev Cell Develop Biol 21: 319-346.
Whitchurch, C. B., Tolker-Nielsen, T., Ragas, P. C., Mattick, J. S. (2002) Extracellular DNA required for bacterial biofilm formation. Science 295: 1487.
Whitfield, C., Valvano, M. (1993) Biosynthesis and expression of cell-surface polysaccharides in Gram-negative bacteria. Adv Microbiol Phys 35: 135-146.
Wiersinga, W. J., van der Poll, T., White, N. J., et al. (2006) Melioidosis: insights into the pathogenicity of *Burkholderia pseudomallei*. Nat Rev Microbiol 4: 272-282.
Williams, P., Camara, M. (2009) Quorum sensing and environmental adaptation in *Pseudomonas aeruginosa*: a tale of regulatory networks and multifunctional signal molecules. Curr Opin Microbiol 12: 182-191.
Williams, P., Camara, M., Hardman, A., et al. (2000) Quorum sensing and the population-dependent control of virulence. Philos Trans R Soc Lond B Biol Sci 355: 667-680.
Wilson, T., Hasting, W. J. (1998) Bioluminescence. Annu Rev Cell Dev Biol 14: 197-230.
Wortham B. W., Patel, C. N., Oliveira, M. A. (2007) Polyamines in bacteria: pleiotropic effects yet specific mechanisms. Adv Exp Med Biol 603: 106-115.
Wu, Y., Ding, Y., Cohen, Y., Cao, B. (2015) Elevated level of the second messenger c-di-GMP in *Comamonas testosteroni* enhances biofilm formation and biofilm-based biodegradation of 3-chloroaniline. Appl Microbiol Biotechnol 99: 1967-1976.
Wu, S., Baum, M. M., Kerwin, J., Guerrero, D., et al. (2014) Biofilm-specific extracellular matrix proteins of nontypeable *Haemophilus influenza* Pathog Dis 72: 143-160.

Wu, Y., Vulić, M., Keren, I., Lewis, K. (2012). Role of oxidative stress in persister tolerance. Antimic Agents Chemoth 56: 4922-4926.
Wu, X., Wang, X., Drlica, K., Zhao, X. (2011) A toxin-antitoxin module in *Bacillus subtilis* can both mitigate and amplify effects of lethal stress. PLoS ONE 6: e23909.
Xie, K., Peng, H., Hu, H., Wang, W., Zhang, X. (2013) OxyR, an important oxidative stress regulator to phenazines production and hydrogen peroxide resistance in *Pseudomonas chlororaphis* GP72. Microbiol Res 168: 646-653.
Yildiz, F.H., Liu, X. S., Heydorn, A., Schoolnik, G. K. (2004) Molecular analysis of rugosity in a *Vibrio cholerae* O1 El Tor phase variant. Mol Microbiol 53: 497–515.
Yin, Y., Withers, T.R., Wang, X., Yu, H.D. (2013) Evidence for sigma factor competition in the regulation of alginate production by *Pseudomonas aeruginosa*. PLoS ONE 8: e72329.
Young, M. E., Alakomi H.-L., Fortune I., Gorbushina A. A., Krumbein W. E., et al. (2008) Development of a biocidal treatment regime to inhibit biological growths on cultural heritage: BIODAM. Environ Geol 56: 631-641.
Zafra, O., Lamprecht-Grandío, M., de Figueras, C. G., González-Pastor, J. E. (2012) Extracellular DNA release by undomesticated *Bacillus subtilis* is regulated by early competence. PloS One 7: e48716.
Zardus, J. D., Nedved, B. T., Huang, Y., Tran, C., Hadfield, M.G. (2008) Microbial biofilms facilitate adhesion in biofouling invertebrates. Biol Bull 214: 91-98.
Zhang, Y., Heym, B., Allen, B., Young, D., Cole, S. (1992) The catalase-peroxidase gene and isoniazid resistance of *Mycobacterium tuberculosis*. Nature 358: 591-593.
Zhao, X., Drlica, K. (2014) Reactive oxygen species and the bacterial response to lethal stress. Curr Opin Microbiol 21: 1–6.
Zheng, L., Chen, Z., Itzek, A., Ashby, M., Kreth, J. (2011) Catabolite control protein A controls hydrogen peroxide production and cell death in *Streptococcus sanguinis*. J Bacteriol 193: 516-526.
Zheng, M., Wang, X., Templeton, L. J., Smulski, D.R., La Rossa, R. A. et al. (2001) DNA microarray-mediated transcriptional profiling of the *Escherichia coli* response to hydrogen peroxide. J Bacteriol 183: 4562-4570.
Zheng, M., Aslund, F., Storz, G. (1998) Activation of the OxyR transcription factor by reversible disulfide bond formation. Science 279: 1718-1721.
Zlosnik, J. E., Hird, T. J., Fraenkel, M. C., Moreira, L. M., Henry, D. A., et al. (2008) Differential mucoid exopolysaccharide production by members of the *Burkholderia cepacia* complex. J Clin Microbiol 46: 1470-1473.
Zogaj, X., Bokranz, W., Nimtz, M., Romling, U. (2003) Production of cellulose and curli fimbriae by members of the family Enterobacteriaceae isolated from the human gastrointestinal tract. Infect Immun 71: 4151-4158.
Zorraquino, V., García, B., Latasa, C., et al. (2013) Coordinated cyclic-di-GMP repression of *Salmonella* motility through YcgR and cellulose. J Bacteriol 195: 417-428.

8. Acknowledgement

This work was supported by fondazione Cariplo and german bilateral Vigoni project.

Thanks to Paolo Landini and Francesca Cappitelli for the opportunity to conduct this PhD study. Having two supervisors can be demanding, but it worst it. I am proud of our collaboration and I hope to have the chance to work again with both of them.
Thanks to Federica Villa, my scientific muse.
Thanks to Thomas Bjarnsholt and Gaziella Cappelletti for being part of my thesis committee.
Thanks to Valeria Marzano and Alberto Vitali for their time and experience.
Thanks to Elio for the figure 2 of this thesis and the long distance support.
Thanks to Tim Tolker-Nielsen, Morten Levin Rybtke and Mustafa Fazli: I learned ten times what I expected in my two months in Copenhagen. Thanks to the rest of the group and especially to Lise and Julie, my Danish friends. Thanks to Chiara Villa, a precious Italian friend in Denmark.
Thanks to the FC lab (Andrews, FedeT, Mauri, Lucy, Cris, Garu), Micro4yoU (Anna, Luigiao, Manu, Violet) and the DD lab (BG, Bessem, Aurorita, Bepps, Eri, Ma, Ramo, Fra, Fusillo's, EleRolli, Davi, Matte, Lore): it wouldn't have been the same without you!
Thanks to the rest of DeFENS, all the FC lab students and our foreign guests.
Thanks to Alice and Gianluca, who contribute to this PhD with their traineeship.
Thanks to Dynamo Camp and A piedi nudi to remind me that I have a beautiful life.
Above all, thanks to Stefano, my family and all my friends to remind me that work is just a part of my beautiful life.

PART II

Contents

Effects of chronic sub-lethal oxidative stress on *Azotobacter vinelandii* biofilm genesis

Federica Villa,[1] William Remelli,[1] Fabio Forlani,[1] Michela Gambino,[2] Paolo Landini,[2] and Francesca Cappitelli[1,*]

[1] Dipartimento di Scienze per gli Alimenti, la Nutrizione e l'Ambiente, Università degli Studi di Milano, via Celoria 2, 20133 Milano, Italy.

[2] Dipartimento di Scienze Biomolecolari e Biotecnologie, Università degli Studi di Milano, via Celoria 26, 20133 Milano, Italy.

*Corresponding author: Francesca Cappitelli, Università degli Studi di Milano, via Celoria 2, 20133 Milano, Italy. Phone: +39-0250319121. Fax: +39-0250319238. E-mail: francesca.cappitelli@unimi.it

ABSTRACT

This work reported how chronic sub-lethal oxidative stress affected biofilm genesis and characteristics of the model bacterium *Azotobacter vinelandii*. To get a continuous source of reactive oxygen species, a strain exposed to chronic sub-lethal oxidative stress as deprived of the gene coding for the antioxidant rhodanese-like protein RhdA (MV474) was employed. In this research MV474 biofilm showed i) seven-fold higher growth rate, ii) induction of catalase and alkyl-hydroxyl-peroxidase enzymes, iii) higher average thicknesses due to increased production of a polysaccharide-rich extracellular matrix and iv) minor susceptibility to hydrogen peroxide than the wild-type strain (UW136). MV474 had a 10-fold and 6-fold increased swimming and swarming activity respectively when compared with UW136. In addition, the level of oxidative stress in the MV474 swarming colony was higher compared to that of UW136, with cells in the center experiencing the highest one. Overall, chronic sub-lethal oxidative events promote the sessile behavior in *Azotobacter vinelandii*.

Keywords: oxidizing biocides; chronic sub-lethal oxidative stress; biofilm; *Azotobacter vinelandii*

INTRODUCTION

Despite extensive research efforts, past and present treatment regimes to control unwanted effects of biofilms has focused on the employment of biocides (Bridier et al. 2011). Oxidizing agents, such as hydrogen peroxide, are increasingly used in a number of medical, food and industrial applications due to their broad spectrum activities, the lack of environmental toxicity following their complete degradation and their inexpensiveness (Linley et al. 2012). Oxidizing biocide formulations are widely used for wounds irrigation, topical medication, surfaces and facilities disinfection, packaging sterilization, water and wastewater treatments (Shintani 2009; Bridier et al. 2011; Linley et al. 2012; Morgenthau et al. 2012). In addition, biocidal active substances are incorporated within a multitude of consumer products, as ingredients used in personal care and household products, together with pharmaceuticals (Gilbert and McBain 2003; Hahn et al. 2010).

Oxidizing biocides induce the production and/or accumulation of reactive oxygen species (ROS). However, there is accumulating evidence suggesting that many non-oxidizing biocides and antibiotics with different sites of action rely, in part, on the elevation in ROS that they elicit (Zuber 2009; Kuczyńska-Wiśnik et al. 2010).

Despite the fact that biocides are generally used at high concentrations to exert the killing action, downstream of the treated area there is likely to be a continuum of biocide concentration ranging from treatment concentration to nil (Gilbert and McBain 2003). Thus, there will be sub-inhibitory levels of biocide at some point along this concentration gradient in all domestic, health care and industrial systems (Mc Cay et al. 2010). In addition, as biocides are used in such large volumes, sooner or later they can be found in natural environments at low (sub-lethal) concentrations leading to a continuous exposure of water and soil microflora (Scenihr 2010).

Thus, the large scale release of these agents by human activities has added a chronic sub-lethal oxidative stress to the bacterial populations, but their response is for most part

unknown. This is an important gap to fill as might result in a reconsideration of the unexpected, and therefore unexplored, effects of low level of biocides on bacterial biofilm formation in both natural and engineered ecosystems to predict their impacts and successful treatment outcomes.

The present study was designed to explore the effects of chronic sub-lethal oxidative stress on bacterial biofilm genesis and characteristics. To address in more detail the impact on the natural environment, the soil bacterium *Azotobacter vinelandii* was used as model system. In the attempts to generate a continuous source of ROS, the target gene *rhdA* coding for the rhodanese-like protein RhdA, was disrupted by deletion generating a strain exposed to chronic sub-lethal oxidative stress (Cereda et al. 2007, 2009; Remelli et al. 2010; Cartini et al. 2011). The picture emerged from recent studies indicates that RhdA (thiosulfate:cyanide sulfurtransferase, E.C. 2.8.1.1, catalyzing in vitro the transfer of a sulfane sulfur atom from thiosulfate to cyanide) displays further activities other than detoxification, playing a key role in maintaining the cellular redox balance in planktonic cells (Cereda et al. 2009; Remelli et al. 2010). Although Remelli et al. (2010) highlighted the potential of RhdA to sustain oxidative imbalance in *A. vinelandii* planktonic cells, no RhdA studies have focused on surface-associated growth model. Thus, using *A. vinelandii* oxidant sensitive strain, we also provided insights into the connection between stress-inducible biofilm formation and rhodanese-like proteins orthologous to RhdA.

MATERIALS AND METHODS

Bacterial strains and growth conditions. The *A. vinelandii* strains used in this study were the wild type strain UW136 and the strain MV474, in which the *rhdA* gene was disrupted by deletion (Colnaghi et al. 1996), that is exposed to chronic sub-lethal oxidative stress. The microorganisms were maintained at -80 °C in suspensions containing 20%

glycerol and 2% peptone, and were grown aerobically in Burk's medium supplemented with 1% sucrose and 15 mM ammonium acetate (BSN medium) for 30 h at 30°C.

Biofilm formation and quantification. Considering the ecological role of *A. vinelandii*, living in habitats such as soil, where water availability is influenced by the solute and matric potentials (Chang and Halverson 2003), the colony-biofilm culturing system to reproduce at lab-scale subaerial biofilm was selected. Colony biofilms of both *A. vinelandii* strains were prepared following the method reported by Anderl et al. (2000). Briefly, 50 µl cell suspension containing 7.5 x 10^5 cells were used to inoculate sterile black polycarbonate filter membranes (0.22 µm pore size and 25 mm diameter, Millipore) resting on agar BSN culture medium. The plates were inverted and incubated at 30°C for 14 days, with the membrane-supported biofilm transferred to fresh culture medium every 48 h. Membranes were collected at 4, 6, 8, 11 and 14 days and transferred to 10 ml glass test tubes pre-filled with 5 ml sterile phosphate buffered saline (PBS, 10 mM phosphate buffer, 0.3 M NaCl pH 7.4 at 25 °C, Sigma-Aldrich). The colony biofilms were vortexed vigorously for 1 min to separate the cells from the membrane. In order to break apart clumps of cells, two cycles of 30 s at 20% power sonication (Branson 3510, Branson Ultrasonic Corporation, Dunburry, CT) followed by 30 s vortex mixing were applied. The resulting cell suspensions were serially diluted, plated on plate count agar (PCA, Sigma Aldrich), incubated 36 h at 30°C and colony forming units (CFU) per membrane were enumerated using the drop-plate method (Herigstad et al. 2001). The specific growth rate of bacteria in colony biofilms was estimated from the CFU data vs. time (h) by the Gompertz model (Zwietering et al. 1990) using the GraphPad Prism software (version 5.0, San Diego, CA, USA). Experiments were performed in triplicate.

Level of oxidative stress. The level of oxidative stress in UW136 and MV474 biofilms was determined by using 2',7'-dichlorofluorescein diacetate (H_2DCFDA) assay according to Jakubowski et al. (2000). The fluorescence of the supernatant was measured using the fluorometer VICTOR™ *X* Multilabel Plate Readers (Perkin Elmer), excitation 490 nm and emission 519 nm. The emission values were normalized by the protein concentration. Experiments were conducted in triplicates.

Enzymatic activities. Biofilm biomass was collected at 4, 6, 8, 11 and 14 days and transferred into a glass test tubes pre-filled with 2 ml lysing buffer (10 mM Tris-HCl, 100 mM NaCl, pH 8). Cell-free extracts of UW136 and MV474 biofilms were obtained by sonication (six 30-s sonication cycles followed by 1 min cooling periods, all on ice, in Sonoplus UW-2070), and cell debris was removed by centrifugation for 15 min at 10,000 x *g*. The protein concentration was determined by the Bradford assay (Bradford 1976) using bovine serum albumin as a standard.

Thiosulfate:cyanide sulfurtransferase (TST) activity was tested by the discontinuous method described by Sörbo (1953) that quantifies the product, thiocyanate, based on the absorption of the ferric thiocyanate complex. One unit of TST activity is defined as the amount of enzyme that produces 1 µmol thiocyanate per minute at 37°C.

Catalase activity was determined in cell-free cultures as described by Cereda et al. (2009) in which the disappearance of peroxide is followed spectrophotometrically at 240 nm. One unit of catalase activity is defined as the amount of enzyme that decomposes 1 µmol of H_2O_2 per min at 37 °C.

Aconitase activity was tested by using cell-free extracts anaerobically prepared following the formation of cis-aconitate from citrate at 240 nm at 30 °C (Cereda et al. 2007). One unit was defined as the amount of enzyme necessary to produce 1 µmol of cis-aconitate per minute ($\varepsilon_{240\ nm}$ = 3.6 mM^{-1} x cm^{-1}).

All the experiments were performed in triplicate.

Expression analysis of alkyl hydroperoxide reductase gene (*ahpC*) using RT-PCR. Biofilm biomass was collected at 4, 6, 8 and 14 days and total RNA was isolated using the RNeasy minikit (QIAGEN) according to the manufacturer's protocols. Reverse transcription was performed on 1,200 ng of total RNA, using RevertAid™ H Minus First Strand cDNA Synthesis Kit (Fermentas Int. Inc., Italy) and random hexamer primer. Quantitative real-time PCR was performed as previously described by Remelli et al. (2010). Negative controls were performed with 2 ng non-reverse transcribed RNA as a template, and in the absence of a template. In positive controls, genomic DNA was used as a template. Data were elaborated according to Livak and Schmittgen (2001) using 16S rRNA as a reference. Relative expression levels were obtained by normalizing the *ahpC* transcript levels to that of the UW136 at day 4 (that was assigned a value of 1).

SDS polyacrylamide gel electrophoresis and immunoblotting. Biofilm biomass was collected at 4, 6 and 14 days. Denaturing gel electrophoresis (SDS-PAGE) was done according to Laemmli (1970) by using the whole cell lysates obtained by heat denaturation of cellular pellets in Laemmli buffer containing 0.35 M β-mercaptoethanol. Western blot analyses were carried out by a standard protocol using anti-RhdA antiserum (Remelli et al. 2010). Red Ponceau S-stained blotted membranes, and immunolabeled membranes were digitized with an Expression 1680 Pro scanner (Epson Italia S.p.A., Milan, Italy).

Extraction and characterization of the extracellular polymeric substances (EPS). Approximately 0.4 g of 14-days old biofilm biomass of both wild-type and oxidant sensitive strains were collected and resuspended in 2 ml 2% ethylenediaminetetraacetic acid (EDTA, Sigma Aldrich, Italy). Biofilm cell suspensions were shaken at 300 rpm for 3 h at

4℃. After incubation, the samples were centrifuged for 20 min, 8,000 *x g* at 4℃ and the supernatant filtered through 0.2 µm polyethersulfone membranes (S623; Whatman, Florhan Park, NJ). Then, one half of the eluate was used for quantification of proteins and carbohydrates and cell lysis analysis, while the second half was used for extracellular DNA (eDNA) precipitation by the cetyltrimethylammonium bromide (CTAB)-DNA method as described by Corinaldesi et al. (2005). The method of Bradford (1976) was applied for analyzing protein concentrations, whereas the optimized microplate phenol–sulfuric acid assay was applied for carbohydrate determination (Masuko et al. 2005) using glucose as the standard. The results obtained were normalized by the weight of the wet biofilm biomass. Experiments were performed in triplicate.

Biofilm cryosectioning, staining and microscopic examination. Fourteen days-old colony biofilms were covered carefully with a layer of Killik (Bio Optica, Italy) and placed on dry ice until completely frozen. Frozen samples were sectioned at -19℃ using a Leitz 1720 digital cryostat (Leica, Italy). The 10-µm thick cryosections were mounted on slide glasses treated with Vectabond (Vector laboratories, Italy), a non-protein tissue section adhesive. The lectin Concanavalin A-Texas Red conjugate (ConA, Invitrogen, Italy) was used to visualize the polysaccharide component of EPS, whereas Syto 9 green fluorescent nucleic acid stain (Invitrogen, Italy) was used to display biofilm cells. Biofilm sections were incubated with 200 µg μl^{-1} ConA and 5 mM Sito-9 (Invitrogen) dye solution in PBS at room temperature in the dark for 30 min and then rinsed with PBS. Biofilm sections were visualized using a Leica TCSNT confocal laser scanning microscope with excitation at 488 nm, and emission ≥ 530 nm. Images were captured with a 10X/NA 0.45 dry lens objective and analyzed with the software Imaris (Bitplane Scientific Software, Zurich, Switzerland). The sections were also examined by fluorescence microscopy using Leica DM 4000 B

microscope at a magnification of 100X and biofilm thickness measured as reported by Villa et al. (2011).

Biofilm susceptibility assay. A volume of 2-chlorobenzoic acid and hydrogen peroxide stock solutions was added to molten culture medium BSN to create a biocide-amended agar for biofilm experiments. The final biocide concentration in biofilm assays were 6 mM 2-chlorobenzoic acid and 4.5 mM hydrogen peroxide. Six-days old and 14-days old biofilms of both strains were aseptically transferred to either biocide-containing agar or a control plate where they were incubated for an additional 16 h at room temperature. After this time, biofilm biomass was collected, physically disaggregated, serially diluted and plated on PCA as reported above. Antimicrobial efficacy was expressed as $\log_{10}$ microbial survival. The $\log_{10}$ reduction was calculated relative to the cell count in the control samples without biocides. All antimicrobial experiments were conducted in triplicate.

Motility assay and level of oxidative stress in swarming colonies. The swimming motility plates were prepared with 10 g l^{-1} tryptone, 5 g l^{-1} NaCl and 0.3% (wt/vol) agarose. Swim plates were incubated at 30 °C for 24 h. Swarming media consisted of 0.5% (wt/vol) Bacto-agar with 8 g l^{-1} Difco nutrient broth, to which 5 g l^{-1} glucose was added. Both swarm and swim plates were allowed to dry at room temperature for 4 h before being used. Plates were inoculated with a 5 µl of a 28 h-old culture of both strains in BSN, onto the top of the agar and incubated at 30 °C for 48 h. Results were expressed as the diameter (mm) of the area of observed motility at the agar surface.

Cells localized in both the center of swarming colonies and the tip of swarming colony migrating front were harvested using an inoculation loop and transferred into 50 mM sodium phosphate buffer pH 7.4. Levels of oxidative stress were measured as previously

described for UW136 and MV474 biofilms. The results obtained were normalized by the weight of the collected biomass. All the experiments were performed in triplicate.

Statistical analysis. T-test or analysis of variance (ANOVA) via a software run in MATLAB environment (Version 7.0, The MathWorks Inc, Natick, USA) were applied to statistically evaluate any significant differences among the samples. Tukey's honestly significant different test (HSD) was used for pairwise comparison to determine the significance of the data. Statistically significant results were depicted by *p*-values < 0.05.

RESULTS

Chronic sub-lethal oxidative stress increases *A. vinelandii* biofilm formation.

MV474 biofilm grew about seven-fold faster than the wild-type strain (Growth $rate_{UW136}$: $5.10 \times 10^6 \pm 2.87 \times 10^5$ CFU h^{-1}; Growth $rate_{MV474}$: $3.46 \times 10^7 \pm 4.34 \times 10^6$ CFU h^{-1}) (Figure 1a). Biofilm biomass raised significantly in MV474 after day 4, reaching a plateau at day 11. MV474 retains only a residual TST activity (about 17%) with respect to that revealed in UW136 (Figure 1b). The residual TST activity was not correlated with the presence of RhdA in MV474 (Figure 1c). The TST activity in UW136 increased during the initial stages of biofilm development, reaching a maximum level at day 6, then decreased and remained steady during biofilm maturation. Western blot analysis demonstrated that the TST activity of UW136 is assignable to the expressed RhdA (Figure 1c).

In both UW136 and MV474, the level of endogenously generated oxidative stress was found to progressively decrease over time, reaching minimum levels in mature biofilm (Figure 2a). Interestingly, MV474 exhibited a peak at day 4 (two-fold increase level compared with UW136), followed by a dramatic decline at day 6. The oxidative stress levels in both UW136 and MV474 remained steady and comparable after day 8.

The levels of catalase activity were higher in MV474 biofilm than in UW136 biofilm. However, the enzyme activity decreased over time in MV474 while it was constant throughout the UW136 biofilm development (Figure 2b).

Expression analysis of *ahpC* gene revealed that at day 4 the level of *ahpC* transcript in MV474 was approximately seven-fold higher than in UW136 (Figure 2c). During biofilm growth *ahpC* gene expression in MV474 biofilm decreased over time in line with oxidative events previously observed. By contrast, the modulation of *ahpC* transcript occurred in *A. vinelandii* wild-type biofilm showed an opposite trend. The *ahpC* transcript in UW136 biofilm was greatly induced after 6 days, when compared with the gene transcriptional level observed in MV474 biofilm (Figure 2c).

Aconitase activity was overall higher in MV474biofilm that in the wild-type biofilm, and it decreased over time (Figure 2d). In the case of UW136, levels of aconitase activity were kept constant throughout the biofilm development.

The biofilm grown under chronic sub-lethal oxidative stress exhibits a polysaccharide-rich extracellular polymeric matrix.

The polysaccharide/protein ratios of the wild type strain and the oxidant sensitive strain biofilms were 0.84 mg $g^{-1}_{biomass}$ and 4.25 mg $g^{-1}_{biomass}$ respectively (Figure 3). Thus, the MV474 biofilm had a considerably higher polysaccharide content, whereas the UW136 biofilm produced an equal amount of proteins and carbohydrates. No statistically significant difference in the eDNA content between UW136 and MV474 was observed.

The strain exposed to chronic sub-lethal oxidative stress forms a thick biofilm at the solid/air interface.

The fluorescently-labelled ConA, mainly accumulated inside the cell-free void of mature microcolonies, demonstrated the presence of the EPS fraction confined in the central part

of the biofilm and the growth of a subaerial biofilm. In addition, MV474 strain synthesized a polysaccharide-richer matrix (Figure 4).

Images captured from frozen sections showed that MV474 and UW136 biofilm retained similar morphological patterns. Interestingly, *A. vinelandii* subaerial biofilms showed a more patchy architecture with empty holes at the bottom of the structure close to the solid surface. Cryosectioning combined with microscopy revealed that MV474 biofilm (biofilm thickness 328 ± 36 µm) was significantly thicker than the biofilm formed by the UW136 (biofilm thickness 217 ± 46 µm).

The biofilm grown under chronic sub-lethal oxidative stress is resistant to hydrogen peroxide but not to 2-chlorobenzoic acid.

Six- and 14-days old UW136 biofilm experienced a 2.10 ± 0.05 $\log_{10}$ reduction and 1.59 ± 0.15 $\log_{10}$ reduction in the CFU number after 2-chlorobenzoic acid treatment (Figure 5). The $\log_{10}$ reductions observed for the MV474 biofilms (6-days old 1.70 ± 0.15; 14-days old 1.33 ± 0.10) were not statistically different from that of the wild-type. However, 6- and 14-days old MV474 biofilm exhibited a 0.65 ± 0.08 and 0.11 ± 0.07 $\log_{10}$ CFU reduction after exposure to hydrogen peroxide, which indicated that it was statistically significant less susceptible than the UW136 biofilm (6-days old 0.65 ± 0.08; 14-days old 1.81 ± 0.04) treated with the same biocide.

The strain exposed to chronic sub-lethal oxidative stress shows an increased flagella-driven motility and an increased level of ROS in swarming colonies.

MV474 sustained a surface-associated movement resulting in a faster and efficient colonization of the polycarbonate membrane (Figure 6a,b). MV474 showed a 10-fold and 6-fold increase in both swimming and swarming movement respectively compared to UW136 (Figure 6c,d).

The level of oxidative stress in MV474 swarmer cell population was higher compared to UW136 (Figure 6e). The MV474 cell subpopulation harvested at the swarming migration front appeared to be under less oxidative stress than the MV474 cell subpopulation collected at the center (Figure 6e).

DISCUSSION

Oxidizing biocides play an important role in the control of bacterial biofilm in a variety of applications and are thus a precious resource that must be managed so as to be protected from loss of activity over time. In order to preserve the role of oxidizing biocides in infection control and hygiene, it is paramount to know their effects on biofilm genesis and characteristics at sub-inhibitory concentrations, a situation normally encountered in all domestic, health care, industrial and natural systems (Mc Cay et al. 2010). Learning the biofilm response of the soil model bacterium *A. vinelandii* to chronic sub-lethal oxidative stress is thus a relevant task to envisage implications of the current predominant biocide regime.

The results obtained in this study showed the enhanced ability of *A. vinelandii* to develop subaerial biofilm under chronic sub-lethal oxidative events. Cartini et al. (2011) observed that the planktonic growth rates of both wild-type UW136 and MV474 were comparable. Explanations for these apparently contrasting results could be based on the significant differences between the planktonic and the biofilm phenotype in term of physiology, gene expression pattern and morphology. As biofilm constitutes the dominant mode of microbial life in most natural and artificial ecosystems, it is important to focus on the sessile point of view. During the surface-associated growth, chronic oxidative events in MV474 strain generated a stress condition to which the bacterium responds by adopting the biofilm lifestyle more efficiently than the UW136 strain. Bacteria that have been previously exposed to chemical stresses, benzalkonium chloride-adapted *Pseudomonas aeruginosa*,

revealed a higher ability to adhere to surfaces and develop biofilms, especially on benzalkonium chloride-conditioned surfaces, which thereby enhanced resistance to sanitation (Machado et al. 2011).

Recently, Zuroff et al. (2011) examined the antibiotic tolerance of *E. coli* colony biofilm on the LB medium depending on the growth phase. Temporal transcriptional analysis showed that genes associated with a stress response were induced in the early biofilm but not in mature biofilms (Domka et al. 2007). According to these results, the highest TST activity in UW136 was recorded at day 6 indicating that at this biofilm development phase maximum RhdA functionality is claimed. The residual TST activity measured in MV474 biofilm was not modulated with a trend correlated to that observed in wild-type biofilm and could be due to the redundancy of rhodanese-like genes in the *A. vinelandii* genome (Cartini et al. 2011) since no RhdA was immunodetected in MV474 biofilm. Taken together, these data suggested a sensitive growth stage in biofilm development, corresponding to the early stage of biofilm formation. Likely, the elevated oxidative stress level observed in the most vulnerable biofilm growth step, the early stage, might provide the selective pressure to increase MV474 biofilm forming capacity. As the biofilm reaches the mature phase, a reduced metabolic activity and enhanced redox buffer ability may avoid stress inducers, providing an explanation for the low level of ROS detected in MV474 biofilm.

In line with the oxidant events, both the activity of the hydrogen peroxide scavenger catalase and the levels of the *ahpC* transcript were higher in MV474 biofilm than in UW136 and decreased along with the biofilm development. In *E. coli* and other bacteria, the thiol-based redox sensors OxyR positively regulates genes such as those encoding catalase and alkyl hydroperoxide reductase, involved in peroxide scavenging, DNA protection and restoration of the thiol-redox balance of the cell (Pomposiello and Demple 2001; Hishinuma et al. 2006). Some researchers observed an attenuation in biofilm development in mutant strains lacking the redox-sensitive protein OxyR in several microbes, including *E.*

coli (Reisner et al. 2003) *P. aeruginosa* (Sauer et al. 2002), *Serratia marcescens* (Shanks et al. 2007), *Porphyromonas gingivalis* (Wu et al. 2008) and *Tannerella forsythia* (Honma et al. 2009). Although OxyR-regulated responses in *A. vinelandii* are unknown, the presence in *A. vinelandii* chromosome of a gene coding for a protein homologous with OxyR could be taken as an indication that similar adaptive mechanisms exist in *A. vinelandii* (Cereda et al. 2009).

In this study, aconitase, which catalyses the interconversion of citrate and isocitrate in the citric acid and glyoxylate cycles, had an overall activity higher in MV474 than in UW136 biofilm, that decreased over time. AcnB, the major aconitase during normal growth conditions, completely loses activity in response to strong oxidants due to its iron-sulfur cluster (Tang et al. 1999), causing the increased production of aconitase A (AcnA), invulnerable to oxidative inactivation in vivo (Varghese et al. 2003). Cereda et al. (2009) reported the overexpression of AcnA in MV474 planktonic cells. Collectively, enzymatic and transcriptomic data proved that the genesis of MV474 biofilm under chronic sub-lethal oxidative stress conditions made it more prone to develop efficient defensive strategies against ROS injuries than the wild-type developed under physiological/standard conditions. Temporal resolution of both oxidant events and activation of ROS-scavenging systems in *A. vinelandii* may have industrial, medical and agricultural relevance contributing to fine-tuning of ROS levels and their signaling properties.

The oxidative stress affected also the composition of the EPS, producing a polysaccharide-rich extracellular polymeric matrix. ConA derived signal was much stronger in the strain exposed to chronic sub-lethal oxidative stress than the wild-type, indicating that these sugars are mainly composed of mannose and glucose. The increased amounts of polysaccharides favoring adherence (Ahimou et al. 2007; Ying et al. 2010) may be part of a stress response, as it is seen in colanic acid synthesis by *E. coli* and other enterobacterial species (Chen et al. 2004). Also Ionesco and Belkin (2009) observed an

overproduction of exopolysaccharides as adaptive action to the lack of general stress response sigma factor RpoS in *E. coli.* Shemesh and colleagues (2010) reported that sub-lethal doses of the oxidizing biocide chlorine dioxide stimulated biofilm formation in *Bacillus subtilis* as well as in other bacteria inducing matrix gene transcription. In addition, previous studies have shown that several bacteria respond to sub-lethal doses of antibiotics by increasing polysaccharides synthesis and biofilm formation (Rachid et al. 2000; Hoffman et al. 2005).

Both the strains formed a flat biofilm with a compact and uniform architecture in contact with the air and a more patchy structure near the solid surface, creating empty holes at the bottom. These structures might facilitate transport of nutrients and gases deeper into the matrix by diffusion. Biofilm of the strain exposed to chronic oxidative stress is thicker than the wild-type biofilm corroborating the ability of MV474 to produce the highest biofilm biomass.

The hypotheses that oxidative stress repair mechanism might increase the emergence of resistant bacteria and the promotion of cross-resistance to other structurally and functionally unrelated biocides was also investigated. That MV474 biofilm was less susceptible to the effective and fast-acting biocide hydrogen peroxide than UW136 biofilm was not surprising as the catalase activity in the oxidant sensitive strain MV474 was higher than in UW136. However, the MV474 biofilm cells tolerance increased with the biofilm maturity and not with the level of catalase activity per se. A mature biofilm provides high level of protection from external stress like biocides rather that early biofilm due to the barrier properties of the EPS, the physiological state of biofilm organisms and the existence of subpopulations of resistant phenotypes (Hall-Stoodley et al. 2004; Boles and Singh 2008; Simões et al. 2011).

Both UW136 and MV474 showed the same tolerance to 2-chlorobenzoic acid. Warth (1991) reported that the toxicity of chlorinated phenols arises from both specific and nonspecific

chemical interactions with bacterial membranes. Differences in the biocidal mode of action between hydrogen peroxide and chlorobenzoic acid could explain the different susceptibility of MV474 to the different antimicrobial agents.

MV474 strain exhibited a robust migration activity over the polycarbonate surface. This bacterial migration activity is an intrinsically surface-linked phenomenon, leading to a change from an individual (swimming) to a collective "social" behavior (swarming) that allows the rapid exploration and colonization of surfaces. Motility assays of the peritrichous flagellated *A. vinelandii* revealed that MV474 had an increased swimming and swarming activity when compared with the wild-type strain UW136. Swimming and swarming are two important systems of bacterial motility required for the competitive fitness during surface colonization processes (Kearns 2010). Recently, Butler et al. (2010) stated that bacterial swarming is an effective strategy for prevailing against antimicrobials by maintaining high cell density, circulating within the multilayered colony to minimize exposure to the antimicrobials, and the death of individuals that are directly exposed. In addition, the level of oxidative stress in MV474 swarmer cell population was higher compared to that of UW136, and cells remaining in the center of the swarming colony experienced the highest one. Recently, Tremblay and Déziel (2010) demonstrated that in *P. aeruginosa* oxidative stress response genes like *katA* and *katB* (catalase), *ahpF* (alkyl hydroperoxide reductase) and *trxB2* (thioredoxin reductase 2) were up-regulated in swarm center and not in tendril tips. Thus, tendril tip cells function as «scouts» whose main purpose is to rapidly spread on uncolonized surfaces while swarm center population are in a state allowing a permanent settlement of the colonized area (biofilm-like) (Tremblay and Déziel 2010). Decision-making between rapidly colonizing a surface and biofilm formation is central to bacterial survival among competitors and hostile environment (Verstraeten et al. 2008). These results allow us to propose a model explaining the ability of strain exposed to chronic sub-lethal oxidative stress to better colonize the available surface in the biofilm

phenotype: during biofilm growth a high cell density may lead to the accumulation of excessive ROS. Thus, MV474 starts to differentiate in a motile phenotype and migrate over the polycarbonate surface. As cells move out in swarming rafts, the concentration of ROS decreases, and cells are unable to maintain the differentiated state and de-differentiate back to the biofilm phenotype. During growth, ROS build up again, and differentiation/swarming proceeds for a second cycle generating a surface-linked phenomenon.

In summary, the inactivation of rhodanese RhdA acts as continuous generator of sub-lethal oxidative events that promote the social behaviour orchestrating biofilm genesis, the activity of ROS-scavenging systems and the switch between swarming and biofilm-like phenotypes. These findings suggest that sub-inhibitory concentrations of oxidizing biocides may not necessarily produce a burden on bacterial biofilm but in some occasions may enhance some characteristics potentially useful for colonization of specific environments, downscaling the efficacy of biocide treatments. The diversity and adaptability produced by oxidative stress repair mechanism could help biofilm communities survive in harsh environments. In addition, these results contribute to a better understanding of the connection between stress-inducible biofilm formation and rhodanese-like proteins orthologous to RhdA.

Acknowledge

This work was partially supported by Fondazione Cariplo, grant no. 2011-0277.

REFERENCES

Ahimou F, Semmens MJ, Haugstad G, Novak PJ. 2007. Effect of protein, polysaccharide, and oxygen concentration profiles on biofilm cohesiveness. Appl Environ Microbiol 73:2905-2910.

Anderl JN, Franklin MJ, Stewart PS. 2000. Role of antibiotic penetration limitation in *Klebsiella pneumoniae* biofilm resistance to ampicillin and ciprofloxacin. Antimicrob Agents Chemother 44:1818-1824.

Boles BR, Singh PK. 2008. Endogenous oxidative stress produces diversity and adaptability in biofilm communities. Proc Natl Acad Sci USA 105:12503-12508.

Bradford MM. 1976. A rapid and sensitive method for the quantitation of microgram quantities of protein utilizing the principle of protein-dye binding. Anal Biochem 72:248-254.

Bridier A, Briandet R, Thomas V, Dubois-Brissonnet F. 2011. Resistance of bacterial biofilms to disinfectants: a review. Biofouling 27:1017-1032.

Butler MT, Wang Q, Harshey RM. 2010. Cell density and mobility protect swarming bacteria against antibiotics. Proc Natl Acad Sci USA 107:3776-3781.

Cartini F, Remelli W, Dos Santos PC, Papenbrock J, Pagani S, Forlani F. 2011. Mobilization of sulfane sulfur from cysteine desulfurases to the *Azotobacter vinelandii* sulfurtransferase RhdA. Amino Acids 41:141-150.

Cereda A, Carpen A, Picariello G, Iriti M, Faoro F, Ferranti P, Pagani S. 2007. Effects of the deficiency of the rhodanese-like protein RhdA in *Azotobacter vinelandii*. FEBS Lett 581:1625-1630.

Cereda A, Carpen A, Picariello G, Tedeschi G, Pagani S. 2009. The lack of rhodanese RhdA affects the sensitivity of *Azotobacter vinelandii* to oxidative events. Biochem J 418:135-143.

Chang WS, Halverson LJ. 2003. Reduced water availability influences the dynamics, development, and ultrastructural properties of *Pseudomonas putida* biofilms. J Bacteriol 185:6199-6204.

Chen J, Lee SM, Mao Y. 2004. Protective effect of exopolysaccharide colanic acid of *Escherichia coli* O157:H7 to osmotic and oxidative stress. Int J Food Microbiol 93:281-286.

Colnaghi R, Pagani S, Kennedy C, Drummond M. 1996. Cloning, sequence analysis and overexpression of the rhodanese gene of *Azotobacter vinelandii*. Eur J Biochem 236:240-248.

Corinaldesi C, Danovaro R, Dell'Anno A. 2005. Simultaneous recovery of extracellular and intracellular DNA suitable for molecular studies from marine sediments. Appl Environ Microbiol 71:46-50.

Domka J, Lee J, Bansal T, Wood TK. 2007. Temporal gene-expression in *Escherichia coli* K-12 biofilms. Environ Microbiol 9:322-346.

Gilbert P, McBain AJ. 2003. Potential impact of increased use of biocides in consumer products on prevalence of antibiotic resistance. Clin Microbiol Rev 16:189-208.

Hahn S, Schneider K, Gartiser S, Heger W, Mangelsdorf I. 2010. Consumer exposure to biocides--identification of relevant sources and evaluation of possible health effects. Environ Health 9:7.

Hall-Stoodley L, Costerton JW, Stoodley P. 2004. Bacterial biofilms: from the natural environment to infectious diseases. Nat Rev Microbiol 2:95-108.

Herigstad B, Hamilton M, Heersink J. 2001. How to optimize the drop plate method for enumerating bacteria. J Microbiol Methods 44:121-129.

Hishinuma S, Yuki M, Fujimura M, Fukumori F. 2006. OxyR regulated the expression of two major catalases, KatA and KatB, along with peroxiredoxin, AhpC in *Pseudomonas putida*. Environ Microbiol 8:2115-2124.

Hoffman LR, D'Argenio DA, MacCoss MJ, Zhang Z, Jones RA, Miller SI. 2005. Aminoglycoside antibiotics induce bacterial biofilm formation. Nature 436:1171-1175.

Honma K, Mishima E, Inagaki S, Sharma A. 2009. The OxyR homologue in *Tannerella forsythia* regulates expression of oxidative stress responses and biofilm formation. Microbiology 155:1912-1922.

Ionescu M, Belkin S. 2009. Overproduction of exopolysaccharides by an *Escherichia coli* K-12 *rpoS* mutant in response to osmotic stress. Appl Environ Microbiol 75:483-492.

Jakubowski W, Biliński T, Bartosz G. 2000. Oxidative stress during aging of stationary cultures of the yeast *Saccharomyces cerevisiae*. Free Radic Biol Med 28:659-664.

Kearns DB. 2010. A field guide to bacterial swarming motility. Nat Rev Microbiol 8:634-644.

Kuczyńska-Wiśnik D, Matuszewska E, Furmanek-Blaszk B, Leszczyńska D, Grudowska A, Szczepaniak P, Laskowska E. 2010. Antibiotics promoting oxidative stress inhibit formation of *Escherichia coli* biofilm via indole signalling. Res Microbiol 161:847-853.

Laemmli UK. 1970. Cleavage of structural proteins during the assembly of the head of bacteriophage T4. Nature 227:680-685.

Linley E, Denyer SP, McDonnell G, Simons C, Maillard J-Y. Use of hydrogen peroxide as a biocide: new consideration of its mechanisms of biocidal action. J Antimicrob Chemother doi: 10.1093/jac/dks129.

Livak KJ, Schmittgen TD. 2001. Analysis of relative gene expression data using real-time quantitative PCR and the 2(-ΔΔCT) method. Methods 25:402-408.

Machado I, Graça J, Sousa AM, Lopes SP, Pereira MO. 2011. Effect of antimicrobial residues on early adhesion and biofilm formation by wild-type and benzalkonium chloride-adapted *Pseudomonas aeruginosa*. Biofouling. 27:1151-1159.

Masuko T, Minami A, Iwasaki N, Majima T, Nishimura S, Lee YC. 2005. Carbohydrate analysis by a phenol-sulfuric acid method in microplate format. Anal Biochem 339:69-72.

Mc Cay PH, Ocampo-Sosa AA, Fleming GT. 2009. Effect of subinhibitory concentrations of benzalkonium chloride on the competitiveness of *Pseudomonas aeruginosa* grown in continuous culture. Microbiology 156:30-38.

Morgenthau A, Nicolae AM, Laursen AE, Foucher DA, Wolfaardt GM, Hausner M. 2012. Assessment of the working range and effect of sodium dichloroisocyanurate on *Pseudomonas aeruginosa* biofilms and planktonic cells. Biofouling 28:111-120.

Pomposiello PJ, Demple B. 2001. Redox-operated genetic switches: the SoxR and OxyR transcription factors. Trends Biotechnol 19:109-114.

Rachid S, Ohlsen K, Witte W, Hacker J, Ziebuhr W. 2000. Effect of subinhibitory antibiotic concentrations on polysaccharide intercellular adhesin expression in biofilm-forming *Staphylococcus epidermidis*. Antimicrob Agents Chemother 44:3357-3363.

Reisner A, Haagensen JA, Schembri MA, Zechner EL, Molin S. 2003. Development and maturation of *Escherichia coli* K-12 biofilms. Mol Microbiol 48:933-946.

Remelli W, Cereda A, Papenbrock J, Forlani F, Pagani S. 2010. The rhodanese RhdA helps *Azotobacter vinelandii* in maintaining cellular redox balance. Biol Chem 391:777-784.

Sauer K, Camper AK, Ehrlich GD, Costerton JW, Davies DG. 2002. *Pseudomonas aeruginosa* displays multiple phenotypes during development as a biofilm. J Bacteriol 184:1140-1154.

SCENIHR. 2010. Assessment of the Antibiotic Resistance Effects of Biocides.

Shanks RM, Stella NA, Kalivoda EJ, Doe MR, O'Dee DM, Lathrop KL, Guo FL, Nau GJ. 2007. A *Serratia marcescens* OxyR homolog mediates surface attachment and biofilm formation. J Bacteriol 189:7262-7272.

Shemesh M, Kolter R, Losick R. 2010. The biocide chlorine dioxide stimulates biofilm formation in *Bacillus subtilis* by activation of the histidine kinase KinC. J Bacteriol 192:6352-6356.

Shintani H. 2009. Application of vapor phase hydrogen peroxide sterilization to endoscope. Biocontrol Sci 14:39-45.

Simões LC, Lemos M, Pereira AM, Abreu AC, Saavedra MJ, Simões M. 2011. Persister cells in a biofilm treated with a biocide. Biofouling. 27:403-411.

Sörbo, B. 1953. Rhodanese. Acta Chem Scand 7:1137-1145.

Tang Y, Guest JR, Artymiuk PJ, Read RC, Green J. 2004. Post-transcriptional regulation of bacterial motility by aconitase proteins. Mol Microbiol 51:1817-1826.

Tremblay J, Déziel E. 2010. Gene expression in *Pseudomonas aeruginosa* swarming motility. BMC Genomics 11:587.

Varghese S, Tang Y, Imlay JA. 2003. Contrasting sensitivities of *Escherichia coli* aconitase A and B to oxidation and iron depletion. J Bacteriol 185:221-230.

Verstraeten N, Braeken K, Debkumari B, Fauvart M, Fransaer J, Vermant J, Michiels J. 2008. Living on a surface: swarming and biofilm formation. Trends Microbiol 16:496-506.

Villa F, Pitts B, Stewart PS, Giussani B, Roncoroni S, Albanese D, Giordano C, Tunesi M, Cappitelli F. 2011. Efficacy of zosteric acid sodium salt on the yeast biofilm model *Candida albicans*. Microb Ecol 62:584-598.

Warth AD. 1991. Mechanism of action of benzoic acid on *Zygosaccharomyces bailii*: effects on glycolytic metabolite levels, energy production, and intracellular pH. Appl Environ Microbiol 57:3410-3414.

Wu J, Lin X, Xie H. 2008. OxyR is involved in coordinate regulation of expression of *fimA* and *sod* genes in *Porphyromonas gingivalis*. FEMS Microbiol Lett 282:188-195.

Ying W, Yang F, Bick A, Oron G, Herzberg M. 2010. Extracellular polymeric substances (EPS) in a hybrid growth membrane bioreactor (HG-MBR): viscoelastic and adherence characteristics. Environ Sci Technol 44:8636-8643.

Zuber P. 2009. Management of oxidative stress in *Bacillus*. Annu Rev Microbiol 63:575-597.

Zuroff TR, Bernstein H, Lloyd-Randolfi J, Stewart PS, Carlson RP. 2010. Robustness analysis of culturing perturbations on *Escherichia coli* colony biofilm beta-lactam and aminoglycoside antibiotic tolerance. BMC Microbiol 10:185.

Zwietering MH, Jongenburger I, Rombouts FM, van 't Riet K. 1990. Modeling of the bacterial growth curve. Appl Environ Microbiol 56:1875-1881.

Figure captions

Figure 1. Growth dynamic (a) and TST activity (b) in *A. vinelandii* biofilms. Data represent the mean ± standard deviation of three independent measurements. The graph provides the *p*-values obtained by ANOVA analysis. According to post-hoc analysis (Tukey's HSD, $p<0.05$), means sharing the same letter are not significantly different from each other. Panel (c) displays the RhdA expression in *A. vinelandii* UW136 and MV474 strains during biofilm development. A 30 kDa protein was immunodetected, corresponding to the monomeric form of RhdA.

Figure 2. Oxidative events (a), catalase activity (b), relative expression of *ahpC* gene (c) and aconitase activity (d) in biofilms of *A. vinelandii* UW136 and MV474 strains. Data represent the mean ± standard deviation of three independent measurements. The graph provides the *p*-values obtained by ANOVA analysis. According to post-hoc analysis (Tukey's HSD, $p<0.05$), means sharing the same letter are not significantly different from each other.

Figure 3. EPS biochemical composition in *A. vinelandii* UW136 and MV474 biofilms. Data represent the mean ± standard deviation of three independent measurements. The graph provides the *p*-values obtained by Student's t-test analysis. A star (*) indicates statistically significant difference at the 95% confidence level between wild-type and oxidant sensitive strains.

Figure 4. Cryosectioning images from *A. vinelandii* subaerial UW136 and MV474 biofilms. Live cells were stained in green with Syto9, whereas the polysaccharide component of the EPS matrix was stained in red with Texas Red-labelled Concanavalin A. Scale bars represent 70 µm or 100 µm.

Figure 5. Susceptibility of UW136 and MV474 biofilms to antimicrobial agents observed as $\log_{10}$ reduction in the number of CFU after exposure to 6 mM 2-chlorobenzoic acid (2-CBA) and 4.5 mM hydrogen peroxide (HP). Data represent the mean ± standard deviation of three independent measurements. The graph provides the *p*-values obtained by ANOVA analysis. According to post-hoc analysis (Tukey's HSD, $p<0.05$), means sharing the same letter are not significantly different from each other.

Figure 6. Surface-associated behaviours influenced by the oxidative stress. Panels (a) and (b) display the pattern formation over a polycarbonate membrane of biofilms of UW136 and MV474 *A. vinelandii* strains respectively. Panel (c) shows swarming motility of UW136 and MV474 strains. Panel (d) displays swimming and swarming colony expansion radius of UW136 and MV474 strains. Data represent the mean ± standard deviation of three independent measurements. The graph provides the *p*-values obtained by Student's t-test analysis. A star (*) indicates statistically significant difference at the 95% confidence level between wild-type and oxidant sensitive strains. Panel (e) reports the level of oxidative stress of the swarmer cell population harvested at the center of swarming colony and at the edge of a swarming colony migration front. Data represent the mean ± standard deviation of three independent measurements. The graph provides the *p*-values obtained by ANOVA analysis. According to post-hoc analysis (Tukey's HSD, $p<0.05$), means sharing the same letter are not significantly different from each other.

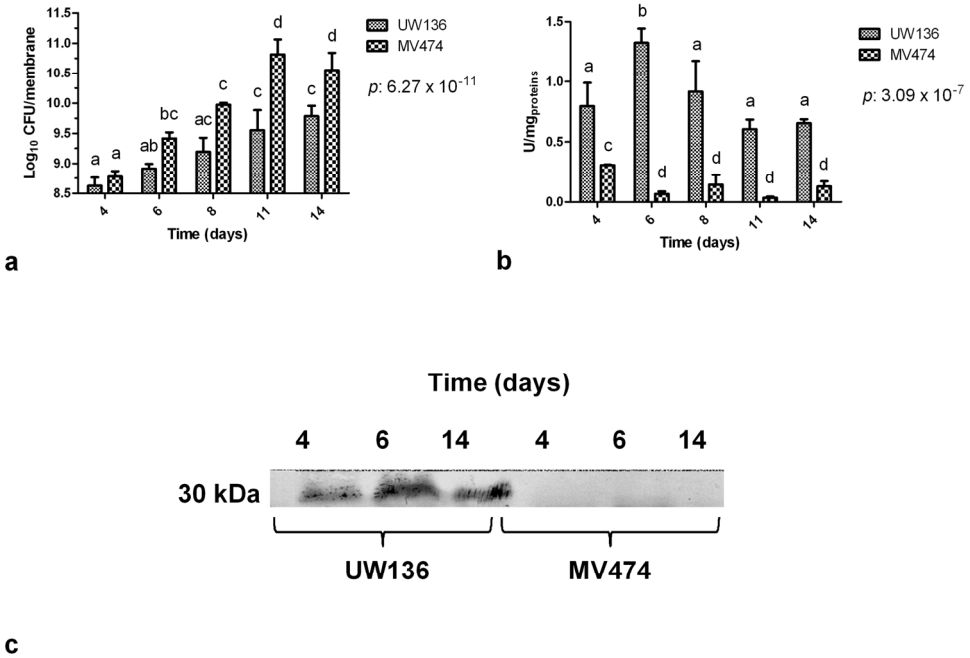

Growth dynamic (a) and TST activity (b) in A. vinelandii biofilms. Data represent the mean ± standard deviation of three independent measurements. The graph provides the p-values obtained by ANOVA analysis. According to post-hoc analysis (Tukey's HSD, $p<0.05$), means sharing the same letter are not significantly different from each other. Panel (c) displays the RhdA expression in A. vinelandii UW136 and MV474 strains during biofilm development. A 30 kDa protein was immunodetected, corresponding to the monomeric form of RhdA.
185x129mm (300 x 300 DPI)

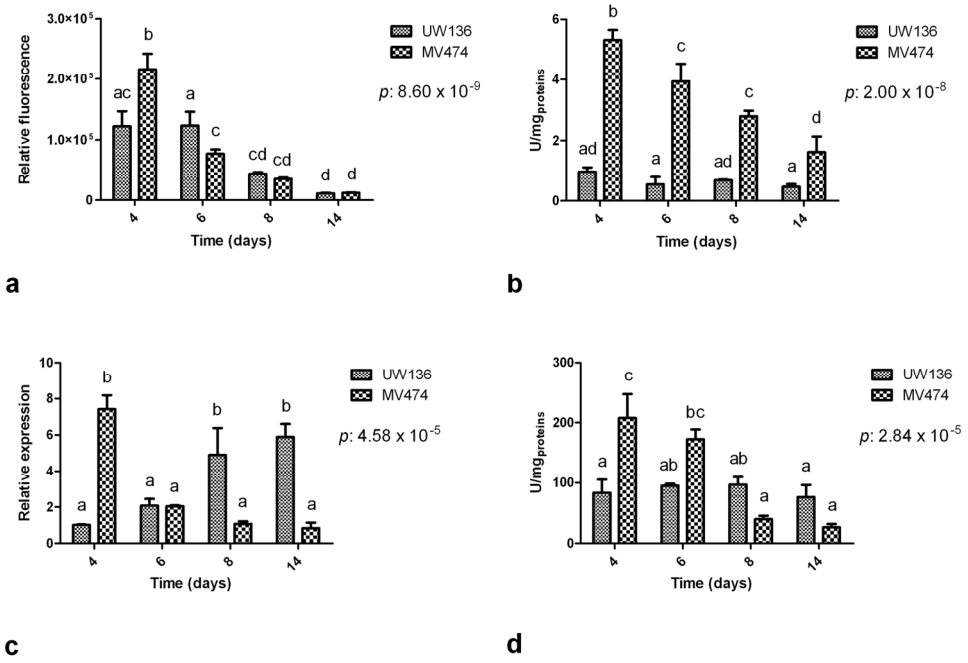

Oxidative events (a), catalase activity (b), relative expression of ahpC gene (c) and aconitase activity (d) in biofilms of A. vinelandii UW136 and MV474 strains. Data represent the mean ± standard deviation of three independent measurements. The graph provides the p-values obtained by ANOVA analysis. According to post-hoc analysis (Tukey's HSD, $p<0.05$), means sharing the same letter are not significantly different from each other.

181x127mm (300 x 300 DPI)

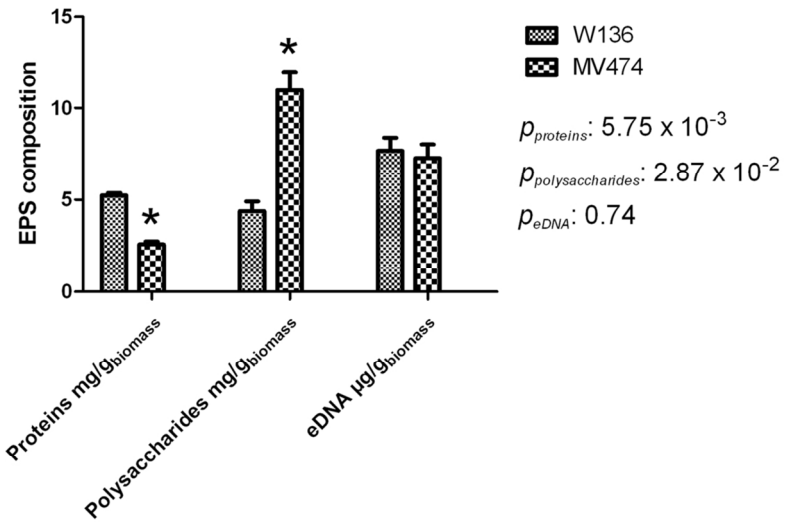

EPS biochemical composition in A. vinelandii UW136 and MV474 biofilms. Data represent the mean ± standard deviation of three independent measurements. The graph provides the p-values obtained by Student's t-test analysis. A star (*) indicates statistically significant difference at the 95% confidence level between wild-type and oxidant sensitive strains.
121x79mm (300 x 300 DPI)

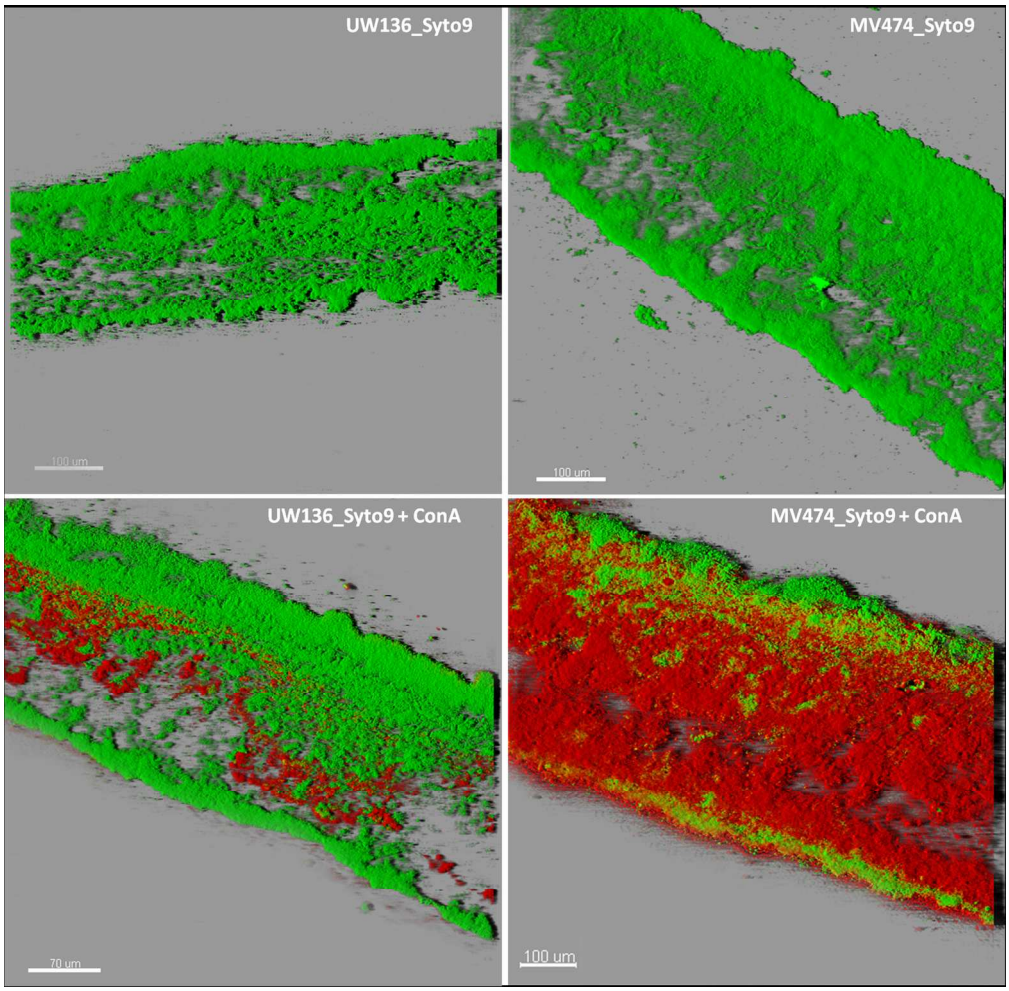

Cryosectioning images from A. vinelandii subaerial UW136 and MV474 biofilms. Live cells were stained in green with Syto9, whereas the polysaccharide component of the EPS matrix was stained in red with Texas Red-labelled Concanavalin A. Scale bars represent 70 μm or 100 μm.
161x158mm (300 x 300 DPI)

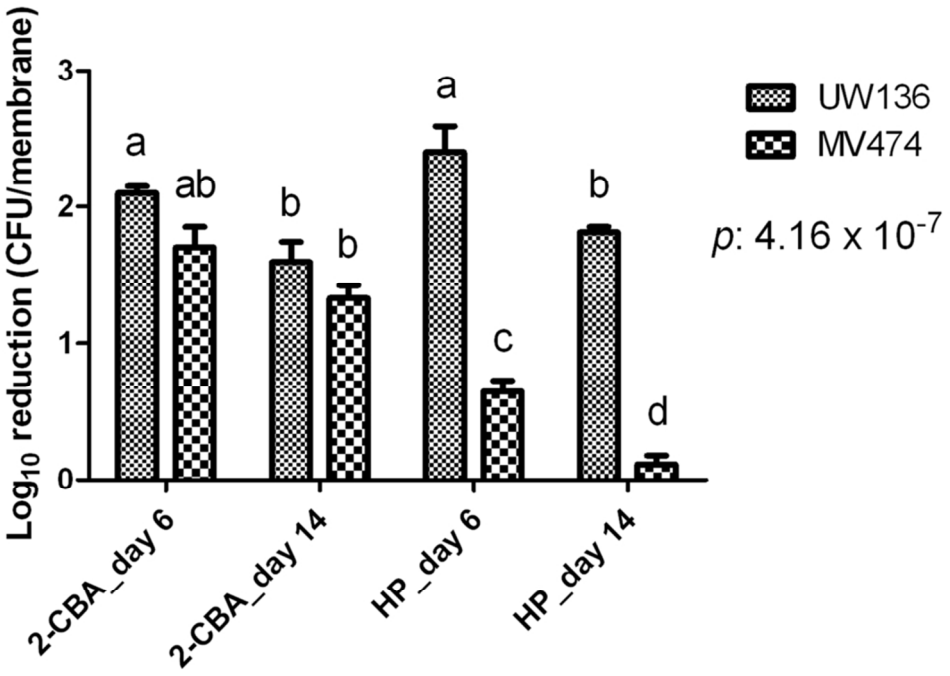

Susceptibility of UW136 and MV474 biofilms to antimicrobial agents observed as log10 reduction in the number of CFU after exposure to 6 mM 2-chlorobenzoic acid (2-CBA) and 4.5 mM hydrogen peroxide (HP). Data represent the mean ± standard deviation of three independent measurements. The graph provides the p-values obtained by ANOVA analysis. According to post-hoc analysis (Tukey's HSD, $p<0.05$), means sharing the same letter are not significantly different from each other.
88x62mm (300 x 300 DPI)

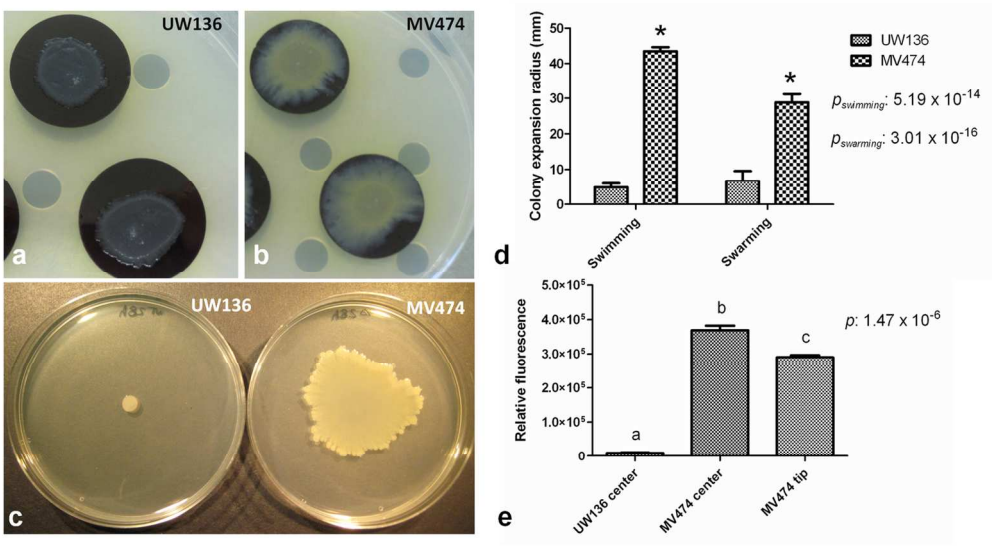

Surface-associated behaviours influenced by the oxidative stress. Panels (a) and (b) display the pattern formation over a polycarbonate membrane of biofilms of UW136 and MV474 A. vinelandii strains respectively. Panel (c) shows swarming motility of UW136 and MV474 strains. Panel (d) displays swimming and swarming colony expansion radius of UW136 and MV474 strains. Data represent the mean ± standard deviation of three independent measurements. The graph provides the p-values obtained by Student's t-test analysis. A star (*) indicates statistically significant difference at the 95% confidence level between wild-type and oxidant sensitive strains. Panel (e) reports the level of oxidative stress of the swarmer cell population harvested at the center of swarming colony and at the edge of a swarming colony migration front. Data represent the mean ± standard deviation of three independent measurements. The graph provides the p-values obtained by ANOVA analysis. According to post-hoc analysis (Tukey's HSD, $p<0.05$), means sharing the same letter are not significantly different from each other.
139x76mm (300 x 300 DPI)

Journal of Applied Microbiology

Journal of Applied Microbiology ISSN 1364-5072

ORIGINAL ARTICLE

Effects of sublethal doses of silver nanoparticles on *Bacillus subtilis* planktonic and sessile cells

M. Gambino[1], V. Marzano[2], F. Villa[3], A. Vitali[2], C. Vannini[4], P. Landini[1] and F. Cappitelli[3]

1 Department of Biosciences, Università degli Studi di Milano, Milan, Italy
2 Institute of Chemistry of Molecular Recognition, Consiglio Nazionale delle Ricerche (CNR), Rome, Italy
3 Department of Food, Environmental and Nutritional Sciences, Università degli Studi di Milano, Milan, Italy
4 Department of Biotecnology and Life Science, Università degli Studi dell'Insubria, Varese, Italy

Keywords
Bacillus, biofilms, proteomics, rhizosphere, stress response.

Correspondence
Paolo Landini, Department of Biosciences, Università degli Studi di Milano, Via Celoria 26, 20133 Milan, Italy.
E-mail: paolo.landini@unimi.it
and
Francesca Cappitelli, Department of Food, Environmental and Nutritional Sciences, Università degli Studi di Milano, Via Celoria 2, 20133 Milan, Italy.
E-mail: francesca.cappitelli@unimi.it

2014/2544: received 12 December 2014, revised 10 February 2015 and accepted 14 February 2015

doi:10.1111/jam.12779

Abstract

Aims: Due to their antimicrobial activity, silver nanoparticles (Ag-NPs) are being increasingly used in a number of industrial products. The accumulation of Ag-NPs in the soil might affect plant growth-promoting rhizobacteria and, in turn, the plants. We describe the effects of Ag-NPs on the soil bacteria *Azotobacter vinelandii* and *Bacillus subtilis*.
Methods and Results: In growth-inhibition studies, *A. vinelandii* showed extreme sensitivity to Ag-NPs, compared to *B. subtilis*. We investigated the effects of Ag-NPs at subinhibitory concentrations, both on planktonic and sessile *B. subtilis* cells. As determined by 2,7-dichlorofluorescein-diacetate assays, Ag-NPs increase the formation of reactive oxygen species in planktonic cells, but not in sessile cells, suggesting the activation of scavenging systems in biofilms. Consistently, proteomic analysis in *B. subtilis* Ag-NPs-treated biofilms showed increased production of proteins related to quorum sensing and involved in stress responses and redox sensing. Extracellular polysaccharides production and inorganic phosphate solubilization were also increased, possibly as part of a coordinated response to stress.
Conclusions: At low concentrations, Ag-NPs killed *A. vinelandii* and affected cellular processes in planktonic and sessile *B. subtilis* cells.
Significance and Impact of the Study: Re-direction of gene expression, linked to selective toxicity, suggests a strong impact of Ag-NPs on soil bacterial communities.

Introduction

Nanoparticles (NPs) are defined as material that is at least one dimension below 100 nm (Handy *et al.* 2008). Such a small size confers NPs features that are different from the bulk material, i.e. higher chemical reactivity, resistance and electrical conductivity and, potentially, higher biological activity (Nel *et al.* 2006).

Silver NPs (Ag-NPs) are widely used for medical and industrial applications, e.g. for biological implants, air and water treatment filters, clothing, paints, cosmetics and food storage containers (Duncan 2011; Levard *et al.* 2012). The NP formulation increases the antimicrobial properties of silver, making Ag-NPs effective against a broad spectrum of bacterial and fungal species (Sotiriou and Pratsinis 2011; Guo *et al.* 2013), including antibiotic-resistant strains (Schacht *et al.* 2013).

The growing diffusion of Ag-NPs in commercially available products used daily (Benn and Westerhoff 2008) leads to a NP dispersal in the environment that is difficult to track and quantify. The release of Ag-NPs into the environment mainly occurs through the application of sewage sludge to agricultural land (Schlich *et al.* 2013). This procedure is still adopted in many countries (Gottschalk and Sonderer 2009), although the sludge may contain substantial amounts of heavy metals (Bourioug *et al.* 2015) and transfer them to soil. Despite scientific models identified the soil as a major NP sink (Mueller *et al.* 2009), their actual concentrations in the environment are often unknown, and their biological

activity still needs to be investigated (Whitley *et al.* 2013).

Some soil micro-organisms, defined as plant growth-promoting rhizobacteria (PGPR), promote plant growth through several indirect or direct mechanisms, such as nutrient uptake, regulation of plant physiology by mimicking the synthesis of plant hormones and increase in mineral and nitrogen availability in the soil (Philippot *et al.* 2013). PGPR can also increase heavy metal solubility, helping plants withstand pollutants contamination (Vacheron *et al.* 2013).

Previous studies have shown that exposure to Ag-NPs leads to significant mortality in various bacteria, mainly through membrane damage (Hachicho *et al.* 2014) and oxidative stress, via Ag-NP-induced reactive oxygen species (ROS) (Fabrega *et al.* 2009). While antimicrobial activity and efficacy of Ag-NP has been the focus of a variety of studies, aiming to use Ag-NPs as an alternative to antibiotics (Rai *et al.* 2012), little information is available regarding the possible effects of sublethal doses. To identify mechanisms activated by bacteria to face Ag-NP presence in soil, we have studied the effects of Ag-NPs at concentrations up to 10 mg l^{-1} on two plant growth-promoting rhizobacteria: the Gram-negative nitrogen-fixing bacterium *Azotobacter vinelandii*, and *Bacillus subtilis*, a Gram-positive bacterium. We found that 10 mg l^{-1} Ag-NPs strongly inhibited *A. vinelandii* growth and induced the oxidative stress response and exopolysaccharide production in *B. subtilis*. Our results suggest that Ag-NPs, at a concentration range locally found in the soil environment, can induce ROS production and select soil microbial population. Interestingly, we also found that, in *B. subtilis*, plant growth-promoting activities, in particular, inorganic phosphate solubilization, were activated by sublethal Ag-NP concentrations. Possible implications on soil microbial community are discussed.

Materials and methods

Bacterial strains and growth conditions

Bacillus subtilis wild type strain Cu1065 and *Azotobacter vinelandii* wild type strain UW136 were maintained at −80°C in suspensions containing 20% glycerol. *Bacillus subtilis* was grown aerobically in Tryptic Soy Broth (TSB) medium for 12 h at 30°C. *Azotobacter vinelandii* was grown in Burk's medium supplemented with 1% sucrose and 15 mmol l^{-1} ammonium acetate for 30 h at 30°C. Silver nanoparticles (Ag-NPs; 10 nm OECD PVP BioPure Silver Nanoparticles, nanoComposix, San Diego, CA, USA) were stored at 4°C as 1 mg ml^{-1} suspension in water, and were added to liquid medium, or uniformly distributed on the agar surface, immediately prior to the start of the experiments. According to the supplier, purchased Ag-NPs have a diameter of 8·3 ± 1·5 nm, hydrodynamic diameter smaller than 20 nm and negative zeta potential (−19 mV).

Effects of Ag-NPs on planktonic growth

Bacillus subtilis and *A. vinelandii* growth in the presence of Ag-NPs at various concentrations (0, 0·01, 0·1, 1, 10, and 100 mg l^{-1}) was monitored, registering the optical density (OD) at 600 nm every 45 min with a microtitre reader (Biotek-Power Wave XS2, BioTek, Winooski, VT, USA). The results were confirmed plating cell suspensions from stationary phase serially diluted on agarized media, incubated at 30°C (overnight for *B. subtilis*, 36 h for *A. vinelandii*) and the colony forming units (CFU) were enumerated using the drop-plate method (Herigstad *et al.* 2001). Experiments were conducted in triplicate. Growth curves were used to calculate the generation time for each condition.

Transmission electron microscopy study

Samples for transmission electron microscopy (TEM) analysis were collected from liquid cultures both in exponential and stationary phases, respectively, after 3 and 8 h of growth in contact with 0 and 10 mg l^{-1} of NPs. Cells were centrifuged (30 min, 7000 ***g***) and fixed in an equal volume of 2·5% glutaraldehyde in cacodylate buffer (pH 7·4) at 4°C overnight. The samples were then rinsed with 0·1 mol l^{-1} cacodylate buffer followed by postfixation in cacodylate buffer supplemented with 1% (w/v) osmium tetroxide. Fixed cell suspensions were washed with cacodylate buffer, dehydrated in an ethanol gradient (once for 15 min in 25%, 50%; once for 1 h in 70%; once for 15 min in 90%, 95% and two times for 15 min in 100%) and then in propylene oxide for 20 min. The samples were infiltrated and finally embedded in Epon Araldite at 60°C for 24 h. The polymerized samples were sectioned into ultra-thin slices (80 nm in thickness) and placed on collodion-coated copper grid (400 meshes). The slices were examined by TEM with Leo912ab (Zeiss, Jena, Germany) at 80 kV.

Ten images with a reduced enlargement of both the control and the treated samples were analysed after exposure to uranyl acetate (10 min) and to lead citrate (5 min) to count live and dead cells, considering cells with no significant morphological alterations as live cells.

TEM analysis was also used to verify the absence of aggregated NPs in the conditions used.

Biofilm formation

Colony biofilms of *B. subtilis* were prepared following the method reported (Anderl *et al.* 2000). Briefly, 10 μl of

cell suspension containing $1{\cdot}5 \times 10^6$ cells were used to inoculate sterile black polycarbonate filter membranes (0·22 mm pore size, Whatman, UK) that were placed on TSA plates, at 30°C, either in the absence or in the presence of Ag-NPs (1 or 10 mg l^{-1}). Ag-NPs were poured on agar plates to be adsorbed. The membranes were transferred every 48 h to fresh media, and grown for 8 days in total.

Colony biofilm quantification with Bradford assay and ATP assay

Total protein amount and average ATP consumption were determined to assess relative amounts of biomass and metabolic activity in colony biofilms.

For protein determination, a membrane was collected every 24 h and resuspended in a 10-ml tube with 2 ml of sterile phosphate buffered saline (PBS, 10 mmol l^{-1} phosphate buffer, 0·3 mol l^{-1} NaCl, pH 7·4). Cells were broken by five cycles of 30 s sonication with 30 s intervals; cell lysates were centrifuged for 15 min at 4°C at 19 000 ***g*** and the supernatant was collected. The protein amount was quantified by Bradford assay (Bradford 1976), using bovine serum albumin as the standard. Experiments were performed in triplicate.

Bacterial metabolic activity in colony biofilm was assessed using the biomass detection kit (Promicol, Sittard, The Netherlands). The experiments were performed according to the manufacturer's protocol using the FB 14 Vega bioluminometer (Berthold Detection Systems, Pforzheim, Germany). Relative light units per second (RLU s^{-1}) values were converted to ATP concentrations (nmol ml^{-1}) using the standard provided. Colony biofilm was resuspended in 100 mmol l^{-1} Tris (pH 7·75), vortexed and sonicated for 30 s (Kobayashi *et al.* 2009). A calibration curve was generated by measuring RLU s^{-1} in *B. subtilis* planktonic cells. The tests were performed in triplicate.

Level of oxidative stress on planktonic and sessile cells

The level of oxidative stress in planktonic and sessile cells of *B. subtilis* was determined using the 2,7-dichlorofluorescein-diacetate (H_2DCFDA) assay (Jakubowski *et al.* 2000).

Bacillus subtilis planktonic cells grown at 30°C for 12 h in TSB, with either 0, 1 or 10 mg l^{-1} of Ag-NPs, were washed with PBS and resuspended in 50 mmol l^{-1} PBS, while, for the colony biofilm, one membrane biofilm was collected for 8 days, scraped and homogeneously resuspended in 2 ml of 50 mmol l^{-1} PBS.

Seven hundred and fifty microlitre of cell suspension was incubated with 10 μmol l^{-1} H_2DCFDA at 30°C for 30 min, vortexed and centrifuged. The supernatant was collected to measure fluorescence relative to the extracellular ROS presence. To evaluate intracellular ROS concentrations in either planktonic or biofilm cultures, cells were washed three times and broken with five cycles of 30 s sonication with 30 s intervals. The fluorescence of the supernatant collected before (outer oxidative stress) and after cell sonication (inner oxidative stress) was measured using the fluorometer VICTOR TM X Multilabel Plate Readers (Perkin Elmer, Milan, Italy), excitation 490 nm and emission 519 nm. The emission values were normalized against the protein concentration, obtained from the remaining 750 μl of cell suspension with the Bradford assay. Experiments were conducted in triplicate.

Extraction and characterization of the extracellular polymeric substances (EPS)

Extracellular polymeric substance extraction and characterization was conducted as described by Villa *et al.* (2012) on 5-day-old biofilm biomass, grown in contact with 0 and 10 mg l^{-1} Ag-NPs. The cetyltrimethylammonium bromide (CTAB)-DNA method described by Corinaldesi *et al.* (2005) was used to quantify the extracellular DNA (eDNA). The Bradford method was applied to analyse protein concentrations, whereas the optimized microplate phenol-sulphuric acid assay was applied for carbohydrate determination (Masuko *et al.* 2005) using glucose as the standard. The results obtained were normalized by the cellular protein concentration. Experiments were performed in triplicate.

Proteomic analysis

Protein extracts were obtained by lysing, homogenizing and sonicating the whole colony biofilm (ten 5-day-old biofilms for each condition), grown either in the presence or in the absence of 10 mg l^{-1} Ag-NPs, in lysis buffer (10 mmol l^{-1} Tris-HCl pH 7·5, 100 mmol l^{-1} NaCl) with protease inhibitor. Protein extracts were precipitated by adding a cold mix of ethanol, methanol and acetone (ratio 2 : 1 : 1, v/v), and redissolved in 6 mol l^{-1} urea, 100 mmol l^{-1} triethylammonium bicarbonate buffer pH 8·5. After reduction with 10 mmol l^{-1} dithiothreitol and alkylation with 20 mmol l^{-1} iodoacetamide, equal amounts of protein samples were digested 50 : 1 (w/w) with sequence grade trypsin (Promega, Madison, WI, USA) at 37°C overnight. In-solution dimethyl labelling on peptides was performed as described by Boersema *et al.* (2009) with sodium cyanoborohydride ($NaBH_3CN$), formaldehyde (CH_2O, light labelling) and deuterated formaldehyde (CD_2O, heavy labelling). In Experiment A,

tryptic peptides deriving from control and Ag-NP-treated biofilm were reacted with light and heavy formaldehyde respectively. A second experiment (Experiment B) was also performed, inverting the isotope labelling. After mixing equal quantities of labelled tryptic peptides, the samples were loaded on 18-cm Immobiline DryStrip gels (GE Healthcare, Uppsala, Sweden), pH 3–10, for peptide separation. Isoelectric-focused strips were cut in 18 pieces and extracted peptides were analysed by liquid chromatography-electrospray ionization-tandem mass spectrometry (LC-ESI-MS/MS) on an Ultimate 3000 Micro HPLC apparatus (Dionex, Sunnyvale, CA, USA) equipped with a FLM-3000-Flow manager module directly coupled to an LTQ Orbitrap XL hybrid FT mass spectrometer (Thermo Fisher Scientific, Waltham, MA, USA). Reverse-phase chromatography was performed on a Jupiter C18, 5 μm, 150 × 1·0 mm column (Phenomenex, Torrance, CA, USA) and a 95-min run (gradient 1·6–44% acetonitrile in water with 0·1% formic acid over 60 min) at a flow rate of 80 μl min^{-1}. Mass spectra were collected in FT-IT data-dependent scan mode (MS scan at 60 000 of resolution in the Orbitrap and MS/MS scan on the three most intense peaks in the linear ion trap, mass range 300–2000 Da). Selected peptide charge states were isolated with a width of m z^{-1} 6–10 and activated for 30 ms using 35% normalized collision energy and an activation q of 0·25. Protein identification and quantification was obtained with the embedded ion-accounting algorithm (Sequest HT) of the software PROTEOME DISCOVERER (ver. 1.4, Thermo) after searching a UniProtKB/Swiss-Prot Protein Knowledgebase (release 2013_08 of 24-Jul-13 containing 540732 sequence entries; taxonomical restrictions: *Bacillus subtilis*, 4188 sequence entries). The search parameters were 10 ppm tolerance for precursor ions and 0·8 Da for product ions, two missed cleavages, carbamydomethylation of cysteine as fixed modification, oxidation of methionine as variable modification, light and heavy dimethylation of peptide N-termini and lysine residues as fixed modification on two different search nodes. We filtered the data applying a q-value threshold of 0.05 based on Percolator algorithm (false discovery rate under is 5%; i.e., the expected fraction of incorrect peptide spectrum match in the entire data set is less than 5%, calculated on a decoy database). Relative peptide abundance was calculated from extracted ion chromatograms of the different isotopic variants with 1·5 fold change in the threshold value for up/down regulation.

Bioinformatic analysis

Modulated proteins identified by proteomic analysis were further analysed by the Protein Analysis Through Evolutionary Relationships Classification System (PANTHER, ver. 9.0, http://www.pantherdb.org) (Mi *et al.* 2013) to highlight the most relevant Gene Ontology (GO) terms and the enriched functional-related protein groups. By the PANTHER Statistical overrepresentation tool, the over- and under-representation of any protein class was assayed using the binomial test (Cho and Campbell 2000) with Bonferroni correction for multiple comparisons, comparing the protein list to the whole *B. subtilis* proteome. The most significant categories were identified by calculating the related significance (*P*-value).

In vitro PGPR and motility assays

PGPR assays were performed inoculating planktonic cells either in direct contact with Ag-NPs or just pre-exposed to Ag-NPs. In the first case, media used for PGPR assays were inoculated with 100 μl of culture of *B. subtilis* at 0·3 as OD600nm either in the absence or in the presence of 10 mg l^{-1} Ag-NPs. In the case of pre-exposition to Ag-NPs, 100 μl of *B. subtilis* grown in the absence or in the presence of 10 mg l^{-1} Ag-NPs for 24 h at 30°C, washed in PBS and resuspended to obtain 0·3 as OD600nm, were used as inoculum for the PGPR assays.

Indole-3-acetic acid (IAA) production was detected as described by Brick *et al.* (1991). Bacterial cultures were grown for 72 h in TSB supplemented with tryptophan (500 mg ml^{-1}). After centrifugation, the supernatant (2 ml) was mixed with 40 μl of orthophosphoric acid and 4 ml of the Salkowski reagent (35% of perchloric acid, 1 ml 0·5 mol l^{-1} $FeCl_3$ solution). After incubating for 25 min, the OD530nm was taken. Concentration of IAA produced by the cultures was measured using a calibration curve of IAA in the range of 10–100 mg ml^{-1}.

To verify the capacity to solubilize inorganic phosphate, the colorimetric method described by Ahmad *et al.* (2008) was used. After 72 h of growth at 30°C, the OD600nm of centrifuged bacterial cultures was measured. Values obtained from inoculated medium were subtracted from the control.

Production of siderophores was studied by cultivating the isolates on chrome azurol sulphate (CAS) agar plate, prepared as described by Schwyn and Neilands (1987). After solidification, the TSA plates were cut into halves and one half was replaced by CAS agar. The halves containing TSA were inoculated and the plates were incubated at 30°C for a week. The chromatic change in the CAS agar was evaluated to state the siderophore production.

Nitrogen fixation was evaluated by inoculating the medium described by Tarrand *et al.* (1978). After 72 h of growth at 30°C, 100 μl of grown bacteria were inoculated

again in new medium and let to grow at 30°C for a week, and then the OD600nm was measured.

Each assay was conducted with 10 replicates for control and 10 replicates for treated cells.

Swarming and swimming motility were determined as previously described by Villa *et al.* (2012) in TSB medium added either with 0·3% (w/v) agar (for swimming motility) or with 0·7% (w/v) agar (for swarming motility). Plates were allowed to dry for 2 h and were inoculated with 10 μl of a 24 h-old culture of *B. subtilis*, incubated with either 0 or 10 mg l^{-1} Ag-NPs, washed with PBS, resuspended to obtain 0·3 as OD600nm, added to the top of the agar and incubated at 30°C for 48 h. Results were expressed as the diameter (cm) of the area of observed motility.

Statistical analysis

A *t*-test or analysis of variance (ANOVA) via GRAPHPAD Software (San Diego, CA) was applied to statistically evaluate any significant differences among the samples. Tukey's Honestly Significant Difference test (HSD) was used for pairwise comparison to determine the significance of the data. Statistically significant results were depicted by *P*-values 0·05.

Results

Effect of Ag-NPs on planktonic growth of rhizobacteria *Azotobacter vinelandii* and *Bacillus subtilis*

In order to evaluate Ag-NP effects on two important representatives of rhizobacteria, namely *A. vinelandii* and *B. subtilis*, we performed growth inhibition tests in liquid media. Ag-NP concentrations chosen ranged from 0·1 mg l^{-1}, i.e. a concentration close to the proposed 'no-effect' concentration in soil (0·05 mg kg^{-1}; Schlich *et al.* 2013) to 100 mg l^{-1}. As shown in Fig. 1b, Ag-NPs inhibited *A. vinelandii* growth, albeit partially, already at concentrations as low as 0·1 mg l^{-1}. Low OD values are caused by the low-oxygen concentration in the medium; however, similar sensitivity has been observed also in *A. vinelandii* cultures grown with vigorous shaking. In contrast, *B. subtilis*, growth rate was only affected at 100 mg l^{-1} Ag-NPs, with consistent decrease in biomass accumulation (Fig. 1a). Determination of generation times during growth phase confirmed that, unlike *B. subtilis* (Fig. 1a), *A. vinelandii* growth rate was already affected at the lowest concentration tested (Fig. 1b). These results were also confirmed by viable counts on aliquots of stationary phase cultures treated with various Ag-NP concentrations, showing reduction in CFU consistent with reduction in OD600nm (data not shown). The results of this experiment would suggest that, even at concentrations as low as 0·1 mg l^{-1}, Ag-NPs might affect the composition of soil bacterial community by selective bacterial growth inhibition. We investigated whether 10 mg ml^{-1} Ag-NPs, a subinhibitory concentration in *B. subtilis*, might trigger the specific cellular responses in this bacterium.

Study of the interaction between Ag-NPs and *Bacillus subtilis* by TEM observations

Interaction of Ag-NPs with *B. subtilis* cells was monitored by direct TEM observations, which showed that no Ag-NP aggregates were present in the media used for bacterial growth. Planktonic cultures, grown either in the absence or in the presence of 10 mg l^{-1} Ag-NPs, were observed to determine the specific localization of Ag-NPs, and possible effects on cell morphology. During exponential phase (Fig. 2a–c), Ag-NPs appear to gather preferentially as aggregates around specific cells, with a nonhomogenous distribution (Fig. 2b). Ag-NPs were also visible inside the microbial cells, as single or aggregated Ag-NPs (Fig. 2c). Phase contrast images revealed that the cell walls of bacteria with internalized Ag-NPs showed no interruption, and the cells were not affected morphologically (data not shown).

During the stationary phase (Fig. 2d–f), for both control and treated samples, the cell wall was no longer stretched, resulting in a rougher surface. As highlighted in Fig. 2d–f, both in control and treated samples, some dead or dying cells were present. Interestingly, in the treated samples, the Ag-NPs gather preferentially within the dead cells or on what remains of the cell wall (Fig. 2e,f). This would suggest that Ag-NPs might be more toxic to *B. subtilis* cultures during stationary phase. To verify this, intact *vs* lysed *B. subtilis* cells were counted in TEM pictures on a total of six thousand cells, both for control and treated (10 mg l^{-1} Ag-NPs) samples during stationary phase. No statistically significant differences were observed (control: 2·83 $\pm$ 0·02% dead/live cells; treated: 4·00 $\pm$ 0·01% dead/live cells), confirming that, at 10 mg l^{-1}, Ag-NPs does not affect the *B. subtilis* viability.

Effect of Ag-NPs on sessile growth of *Bacillus subtilis*

Ag-NPs accumulating in soil are likely to interact with *B. subtilis* growing as a biofilm, rather than in planktonic cells. For this reason, we tested inhibition of colony biofilm by Ag-NPs. This condition mimics growth in soil, in which bacteria are attached to a solid surface and where water availability is influenced by the solute potentials (Chang and Halverson 2003). *Bacillus subtilis* colony biofilm showed rapid growth, reaching maturity in 4 days.

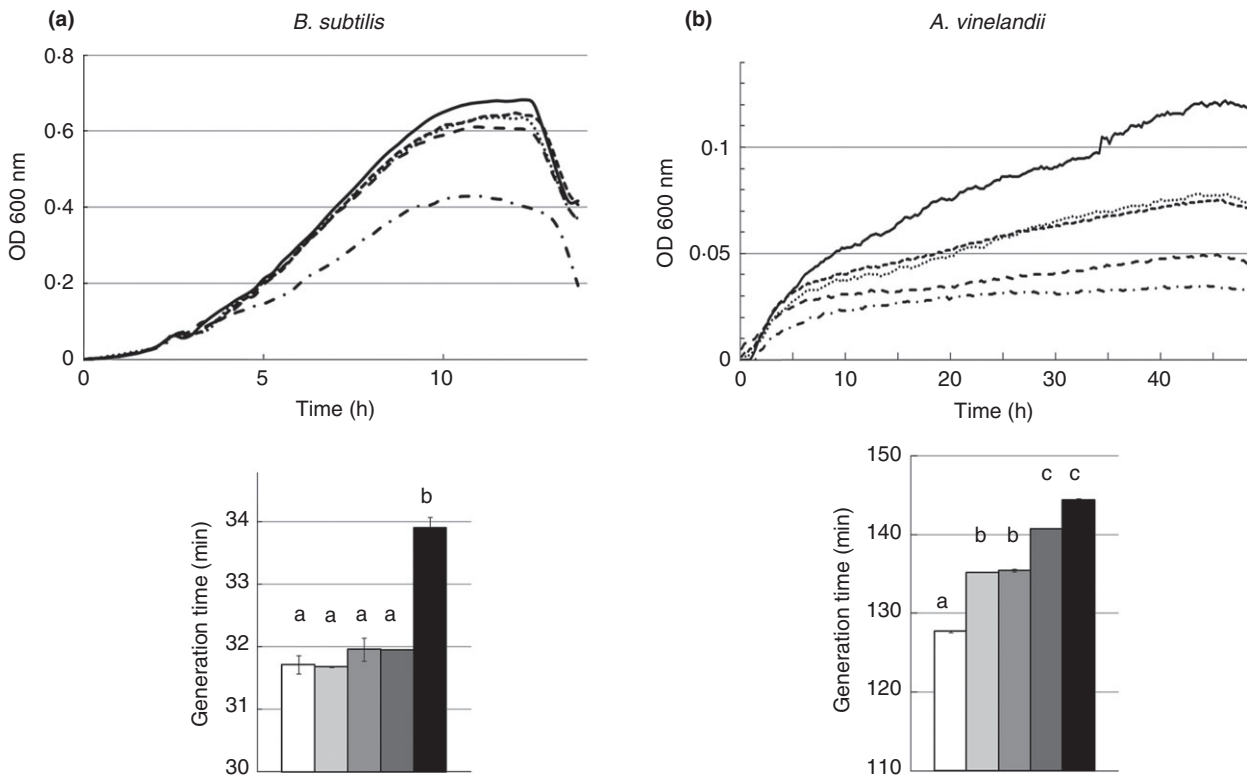

Figure 1 Growth curves of *Bacillus subtilis* (a) and *Azotobacter vinelandii* (b) in the presence of Ag-NP concentrations from 0 to 100 mg l^{-1}. Relative generation times were calculated for each condition. Data represent the means ± the SD of three independent measurements. Letters provide the graphical representation for *post hoc* comparisons. The histogram provides the *P*-values obtained by ANOVA analysis. According to *post hoc* analysis (Tukey's HSD, $P < 0{\cdot}05$), means sharing the same letter are not significantly different from each other. ——0 mg l^{-1}, ·····0·1 mg l^{-1}, ------1 mg l^{-1}, - - - -10 mg l^{-1}, -·-·-100 mg l^{-1}. □0 mg l^{-1}, □0·1 mg l^{-1}, □1 mg l^{-1}, □10 mg l^{-1}, ■100 mg l^{-1}.

At later times, the colony biofilm seemed to undergo a phase of dispersion, as suggested by a reduction in total proteins (Fig. 3). Although the presence of 10 mg l^{-1} of Ag-NPs did not hinder biofilm biomass as determined both by total protein determination (Fig. 3) and ATP consumption levels (Fig. S4), it appeared to slow down the growth rate, in particular at days 2 and 3, corresponding to the exponential phase of biofilm growth. In this growth phase, the lower ATP concentration of Ag-NP-treated biofilm with respect to the control, suggested a more extended lag phase in the presence of Ag-NPs. In contrast, the presence of 1 mg l^{-1} of Ag-NPs seemed to enhance biofilm growth by day 4.

Level of oxidative stress in planktonic cells and biofilm of *Bacillus subtilis*

Results of the biofilm growth-inhibition experiments highlight a phase of adaptation to Ag-NPs of biofilms that is not visible in the planktonic cells. As inhibition of bacterial growth by Ag-NP might be associated with the induction of oxidative stress, we measured Ag-NP-induced ROS production both in planktonic (Fig. 4) and biofilm (Fig. 5) cells. Due to the complex structure of the biofilm, ROS production was determined both intracellularly and in the biofilm matrix. In planktonic cells, collected during stationary phase, 10 mg l^{-1} Ag-NP increased the intracellular ROS concentrations by 3 fold compared to the untreated control (Fig. 4). The effect of 1 mg l^{-1} Ag-NPs was also tested, and, surprisingly, determined a reduction in intracellular ROS levels, possibly suggesting that at low concentrations, Ag-NPs might induce an adaptive response to oxidative stress, leading to a reduction in detectable ROS.

A different picture emerged from experiments on biofilm cells: indeed, ROS levels were lower or similar in Ag-NP-treated samples in comparison to the control throughout biofilm growth (Fig. 5). High levels of ROS were detected in the extracellular matrix, regardless of the presence of Ag-NPs (Fig. 5a). In contrast, intracellular ROS formation in biofilm cells was lower than those measured in the planktonic cells (Figs 4 and 5b) being undetectable on days 3–4, i.e. during the late exponential/stationary phase of biofilm formation, while reaching a

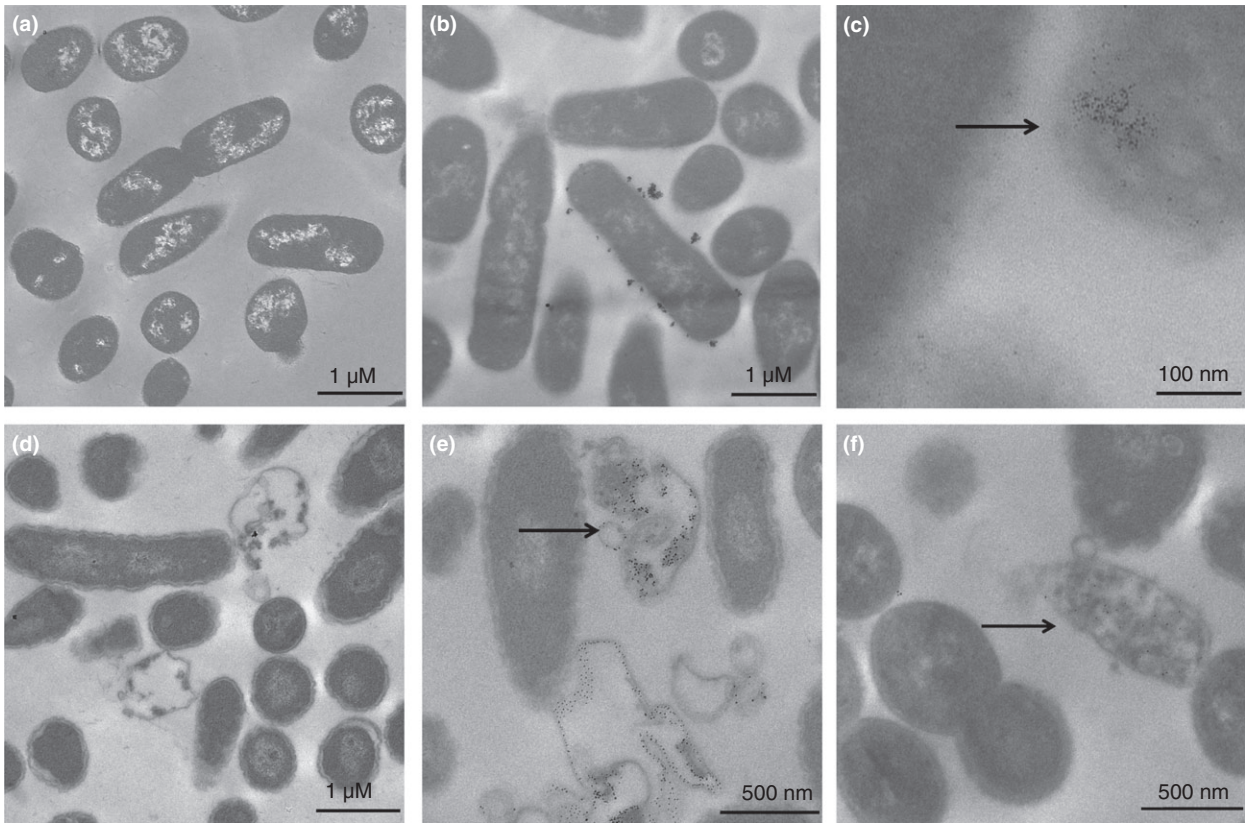

Figure 2 Transmission electron microscopy images of *Bacillus subtilis* planktonic cells grown with 0 (a, d) and 10 mg l^{-1} of Ag-NPs (b, c, e, f), during exponential (a, b, c) and stationary phase (d, e, f). Arrows indicate Ag-NPs localized inside the cells.

peak on day 8 (Fig. 5b). In biofilm cells, exposure to Ag-NPs reduced the intracellular ROS concentrations, with the only exception of day 1 for the higher Ag-NP concentration tested (10 mg l^{-1}).

To gather additional information on their effects on *B. subtilis* biofilm, we characterized the composition of the biofilm matrix in the presence and in the absence of Ag-NPs. In particular, we quantified the amounts of proteins, EPS and eDNA. Exposure to either 1 or 10 mg l^{-1} of Ag-NPs did not affect protein or eDNA amounts, while significantly stimulating EPS production in the biofilm matrix (*c.* 2·5-fold; Fig. 6).

Quantitative proteomics and bioinformatic data mining

To further evaluate the impact of Ag-NPs on *B. subtilis*, we determined the total protein composition from whole colony biofilm grown in the presence or absence of 10 mg l^{-1} Ag-NPs by proteomic analysis. Biomass was collected during the stationary phase. The data revealed a total of 19 proteins differentially expressed at significant levels in the Ag-NP-treated samples compared to the control (Table 1, Tables S1 and S2). No down-regulated proteins in Ag-NP-treated biofilm were detected.

Data were further analysed by the Statistical overrepresentation test of the software PANTHER to highlight the most relevant GO term group annotation associated with our proteomic dataset. This analysis showed a statistically significant higher expression of proteins with oxidoreductase activity (*P*-value = 0·0487) (Table S3).

As shown in Table 1, Ag-NPs appeared to positively affect the production of proteins either belonging to stress responses or able to sense the cell's redox potential. Indeed, two proteins directly involved in the response to oxidative stress (Alkyl hydroperoxide reductase subunit C and FeS cluster assembly protein SufD) and two proteins were able to sense the redox conditions (Thioredoxin A and the iron–sulphur cluster protein YutI) were more expressed in the presence of Ag-NPs. In addition, exposure to Ag-NPs also induced other stress response-related proteins, namely, oxalate decarboxylase (OxdC), involved in protection against low-pH stress (MacLellan *et al.* 2009), Tig (trigger factor), a chaperone protein activated in response to heat-shock (Reyes and Yoshikawa 2002), and the cell wall-associated protease WprA, induced by phosphate starvation

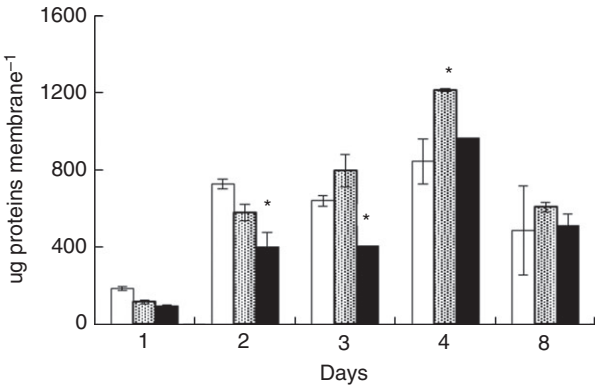

Figure 3 Total protein amounts from *Bacillus subtilis* biofilm in the presence of 0, 1 and 10 mg l^{-1} of Ag-NPs over time. Data represent the means ± the SD of three independent measurements of proteins for each membrane. The histograms provide the *P*-values obtained by ANOVA analysis. *Post hoc* comparisons results (Tukey's HSD, $P < 0{\cdot}05$) are summarized with asterisks to underline the most relevant differences of Ag-NP-treated samples with respect to control. □0 mg l^{-1}, ▨1 mg l^{-1}, ■10 mg l^{-1}, $P < 0{\cdot}0001$.

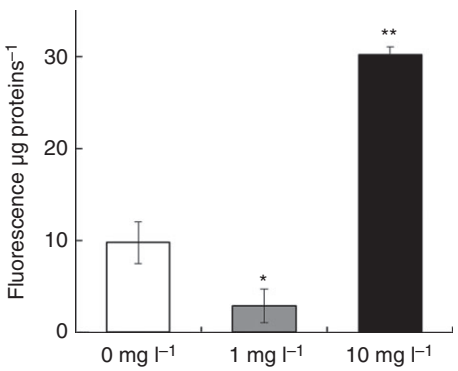

Figure 4 Intracellular reactive oxygen species concentrations in *Bacillus subtilis* planktonic cells. The histograms provide the *P*-values obtained by ANOVA analysis. *Post hoc* comparison results (Tukey's HSD, $P < 0{\cdot}05$) are summarized with asterisks to underline the most relevant differences in Ag-NP-treated samples with respect to the control. $P < 0{\cdot}0001$.

and necessary for the secretion of the peroxidase YwbN (Monteferrante *et al.* 2013). Our results suggest Ag-NP induction of some quorum-sensing related genes, as indicated by increased production of SrfAB, DegU, OppF and CotE proteins. DegU is able to induce competence in *B. subtilis* through positive regulation of *comK* (D'Souza 1994; Kobayashi 2007); *oppF* is part of *oppABCDF* operon, encoding Opp, an oligopeptide permease (Lazazzera 2001), which allows uptake of quorum-sensing related peptides. Interestingly, the *srfAB* gene, encoding a subunit of surfactin synthase, also contains the competence-stimulating peptide ComS (Zafra *et al.* 2012), another quorum-sensing signal. Finally, another Ag-NP-induced protein, CotE, is produced during sporulation, which is subject to a complex regulation in *B. subtilis* that also requires high cell density and production of quorum-sensing signals (Hilbert and Piggot 2004).

Plant growth-promoting activity and motility

Bacillus subtilis is considered as an important PGPR (Saharan and Nehra 2011). As Ag-NPs in soil might affect plant growth through modulation of PGPR composition and metabolic activities, their effects on PGP activities in *B. subtilis* (Barriuso *et al.* 2008) were evaluated, either pre-exposed to or grown in presence of Ag-NPs (10 mg l^{-1}) (Fig. 7). Although the bacteria in the rhizosphere are thought to be mostly present as a biofilm, no reliable assays are currently available to test the PGPR activities on sessile cells. Thus, we tested the effects of Ag-NPs on *B. subtilis* planktonic cells. Among the different PGP activities, we examined nitrogen fixation and phosphate solubilization, as they increase bioavailability of nitrogen and phosphate in soil, essential for plant growth (Bhattacharyya and Jha 2012). We also determined the production of IAA, an auxin phytohormone that regulates plant development and stimulates nitrogen, phosphorous and potassium uptake by plants (Etesami *et al.* 2009); finally, we measured production of siderophores, high-affinity iron chelating compounds used to solubilize mineral iron and promote its bioavailability (Saharan and Nehra 2011). The *B. subtilis* showed no nitrogen fixation activity in the conditions tested, while comparable levels of IAA and siderophore production were measured either in the presence or in the absence of Ag-NPs. In contrast, treatment with 10 mg l^{-1} of Ag-NPs increased the ability of *B. subtilis* to solubilize inorganic phosphate (OD600nm control: 0·754 ± 0·139; treated: 1·882 ± 0·145).

In order to carry out their beneficial activity on plants, bacteria must be able to colonize plant roots effectively (Achouak *et al.* 2004). Two different mechanisms of flagellar motilities can be involved in this process. Swimming is an individual motility (Kearn and Whittington 1991), necessary for the adhesion phase; whereas, swarming is the coordinated motility of a whole colony, and can be affected by signal molecules (Verstraeten *et al.* 2008). We tested Ag-NPs for possible effects on cell motility: exposure to 10 mg l^{-1} Ag-NPs failed to affect either swimming (control: 1·42 ± 0·13 cm; treated: 1·50 ± 0·21 cm) or swarming motility (control: 1·56 ± 0·05 cm; treated: 1·58 ± 0·08 cm).

Discussion

Due to the constant increase in their utilization in a variety of industrial products, the possible accumulation of

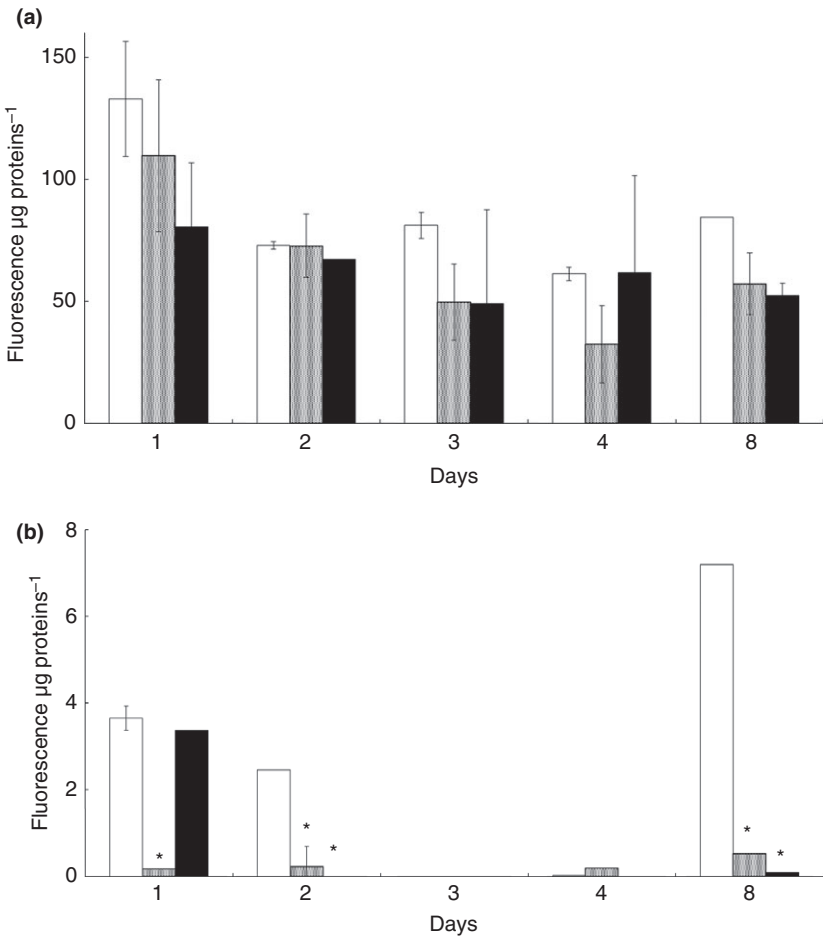

Figure 5 Reactive oxygen species detection outside (a) and inside (b) the cells of *Bacillus subtilis* biofilm in the presence of 0, 1 and 10 mg l^{-1} of Ag-NPs. The histograms provide the *P*-values obtained by ANOVA analysis. *Post hoc* comparison results (Tukey's HSD, $P < 0{\cdot}05$) are summarized with asterisks to underline the most relevant differences in Ag-NP-treated samples with respect to the control. □0 mg l^{-1}, ▩1 mg l^{-1}, ■10 mg l^{-1}, $P < 0{\cdot}0001$.

Ag-NPs in soil raises concerns, also since the extents of their biological effects, especially at low concentrations, have not been clearly determined yet. It has been proposed that 0·05 mg kg^{-1} of soil might represent a 'no-effect concentration' for Ag-NPs (Schlich *et al.* 2013). In this work, we have shown that Ag-NPs, already at 0·1 mg l^{-1}, i.e. at a concentration close to the proposed 'no-effect concentration', can affect growth of *A. vinelandii*, an important rhizosphere bacterium, reducing both its growth rate and the amount of culture biomass. In contrast, growth of the Gram-positive rhizosphere bacterium *B. subtilis* was only affected at 10 mg l^{-1}. Such discrepancy seems to depend on an increased sensitivity of *A. vinelandii*, rather than of Gram-negative bacteria, as *Escherichia coli* showed a similar response to Ag-NPs as *B. subtilis* (data not shown). Our observation suggests that, already at concentrations thought to be devoid of biological activity, Ag-NPs could impact the composition of rhizosphere microbial community by affecting the growth of specific bacteria.

Despite being *c.* 200-fold higher than the proposed 'no-effect concentration' in soil, exposure of soil bacteria to Ag-NPs at 10 mg l^{-1} or more can occur locally, in particular, in instances of utilization of sewage sludge, rich in Ag-NPs, as manure on agricultural soil, a procedure still widely used in many European countries (Schlich *et al.* 2013). Our results suggest that, at this concentration, Ag-NPs can enter *B. subtilis* cells grown in liquid cultures and accumulate in their cytoplasm, triggering ROS formation. However, a more complex picture emerges from the exposure to Ag-NPs of *B. subtilis* colony biofilms, a condition more likely to resemble bacterial growth and physiology in the soil environment. Despite showing some reduction in initial growth rate, fully overcome in the later stages of biofilm development, 10 mg l^{-1} Ag-NPs failed to trigger ROS formation, either in the biofilm matrix or inside the biofilm cells. Intracellular ROS levels were actually decreased upon exposure to Ag-NPs. However, exposure to 10 mg l^{-1} Ag-NPs strongly induced the polysaccharide production in the biofilm matrix, suggesting that the ATP consumption required by this process might be responsible for reduced growth rate in the presence of Ag-NPs in the earlier stages of biofilm formation.

Higher polysaccharide production is often induced as part of a response to environmental stresses (Sutherland 2011). Polysaccharide overproduction in the EPS matrix might be involved in Ag-NP absorption, thus preventing them from entering the bacterial cells, and limiting ROS formation and diffusion, consistent with previous observations (Peulen and Wilkinson 2011).

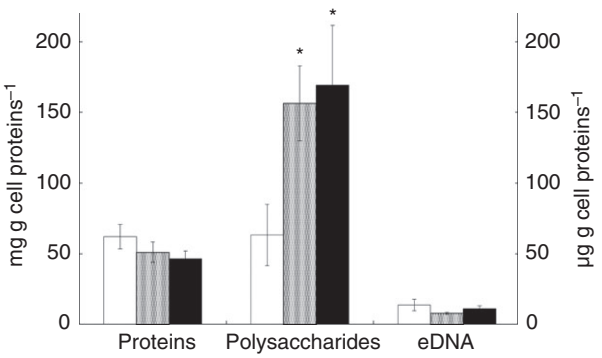

Figure 6 Biochemical composition of mature biofilm matrix of *Bacillus subtilis*. Protein and polysaccharide values are expressed as mg g^{-1} of total cell proteins, while eDNA values are expressed as μg g^{-1} of total cell proteins. Data represent the means ± the SD of three independent measurements. The histograms provide the *P*-values obtained by ANOVA analysis. *Post hoc* comparison results (Tukey's HSD, $P < 0{\cdot}05$) are summarized with asterisks to underline the most relevant differences in Ag-NP-treated samples with respect to the control. □0 mg l^{-1}, ▨1 mg l^{-1}, ■10 mg l^{-1}, $P < 0{\cdot}0001$.

In addition to the buffering effect of the polysaccharide matrix, reduction in ROS levels in biofilm cells might suggest that, at the concentrations tested, Ag-NPs might trigger an adaptive response to oxidation stress. To verify this hypothesis, we carried out a proteomic analysis in *B. subtilis* biofilm either in the presence or in the absence of 10 mg l^{-1} Ag-NPs. The high amount of polysaccharides in the EPS, resulting in 50 and 75% of the matrix weight in the control and Ag-NP-treated biofilms, respectively, made extraction of proteins for proteomic analysis very challenging (Bodzon-Kulakowska *et al.* 2007). Although this resulted in relatively low scores for some proteins, our proteomic analysis allowed us to identify cellular processes induced in response to Ag-NP treatment of *B. subtilis* biofilm, namely, stress responses and quorum sensing. Indeed, we could detect higher expression of the subunit C of alkyl hydroperoxide reductase, an important enzyme in oxidative stress response (Antelmann *et al.* 1996). Another protein induced in response to Ag-NPs was SufD, part of a FeS cluster assembly

Table 1 Differentially expressed proteins identified by LC-ESI-MS/MS. The following parameters are listed: alphanumeric unique protein sequence identifier (Accession) provided by UniProtKB/Swiss-Prot protein Knowledgebase, protein name (Description), Gene name and numeric unique gene sequence identifier (Gene ID) provided by NCBI, Function and mean of the ratio of the heavy and light quantification channels (Ag-NPs/Ctrl)

Accession	Description	Gene name [gene ID]	Function	Ag-NPs/Ctrl
Stress response				
O32165	FeS cluster assembly protein SufD	sufD [938871]	Repair under oxidative stress	10·52
O32119	Putative nitrogen fixation proteins	yutI [936658]	Iron–sulphur cluster assembly	3·38
O34714	Oxalate decarboxylase OxdC	oxdC [938620]	Acidic stress response	1·65
P14949	Thioredoxin	trxA [938187]	Cell redox homeostasis	4·72
P54423	Cell wall-associated protease	wprA [936350]	Proteoglycan peptide bridges in stationary phase	3·37
P80239	Alkyl hydroperoxide reductase subunit C	ahpC [938147]	Oxidative stress response	1·86
P80698	Trigger factor	tig [936610]	Chaperone in heat-shock response	2·39
Primary metabolism				
O31669	Acireductone dioxygenase	mtnD [939322]	Aminoacid biosynthesis	2·04
P21881	Pyruvate dehydrogenase E1 component subunit alpha	pdhA [936005]	Pyruvate metabolism	4·93
P34956	Quinol oxidase subunit 1	qoxB [937303]	ATP synthesis	9·00
P37808	ATP synthase subunit alpha	atpA [936995]	ATP synthesis	2·06
P39062	Acetyl-coenzyme A synthetase	acsA [937324]	Acetate utilization	13·32
P12425	Glutamine synthetase	glnA [940020]	Glutamine synthetase	3·82
Transcription and translation				
P12877	50S ribosomal protein L5	rplE [936981]	tRNA binding	6·40
P17889	Translation initiation factor IF-2	infB [936930]	Protein synthesis	6·62
Quorum sensing				
P13800	Transcriptional regulatory protein DegU	degU [936751]	Recruitment of ComK	5·05
P24137	Oligopeptide transport ATP-binding protein OppF	oppF [936410]	Transmembrane transport	2·15
P14016	Spore coat protein E	cotE [939508]	Sporulation	4·18
Q04747	Surfactin synthase subunit 2	srfAB [938303]	Surfactin biosynthesis	3·16

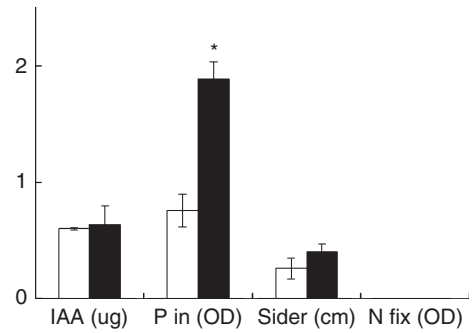

Figure 7 Plant growth-promoting rhizobacterial activities of planktonic cells of *Bacillus subtilis* in the presence of 0, 1 and 10 mg l^{-1} of Ag-NPs. IAA: indole-3-acetic acid production; P in: solubilization of inorganic phosphate; sider: siderophore production; N fix: nitrogen fixation. Data represent the means ± the SD of at least three independent measurements. Statistically significant differences ($P < 0{\cdot}05$) were determined by Student's *t*-test and marked by asterisks. □0 mg l^{-1}, ■10 mg l^{-1}, *P* Pin < 0·0001.

which, in *E. coli*, is sensitive to disruption by ROS or by iron limitation (Layer *et al.* 2007). Thioredoxin (TrxA), another enzyme linked to oxidative stress, was also induced by exposure to Ag-NPs. As many Gram-positive bacteria do not generate glutathione, which is the dominant low-molecular thiol in most Eukaryota and many Gram-negative bacteria (Newton *et al.* 2009), thioredoxins are essential to *B. subtilis* for cellular thiol/disulfide balance and survival under oxidative stress (Lu and Holmgren 2013). Thus, results of proteomic analysis suggested that treatment with Ag-NPs leads to a higher expression of proteins involved in oxidative stress response, which would in turn, lead to more efficient detoxification and removal of ROS, as observed.

In addition to proteins involved in stress responses, exposure to Ag-NPs stimulates the production of competence-related peptides and to induce quorum-sensing mechanisms. Indeed, we observed a higher expression of DegU, a transcription regulator involved in the production of the ComK, a quorum sensing-dependent regulator (Mhatre *et al.* 2014). We also observed a higher expression of the quorum sensing-dependent molecule surfactin coded by the *srfAB* gene. In addition, a fragment of the *srfAB* gene encodes for ComS, a quorum-sensing peptide able to enhance competence (Morikawa 2006). Surfactin triggers matrix production (Lopez *et al.* 2009), which is consistent with the observed higher polysaccharide production in Ag-NP-treated biofilm. It is tempting to speculate that Ag-NPs might also trigger induction of quorum sensing, thus affecting gene expression at large in *B. subtilis* biofilms.

Exposure of *B. subtilis* to Ag-NPs positively affects polysaccharide production, which, by promoting effective colonization of plant roots, plays an important role in the PGP activity by this bacterium (Chen *et al.* 2013). We also found that inorganic phosphate solubilization, which results in increased phosphorous availability in the rhizosphere, was stimulated by Ag-NPs. Although PGP activities were determined on planktonic cultures, due to lack of reliable assays on biofilm cells, our results seem to suggest that sublethal doses of Ag-NPs might exert a positive effect on PGP activity by *B. subtilis*. In conclusion, using *B. subtilis* as a model for rhizosphere organisms, we were able to show that Ag-NPs at subinhibitory concentrations affect pivotal cellular processes such as stress responses, quorum sensing and PGP activities. It is conceivable that similar effects might take place on other soil bacteria: re-direction of cellular processes and of gene expression, linked to selective toxicity on some bacterial species, such as *A. vinelandii*, suggest a strong impact of Ag-NPs on soil bacterial communities.

Acknowledgements

This work was supported by the Fondazione Banca del Monte di Lombardia (grant 2011) (Valutazione della tossicità ambientale indotta da nanoparticelle: focus su batteri del suolo, alghe unicellulari e piante superiori).

Conflict of interest

None declared.

References

Achouak, W., Conrod, S., Cohen, V. and Heulin, T. (2004) Phenotypic variation of *Pseudomonas brassicacearum* as a plant root-colonization strategy. *Mol Plant Microbe Interact* **17**, 872–879.

Ahmad, F., Ahmad, I. and Khan, M.S. (2008) Screening of free-living rhizospheric bacteria for their multiple plant growth promoting activities. *Microbiol Res* **163**, 173–181.

Anderl, J.N., Franklin, M.J. and Stewart, P.S. (2000) Role of antibiotic penetration limitation in *Klebsiella pneumoniae* biofilm resistance to ampicillin and ciprofloxacin. *Antimicrob Agents Chemother* **44**, 1818–1824.

Antelmann, H., Engelmann, S. and Schmid, R. (1996) General and oxidative stress responses in *Bacillus subtilis*: cloning, expression, and mutation of the alkyl hydroperoxide reductase operon. *J Bacteriol* **178**, 6571–6578.

Barriuso, J., Solano, B. and Lucas, J. (2008) Ecology, genetic diversity and screening strategies of plant growth promoting rhizobacteria (PGPR). In *Plant-Bacteria Interactions: Strategies and Techniques to Promote Plant Growth* ed. Ahmad, I., Pichtel, J. and Hayat, S. pp 1–17. Weinheim: WILEY-VCH Verlag GmbH & Co. KGaA.

Benn, T.M. and Westerhoff, P. (2008) Nanoparticle silver released into water from commercially available sock fabrics. *Environ Sci Technol* **42**, 4133–4139.

Bhattacharyya, P.N. and Jha, D.K. (2012) Plant growth-promoting rhizobacteria (PGPR): emergence in agriculture. *World J Microbiol Biotechnol* **28**, 1327–1350.

Bodzon-Kulakowska, A., Bierczynska-Krzysik, A., Dylag, T., Drabik, A., Suder, P., Noga, M., Jarzebinska, J. and Silberring, J. (2007) Methods for samples preparation in proteomic research. *J Chromatogr B* **849**, 1–31.

Bourioug, M., Gimbert, F., Alaoui-Sehmer, L., Benbrahim, M., Aleya, L. and Alaoui-Sossé, B. (2014) Sewage sludge application in a plantation: effects on trace metal transfer in soil-plant-snail continuum. *Sci Total Environ* **502**, 309–314.

Boersema, P.J., Raijmakers, R., Lemeer, S., Mohammed, S. and Heck, A.J. (2009) Multiplex peptide stable isotope dimethyl labeling for quantitative proteomics. *Nat Protoc* **4**, 484–494.

Bradford, M.M. (1976) A rapid and sensitive method for the quantitation of microgram quantities of protein utilizing the principle of protein-dye binding. *Anal Biochem* **72**, 248–254.

Brick, J.M., Bostock, R.M. and Silverstone, S.E. (1991) Rapid *in situ* assay for indoleacetic acid production by bacteria immobilized on nitrocellulose membrane. *Appl Environ Microbiol* **57**, 535–538.

Chang, W.S. and Halverson, L.J. (2003) Reduced water availability influences the dynamics, development, and ultrastructural properties of *Pseudomonas putida* biofilms. *J Bacteriol* **185**, 6199–6204.

Chen, Y., Yan, F., Chai, Y., Liu, H., Kolter, R., Losick, R. and Guo, J.H. (2013) Biocontrol of tomato wilt disease by *Bacillus subtilis* isolates from natural environments depends on conserved genes mediating biofilm formation. *Environ Microbiol* **15**, 848–864.

Cho, R.J. and Campbell, M.J. (2000) Transcription, genomes, function. *Trends Genet* **16**, 409–415.

Corinaldesi, C., Danovaro, R. and Dell Anno, A. (2005) Simultaneous recovery of extracellular and intracellular DNA suitable for molecular studies from marine sediments. *Appl Environ Microbiol* **71**, 46–50.

D'Souza, C. (1994) Identification of comS, a gene of the srfA operon that regulates the establishment of genetic competence in *Bacillus subtilis*. *Proc Natl Acad Sci U S A* **91**, 9397–9401.

Duncan, T.V. (2011) Applications of nanotechnology in food packaging and food safety: barrier materials, antimicrobials and sensors. *J Colloid Interface Sci* **363**, 1–24.

Etesami, H., Alikhani, H.A., Jadidi, M. and Aliakbari, A. (2009) Effect of superior IAA producing rhizobia on N, P, K uptake by wheat grown under greenhouse condition. *World Appl Sci J* **6**, 1629–1633.

Fabrega, J., Fawcett, S.R., Renshaw, J.C. and Lead, J.R. (2009) Silver nanoparticle impact on bacterial growth: effect of pH, concentration, and organic matter. *Environ Sci Technol* **43**, 7285–7290.

Gottschalk, F. and Sonderer, T. (2009) Modeled environmental concentrations of engineered nanomaterials (TiO_2, ZnO, Ag, CNT, fullerenes) for different regions. *Environ Sci Technol* **43**, 9216–9222.

Guo, R., Li, Y., Lan, J., Jiang, S., Liu, T. and Yan, W. (2013) Microwave-assisted synthesis of silver nanoparticles on cotton fabric modified with 3-aminopropyltrimethoxysilane. *J Appl Polym Sci* **130**, 3862–3868.

Hachicho, N., Hoffmann, P., Ahlert, K. and Heipieper, H.J. (2014) Effect of silver nanoparticles and silver ions on growth and adaptive response mechanisms of *Pseudomonas putida* mt-2. *FEMS Microbiol Lett* **355**, 71–77.

Handy, R.D., von der Kammer, F., Lead, J.R., Hassellov, M., Owen, R. and Crane, M. (2008) The ecotoxicology and chemistry of manufactured nanoparticles. *Ecotoxicology* **17**, 287–314.

Herigstad, B., Hamilton, M. and Heersink, J. (2001) How to optimize the drop plate method for enumerating bacteria. *J Microbiol Methods* **44**, 121–129.

Hilbert, D.W. and Piggot, P.J. (2004) Compartmentalization of gene expression during *Bacillus subtilis* spore formation. *Microbiol Mol Biol Rev* **68**, 234–262.

Jakubowski, W., Bilinski, T. and Bartosz, G. (2000) Oxidative stress during aging of stationary cultures of the yeast *Saccharomyces cerevisiae*. *Free Radic Biol Med* **28**, 659–664.

Kearn, G.C. and Whittington, I.D. (1991) Swimming in a sub-adult monogenean of the genus *Entobdella*. *Int J Parasitol* **21**, 739–741.

Kobayashi, K. (2007) Gradual activation of the response regulator DegU controls serial expression of genes for flagellum formation and biofilm formation in *Bacillus subtilis*. *Mol Microbiol* **66**, 395–409.

Kobayashi, H., Oethinger, M., Tuohy, M.J., Procop, G.W. and Bauer, T.W. (2009) Improved detection of biofilm-formative bacteria by vortexing and sonication: a pilot study. *Clin Orthop Relat Res* **467**, 1360–1364.

Layer, G., Gaddam, S.A., Ayala-Castro, C.N., Ollagnier-de Choudens, S., Lascoux, D., Fontecave, M. and Outten, F.W. (2007) SufE transfers sulfur from SufS to SufB for iron-sulfur cluster assembly. *J Biol Chem* **282**, 13342–13350.

Lazazzera, B. (2001) The intracellular function of extracellular signaling peptides. *Peptides* **22**, 1519–1527.

Levard, C., Hotze, E.M., Lowry, G.V. and Brown, G.E. (2012) Environmental transformations of silver nanoparticles: impact on stability and toxicity. *Environ Sci Technol* **46**, 6900–6914.

Lopez, D., Vlamakis, H., Losick, R. and Kolter, R. (2009) Paracrine signaling in a bacterium. *Genes Dev* **23**, 1631–1638.

Lu, J. and Holmgren, A. (2013) The thioredoxin antioxidant system. *Free Radic Biol Med* **66**, 75–87.

MacLellan, S.R., Helmann, J.D. and Antelmann, H. (2009) The YvrI alternative sigma factor is essential for acid stress

induction of oxalate decarboxylase in *Bacillus subtilis*. *J Bacteriol* **191**, 931–939.

Masuko, T., Minami, A., Iwasaki, N., Majima, T., Nishimura, S. and Lee, Y.C. (2005) Carbohydrate analysis by a phenolsulfuric acid method in microplate format. *Anal Biochem* **339**, 69–72.

Mhatre, E., Monterrosa, R.G. and Kovacs, A.T. (2014) From environmental signals to regulators: modulation of biofilm development in Gram-positive bacteria. *J Basic Microbiol* **54**, 616–632.

Mi, H., Muruganujan, A. and Thomas, P.D. (2013) PANTHER in 2013: modeling the evolution of gene function, and other gene attributes, in the context of phylogenetic trees. *Nucleic Acids Res* **41**, 377–386.

Monteferrante, C.G., MacKichan, C., Marchadier, E., Prejean, M.V., Carballido-Lopez, R. and van Dijl, J.M. (2013) Mapping the twin-arginine protein translocation network of *Bacillus subtilis*. *Proteomics* **13**, 800–811.

Morikawa, M. (2006) Beneficial biofilm formation by industrial bacteria *Bacillus subtilis* and related species. *J Biosci Bioeng* **101**, 1–8.

Mueller, P., Jacobsen, N.R., Folkmann, J.K., Danielsen, P.H., Mikkelsen, L., Hemmingsen, J.G., Vesterdal, L.K., Forchhammer, L. *et al.* (2009) Role of oxidative damage in toxicity of particulates. *Free Radical Res* **44**, 1–46.

Nel, A., Xia, T., Madler, L. and Li, N. (2006) Toxic potential of materials at the nanolevel. *Science* **311**, 622–627.

Newton, G.L., Rawat, M., La Clair, J.J., Jothivasan, V.K., Budiarto, T., Hamilton, C.J., Claiborne, A., Helmann, J.D. *et al.* (2009) Bacillithiol is an antioxidant thiol produced in *Bacilli*. *Nat Chem Biol* **5**, 625–627.

Peulen, T.O. and Wilkinson, K.J. (2011) Diffusion of nanoparticles in a biofilm. *Environ Sci Technol* **45**, 3367–3373.

Philippot, L., Raaijmakers, J.M., Lemanceau, P. and van der Putten, W.H. (2013) Going back to the roots: the microbial ecology of the rhizosphere. *Nat Rev Microbiol* **11**, 789–799.

Rai, M.K., Deshmukh, S.D., Ingle, A.P. and Gade, A.K. (2012) Silver nanoparticles: the powerful nanoweapon against multidrug-resistant bacteria. *J Appl Microbiol* **112**, 841–852.

Reyes, D. and Yoshikawa, H. (2002) DnaK chaperone machine and trigger factor are only partially required for normal growth of *Bacillus subtilis*. *Biosci Biotechnol Biochem* **66**, 1583–1586.

Saharan, B. and Nehra, V. (2011) Plant growth promoting rhizobacteria: a critical review. *Life Sci Med Res* **21**, 1–30.

Schacht, V.J., Neumann, L.V., Sandhi, S.K., Chen, L., Henning, T., Klar, P.J., Theophel, K., Schnell, S. *et al.* (2013) Effects of silver nanoparticles on microbial growth dynamics. *J Appl Microbiol* **114**, 25–35.

Schlich, K., Klawonn, T., Terytze, K. and Hund-Rinke, K. (2013) Hazard assessment of a silver nanoparticle in soil applied via sewage sludge. *Environ Sci Europe* **25**, 1–14.

Schwyn, B. and Neilands, J.B. (1987) Universal chemical assay for the detection and determination of siderophores. *Anal Biochem* **160**, 47–56.

Sotiriou, G.A. and Pratsinis, S.E. (2011) Engineering nanosilver as an antibacterial biosensor and bioimaging material. *Curr Opin Chem Eng* **1**, 3–10.

Sutherland, I.W. (2011) Biofilm exopolysaccharides: a strong and sticky framework. *Microbiology* **147**, 3–9.

Tarrand, J.J., Krieg, N.R. and Dobereiner, J. (1978) A taxonomic study of the *Spirillum lipoferum* group, with descriptions of a new genus, *Azospirillum* gen. nov. and two species, *Azospirillum lipoferum* (Beijerinck) comb. nov. and *Azospirillum brasilense* sp. nov. *Can J Microbiol* **24**, 967–980.

Vacheron, J., Desbrosses, G., Bouffaud, M.L., Touraine, B., Moenne-Loccoz, Y., Muller, D., Legendre, L., Wisniewski-Dye, F. *et al.* (2013) Plant growth-promoting rhizobacteria and root system functioning. *Front Plant Sci* **4**, 1–19.

Verstraeten, N., Braeken, K., Debkumari, B., Fauvart, M., Fransaer, J., Vermant, J. and Michiels, J. (2008) Living on a surface: swarming and biofilm formation. *Trends Microbiol* **16**, 496–506.

Villa, F., Remelli, W., Forlani, F., Gambino, M., Landini, P. and Cappitelli, F. (2012) Effects of chronic sub-lethal oxidative stress on biofilm formation by *Azotobacter vinelandii*. *Biofouling* **28**, 823–833.

Whitley, A.R., Levard, C., Oostveen, E., Bertsch, P.M., Matocha, C.J., von der Kammer, F. and Unrine, J.M. (2013) Behavior of Ag nanoparticles in soil: effects of particle surface coating, aging and sewage sludge amendment. *Environ Pollut* **182**, 141–149.

Zafra, O., Lamprecht-Grandio, M., de Figueras, C.G. and Gonzalez-Pastor, J.E. (2012) Extracellular DNA release by undomesticated *Bacillus subtilis* is regulated by early competence. *PLoS ONE* **7**, e48716, 1–15.

Supporting Information

Additional Supporting Information may be found in the online version of this article:

Table S1 Detailed information about proteins identified as differentially expressed by quantitative proteomics by stable isotope dimethyl labelling.

Table S2 Information about peptides from proteins identified by LC-ESI-MS/MS experiments.

Table S3 Functional characterization of the proteins modulated in expression belonging to the dataset relative to proteomic analysis of the NP-treated condition compared with the control colony biofilm.

Figure S1 ATP concentration in colony biofilm of *B. subtilis* in the presence of 0 and 10 mg l^{-1} of Ag-NPs over time.

Accession	Gene ID	Description GN= gene name - [Entry name]	Experiment	Nanoparticles/Ctrl Ratio	Nanoparticles/Ctrl Count	Nanoparticles/Ctrl Variability [%]	Coverage	# Unique Peptides	# Peptides	# PSMs	Score
O31669	939322	Acireductone dioxygenase GN=mtnD - [MTND_BACSU]	A	1.90	2	1.6	7.87	1	1	5	11.87
			B	2.17	1		7.87	1	1	4	6.71
O32119	936658	Putative nitrogen fixation protein YutI GN=yutI - [YUTI_BACSU]	A	2.11	1		14.41	1	1	3	7.83
			B	4.64	2	26.0	14.41	1	1	4	7.46
O32165	938871	FeS cluster assembly protein SufD GN=sufD - [SUFD_BACSU]	A	11.08	1		3.66	1	1	3	8.90
			B	9.96	1		3.66	1	1	4	10.97
O34714	938620	Oxalate decarboxylase OxdC GN=oxdC - [OXDC_BACSU]	A	1.53	1		3.38	1	1	3	7.25
			B	1.77	1		3.38	1	1	3	6.60
P12425	940020	Glutamine synthetase GN=glnA - [GLNA_BACSU]	A	4.05	1		1.80	1	1	4	7.50
			B	3.58	1		1.80	1	1	3	7.08
P12877	936981	50S ribosomal protein L5 GN=rplE - [RL5_BACSU]	A	7.19	1		8.38	1	1	3	10.16
			B	5.61	1		8.38	1	1	4	12.81
P13800	936751	Transcriptional regulatory protein DegU GN=degU - [DEGU_BACSU]	A	5.29	1		9.61	1	1	6	28.20
			B	4.81	2	18.6	9.61	1	1	7	26.75
P14016	939508	Spore coat protein E GN=cotE - [COTE_BACSU]	A	3.90	4	22.8	8.84	1	1	12	52.62
			B	4.46	6	15.9	8.84	1	1	14	39.88
P14949	938187	Thioredoxin GN=trxA - [THIO_BACSU]	A	3.26	1		11.54	1	1	2	5.56
			B	6.18	1		11.54	1	1	2	4.47
P17889	939630	Translation initiation factor IF-	A	6.71	2	7.3	1.54	1	1	4	5.91
			B	6.54	1		1.54	1	1	6	12.10

		2 GN=infB - [IF2_BACSU]									
P21881	936005	Pyruvate dehydrogenase E1 component subunit alpha GN=pdhA - [ODPA_BACSU]	A	3.71	1		3.77	1	1	3	9.23
			B	6.15	1		3.77	1	1	1	2.31
P24137	936410	Oligopeptide transport ATP-binding protein OppF GN=oppF - [OPPF_BACSU]	A	2.13	2	1.4	6.56	1	1	8	29.34
			B	2.18	3	2.0	6.56	1	1	9	25.96
P34956	937303	Quinol oxidase subunit 1 GN=qoxB - [QOX1_BACSU]	A	9.78	1		1.69	1	1	3	6.31
			B	8.23	1		1.69	1	1	3	7.45
P37808	936995	ATP synthase subunit alpha GN=atpA - [ATPA_BACSU]	A	2.19	10	11.7	5.98	3	3	68	166.79
			B	1.93	11	11.0	5.98	3	3	55	129.84
P39062	937324	Acetyl-coenzyme A synthetase GN=acsA - [ACSA_BACSU]	A	11.33	1		1.92	1	1	3	5.65
			B	15.31	2	1.2	1.92	1	1	4	7.79
P54423	936350	Cell wall-associated protease GN=wprA - [WPRA_BACSU]	A	2.99	2	16.8	2.46	1	1	7	30.33
			B	3.75	2	19.9	2.46	1	1	8	34.79
P80239	938147	Alkyl hydroperoxide reductase subunit C GN=ahpC - [AHPC_BACSU]	A	2.03	2	8.3	17.11	2	2	2	6.08
			B	1.69	1		9.63	1	1	1	2.31
P80698	936610	Trigger factor GN=tig - [TIG_BACSU]	A	2.00	2	13.7	4.01	1	1	6	26.15
			B	2.78	1		17.69	3	3	9	29.57
Q04747	938303	Surfactin synthase subunit 2 GN=srfAB - [SRFAB_BACSU]	A	4.10	1		1.31	2	3	8	17.77
			B	2.22	1		2.29	4	4	7	18.63

Supporting Information 1 Detailed information about proteins identified as differentially expressed by quantitative proteomics by stable isotope dimethyl labeling. The dataset is relative to the differential proteomic analysis of the NPs treated condition compared with the control colony biofilm and to biological replicates results with the same trend of regulation: Heavy/Light (Experiment A) or Light/Heavy (Experiment B) = NPs/Ctrl. In the table are listed the following parameters: alphanumeric unique protein sequence identifier (Accession), protein name (Description), protein identifier characters with a naming convention [Entry name] provided by UniProtKB/Swiss-Prot protein knowledgebase; numeric unique gene sequence identifier (Gene ID) provided by NCBI and gene name; percentage of protein sequence covered by identified peptides (Coverage); ratio of the quantification values of the heavy and light quantification channels (Heavy/Light or Light/Heavy = Nanoparticles/Ctrl), number of peptide ratios that were actually used to calculate the protein ratio (Heavy/Light or Light/Heavy Count); the variability of the peptide ratios that were used to calculate the protein ratio Heavy/Light or Light/Heavy (Variability [%]); number of peptides unique to the protein (# Unique Peptides), number of the identified peptides matching to the protein (# Peptides), total number of identified peptide sequences (peptide spectrum matches) (# PSMs), protein identification's SEQUEST Score.

Accession	Experiment	Sequence	MH+ [Da]	Charge	m/z [Da]	Mass Error	# Missed Cleavages	Modifications	RT	# PSMs	NPs/ Ctrl ratio	NPs/ Ctrl Count	NPs/Ctrl Variability [%]	q-Value	PEP
O31669	A	LNPGDLISVPENIR	1568.89	2	784.95	-0.89 mmu/-1.13 ppm	0	N-Term(Dimethyl:2H(4))	41.43	5	1.90	2	1.58	0	0.000009146
	B	LNPGDLISVPENIR	1564.86	2	782.93	-3.65 mmu/-4.67 ppm	0	N-Term(Dimethyl)	39.73	4	2.17	1		0	0.001979
O32119	A	DGGDCELVDVDEGIVK	1775.84	2	888.42	-0.93 mmu/-1.05 ppm	0	N-Term(Dimethyl); C5(Carbamidomethyl); K16(Dimethyl)	34.85	1				0	0.05299
		DGGDCELVDVDEGIVK	1783.88	2	892.45	-1.2 mmu/-1.34 ppm	0	N-Term(Dimethyl:2H(4)); C5(Carbamidomethyl); K16(Dimethyl:2H(4))	34.93	2	2.11	1		0	0.001858
	B	DGGDCELVDVDEGIVK	1775.83	2	888.42	-4.54 mmu/-5.11 ppm	0	N-Term(Dimethyl); C5(Carbamidomethyl); K16(Dimethyl)	33.82	4	4.64	2	26.01	0	0.000477
O32165	A	ALIDIENEDKTLYVQR	1984.12	3	662.04	-0.97 mmu/-1.46 ppm	1	N-Term(Dimethyl:2H(4)); K10(Dimethyl:2H(4))	36.63	3	11.08	1		0	4.002E-07
	B	ALIDIENEDKTLYVQR	1976.06	3	659.36	-3.05 mmu/-4.62 ppm	1	N-Term(Dimethyl); K10(Dimethyl)	35.34	4	9.96	1		0	0.002172
O34714	A	LLEQEPIESEGGK	1484.78	2	742.90	-0.73 mmu/-0.98 ppm	0	N-Term(Dimethyl); K13(Dimethyl)	25.37	2	1.53	1		0	0.06406
		LLEQEPIESEGGK	1492.83	2	746.92	-1.18 mmu/-1.58 ppm	0	N-Term(Dimethyl:2H(4)); K13(Dimethyl:2H(4))	25.39	1				0	0.006101
	B	LLEQEPIESEGGK	1484.78	2	742.89	-4.52 mmu/-6.08 ppm	0	N-Term(Dimethyl); K13(Dimethyl)	24.27	3	1.77	1		0	0.004511

P12425	A	EIEWDMFR	1157.56	2	579.28	-0.17 mmu/-0.29 ppm	0	N-Term(Dimethyl:2H(4))	43.28	4	4.05	1		0	0.09111
	B	EIEWDMFR	1153.53	2	577.27	-2.75 mmu/-4.77 ppm	0	N-Term(Dimethyl)	41.31	3	3.58	1		0	0.002036
P12877	A	EQLIFPEIDYDKVTK	1934.13	3	645.38	-0.62 mmu/-0.96 ppm	1	N-Term(Dimethyl:2H(4)); K12(Dimethyl:2H(4)); K15(Dimethyl:2H(4))	41.07	3	7.19	1		0	3.336E-08
	B	EQLIFPEIDYDKVTK	1922.05	3	641.35	-2.37 mmu/-3.7 ppm	1	N-Term(Dimethyl); K12(Dimethyl); K15(Dimethyl)	39.37	4	5.61	1		0	0.0002059
P13800	A	ILDFEPTFEVVAEGDDGDEAAR	2427.15	2	1214.08	+0.15 mmu/+0.12 ppm	0	N-Term(Dimethyl:2H(4))	45.23	6	5.29	1		0	2.683E-09
	B	ILDFEPTFEVVAEGDDGDEAAR	2423.11	2	1212.06	-6.34 mmu/-5.23 ppm	0	N-Term(Dimethyl)	43.08	7	4.81	2	18.60	0	9.189E-10
P14016	A	YRDNNYLDDEHEVIAK	2058.03	3	686.68	-1.35 mmu/-1.96 ppm	1	N-Term(Dimethyl:2H(4)); K16(Dimethyl:2H(4))	28.09	12	3.90	4	22.76	0	4.948E-11
	B	YRDNNYLDDEHEVIAK	2049.98	3	684.00	-3.61 mmu/-5.28 ppm	1	N-Term(Dimethyl); K16(Dimethyl)	27.30	14	4.46	6	15.90	0	2.928E-11

P14949	A	IDVDENQETAGK	1382.72	2	691.87	-0.9 mmu/-1.3 ppm	0	N-Term(Dimethyl:2H(4)); K12(Dimethyl:2H(4))	20.44	2	3.26	1		0	0.00006588
	B	IDVDENQETAGK	1374.67	2	687.84	-4.55 mmu/-6.61 ppm	0	N-Term(Dimethyl); K12(Dimethyl)	19.87	2	6.18	1		0	0.03143
P17889	A	LSLDDLFEQIK	1384.82	2	692.91	0 mmu/0 ppm	0	N-Term(Dimethyl:2H(4)); K11(Dimethyl:2H(4))	51.29	4	6.71	2	7.25	0	0.01852
	B	LSLDDLFEQIK	1376.76	2	688.88	-3.1 mmu/-4.49 ppm	0	N-Term(Dimethyl); K11(Dimethyl)	49.18	6	6.54	1		0	0.00699
P21881	A	EIENEWEQKDPLVR	1848.99	3	617.00	-0.86 mmu/-1.4 ppm	1	N-Term(Dimethyl:2H(4)); K9(Dimethyl:2H(4))	33.97	3	3.71	1		0	0.0001206
	B	EIENEWEQKDPLVR	1840.93	3	614.32	-3.86 mmu/-6.29 ppm	1	N-Term(Dimethyl); K9(Dimethyl)	32.57	1	6.15	1		0.043	0.319
P24137	A	LVELAPADELYENPLHPYTK	2368.24	3	790.09	-0.41 mmu/-0.52 ppm	0	N-Term(Dimethyl); K20(Dimethyl)	41.98	1				0	0.08422
		LVELAPADELYENPLHPYTK	2376.29	3	792.77	-1.32 mmu/-1.66 ppm	0	N-Term(Dimethyl:2H(4)); K20(Dimethyl:2H(4))	41.88	7	2.13	2	1.37	0	6.023E-11
	B	LVELAPADELYENPLHPYTK	2368.23	3	790.08	-3.59 mmu/-4.54 ppm	0	N-Term(Dimethyl); K20(Dimethyl)	40.22	7	2.29	2	9.69	0	1.175E-07
		LVELAPADELYENPLHPYTK	2376.28	3	792.76	-4.92 mmu/-6.21 ppm	0	N-Term(Dimethyl:2H(4)); K20(Dimethyl:2H(4))	40.45	2	2.18	1		0	0.000001623
P34956	A	EISGDSWGVGR	1194.60	2	597.81	-0.7 mmu/-1.16 ppm	0	N-Term(Dimethyl:2H(4))	28.44	3	9.78	1		0	0.0005899
	B	EISGDSWGVGR	1190.57	2	595.79	-3.89 mmu/-6.53 ppm	0	N-Term(Dimethyl)	27.22	3	8.22	1		0	0.001844

P37808	A	AIDALIPIGR	1070.68	2	535.84	-2.76 mmu/-5.15 ppm	0	N-Term(Dimethyl:2H(4))	38.36	52	2.15	7	4.43	0	0.00000781
		IMEVPVGEELIGR	1473.83	2	737.42	-0.62 mmu/-0.84 ppm	0	N-Term(Dimethyl:2H(4))	39.94	12	22.79	2	14.35	0	0.0001247
		ELIIGDR	847.52	2	424.26	-0.52 mmu/-1.22 ppm	0	N-Term(Dimethyl:2H(4))	27.64	4	2.45	1		0	0.01237
	B	AIDALIPIGR	1066.66	2	533.83	-2.66 mmu/-4.98 ppm	0	N-Term(Dimethyl)	37.83	42	1.82	8	5.48	0	0.000002794
		IMEVPVGEELIGR	1469.80	2	735.40	-3.02 mmu/-4.1 ppm	0	N-Term(Dimethyl)	38.42	6				0	0.00009816
		ELIIGDR	843.49	2	422.25	-2.06 mmu/-4.89 ppm	0	N-Term(Dimethyl)	26.56	5	3.16	2	21.22	0	0.01187
		IMEVPVGEELIGR	1485.79	2	743.40	-3.34 mmu/-4.5 ppm	0	N-Term(Dimethyl); M2(Oxidation)	34.34	2	12.46	1		0	0.03847
P39062	A	VVVTTPELLER	1287.78	2	644.39	-0.58 mmu/-0.91 ppm	0	N-Term(Dimethyl:2H(4))	35.04	3	11.33	1		0	0.05031
	B	VVVTTPELLER	1283.75	2	642.38	-3.35 mmu/-5.22 ppm	0	N-Term(Dimethyl)	34.01	4	15.31	2	1.16	0	0.05848
P54423	A	VEYLGEEEPEDGGTAEAAAEAK	2321.07	2	1161.04	-0.31 mmu/-0.27 ppm	0	N-Term(Dimethyl); K22(Dimethyl)	28.56	4	3.34	1		0	0.000103152
		VEYLGEEEPEDGGTAEAAAEAK	2329.12	2	1165.06	-1 mmu/-0.86 ppm	0	N-Term(Dimethyl:2H(4)); K22(Dimethyl:2H(4))	28.65	3	2.67	1		0	2.419E-11
	B	VEYLGEEEPEDGGTAEAAAEAK	2321.05	2	1161.03	-7.15 mmu/-6.16 ppm	0	N-Term(Dimethyl); K22(Dimethyl)	27.54	8	3.75	2	19.87	0	1.969E-13
P80239	A	NFDVLDEETGLADR	1625.79	2	813.40	-0.74 mmu/-0.91 ppm	0	N-Term(Dimethyl:2H(4))	37.98	1	1.92	1		0	2.414E-08
		WEEGGETLTPSLDLVGKI	2008.11	2	1004.56	-1.6 mmu/-1.6 ppm	1	N-Term(Dimethyl:2H(4)); K17(Dimethyl:2H(4))	46.40	1	2.15	1		0	0.0008343
	B	WEEGGETLTPSLDLVGKI	2000.05	2	1000.53	-6.59 mmu/-6.59 ppm	1	N-Term(Dimethyl); K17(Dimethyl)	44.55	1	1.69	1		0	0.001262

P80698	A	AENLEVSDEEVDAELTK	1946.95	2	973.98	+0.59 mmu/+0.61 ppm	0	N-Term(Dimethyl); K17(Dimethyl)	33.82	1				0	0.002135
		AENLEVSDEEVDAELTK	1954.99	2	978.00	-0.4 mmu/-0.41 ppm	0	N-Term(Dimethyl:2H(4)); K17(Dimethyl:2H(4))	33.88	5	2.00	2	13.65	0	1.27935E-13
	B	AENLEVSDEEVDAELTK	1946.94	2	973.97	-4.17 mmu/-4.28 ppm	0	N-Term(Dimethyl); K17(Dimethyl)	32.62	3				0	1.238E-11
		ELPELDDEFAKDIDEEVETLAELTEK	3104.51	4	776.88	-3.95 mmu/-5.08 ppm	1	N-Term(Dimethyl); K11(Dimethyl); K26(Dimethyl)	61.27	4				0	0.000002219
		AENLEVSDEEVDAELTK	1954.98	2	977.99	-6.02 mmu/-6.16 ppm	0	N-Term(Dimethyl:2H(4)); K17(Dimethyl:2H(4))	32.81	1	2.78	1		0	1.52082E-08
		EFEQRLQMQGMNLELYTQFSGQDEAALKEQMK	3964.92	5	793.79	-5.59 mmu/-7.04 ppm	2	N-Term(Dimethyl:2H(4)); M8(Oxidation); M11(Oxidation); K28(Dimethyl:2H(4)); M31(Oxidation); K32(Dimethyl:2H(4))	47.81	1				0	0.003066
Q04747	A	QADQGPVEGEVILTPIQR	1982.08	2	991.55	-1.39 mmu/-1.4 ppm	0	N-Term(Dimethyl:2H(4))	35.63	3				0	2.548E-09
		QFLEDPFRPGER	1522.79	3	508.27	-1.25 mmu/-2.46 ppm	0	N-Term(Dimethyl:2H(4))	36.30	4	4.10	1		0	0.01544
		VSFEIVDLYGSDEEMLR	2034.01	2	1017.51	+2.41 mmu/+2.37 ppm	0	N-Term(Dimethyl:2H(4))	47.76	1				0.003	0.1061
	B	QADQGPVEGEVILTPIQR	1978.05	2	989.53	-5.62 mmu/-5.68 ppm	0	N-Term(Dimethyl)	34.17	3				0	6.871E-09
		EQTNYQKDEEYWLDVFKGELPILDLPADFERPAER	4338.13	5	868.43	-6.44 mmu/-7.42 ppm	2	N-Term(Dimethyl); K7(Dimethyl); K17(Dimethyl)	58.81	2	2.22	1		0	0.006192
		QFLEDPFRPGER	1518.76	3	506.93	-2.75 mmu/-5.43 ppm	0	N-Term(Dimethyl)	35.29	1				0	0.05884
		VSFEIVDLYGSDEEMLR	2029.97	2	1015.49	-6.15 mmu/-6.06 ppm	0	N-Term(Dimethyl)	45.63	1				0.035	0.2962

Supporting Information S2 Information about peptides from proteins identified by LC-ESI-MS/MS experiments. The dataset is relative to the differential proteomic analysis of the NPs treated condition compared with the control colony biofilm and to biological replicates results with the same trend of regulation: Heavy/Light (Experiment A) or Light/Heavy (Experiment B) = Nanoparticles (NPs) / Ctrl. In the table are listed the peptides following parameters: alphanumeric unique protein sequence identifier (Accession) to which the peptide corresponds; the identified amino acidic peptide Sequence; the calculated protonated monoisotopic peptide mass, in daltons [MH+ (Da)]; Charge state of the precursor ion; mass-to-charge ratio (m/z) of the precursor ion, in daltons; the calculated peptide Mass Error in milli-mass units or parts per million (mmu/ppm); number of Missed Cleavages; peptides Modification [Dimethyl = Light labeling = + 28.03130 Da; Dimethyl:2H(4) = Heavy labeling = + 32.05641 Da; Carbamidomethyl = + 57.02146 Da; Oxidation = + 15.99492 Da] at the reported amino acids position or peptides N-terminal; retention time of the precursor ion, in minutes (RT); total number of identified peptide sequences (peptide spectrum matches) (# PSMs); ratio of the quantification values of the heavy and light quantification channels (Heavy/Light or Light/Heavy = NPs/Ctrl), number of peptide ratios that were actually used to calculate the protein ratio (NPs/Ctrl Count); the variability of the peptide ratios that were used to calculate the protein ratio Heavy/Light or Light/Heavy (NPs/Ctrl Variability [%]);the Percolator q-value (= false discovery rate) and posterior error probability (PEP) values that discriminate correct from incorrect peptide spectrum matches and calculates accurate statistics.

Molecular Function	# proteins *B. subtilis* Reference list	# proteins NPs/Ctrl list (experimental)	# proteins NPs/Ctrl list (expected)	Over representation	p-value	UniProtKB Protein Accession	GO Molecular Function	UniProtKB Protein Accession	GO Molecular Function
oxidoreductase activity	316	7	1.43	+	4.87E-02	P17889	GTPase activity;translation initiation factor activity;translation elongation factor activity;translation initiation factor activity;translation elongation factor activity;protein binding;translation initiation factor activity;translation elongation factor activity	P17889	GTPase activity;translation initiation factor activity;translation elongation factor activity; translation initiation factor activity;translation elongation factor activity;protein binding;translation initiation factor activity;translation elongation factor activity
								P24137	ATPase activity, coupled to transmembrane movement of substances;transmembrane transporter activity
								P34956	oxidoreductase activity
								O31669	oxidoreductase activity
								P21881	oxidoreductase activity
								O32119	
								O32165	protein binding
								O34714	
								P13800	methyltransferase activity;protein kinase activity
								P80698	
								P37808	hydrolase activity;receptor activity;anion channel activity;ligand-gated ion channel activity;cation transmembrane transporter activity;proton-transporting ATP synthase activity, rotational mechanism;single-stranded DNA binding
								P14949	oxidoreductase activity
								P12425	ligase activity
								P12877	structural constituent of ribosome;nucleic acid binding
								P14016	
								P39062	oxidoreductase activity;ligase activity
								P54423	serine-type peptidase activity
								Q04747	oxidoreductase activity;ligase activity
								P80239	oxidoreductase activity;peroxidase activity

Supporting Information 3 Functional characterization of the proteins modulated in expression belonging to the dataset relative to proteomic analysis of the NPs treated condition compared with the control colony biofilm. PANTHER Statistical over-representation test has been used to search for under- and over-represented biological processes. In the table are listed the following parameters: Molecular Function Category; number of reference database proteins (total 4193 proteins of *B. subtilis*) related to the specific category; number of experimental proteins related to the specific category; number of expected proteins related to the specific category for the experimental dataset; trend of over-representation; calculated p-value; accession number of the differentially expressed proteins with their Gene Ontology molecular functions (bold proteins contribute to the over-represented function).

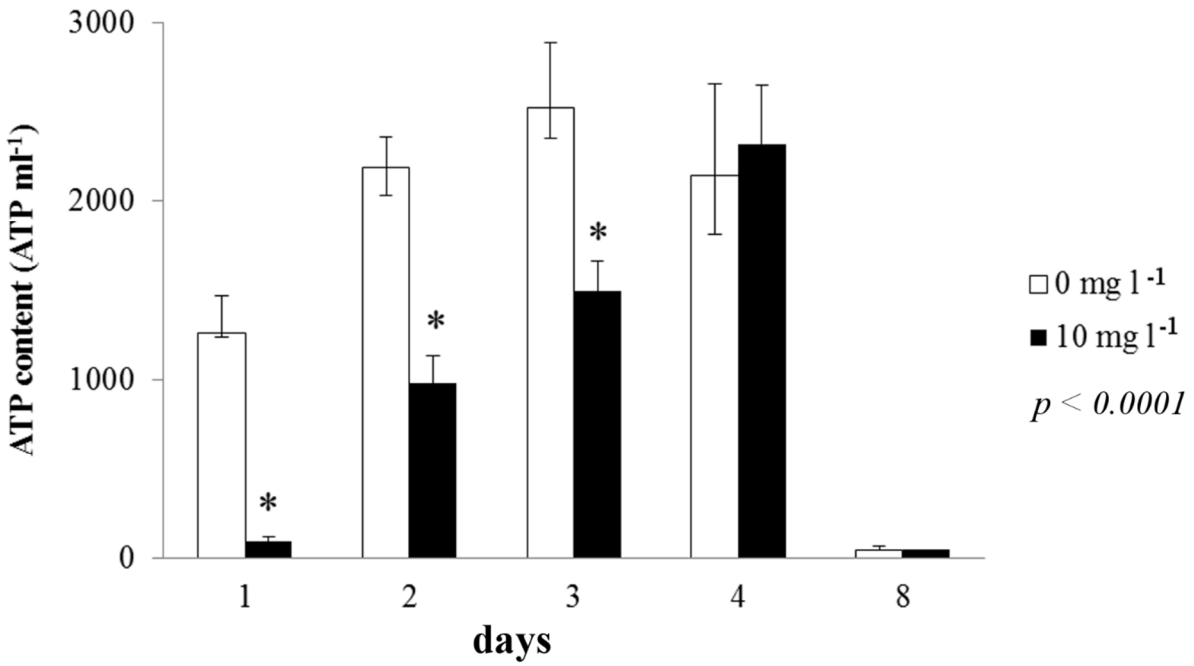

Supporting Information 4 ATP concentration in colony biofilm of *B. subtilis* in the presence of 0 and 10 mg/l of Ag-NPs over time. Data represent the means + the SD of three independent measurements. The histograms provide the p-values obtained by ANOVA analysis. Posthoc comparison results (Tukey's HSD, $p < 0.05$) are summarized with asterisks to underline the most relevant differences of Ag-NPs treated samples with respect to control

A Gateway-compatible allelic exchange system for generation of in-frame and unmarked gene deletions in *Burkholderia cenocepacia*

Fazli M[1], Harrison JJ[2], Gambino M[3], Givskov M[4,5], Tolker-Nielsen T[4#]

[1]Department of Biology, Faculty of Science, University of Copenhagen, Copenhagen, Denmark.

[2]Department of Biological Sciences, University of Calgary, Calgary, Alberta, Canada

[3]Department of Food, Environmental and Nutritional Sciences, University of Milan, Milan, Italy.

[4]Costerton Biofilm Center, Department Immunology and Microbiology, Faculty of Health and Medical Sciences, University of Copenhagen, Copenhagen, Denmark.

[5]Singapore Centre on Environmental Life Sciences Engineering, Nanyang Technological University, Singapore, Singapore.

 # Corresponding author: Tim Tolker-Nielsen.

Department of Immunology and Microbiology

Faculty of Health Sciences, University of Copenhagen

Blegdamsvej 3B, DK-2200 Copenhagen N, Denmark.

Phone: +45 3532 6656 Fax: +45 353 27853.

E-mail: ttn@sund.ku.dk

Running title: Deletion mutagenesis in *Burkholderia cenocepacia*

Keywords: *Burkholderia cenocepacia*, *Burkholderia* species, deletion mutagenesis, Gateway Recombineering

Abstract

Burkholderia cenocepacia is an emerging opportunistic pathogen causing life-threatening infections in immunocompromised individuals and in patients with cystic fibrosis, which are often difficult, if not impossible, to treat. Understanding the genetic basis of virulence in this emerging pathogen is important for the development of novel treatment regimes. Generating deletion mutations in genes predicted to encode virulence determinants is fundamental to investigating the mechanisms of pathogenesis. However, there is a lack of appropriate selectable and counter-selectable markers for use in *B. cenocepacia*, making its genetic manipulation problematic. Here we describe a Gateway-compatible allelic exchange system based on the counter-selectable *pheS* gene and I-SceI homing endonuclease. The system provides efficiency in cloning homology regions of target genes, and allows the generation of precise and unmarked gene deletions in *B. cenocepacia*. As a proof of concept, we demonstrate its utility by deleting the *Bcam1349* gene, encoding a c-di-GMP responsive regulator protein important for biofilm formation.

Introduction

Burkholderia cenocepacia is a member of a group of closely related Gram-negative bacteria referred to as the *Burkholderia cepacia complex* (Bcc). Bcc contains at least 18 different species that thrive in diverse ecological niches including clinical, industrial and natural environments. These bacteria possess very large genomes separated in multiple replicons and hence are considered one of the most versatile groups of Gram-negative bacteria (1, 2). Some Bcc species have biotechnological potential use in processes such as enhancement of plant growth or breakdown of pollutants, while others are opportunistic pathogens causing life-threatening infections in immunocompromised individuals and in patients with cystic fibrosis (CF) (3). Although all members of Bcc have been isolated from CF

patients, *B. cenocepacia* accounts for the majority of these isolates, comprising the most virulent and transmissible strains, associated with poor clinical course and high mortality (4). Therefore, research on the virulence mechanisms of Bcc bacteria has largely focused on *B. cenocepacia*.

The genomes of several *B. cenocepacia* strains have recently been sequenced (5, 6, 7), enabling bioinformatics-based predictions of virulence determinants in this pathogen. Although a number of genes associated with virulence in *B. cenocepacia* has been identified (4, 8, 9) and tested in various infection models (10, 11), it seems likely that the list of the genes implicated in virulence is far from complete and will expand with genetic tools becoming available to manipulate *B. cenocepacia* strains. The deletion of genes potentially associated with virulence is a powerful way to investigate their function in bacterial physiology and pathogenesis. Most of the virulence traits of *B. cenocepacia*, such as antibiotic resistance, motility, biofilm formation, cell invasion and intracellular survival, are multifactorial involving more than one gene, thus multiple gene deletions may need to be generated in one strain to fully assess the genetic basis of a particular virulence trait. This requires an efficient method to generate gene deletions, which are preferably not marked with antibiotic resistance cassettes, as this would prevent the ability to mutate more than a single gene in one particular strain, and moreover, may cause polar effects on adjacent genes. During the past few years a number of elegant systems has been developed for generation of unmarked gene deletions in *B. cenocepacia* (12, 13) as well as in other *Burkholderia* species (14, 15, 16). In these systems regions of homology containing a mutant allele of a target gene are cloned into a suicide vector. These vectors are then transferred into the bacterial host by conjugation. The integration of the plasmid into the chromosome by homologous recombination is selected by antibiotic resistance encoded by a gene on the plasmid, leading to formation of merodiploids, which contain both the mutant and wild type alleles of the target gene. The resolution of merodiploids by excision of the integrated plasmid in a second homologous recombination event results in a population of cells in which a significant

fraction contains the desired gene deletion. This latter step usually requires counter-selection for the integrated plasmid since the second homologous recombination can be an exceptionally rare event.

Sucrose counter-selection based on the *sacB* gene (15, 17), and an engineered counter selectable marker based on the *Burkholderia pseudomallei pheS* gene encoding the α-subunit of phenylalanyl tRNA synthase (14) have been used in some *Burkholderia* species. However, they appear to be inappropriate and leaky counter selectable markers for generation of *B. cenocepacia* gene deletions in our laboratory. Another way to stimulate the second homologous recombination event and consequently the resolution of merodiploids is based on the yeast homing endonuclease I-SceI, which recognizes a specific 18-bp sequence (12, 15). After an allelic exchange vector carrying the I-SceI recognition site has integrated into the chromosome, a replicative second plasmid constitutively expressing the I-SceI enzyme is introduced into the merodiploid bacteria. The I-SceI enzyme creates a double-stranded DNA break at the I-SceI site within the integrated plasmid, which stimulates a second homologous recombination event by the host's DNA repair system. The excision of the integrated plasmid results in a population of cells carrying either the wild type or the mutant allele, which can be identified by PCR and partial sequencing.

Another major limitation of allelic exchange vectors for *Burkholderia* species is their dependence on restriction and ligation enzymes for cloning. Restriction-free cloning based on the Gateway recombineering technology (18) is an alternative method that can expedite the construction of gene replacement vectors containing mutant alleles.

Here we present a Gateway-compatible allelic exchange system for *Burkholderia* species that utilizes the I-SceI homing endonuclease and *pheS*-based counter-selection. We further describe the application of this system for generating in-frame and unmarked gene deletions in *B. cenocepacia* H111. As a proof of concept, we describe the deletion and complementation of the *Bcam1349* gene, which is a regulator of biofilm formation in *B. cenocepacia* H111. In addition, we also provide

Applied and Environmental Microbiology

evidence that the system can be used to make gene deletions in *Burkholderia thailandensis*, indicating that it may be used in other *Burkholderia* species as well.

Experimental procedures

Strains, plasmids, and growth conditions

The bacterial strains and plasmids used in this study are listed in Table 1. All *B. cenocepacia* and *Escherichia coli* strains were grown at 37°C. Luria broth (LB) medium was used for overnight batch cultivation of all bacteria unless otherwise stated. Solid media were prepared with 2% (w/v) agar. Eighty micrograms tetracycline (Tet) mL^{-1} (liquid medium), 120 micrograms µg Tet mL^{-1} (solid medium), 25 µg gentamicin-sulfate (Gm) mL^{-1}, 100 µg kanamycin-sulfate (Km) mL^{-1} and 100 µg trimethoprim (Tp) mL^{-1} were used for *B. cenocepacia* strains, and 20 µg Tet mL^{-1}, 10 µg Gm mL^{-1}, 50 µg Km mL^{-1}, 50 µg Tp mL^{-1}, 100 µg ampicillin (Ap) mL^{-1} and 25 µg chloramphenicol (Cm) mL^{-1} were used for *E. coli* strains where appropriate. After conjugal transfer of plasmids into *B. cenocepacia*, AB-agar medium (19) supplemented with 10 $mmolL^{-1}$ Na-citrate and appropriate antibiotics were used to select for *B. cenocepacia* tranconjugants. For use in self curing of the pDAI-SceI-*pheS* plasmid, 0.1% (w/v) *p*-chlorophenylalanine (cPhe; DL-4- chlorophenylalanine; Sigma-Aldrich) was autoclaved together with B-salts solution, and A-salts solution and the carbon source of choice were added thereafter.

Construction of Gateway-compatible allelic exchange vectors

The *attB1* and *attB2* flanked Gateway donor site was amplified by PCR from pDONR221 using the primers GWE-SceI-F (flanked by *Hind*III and I-SceI restriction sites) and GWE-R (flanked by *Xba*I site). The resulting 2.6-kb PCR product was digested with *Hind*III and *Xba*I, and cloned into *HindIII*/*Xba*I digested plasmids pEX18Tp-*pheS*, pEX18Gm-*pheS* and pEX18Km-*pheS* (14),

resulting in the allelic exchange vectors pDONRPEX18Tp-SceI-*pheS*, pDONRPEX18Gm-SceI-*pheS* and pDONRPEX18Km-SceI-*pheS*, respectively (Fig. 1). The insertion of the Gateway donor site was confirmed by restriction analysis and partial sequencing of the newly generated vectors. These vectors are maintained in *E. coli* DB3.1 strain, which contains a *gyrA462* mutation (Invitrogen).

Construction of the I-SceI expression vector pDAI-SceI-*pheS*

To construct pDAI-SceI-*pheS* (Fig. 1), a ~1.2-kb fragment containing the *pheS* gene was excised from pUC57-pheS (14) by restriction with *Xba*I and *Sph*I, and was ligated into the *Xba*I/*Sph*I digested plasmid pDAI-SceI (12). The presence of the insertion was verified by restriction analysis.

Construction of the gene replacement vector pENTRPEX18Tp-SceI-*pheS-Bcam1349*

The upstream fragment of *Bcam1349* gene was amplified using the primers Bcam1349-UpF-GWR and Bcam1349-UpR-tail, and the downstream fragment of *Bcam1349* gene was amplified using the primers Bcam1349-DnF and Bcam1349-DnR-GWL (Table 2). Both fragments were amplified using Phusion High-Fidelity DNA polymerase (Thermo Scientific) according to the manufacturer's instructions and the following thermal cycling conditions: 98 °C for 2 min; 25 cycles of 98 °C for 15 sec, 64 °C for 30 sec and 72 °C for 1 min; a final extension step of 72 °C for 7 min. The PCR fragments were purified using Wizard SV Gel and PCR Clean-Up System (Promega), and their concentrations were determined spectrophotometrically. The up- and downstream fragments were fused together and amplified using the primers GW-*attB*1 and GW-*attB*2 (Table 2) in splicing-by-overlap extension (SOE) PCR (20) to generate the *Bcam1349* mutant allele as follows. Equal amounts (50 ng) of each up- and downstream fragments and the other components of the PCR reaction except the primers GW-*attB*1 and GW-*attB*2 were mixed. The PCR reaction was carried out using the following thermal cycling conditions: 98 °C for 2 min; 3 cycles of 98 °C for 15 sec, 64 °C for 30 sec and 72 °C for 1 min; and a final extension step of 72 °C for 1 min. The final extension step was paused at 30 sec, the primers GW-*attB*1 and GW-*attB*2 were added, and the thermal cycling was

continued with 27 cycles of 98 °C for 15 sec, 64 °C for 30 sec and 72 °C for 2 min; and a final extension step of 72 °C for 7 min. The PCR product was then purified and verified by restriction analysis.

BP clonase reaction for recombinational transfer of the mutant allele into the allelic exchange vector pDONRPEX18Tp-SceI-*pheS* was performed at 25 °C overnight as described in the Gateway cloning manual (Invitrogen), using only half of the recommended amount of BP Clonase II enzyme mix (Invitrogen). The BP clonase reaction product was transferred into chemically competent *E. coli* DH5α cells. The transformants growing on LB-agar plates containing 50 µg Tp mL^{-1} were screened by colony PCR using the primers GWE-SceI-F and GWE-R for insertion of the deletion allele. A number of positive clones were streaked on LB-agar plates containing 50 µg Tp mL^{-1} for purification, plasmid isolation and partial sequencing.

Construction of pYedQ2 and the complementation plasmid pMF564

The pYedQ2 plasmid which was used to elevate intracellular c-di-GMP levels was constructed as follows. The *yedQ* expression cassette was excised from the plasmid pYedQ (21) by restriction with *Bam*HI and *Hind*III, and was inserted into the *Bam*HI/*Hind*III digested broad-host-range cloning vector pBBR1MCS-5 (22). The presence of the insertion was confirmed by restriction analysis.

The complementation plasmid pMF564 was constructed as follows. The vector pBBR1MCS-5 was digested with *Sph*I and blunt-ended by T4 DNA polymerase. The linearized vector was further digested with *Xba*I and de-phosphorylated by shrimp-alkaline phosphatase. The *Sph*I/*Xba*I digestion removed the P_{lac} promoter and the related regulatory sequences from the plasmid. A ~1.5-kb fragment containing the *Bcam1349* gene and its ~0.7-kb upstream DNA sequence was PCR amplified using the primers Bcam1349-RBS-F and Bcam1349-RBS-R, which were flanked by *Sma*I and *Xba*I restriction sites, respectively. The PCR fragment was digested with *Sma*I and *Xba*I and

cloned into the previously linearized vector, yielding the complementation plasmid pMF564. The presence of the insertion was confirmed by restriction analysis.

Mutagenesis of *B. cenocepacia* H111

The gene replacement vector pENTRPEXTp-SceI-*pheS-Bcam1349* was introduced by conjugation into *B. cenocepacia* via tri-parental mating as described previously (23). The co-integrants were selected for Tp resistance on AB-citrate agar plates containing 100 µg Tp mL^{-1}. Four Tp resistant colonies were streaked on the same selective plates, and the growing colonies were screened for integration of the plasmid by colony PCR using the primers Bcam1349-F and Bcam1349-R (Table 2). A single positive merodiploid clone was transformed with pDAI-SceI-*pheS* by tri-parental mating to stimulate the second homologous recombination event and resolve the merodiploid state. The transconjugants were screened for Tet resistance on AB-citrate agar plates containing 120 µg Tet mL^{-1}. Batches of 10 Tet resistant colonies were screened for the loss of the wild type allele and the presence of the desired gene deletion by colony PCR using the primers Bcam1349-F and Bcam1349-R. Two positive clones were purified by streaking and growing on AB-citrate agar plate. Thereafter a single colony for each clone was picked and grown in 1 ml AB-glucose medium containing 0.1% (w/v) cPhe at 37 °C overnight in order to stimulate the loss of pDAI-SceI-*pheS* via the counter-selectable marker *pheS* on the plasmid. Ten-fold serial dilutions of the overnight grown cultures were plated on LB-agar plates without any antibiotic, and 20 of the growing colonies for each clone were patched on LB-agar plates with or without tetracycline using sterile tooth pick to screen for Tet sensitivity, which indicated the loss of the plasmid pDAI-SceI-*pheS*. A single positive colony for each clone was selected and stored at -80 °C.

Phenotypic characterization of the *B. cenocepacia Bcam1349* deletion mutant

The colony morphology, pellicle formation and flow-cell biofilm formation assays were performed as described previously (24).

Results and Discussion

Features of the Gateway-compatible allelic exchange vectors

The allelic exchange vectors pEX18Tp-*pheS*, pEX18Gm-*pheS* and pEX18Km-*pheS*, which contain different antibiotic resistance markers, were first described by Barrett and colleagues (14). These vectors are derivatives of a set of pEX-family vectors (25) in which the counter-selectable marker *sacB* gene was replaced with a mutant allele of the *B. pseudomallei pheS* gene. Here, we modified these vectors for use as Gateway-compatible donor vectors to clone regions of homology containing the deleted allele of a target gene. This was carried out by cloning the Gateway donor cassette from pDONR221 into the multicloning site of the above vectors. The 18-bp I-SceI recognition site was incorporated into the vectors as a tail to the forward primer during PCR amplification of the donor cassette. The resulting vectors (Fig. 1) contain sequences *attP*1 and *attP*2 required for recombination-based cloning and the *ccdB* gene as a counter selectable marker, which kills *gyrA*$^{+}$ host cells such as *E. coli* DH5α by inducing gyrase-mediated double-stranded DNA breaks, providing positive selection for *E. coli* clones bearing plasmids with cloned inserts. Additionally, the vectors contain the counter-selectable *pheS* gene (14) driven by the P_{S12} promoter of the *B. pseudomallei rpsL* gene (26) and the I-SceI recognition site for downstream resolution of merodiploids. Although the mutant *pheS* gene was shown to be efficient in killing *Burkholderia thailandensis* cells in the presence of cPhe when expressed as a single copy from the gene replacement vector integrated on the chromosome (14), it was inefficient in killing *B. cenocepacia* H111 cells, and the resolution of merodiploids was almost impossible when the cells were grown in the presence of cPhe. Therefore, we incorporated the I-SceI site into the gene replacement vectors for downstream resolution of merodiploids. We preferred to keep the *pheS* gene on the gene replacement

vectors as it can efficiently be utilized as a counter selectable marker in strains such as *B. thailandensis* (14).

Features of the I-SceI expression vector pDAI-SceI-*pheS*

The vector pDAI-SceI-*pheS* (Fig. 1) that constitutively expresses the I-SceI endonuclease is a derivative of the vector pDAI-SceI, features of which was previously described by Flannagan and colleagues (12). Although the mutant *pheS* gene was not efficient in killing *B. cenocepacia* cells in the presence of cPhe when expressed as a single copy on the chromosome, it effectively killed almost all *B. cenocepacia* cells when expressed from the multicopy plasmid pBBR1MCS-Km-*pheS* (14) (Fig. S1), indicating that the mutant *pheS* gene has to be present in multiple copies in the cells to provide effective counter selection in *B. cenocepacia*. Based on this finding, we modified pDAI-SceI by cloning the mutant *B. pseudomallei pheS* gene from pUC57-*pheS* (14) into the multicloning site of pDAI-SceI to expedite self-curing of the plasmid. In the presence of 0.1% cPhe, the mutant *pheS* gene enables efficient killing of *B. cenocepacia* cells containing pDAI-SceI-*pheS* and curing of the *B. cenocepacia* deletion mutants from the plasmid once they are obtained after the resolution of merodiploids. In this way, the deletion mutants become ready for subsequent rounds of mutagenesis.

Construction of the *B. cenocepacia Bcam1349* deletion mutant

Using the allelic exchange system described here, we have successfully generated gene deletions both in *B. cenocepacia* H111 and *B. thailandensis* (Supplementary material). As a proof of concept, we present the procedure that was used to delete the *Bcam1349* gene. This gene encodes a c-di-GMP responsive CRP/FNR superfamily transcription factor, and regulates biofilm formation in *B. cenocepacia* H111 (23, 24). We previously showed that elevated intracellular levels of c-di-GMP promoted wrinkled colony formation on solid medium, robust pellicle formation at the air-liquid interface of static liquid cultures, and increased biofilm formation in flow-cells. However, despite

having high intracellular c-di-GMP levels, a transposon insertion mutant of *Bcam1349* did not form wrinkled colonies, pellicle or thick flow-cell biofilms (23).

We created the *Bcam1349* mutant allele in two consecutive PCR rounds using three primer pairs (Table 2). Two of them were gene specific, and one of them was common and can be used routinely. Gene specific primers were designed to amplify fragments ranging from 0.8- to 1-kb in size. The fragments were chosen so that the gene specific UpF-GWR primer is placed within 10-100bp after the gene start and the gene specific primer DnR-GWL is placed within 10-100 bp before the stop codon. The gene specific primers were compared to the *B. cenocepacia* H111 genome to make sure that they will not fully anneal to unspecific regions in the genome. In the first PCR round, the gene specific primers were used to amplify up- and downstream homology regions of the target gene. We usually obtained single major PCR products of the right size, which were subsequently purified with a PCR clean-up kit and used in the second PCR round. However, if there are multiple bands, the entire PCR reactions should be loaded on an agarose gel and fragments with the right size should be gel extracted. In the second PCR round, equal amounts of up- and downstream PCR fragments were fused together and amplified with the common primers GW-*attB*1 and GW-*attB*2 (Table 2), incorporating the *attB*1 and *attB*2 recombination sites at either end of the deletion allele. We usually obtained a single major PCR product of the right size (~2-kb) at this step.

We recombined the *Bcam1349* mutant allele into pDONRPEX18Tp-SceI-pheS using BP clonase and transferred the entire BP reaction product into *E. coli* DH5α cells. Tp resistant transformants were selected and the presence of the correct plasmid was checked by colony PCR using the primers GWE-SceI-F and GWE-R. Alternatively M13-F and M13-R primers can be used. Plasmids were isolated from a number of positive clones, and the presence of the deletion allele was verified by restriction analysis and partial sequencing.

The resulting gene replacement vector pENTRPEX18Tp-SceI-*pheS*-*Bcam1349* was transferred into *B. cenocepacia* by tri-parental mating giving rise to Tp resistant merodiploids (Fig. 2A). The integration of the nonreplicative vector into the chromosome can normally be verified by colony PCR using the gene specific UpF-GWR and DnR-GWL primers, often resulting in two PCR products corresponding to the wild type and deletion alleles (Fig. 2B). However we had to use another pair of primers, Bcam1349-F and Bcam1349-R, to verify integration of the vector, as the former primer pair did not result in any PCR products. During the generation of deletion mutants of other genes, we also noticed that it is not always possible to see a PCR product corresponding to the wild type allele as its amplification may not be favoured due to its relatively large size compared to the deletion allele. A single merodiploid clone was selected and transformed with pDAI-SceI-*pheS* by conjugation to stimulate the second homologous recombination event via generation of a double-stranded DNA break by I-SceI endonuclease expressed from the plasmid. Depending on the location of the second recombination event, the resolution of the merodiploid state either restored the wild type allele or generated the desired gene deletion (Fig. 2A). Eight Tet resistant colonies were selected and verified for *Bcam1349* deletion by colony PCR. In our experience, at least one colony always contained the desired gene deletion (Fig. 2B). Finally, the deletion mutant was cured from the plasmid pDAI-SceI-*pheS* by growing the mutant in liquid medium containing 0.1% cPhe as described in the experimental procedures. The counter-selection medium with cPhe should not contain any competing phenylalanine for efficient counter selection. We therefore prefer to use AB-minimal medium supplemented with glucose as carbon source. However in the case of deleting genes essential for growth in minimal medium, the mutants can alternatively be cured from the plasmid pDAI-SceI-pheS by growing them in serial passages in rich medium without cPhe and Tet, which is required for maintenance of the plasmid.

Phenotypic characterization of the *Bcam1349* deletion mutant

We previously demonstrated that a transposon insertion mutant of *Bcam1349* did not form wrinkled colonies, robust pellicle or thick flow-cell biofilms despite having high intracellular c-di-GMP levels (22). To characterize the *Bcam1349* deletion mutant obtained here, we first transformed it with the plasmid pYedQ2, which contains the *E. coli* diguanylate cyclase protein YedQ and leads to elevated intracellular levels of c-di-GMP in *B. cenocepacia* (23). Unlike the pYedQ2-containing wild type, the pYedQ2-containing *Bcam1349* mutant formed smooth colonies on AB-agar medium (Fig. 3A) and did not form robust pellicles in static liquid culture (Fig. 3B). Furthermore, we tested biofilm formation ability of the *Bcam1349* mutant in a flow-cell biofilm system. In accordance with the previous results, the *Bcam1349* mutant was markedly impaired in biofilm formation compared to the wild type strain (Fig. 4). To rule out the possibility that the observed biofilm defect was due to a secondary mutation obtained during the mutagenesis procedure, we genetically complemented the mutant strain with an intact copy of the *Bcam1349* gene and its 0.7-kb upstream DNA sequence on a replicative plasmid (pMF564). After complementation of the mutant strain, the biofilm formation ability was restored to wild type levels (Fig. 4), indicating that the biofilm defect was indeed a result of *Bcam1349* deletion.

Conclusion

The Gateway-compatible allelic exchange system described here takes advantage of the bacteriophage lambda based site-specific recombination instead of the traditional cloning procedures based on restriction enzymes and ligase, and provides flexibility and efficiency. With proper primer design, the system allows precise in-frame deletion of open reading frames without generating truncated genes, reducing the risk of undesired polar effects. Moreover, the unmarked nature of the deletion procedure enables repetitive rounds of gene deletions in a single strain. We believe that the allelic exchange system described here will be useful in understanding the genetic basis of virulence

in *B. cenocepacia* and in systematic analysis of functions of genes in the physiology of this emerging pathogen and other *Burkholderia* species with medical relevance or potential biotechnological use. Furthermore, the allelic exchange system may enable the engineering of *Burkholderia* strains that retain their biotechnologically useful functions, but are attenuated for virulence.

Acknowledgements

This work was supported by grants from the Lundbeck Foundation to MF, and the Danish Council for Independent Research to TTN.

References

1. Coenye T, Vandamme P. 2003. Diversity and significance of Burkholderia species occupying diverse ecological niches. Environ. Microbiol. 5:719-729.
2. Mahenthiralingam E, Baldwin A, Dowson CG. 2008. Burkholderia cepacia complex bacteria: opportunistic pathogens with important natural biology. J Appl. Microbiol. 104:1539-1551.
3. Chiarini L, Bevivino A, Dalmastri C, Tabacchioni S, Visca P. 2006. Burkholderia cepacia complex species: health hazards and biotechnological potential. Trends Microbiol. 14:277-286.
4. Drevinek P, Mahenthiralingam E. 2010. Burkholderia cenocepacia in cystic fibrosis: epidemiology and molecular mechanisms of virulence. Clin. Microbiol. Infect. 16:821-830.
5. Holden MT, Seth-Smith HM, Crossman LC, Sebaihia M, Bentley SD, Cerdeño-Tárraga AM, Thomson NR, Bason N, Quail MA, Sharp S, Cherevach I, Churcher C, Goodhead I, Hauser H, Holroyd N, Mungall K, Scott P, Walker D, White B, Rose H, Iversen P, Mil-Homens D,

329 Rocha EP, Fialho AM, Baldwin A, Dowson C, Barrell BG, Govan JR, Vandamme P, Hart
330 CA, Mahenthiralingam E, Parkhill J. 2009. The genome of Burkholderia cenocepacia J2315,
331 an epidemic pathogen of cystic fibrosis patients. J. Bacteriol. 191:261-277.

332 6. Varga JJ, Losada L, Zelazny AM, Kim M, McCorrison J, Brinkac L, Sampaio EP, Greenberg
333 DE, Singh I, Heiner C, Ashby M, Nierman WC, Holland SM, Goldberg JB. 2013. Draft
334 genome sequences of Burkholderia cenocepacia ET12 lineage strains K56-2 and BC7.
335 Genome. Announc. 1:e00841-13.

336 7. Carlier A, Agnoli K, Pessi G, Suppiger A, Jenul C, Schmid N, Tümmler B, Pinto-Carbo M,
337 Eberl L. Genome sequence of Burkholderia cenocepacia H111, a cystic fibrosis airway
338 isolate. Genome Announc. 2:e00298-14.

339 8. Suppiger A, Schmid N, Aguilar C, Pessi G, Eberl L. 2013. Two quorum sensing systems
340 control biofilm formation and virulence in members of Burkholderia cepacia complex.
341 Virulence. 4:400-409.

342 9. Fazli M, Almblad H, Rybtke ML, Givskov M, Eberl L, Tolker-Nielsen T. Regulation of
343 biofilm formation in Pseudomonas and Burkholderia species. Environ. Microbiol. 16:1961-
344 1981.

345 10. Uehlinger S, Schwager S, Bernier SP, Riedel K, Nguyen DT, Sokol PA, Eberl L. 2009.
346 Identification of specific and universal virulence factors in Burkholderia cenocepacia strains
347 by using multiple infection hosts. Infect. Immun. 77:4102-10.

348 11. Schwager S, Agnoli K, Köthe M, Feldmann F, Givskov M, Carlier A, Eberl L. 2013.
349 Identification of Burkholderia cenocepacia strain H111 virulence factors using
350 nonmammalian infection hosts. Infect. Immun. 81:143-53.

351 12. Flannagan RS, Linn T, Valvano MA. 2008. A system for construction of targeted unmarked
352 gene deletions in the genus Burkholderia. Environ. Microbiol. 10:1652-60.

13. Aubert DF, Hamad MA, Valvano MA. 2014. A markerless deletion method for genetic manipulation of Burkholderia cenocepacia and other multidrug-resistant gram-negative bacteria. Methods Mol. Biol. 1197:311-27.

14. Barrett AR, Kang Y, Inamasu KS, Son MS, Vukovich JM, Hoang TT. 2008. Genetic tools for allelic replacement in Burkholderia species. Appl. Environ. Microbiol. 74:4498-508.

15. López CM, Rholl DA, Trunck LA, Schweizer HP. 2009. Versatile dual-technology system for markerless allele replacement in Burkholderia pseudomallei. Appl. Environ. Microbiol. 75:6496-503.

16. Hamad MA, Zajdowicz SL, Holmes RK, Voskuil MI. 2009. An allelic exchange system for compliant genetic manipulation of the select agents Burkholderia pseudomallei and Burkholderia mallei. Gene. 430:123-31.

17. Logue CA, Peak IR, Beacham IR. 2009. Facile construction of unmarked gene deletion mutants in Burkholderia pseudomallei using sacB counter-selection in sucrose-resistant and sucrose-sensitive isolates. J. Microbiol. Methods. 76:320-3.

18. Katzen F. 20007. Gateway recombinational cloning: a biological operating system. Expert Opin. Drug Dicov. 2:571-89.

19. Clark DJ, Maaløe O. 1967. DNA replication and division cycle in Escherichia coli. J. Mol. Biol. 23:99-112.

20. Horton RM, Hunt HD, Ho SN, Pullen JK, Pease LR. 1989. Engineering hybrid genes without the use of restriction enzymes: gene splicing by overlap extension. Gene. 77:61-8.

21. Ausmees N, Mayer R, Weinhouse H, Volman G, Amikam D, Benziman M, Lindberg M. 2001. Genetic data indicate that proteins containing GGDEF domain possess diguanylate cyclase activity. FEMS Microbiol. Lett. 204:163-7.

22. Kovach ME, Elzer PH, Hill DS, Robertson GT, Farris MA, Roop RM 2nd, Peterson KM. 1995. Four new derivatives of the broad-host-range cloning vector pBBR1MCS, carrying different antibiotic-resistance cassettes. Gene. 166:175-6.

23. Fazli M, O'Connell A, Nilsson M, Niehaus K, Dow JM, Givskov M, Ryan RP, Tolker-Nielsen T. 2011. The CRP/FNR family protein Bcam1349 is a c-di-GMP effector that regulates biofilm formation in the respiratory pathogen Burkholderia cenocepacia. Mol. Microbiol. 82:327-41.

24. Fazli M, McCarthy Y, Givskov M, Ryan RP, Tolker-Nielsen T. 2013. The exopolysaccharide gene cluster Bcam1330-Bcam1341 is involved in Burkholderia cenocepacia biofilm formation, and its expression is regulated by c-di-GMP and Bcam1349. Microbiologyopen. 2:105-22.

25. Hoang TT, Karkhoff-Schweizer RR, Kutchma AJ, Schweizer HP. 1998. A broad-host-range Flp-FRT recombination system for site-specific excision of chromosomally-located DNA sequences: application for isolation of unmarked Pseudomonas aeruginosa mutants. Gene. 212:77-86.

26. Yu M, Tsang JS. 2006. Use of ribosomal promoters from Burkholderia cenocepacia and Burkholderia cepacia for improved expression of transporter protein in Escherichia coli. Protein Expr. Purif. 49:219-27.

27. Kessler B, de Lorenzo V, Timmis KN. 1992. A general system to integrate lacZ fusions into the chromosomes of gram-negative eubacteria: regulation of Pm promoter in the TOL plasmid studied with all controlling elements in monocopy. Mol. Gen. Genet. 233:293–301

28. Choi KH, Schweizer HP. 2005. An improved method for rapid generation of unmarked Pseudomonas aeruginosa deletion mutants. BMC Microbiol. 5:30.

399 29. Peano C, Chiaramonte F, Motta S, Pietrelli A, Jaillon S, Rossi E, Consolandi C, Champion
400 OL, Michell SL, Freddin L, Falciola L, Basilico F, Garlanda C, Mauri P, De Bellis G,
401 Landini P. 2014. Gene and protein expression in response to different growth temperatures
402 and oxygen availability in Burkholderia thailandensis. PLOS One. 9:e93009.

403

404 Tables and Figure Legends

405 **Table 1.** Bacterial strains and plasmids used in the study.

406 **Table 2.** Primers used in the study.

407 **Figure 1.** Maps of the allelic exchange vectors and the I-SceI expression vector constructed in this
408 study. (A, B and C) The gene replacement vectors, each containing a different antibiotic resistance
409 marker, were constructed by cloning the Gateway cassette into the *Xba*I/*Hind*III site of a set of pEX
410 family vectors based on the mutant *pheS* gene (14). *attP*1 and *attP*2, lambda recombination sites;
411 CmR, choloramphenicol acetyltransferase-encoding gene; *ccdb*, gene encoding gyrase-modifying
412 enzyme; *dhfr*, dihydrofolate reductase-encoding gene; *aac1*, Gm-acetyltransferase-encoding gene;
413 *kanR*, confers resistance to kanamycin; *pheS*, mutant gene for the α-subunit of phenylalanyl tRNA
414 synthase; P_{S12}, *B. pseudomallei rpsL* gene promoter; I-SceI, I-SceI endonuclease recognition site;
415 ColE1, origin of replication; *ori*T, conjugal origin of transfer; M13-F and M13-R, primer binding
416 sites for partial sequencing of the DNA sequence cloned into *attP*1-*attP*2 sites. (D) pDAI-SceI-*pheS*
417 was constructed by cloning the *pheS* gene into the XbaI/SphI site of plasmid pDAI-SceI (12). *tetA*
418 and *tetR*, genes encoding tetracycline specific efflux protein and repressor protein, respectively; *mob*,
419 region facilitating conjugal transfer; *I-SceI*, gene encoding the I-SceI endonuclease; ori_pBBR1, origin
420 of replication; *rep*, gene encoding pBBR1 replication protein.

Figure 2. Schematic diagram depicting the gene replacement procedure in *B. cenocepacia* H111. (A) Step 1: The gene replacement vector pENTRPEX18Tp-SceI-*pheS*-*Bcam1349* (derivative of pDONRPEX18Tp-SceI-*pheS*) contains regions of homology flanking the *Bcam1349* gene. The vector was transferred into *B. cenocepacia* by conjugation and integrated into the chromosome by the first homologous recombination event, resulting in trimethoprim resistant merodiploids, which were verified by colony PCR (gel image lane 1). Step 2: A merodiploid was transformed with pDAI-SceI-*pheS*. The I-SceI endonuclease expressed from the plasmid introduces a double-stranded DNA break at the I-SceI recognition site on the chromosome. Step 3: The DNA break stimulates the second homologous recombination event through the host DNA repair system. Depending on the location of the second recombination event the resolution of the merodiploid state either generates the desired gene deletion (Step and gel image 3A) or restores the wild type allele (Step and gel image 3B), which is identified by colony PCR.

Figure 3. Phenotypic characterization of *Bcam1349* deletion mutant. Colony morphology on AB-glucose agar medium (A), and pellicle formation in static LB liquid culture (B) of the wild type (WT) and *Bcam1349* mutant strains carrying pYedQ2 and the WT strain carrying pBBR1MCS-5 (vector control).

Figure 4. Flow-cell biofilm formation by the wild type (WT), *Bcam1349* mutant and its complemented counterpart and vector control strains. The CLSM images were acquired after 24 hours incubation at 37 °C.

Table 1. Bacterial strains and plasmids used in the study

Strain or plasmid	Lab ID	Relevant characteristics	Source or reference
Strains			
B. cenocepacia H111	MF108	Clinical isolate from a cystic fibrosis patient	(7)
B. thailandensis CDC2721121	-	Clinical isolate from a patient with pleural infection	(29)
E. coli DH5α	TTN322	Used for standard DNA manipulations	Invitrogen
E. coli DB3.1	TTN312	Host for the Gateway- compatible gene replacement vectors	Invitrogen
Plasmids			
pBBR1MCS5	MF528	Broad-host range cloning vector, Gm^R	(22)
pBBR1MCS2	MF124	Broad-host range cloning vector, Km^R	(22)
pMF564	MF564	*Bcam1349* gene cloned in pBBR1MCS5	This study
pYedQ	MF202	*E. coli yedQ* (*yhcK*) gene cloned in pRK404A	(21)
pYedQ2	MF217	*yedQ* gene cloned in *Hin*dIII/*Bam*HI site in pBBR1MCS5	This study
pRK600	TTN365	Helper plasmid in tri-parental conjugations, Cm^R, ori-ColE1, RK-mob+, RK-tra+	(27)
pDONR221	TTN313	Source of GWE cassette, Gateway donor vector, Km^R	Invitrogen
pBBR1MCS-Km-*pheS*	MF138	The engineered *pheS* cloned in pBBR1MCS2, Km^R	(14)
pEX18Tp-*pheS*	MF322	Gene replacement vector based on *pheS* and Tp^R	(14)
pEX18Gm-*pheS*	MF320	Gene replacement vector based on *pheS* and Gm^R	(14)
pEX18Km-*pheS*	MF321	Gene replacement vector based on *pheS* and Km^R	(14)
pUC57-*pheS*	MF130	Cloning vector containing the engineered *pheS*, Ap^R	(14)
pDAI-SceI	MF339	Cloning vector containing the I-SceI endonuclease, Tet^R	(12)
pDONRPEX18Tp-SceI-*pheS*	MF415	~2.6-kb Gateway donor site cloned in *Xba*I/*Hind*III site of pEX18Tp-*pheS*, Tp^R	This study
pDONRPEX18Gm-SceI-*pheS*	MF356	~2.6-kb Gateway donor site cloned in *Xba*I/*Hind*III site of pEX18Gm-*pheS*, Gm^R	This study
pDONRPEX18Km-SceI-*pheS*	MF414	~2.6-kb Gateway donor site cloned in *Xba*I/*Hind*III site of pEX18Km-*pheS*, Km^R	This study
pENTRPEX18Tp-SceI-*pheS*-*Bcam1349*	MF455	Gene replacement vector containing the *Bcam1349* deletion allele, Tp^R	This study
pENTRPEX18Tp-SceI-*pheS*-*phzF*	MF450	Gene replacement vector containing the phzF deletion allele, Tp^R	This study
pDAI-SceI-*pheS*	MF355	~1.2-kb *Xba*I/*Sph*I *pheS* fragment from pUC57-*pheS* cloned in *Xba*I/*Sph*I site of pDAI-SceI	This study

Applied and Environmental Microbiology

Table 2. Primers used in the study

Primer name	Sequence from 5' to 3'
Gene specific primers	
Bcam1349-UpF-GWL[1]	TACAAAAAAGCAGGCTAACGGGGATTTCGCACGAT
Bcam1349-UpR-tail [2]	**GGACATCGACTGCATCGTCA**AGCTCGAGTGAAGATGAAGCA
Bcam1349-DnF	TGACGATGCAGTCGATGTCC
Bcam1349-DnR-GWR [1]	TACAAGAAAGCTGGGTGAGATTGATCGCCGGCAT
Common primers [3]	
GW-*attB*1	GGGGACAAGTTTGTACAAAAAAGCAGGCT
GW-*attB*2	GGGGACCACTTTGTACAAGAAAGCTGGGT
Primers used to amplify Gateway donor site	
GWE-SceI-F [4]	TACTACAAGCTT**TAGGGATAACAGGGTAAT**AGCATGGATGTTTTCCCAGT
GWE-R [4]	TACTACTCTAGATCAGAGATTTTGAGACACGGG
Other primers [5]	
Bcam1349-F	TACTACCCCGGGTAAATCGCTTATTCGGGCTG
Bcam1349-R	TACTACTCTAGACATTCGTTCCACCGGACAT
Bcam1349-RBS-F	TACTACTCTAGAATTGTCCGGAAATGGATTGGT
Bcam1349-RBS-R	TACTACCCCGGGATTCGTTCCACCGGACAT

[1]Sequences double-underlined are common for all genes amplified and overlap with the GW-*attB* primer sequences (28).
[2]Sequences in bold letters overlap with the gene specific-DnF primer.
[3]Sequences were obtained from the reference 28.
[4]Restriction enzyme sites are single-uderlined and the I-SceI endonuclease recognition site is in bold letters and double-underlined.
[5]Restriction enzyme sites are uderlined

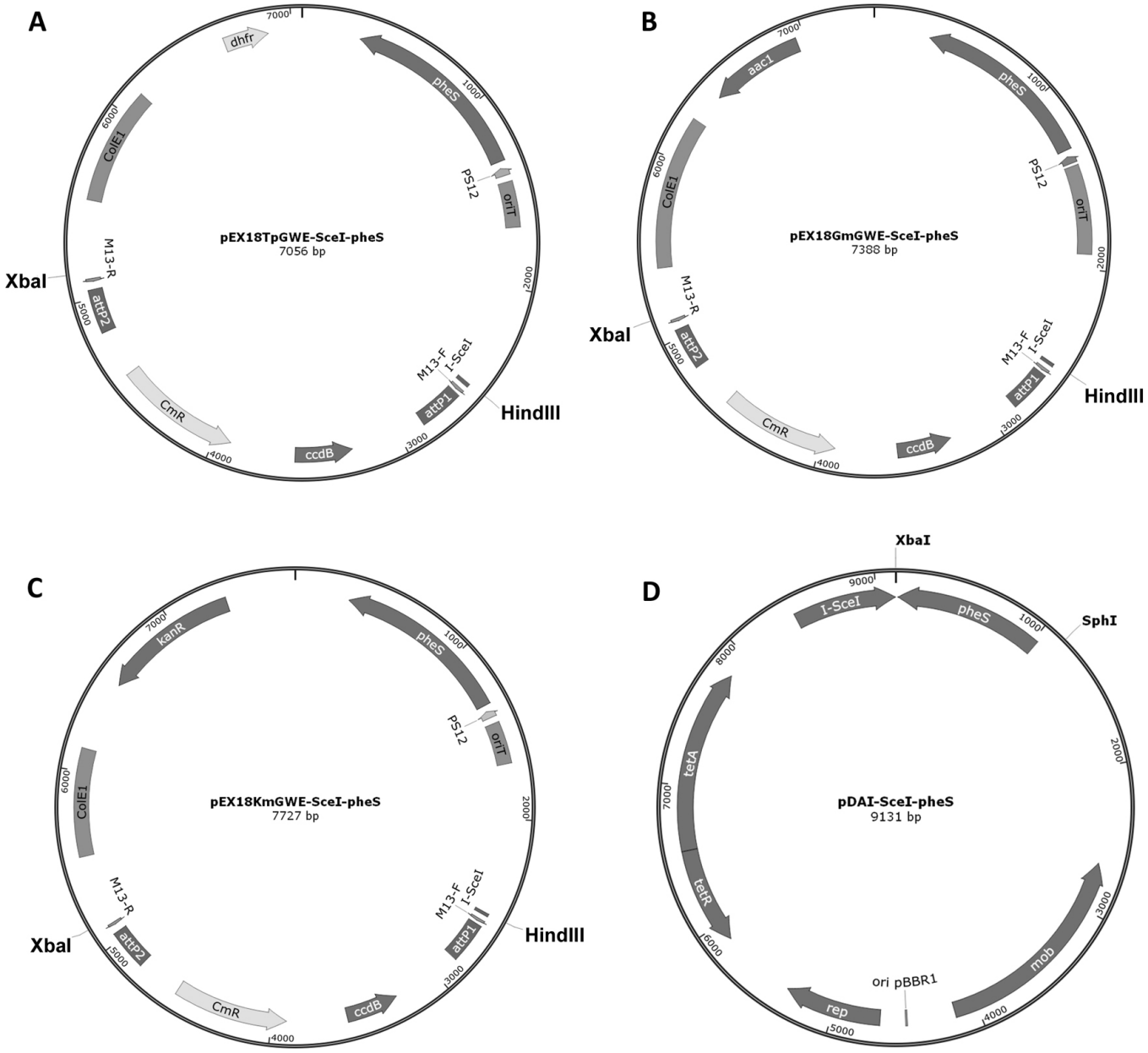

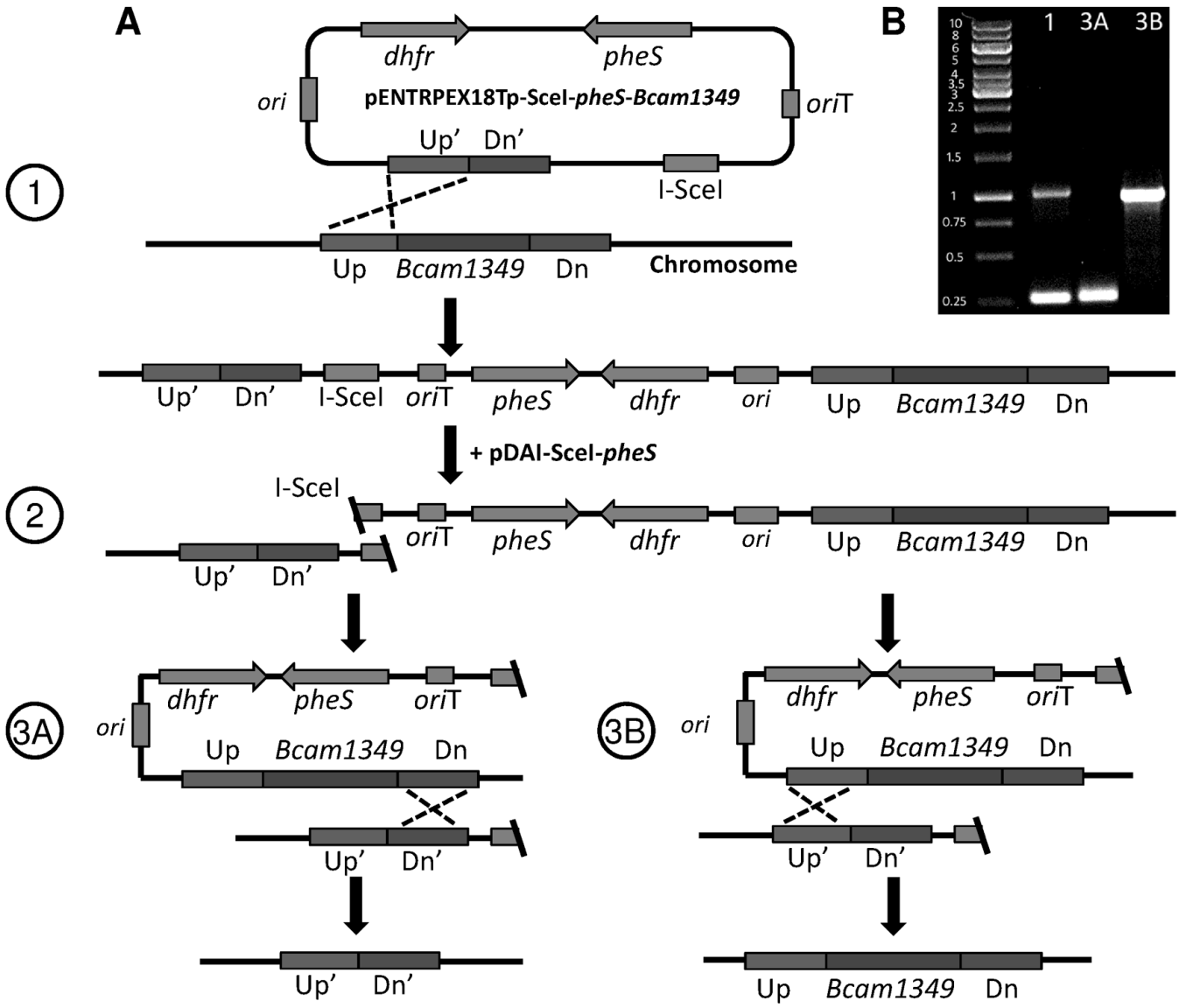

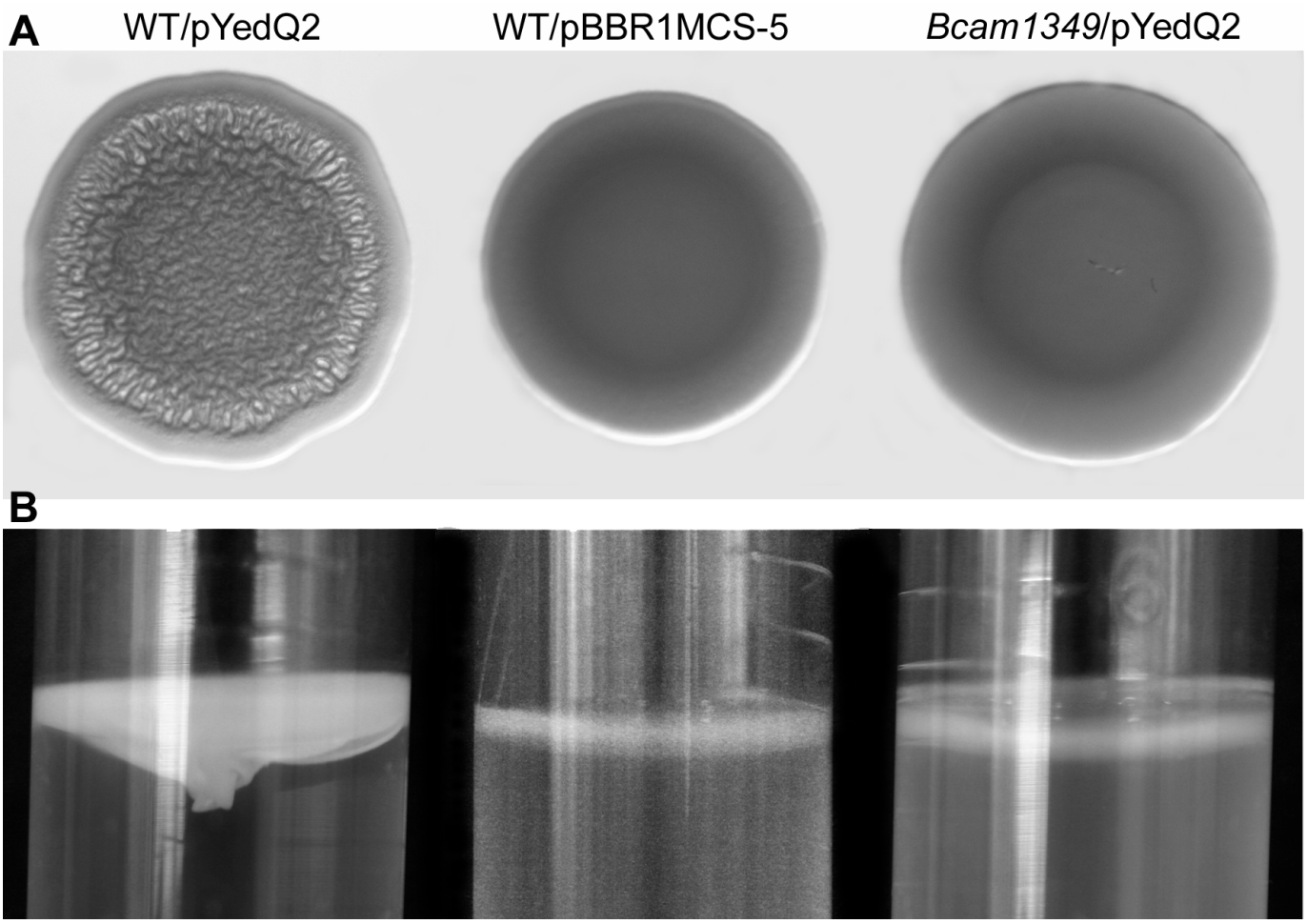

Applied and Environmental Microbiology

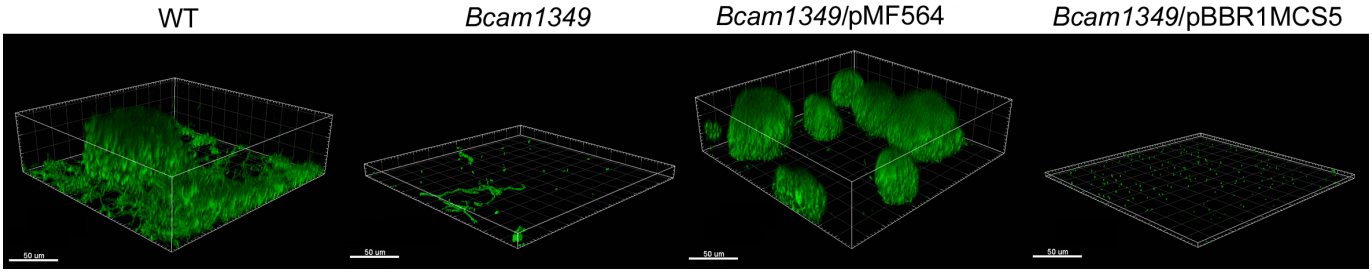

Supplementary material for "A Gateway-compatible allelic exchange system for generation of in-frame and unmarked gene deletions in *Burkholderia cenocepacia*" by Fazli et al.

Killing of *Burkholderia cenocepacia* by chromosomally encoded single copy or plasmid encoded multicopy *pheS* gene

We used three *B. cenocepacia* strains to test the effectiveness of the engineered *pheS* gene in killing *B. cenocepacia* cells in the presence of 0.1% cPhe when expressed as a single copy or a multicopy gene. The *Bcam1349* merodiploid strain served as an example for a bacterium with a single copy *pheS* gene. This strain harbours a single copy *pheS* gene on the gene replacement vector pENTRPEX18Tp-SceI-*pheS-Bcam1349*, which is integrated into the chromosome. Trimethoprim (Tp) was added to the growth medium to maintain the merodiploid state. As an example of multicopy *pheS* gene, we transformed the wild type *B. cenocepacia* strain with the plasmid pBBR1MCS-Km-*pheS* (1). We also transformed the wild type *B. cenocepacia* strain with the plasmid pBBR1MCS2, which served as the vector control strain. Kanamycin (Km) was added to the growth medium for plasmid maintenance. The strains were grown in LB medium with appropriate antibiotics overnight at 37°C. One ml of the overnight grown cultures was harvested, washed twice in 1ml 0.9% NaCl and serially diluted in 0.9% NaCl. Approximately $2x10^5$ CFU were plated on AB-agar medium with appropriate antibiotics and with or without 0.1% cPhe. The plates were incubated at 37°C for 48 hours. The results indicate that the engineered *pheS* gene was not efficient in killing *B. cenocepacia* cells in the presence of cPhe when expressed as a single copy on the chromosome, but it effectively killed almost all *B. cenocepacia* cells when expressed from the multicopy plasmid pBBR1MCS-Km-*pheS* (Fig. S1), demonstrating that the mutant *pheS* gene provides effective counter selection in *B. cenocepacia* when it is present in multiple copies in the cells.

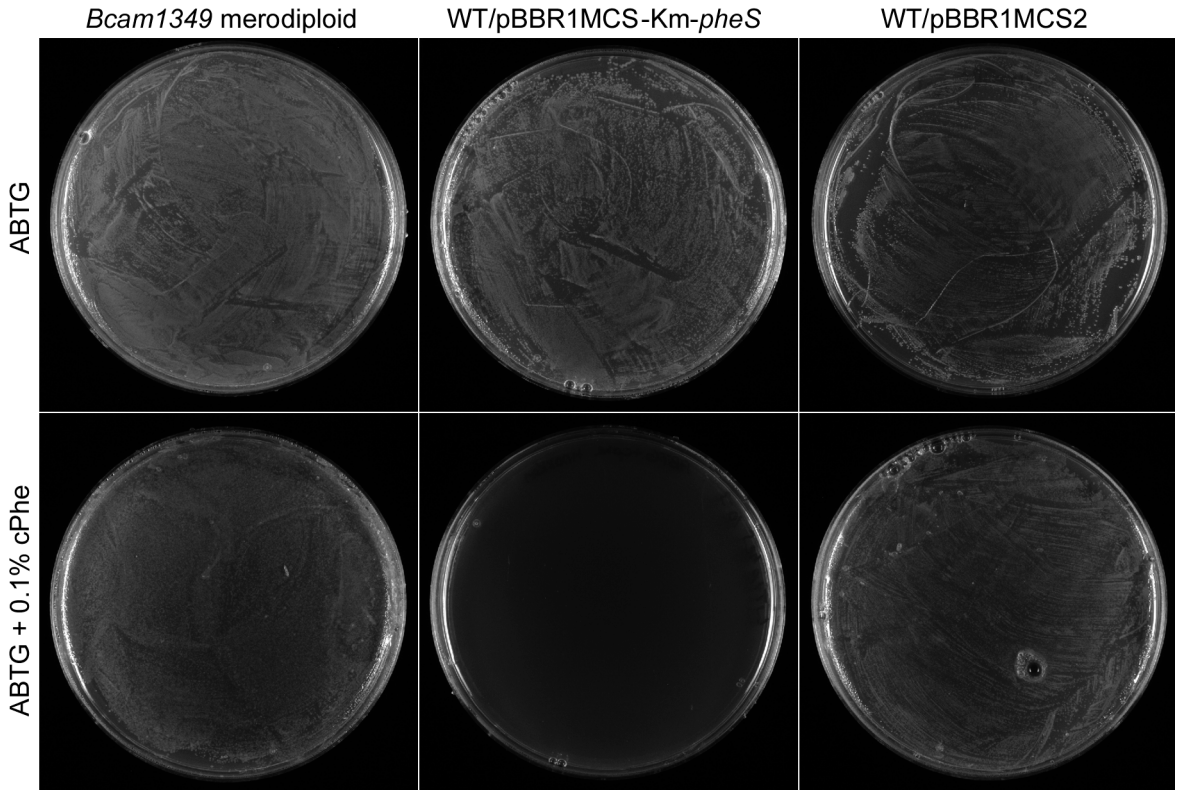

Fig. S1. Killing of *B. cenocepacia* strains by the engineered *pheS* gene in the presence of 0.1% cPhe when expressed in single or multiple copies. *Bcam1349* merodiploid is the single copy *pheS* gene containing strain, WT/pBBR1MCS-Km-pheS is the multicopy *pheS* gene containing strain, and WT/pBBR1MCS2 is the vector control strain. Both Tp and Km were used at 100 μg/ml. An identical amount of cells was plated on AB-agar medium with or without 0.1% cPhe. The images of the plates were acquired after 48 hours of incubation at 37°C.

Construction of the *Burkholderia thailandensis phzF* (BTH_I0859) deletion mutant

Using the allelic exchange system described here, we have successfully deleted the *phzF* (BTH_I0949) gene encoding a putative phenazine biosynthesis protein in *B. thailandensis*. *phzF* is the first gene of a predicted operon containing five genes.

We constructed the gene replacement vector pENTRPEX18Tp-SceI-*pheS*-*phzF* as follows. The ~0.5-kb upstream and downstream fragments of *phzF* gene were amplified using the primer pairs Phz_UpF/Phz_UpR and Phz_DnF/Phz_DnR, respectively (The primer sequences are available upon request). Both fragments were fused together using the primers GW-*attB*1 and GW-*attB*2 in splicing-by-overlap-extension (SOE) PCR to generate the *phzF* deletion allele. The final PCR product was then purified and verified by restriction analysis. BP clonase reaction for recombinational transfer of the mutant allele into the allelic exchange vector pDONRPEX18Tp-pheS was performed at 25 °C overnight as described in the Gateway cloning manual (Invitrogen), using only half of the recommended amount of BP Clonase II enzyme mix (Invitrogen). The BP clonase reaction product was transferred into chemically competent *E. coli* DH5α cells. The transformants growing on LB-agar plates containing 50 µg Tp mL^{-1} were streaked on LB-agar plates containing 50 µg Tp mL^{-1} for purification, plasmid isolation, restriction analysis and partial sequencing.

The gene replacement vector pENTRPEX18Tp-SceI-*pheS*-*phzF* was introduced into *B. thailandensis* via tri-parental mating as described previously (2). The co-integrants were selected for Tp resistance on LB-agar plates containing 100 µg Tp mL^{-1} and 100 µg Amp mL^{-1}. Eight Tp resistant colonies were streaked on the same selective plates, and the growing colonies were screened for integration of the plasmid by colony PCR using the primers Phz_UpF and Phz_DnR. A single positive merodiploid clone was transformed with pDAI-SceI-*pheS* by tri-parental mating to stimulate the second homologous recombination event and resolve the merodiploid state. The transconjugants were screened for Tet resistance on LB-agar plates containing 120 µg Tet mL^{-1} and 100 µg Amp mL^{-1}. Batches of 10 Tet resistant colonies were screened for the loss of the wild type allele and the presence of the desired gene deletion by colony PCR using the primers Phz_UpF and Phz_DnR. Two positive clones were purified by streaking and growing on the same selective plates. Thereafter a single colony for each clone was picked and grown in 1 ml AB-glucose medium containing 0.1% (w/v) cPhe at 37 °C overnight in order to stimulate the loss of pDAI-SceI-*pheS* via the counter-selectable marker *pheS* on the plasmid. Ten-fold serial dilutions of the overnight grown cultures were plated on LB-agar plates without any antibiotic, and 20 of the growing colonies for each clone were patched on LB-agar plates with or without tetracycline to screen for Tet sensitivity, which indicated

the loss of the plasmid pDAI-SceI-*pheS*. A single positive colony for each clone was selected and stored at -80 °C.

References

1. Barrett AR, Kang Y, Inamasu KS, Son MS, Vukovich JM, Hoang TT. 2008. Genetic tools for allelic replacement in Burkholderia species. Appl. Environ. Microbiol. 74:4498-508.
2. Fazli M, O'Connell A, Nilsson M, Niehaus K, Dow JM, Givskov M, Ryan RP, Tolker-Nielsen T. 2011. The CRP/FNR family protein Bcam1349 is a c-di-GMP effector that regulates biofilm formation in the respiratory pathogen Burkholderia cenocepacia. Mol. Microbiol. 82:327-41.

PART III

Contents

Response to oxidative stress of *Burkholderia thailandensis* biofilm.

This section collects unpublished results, as further experiments are necessary to complete theresearch. Data are organized in sections - Abstract, Introduction, Material and methods, Results, Discussion - to better present the main results.

ABSTRACT

The soil saprophyte *Burkholderia thailandensis* is a mostly environmental bacterium and a pathogen of invertebrates, closely related to the pathogenic bacteria *B. pseudomallei* and *B. mallei*. We challenged *B. thailandensis* biofilms with phenazine methosulphate (PMS), a well-known reactive oxygen species (ROS) producer, and evaluated oxidative stress both in planktonic and sessile cells. Planktonic cells treated with PMS showed higher oxidative stress than untreated cells, whereas in PMS-treated biofilms we measured a lower oxidative stress with respect to the control. To better identify the enzymes involved in buffering oxidative stress, we deleted *sodC*, encoding the periplasmic superoxide dismutase, possibly involved in defence against exogenous sources of oxidative stress. Surprisingly, compared to the untreated wild type cells, no additional oxidative stress was measured in the *sodC* mutant planktonic cells and lower oxidative stress was measured in *sodC* biofilms. Even the exposure to PMS did not exacerbate the oxidative stress levels in the mutant strain. Interestingly, we observed that PMS affected in the same way both the wild type and *sodC* biofilm morphology, leading to the accumulation of polysaccharides in the biofilm matrix. These data suggest that polysaccharide biosynthesis might be part of an adaptive response to oxidative stress, both endogenously and exogenously induced. The higher catalase activity measured in wild type biofilms treated with PMS can only partially explain these results. Using transcriptomics experiments, we intend to unravel which genes are involved in the ROS scavenging mechanisms and in the accumulation of polysaccharides, which appear the main strategies to reduce the endogenous and exogenous oxidative stress in *B. thailandensis* biofilms.

INTRODUCTION

Biofilms are heterogenic microbial communities embedded in a self- produced polymeric matrix attached to a surface (Hall-Stoodley et al., 2004). The biofilm

formation is a nearly universal trait enabling bacteria to develop coordinated architectural and survival strategies (Vlamakis et al., 2013) and is now largely accepted that biofilms constitute the predominant microbial lifestyle in natural and engineered ecosystems (McDougald et al., 2011). Both in soil and in the host, bacteria form biofilm to resist to abiotic and biotic stress (Davey et al., 2000; Flemming et al., 2010). Many of these environmental signals, e.g. the immune response, biocides, antibiotics and toxic compound, involve the formation of reactive oxygen species (ROS) (Villa et al., 2012; Albesa et al., 2004; Lushchak, 2011; Gambino et al., 2015), causing oxidative stress in the cells. The biofilm response to oxidative stress is a topic of outstanding importance. The comprehension of mechanisms regulating biofilm in response to oxidative stress may shed light on the molecular strategies to sense environmental signals and adapt accordingly.

The soil saprophyte *Burkholderia thailandensis* is an opportunistic pathogen of invertebrates and is used as a model organism for the human pathogen *B. pseudomallei*, the etiological agent of mieloidosis, a serious disease endemic in South Est Asia and Northern Australia (Wiersinga et al., 2006). The high resistance of the pathogen to the common antibiotics (Cheng and Currie, 2005), its capacity to stay latent for many years (Stevens and Galyov, 2004) and the variety of clinical manifestation of the disease (acute, chronic or latent infections) (Hamad et al., 2011) make mieloidosis difficult to diagnosticate and to eradicate.

In this study, the response to phenazine methosulphate (PMS), a well-known superoxide producer, of a clinical isolate of *B. thailandensis* CDC272 was studied, both in planktonic and sessile cells, to identify which pathways this bacterium activate to avoid oxidative stress. The characterization of a mutant in the gene *sodC*, coding for a periplasmic superoxide dismutase, confirmed the tight linkage between endogenously and exogenously induced oxidative stress and the production of polysaccharides in the biofilm matrix.

MATERIALS AND METHODS

Bacterial strain and growth conditions

The bacterial strains, plasmids and primers used in this study are listed in Table 1. *Burkholderia thailandensis* wild type strain CDC2721121 (also called CDC272; from now on, wt) was maintained at -80°C in suspensions containing 20% glycerol. *B.*

thailandensis wt was grown aerobically in Tryptic Soy Broth (TSB) medium at 30° C, in the dark. Were stated, the two strains were challenged with various concentrations of phenazine methosulphate (PMS; Sigma-Aldrich, Milan, Italy). For the construction of the mutant, *E. coli* and *B. thailandensis* strains were grown on Luria broth (LB) and for the resolution of single croosover, 0.1% (w/v) p-chlorophenylalanine (cPhe; DL-4-chlorophenylalanine; Sigma-Aldrich) was autoclaved together with B-salts solution, and A-salts solution and the carbon source of choice were added thereafter. All media were made solid by addition of 2% (w/v) agar.

Effects of PMS on planktonic growth and adhesion.

B. thailandensis wt and *sodC* growth was monitored in a polystyrene 96-well microtiter (Greiner, Bio-One) in the presence of PMS at various concentrations (from 0 to 300 μM), registering the optical density (OD) at 600 nm every 15 min with a microtiter reader (Biotek-Power Wave XS2). The results were confirmed plating cell suspensions from stationary phase serially diluted on agarized media, incubated at 30°C overnight and the colony forming units (CFU) were enumerated using the drop-plate method (Herigstad et al. 2001). Obtained growth curves were analysed and lag phase and growth rate were calculated according to the by the Gompertz model (Zwietering et al. 1990) using the GraphPad Prism software (version 5.0, San Diego, CA, USA). At the end of the growth, the same microtiter used to monitor the growth was used to quantify adhered cells to the wells surface with 4',6-diamidino-2-phenylindole (DAPI; LifeTechnologies, Italy) staining. The liquid culture was removed, and cells attached to the wells surface were washed gently with PBS and stained for 20 min in the dark with DAPI solution (10 μg/ml), washed twice with PBS, and dried. The OD600nm of crystal violet- stained biofilm cells was determined and normalized to the OD600nm of the planktonic cells from the corresponding liquid cultures; this value is defined as “adhesion units”. The fluorescence was measured using the fluorometer VICTOR TM X Multilabel Plate Readers (Perkin Elmer, Italy), excitation 360 nm and emission 465 nm. Experiments were conducted in triplicate.

Biofilm growth

Colony biofilms of *B. thailandensis* wt and *sodC* mutant strain were prepared following the method reported (Anderl et al. 2000). Briefly, 10 μl of cell suspension containing 1.5 * 10^6 cells were used to inoculate sterile black polycarbonate filter membranes (0.22 mm pore size, Whatman, UK) that were placed on TSA plates, at 30°C, either in the

absence or in the presence of PMS. PMS was poured on agar plates and let adsorb. The membranes were transferred every 24 h to fresh media, and grown for 8 days in total. For protein determination, a membrane was collected every 24 h and resuspended in a 10-ml tube with 2 ml of sterile phosphate base saline (PBS, 10 mmol l-1 phosphate buffer, 0.3 mol l-1 NaCl, pH 7.4; Sigma-Aldrich, Milan, Italy). Cells were broken by 5 cycles of 30 s sonication with 30 s intervals; cell lysates were centrifuged 15 min at 4°C at 19000 g and supernatant was collected. The protein amount was quantified with Bradford assay (Bradford 1976), using bovine serum albumin as a standard. Experiments were performed in triplicate.

Level of oxidative stress on planktonic and sessile cells

The level of oxidative stress in planktonic and sessile cells of *B. thailandensis* wt and *sodC* mutant strain was determined using the 2,7-dichlorofluorescein-diacetate (H_2DCFDA) assay (Jakubowski et al. 2000). *B. thailandensis* planktonic cells grown at 30°C for 6 h in TSB, with either 0, 15 or 150 µM PMS, were washed with phosphate buffer solution (PBS; Sigma-Aldrich, Italy) and resuspended in 50 mmol l-1 PBS. For the colony- biofilm, the protocol described by Gambino et al. (2015) was adopted. One membrane biofilm was collected for 8 days, scraped and homogeneously resuspended in 2 ml of PBS 50 mmol/l. 750 µl of cell suspension was incubated with 10 µmol l-1 H_2DCFDA at 30°C for 30 min, vortexed and centrifuged. The supernatant was collected to measure fluorescence relative to the extracellular reactive oxygen species (ROS) presence. To evaluate intracellular ROS concentrations in either planktonic or biofilm cultures, cells were washed three times and broken with 5 cycles of 30 s sonication with 30 s intervals. The fluorescence of the supernatant collected before (outer oxidative stress) and after cell sonication (inner oxidative stress) was measured using the fluorometer VICTOR TM X Multilabel Plate Readers (Perkin Elmer, Italy), excitation 490 nm and emission 519 nm. The emission values were normalized against the protein concentration, obtained from the remaining 750 µl of cell suspension with the Bradford assay. Experiments were conducted in triplicate.

Construction of *B. thailandensis* deletion *sodC* mutant

The gene identified with the locus tag BTQ_RS04505 on chromosome I of *B. thailandensis* CDC272, homologous to the *B. thailandensis* E264 *sodC* and encoding the periplasmic superoxide dismutase SodC, was deleted using the allelic exchange system and the counterselection based on the *pheS* gene encoding the α-subunit of phenylalanyl

tRNA synthase (Barrett et al., 2008). Gene replacement vector, containing a trimethoprim (Tp) resistance cassette, was generated by PCR overlap extension, as described by Choi and Schweizer (2005). A set of four primers was used to amplify chromosomal regions upstream (*sodC*-UpF and *sodC*-UpR) and downstream (*sodC*-DnF and *sodC*-DnR) of *sodC* gene (table 1). Two additional primers (*sodC*-SeqF and *sodC*-SeqR) were designed to check the deletion site on the chromosome. The PCR fragments were fused together to generate the deletion allele and amplified with primers GW-*attB*1 and GW-*attB*2 incorporating the *att*B1 and *att*B2 recombination sites at either end of the gene replacement cassette. The *attB*1 and *attB*2 flanked Gateway donor site were amplified by PCR from pDONR221 using the primers GWE- F and GWE-R (flanked by XbaI site). The resulting 2.4-kb PCR product was digested with XbaI, and cloned into XbaI digested plasmids pEX18Tp-*pheS* (Barrett et al., 2008) resulting in the allelic exchange vectors pDONRPEX18Tp- *pheS*. Using the Gateway cloning system (Invitrogen, Life Technologies, Denmark), BP clonase reaction for recombinational transfer of the mutant allele into the allelic exchange vector pDONRPEX18Tp-*pheS* was performed at 25 °C overnight. The deletion vector pDONRPEX18Tp-*pheS*-*sodC* was transferred into chemically competent *E. coli* DH5α cells. The presence of the insertion was confirmed by sequencing and restriction analysis. The gene replacement plasmids pDONRPEX18Tp-*pheS*-*sodC* was transferred into *B. thailandensis* wt by tri-parental mating as described previously (Fazli et al. 2011), and the resulting transformants were selected for Tp and Kan resistance on LB agar plates containing 100 μg Tp mL^{-1} and 50 μg Kan ml^{-1}. Six clones were streaked twice on AB-phenylanine agar plates. Resolution of single crossover events was achieved by streaking on plates containing 0.1% (w/v) p-chlorophenylalanine (cPhe; DL-4-chlorophenylalanine; Sigma-Aldrich, Denmark) via the counter- selectable *pheS* marker on the gene replacement plasmid (Barrett et al. 2008). Positive clones were verified by sequencing and and maintained at -80°C in suspensions containing 20% glycerol. All primers and plasmids used are listed in table 1. The *sodC* mutant strain has been tested for every assay described for the wild type strain, in the same conditions.

Primer name	Sequence from 5' to 3'
sodC-UpF	GGGACAAGTTTGTACAAAAAAGCAGGCTCAGCGCGATCTCGACTACCT
sodC-UpR	CGGGAACGCCGGGTCAAAGTCGTCATGATACCGTGA
sodC -DnF	GACCCGGCGTTCCCG
sodC -DnR	GGGGACCACTTTGTACAAGAAAGCTGGGTAGTTCGAGAATTCGAGCGTCA
sodC-SeqF	CGAACTCGATCGGCTTTCT
sodC-SeqR	AGGTCAGACCGATATGCAAG
GWE-F	AAATCTAGATAAGCTCGGGCCCCAAATA
GWE-R	AAATCTAGAGGATATCAGCTGGATGGCAA
GW-*attB*1	GGGGACAAGTTTGTACAAAAAAGCAGGCT
GW-*attB*2	GGGGACCACTTTGTACAAGAAAGCTGGGT

Strain and plasmid	Relevant characteristics	Source
B. thailandensis wild type	*Burkholderia thailandensis* wild type strain CDC2721121 (also called CDC272), a clinical isolate from a patient with pleural infection	Peano et al., 2014
sodC mutant strain	*sodC* deletion mutant in *B. thailandensis* CDC2721121	this study
E. coli DH5α	Used for standard DNA manipulations	Invitrogen
pEX18Tp-*pheS*	Gene replacement vector based on *pheS* and Tp^R	Barrett et al., 2008
pDONRPEX18Tp-*pheS*	~2.4-kb Gateway donor site cloned in XbaI site of pEX18Tp-*pheS*, Tp^R	this study
pDONRPEX18Tp-*pheS*-*sodC*	*sodC* deletion vector	this study

Table 1. List of primers, strains and plasmids used in this work.

Extraction and characterization of the extracellular polymeric substances (EPS)

EPS extraction and characterization was conducted as described by Villa and collaborators (2012) on eight-days old biofilm biomass of both *B. thailandensis* wt and *sodC* mutant, grown upon exposure to 0, 15 and 150 uM PMS. The cetyltrimethylammonium bromide (CTAB)-DNA method described by Corinaldesi and collaborators (2005) was used to quntify extracellular DNA (eDNA). The Bradford method was applied to analyze protein concentrations, whereas the optimized microplate phenol-sulfuric acid assay was applied for carbohydrate determination

(Masuko et al. 2005) using glucose as standard. The results obtained were normalized by the cellular protein concentration. Experiments were performed in triplicate.

Catalase assay

For each replicate, a total protein extraction of the whole biofilm was prepared resuspending one membrane in 2ml of PBS, sonicating (5 cycles of 30 s sonication with 30 s intervals) and centrifuging the suspension to eliminate cell debris. All steps were performed on ice or at 4°C. Catalase assay described by Sinha (1972) was performed on the total biofilm extract. For each replicate, 100 ul of biofilm protein extract was added to 287 umol of H_2O_2 in 10 mM Tris 100 mM NaCl pH 8.00 buffer. Every 60 s, reaction was stopped with catalase reagent (25% (v/v) of 5% $K_2Cr_2O_7$ 5%, 75% (v/v) of 100% acetic acid) and the absorbance at 570 nm was compared with the standard curve. Controls with no H_2O_2 and no biofilm protein extract were also included and were used to calculate H2O2 consumed by catalase activity in the samples. Values were normalized against the protein concentration, obtained from the remaining protein extract with the Bradford assay. Experiments were conducted in triplicate.

Statistical analysis

A t-test or analysis of variance (ANOVA) via Graphpad Software (San Diego California USA) was applied to statistically evaluate any significant differences among the samples. Tukey's honestly significant different test (HSD) was used for pairwise comparison to determine the significance of the data. Statistically significant results were depicted by *p*-values 0.05. Histograms provide the *p*-values obtained by ANOVA analysis. Posthoc comparison results (Tukey's HSD, $p < 0.05$) are summarized with asterisks to underline the most relevant differences with respect to control (wt 0 μM).

RESULTS

Effects of PMS on *B. thailandensis* wt planktonic growth and adhesion.

In order to evaluate the response to oxidative stress in *B. thailandensis*, the superoxide generator PMS (Hassett et al., 1999) was added to the medium and the absorbance was monitored spectrophotometrically (OD 600 nm) for 24 h. The concentrations of 1.5 and 15 μM PMS did not affect the growth curve in the wt, while 150 μM PMS significantly increased the lag phase and reduced the growth rate (Fig. 1). Results were confirmed by total cell count using the drop counting method. As adhesion, that is the very first step of biofilm formation, could influence the measured absorbance of cells in suspension,

we also measured the adhesion of cells to the microtiter surface at the end of the growth by staining DNA with DAPI. No statistically significant difference was detectable between the DAPI fluorescence of untreated cells (3660.1± 641.9 fluorescence units) and the 1.5 and 15 μM PMS treated cells (5198.5±793.6; 3163.8±644.1; 1645.3±818.7 fluorescence units). Conversely, the exposure to 150 μM PMS resulted in a lower fluorescence (1645.3±818.7 fluorescence units), thus in a statistically significant minor adhesion than the control.

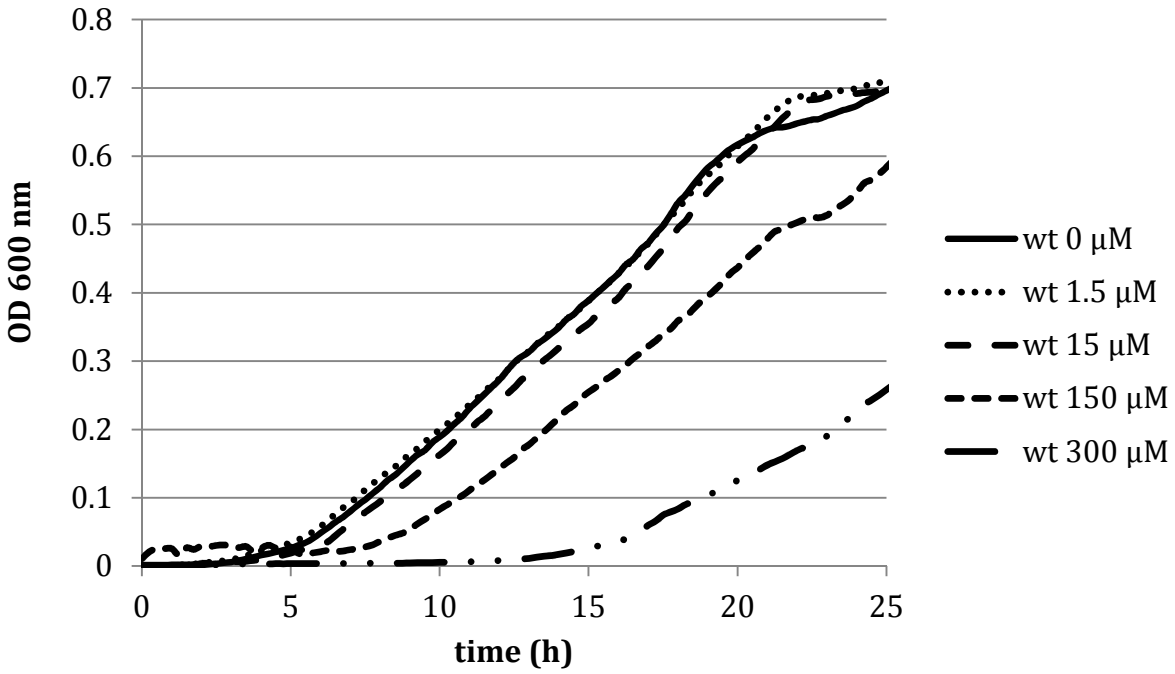

Figure 1. Planktonic growth curve of B.thailandensis wt in the presence of PMS concentrations from 0 to 300 μM.

Effects of PMS on *B. thailandensis* wt biofilm growth.

Biofilm formation is an effective mechanism of resistance to adverse conditions, largely conserved among bacteria. Colony biofilm mimics growth in soil, in which bacteria are attached to a solid surface and where water availability is influenced by the solute potentials (Chang and Halverson, 2003). This method allowed us to test the inhibition of colony biofilm by PMS. *B. thailandensis* colony biofilm reached the maturity in eight days (Fig. 2). The only effect of PMS treatment (both 15 and 150 μM PMS) on the growth curve of biofilm, determined as total protein quantification (see Materials and methods section), was a delay in biomass build-up at the second day of incubation, somehow akin to an extension of the lag phase in planktonic cultures (Fig. 2).

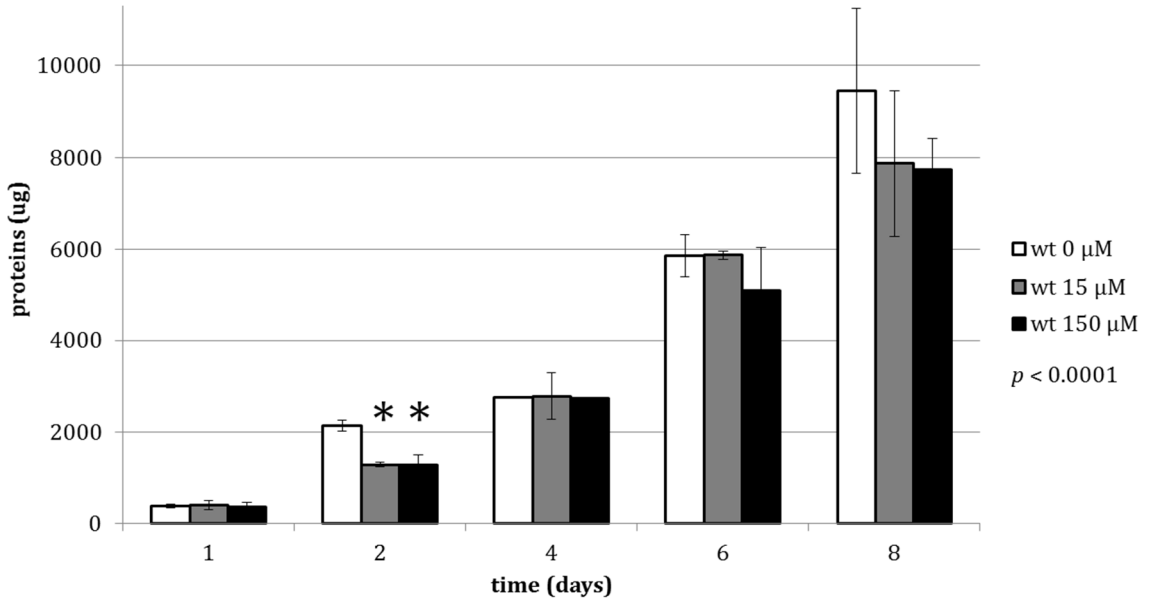

Figure 2. Total protein amounts from B. thailandensis wt biofilm in the presence of 0, 15 and 150 µM PMS over time. Data represent the means ± the SD of three independent measurements of proteins for each membrane. The histograms provide the P-values obtained by ANOVA analysis. Post hoc comparisons results (Tukey's HSD, P < 0.05) are summarized with asterisks to underline the most relevant differences of PMS-treated samples compared to the control.

PMS clearly affected the morphology of the *B. thailandensis* biofilm. *B. thailandensis* wt colony biofilm presented a succession of smooth and rough rings. This easily recognizable structure disappeared in biofilm treated with 15 µM PMS. The effect was even more evident in biofilm treated with 150 µM PMS, leading to the development of thinner and less organized biofilm respect to the untreated biofilm (Fig. 3).

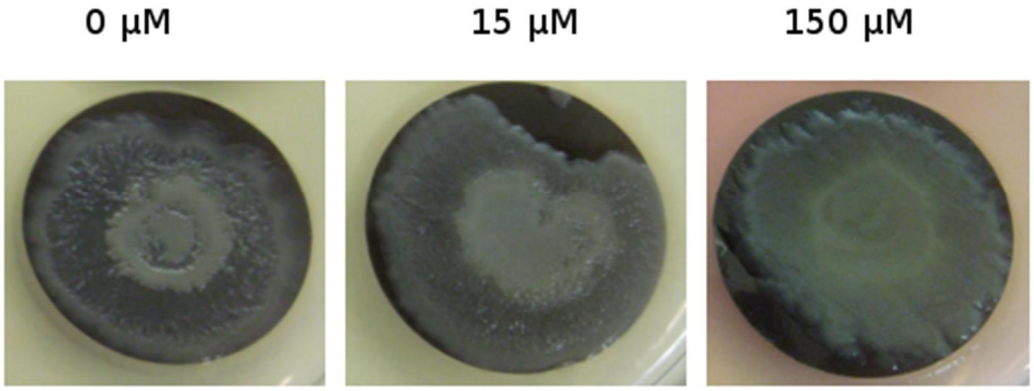

Figure 3. Morphology of C Burkholderia thailandensis wt colony biofilm challenged with 0, 15 and 150 µM PMS.

Levels of oxidative stress in planktonic cells and biofilm of *B. thailandensis* wt.

To directly connect the observed effects on planktonic and sessile growth with the superoxide produced by PMS, we measured the oxidative stress levels using H_2DCFDA, a fluorescent probe sensitive to ROS (Zhao et al., 2014). As biofilms are composed by cells enclosed in a polymeric matrix with known defense properties (Flemming et al., 2010), we measured ROS levels both inside cells (Fig. 4a, inside) and outside the sessile cells (Fig. 4b, outside), i.e., in the biofilm matrix. We found that 150 μM was a concentration able to increase oxidative stress in planktonic cells (42.7±12.6 fluorescence/ μg proteins), whereas oxidative stress in cells exposed to lower PMS concentration (19.9±1.8 fluorescence/ μg proteins) was not significantly different from the control (14.9±0.9 fluorescence/ μg proteins). As illustrated in figure 4, in the biofilm the oxidative stress was higher in the first days of biofilm formation, decreasing at later times. Villa et al. (2012) and Gambino et al. (2015) already reported the same trend for colony biofilms exposed to oxidative stress. All along the biofilm growth, no additional oxidative stress was measurable in the PMS treated samples, both inside and outside cells. In detail, oxidative stress outside cells, ascribable to the biofilm matrix, was statistically significant higher in the control biofilm than in 15 and 150 μM PMS treated biofilms for the first 4 days of growth. Inside cells, oxidative stress is higher in the untreated biofilm only at the first day of growth; after the first day, no difference has been detected (Fig. 4). The decrease in oxidative stress levels in biofilm exposed to PMS led us to hypothesize the activation of effective scavenging mechanisms.

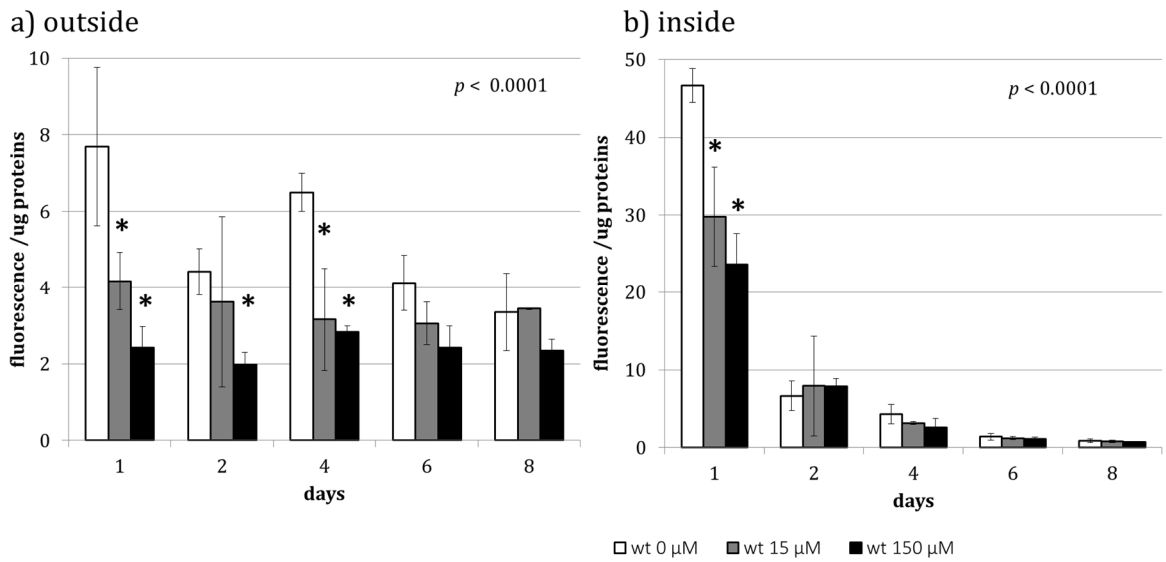

Figure 4. Reactive oxygen species detection outside (a) and inside (b) the cells of Burkholderia thailandensis wt biofilm in the presence of 0, 15 and 150 µM PMS. The histograms provide the P-values obtained by ANOVA analysis. Post hoc comparison results (Tukey's HSD, P < 0.05) are summarized with asterisks to underline the most relevant differences in PMS-treated samples with respect to the control.

Effect of PMS on the *sodC* mutant strain growth as planktonic and sessile cells.

In *B. pseudomallei*, *sodC* encodes for a periplasmic superoxide dismutase, which plays a key role in its virulence and survival in the host cells (Vanaporn et al., 2011), as it protects bacteria from toxic free radicals produced by the host immune system (Sanjay et al., 2011). To verify the involvement of SodC in the PMS response, we built a deletion mutant in the gene coding for this protein, by combining the Gateway allelic exchange system (Choi and and Schweizer, 2005) and the counterselection based on the *pheS* gene (Barrett et al., 2008). As already reported for *Salmonella enterica* serovar Typhimurium (Fang et al., 1999) and *Escherichia coli* (Gorth et al., 1999; Imlay, 2003), the deletion of *sodC* in *B. thailandensis* only caused a slight reduction of the planktonic growth rate – not statistically significant -in respect to the wild type. The effect was more evident in the presence of an exogenous source of oxidative stress. The differences already observed exposing the wt to 150 µM PMS (i.e., the elongation of the lag phase and the decrease in growth rate) were more evident in the mutant (Fig. 5). The adhesion of the *sodC* mutant strain to the microtiter surface (2523.3 ± 814.7 fluorescence unities) was not different from the adhesion of the wt (3660.1 ± 641.9

fluorescence unities), except for the observed decreased adhesion in the presence of 15 μM (1363.4 ± 359.1 fluorescence unities) and 150 μM PMS (1123.25 ± 427.1 fluorescence unities). The decrease was comparable to the effect of 150 μM PMS on the wt (1645.3 ± 818.7 fluorescence unities).

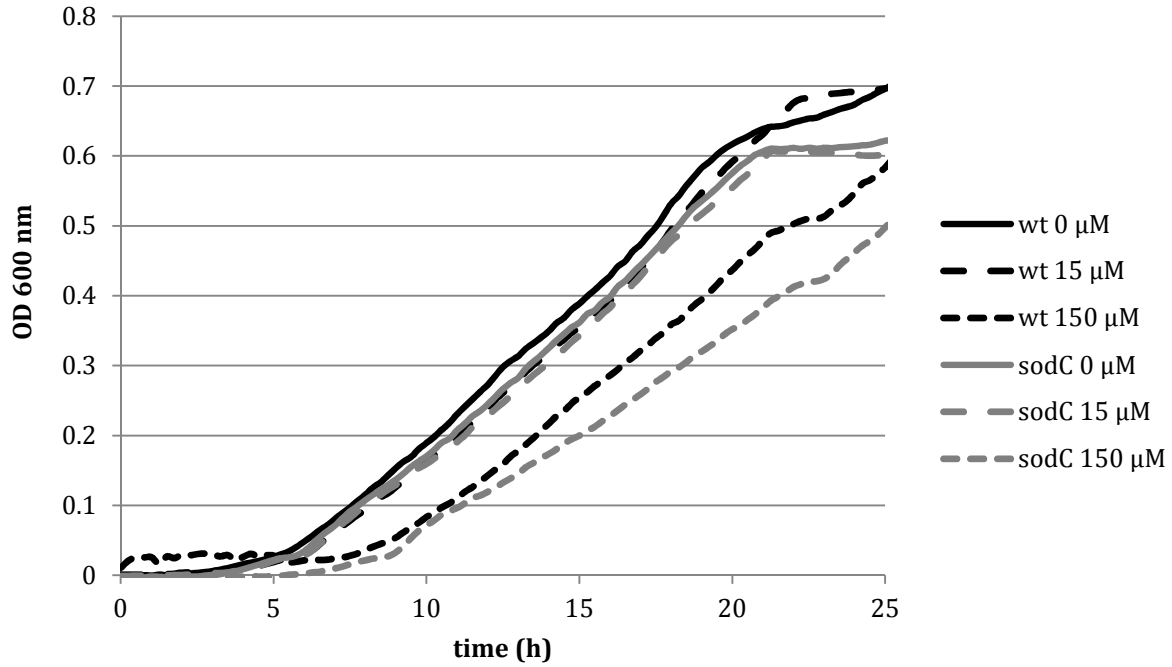

Figure 5. Planktonic growth curve of B. thailandensis wt and sodC mutant strain in the PMS concentrations from 0 to 150 μM.

Colony biofilm morphology in the *sodC* mutant strain did not reveal any difference with the wt colony biofilm, not even upon exposure to PMS, which, as for the wt strain, led to the development of a less structured biofilm. However, monitoring the biofilm growth, at day 2 the mutant biofilm treated with 150 μM PMS is the only one with an extended lag phase (Fig. 6), whereas we previously observed that in wt biofilm the exposure to 15 uM PMS could have this effect, too (Fig. 2).

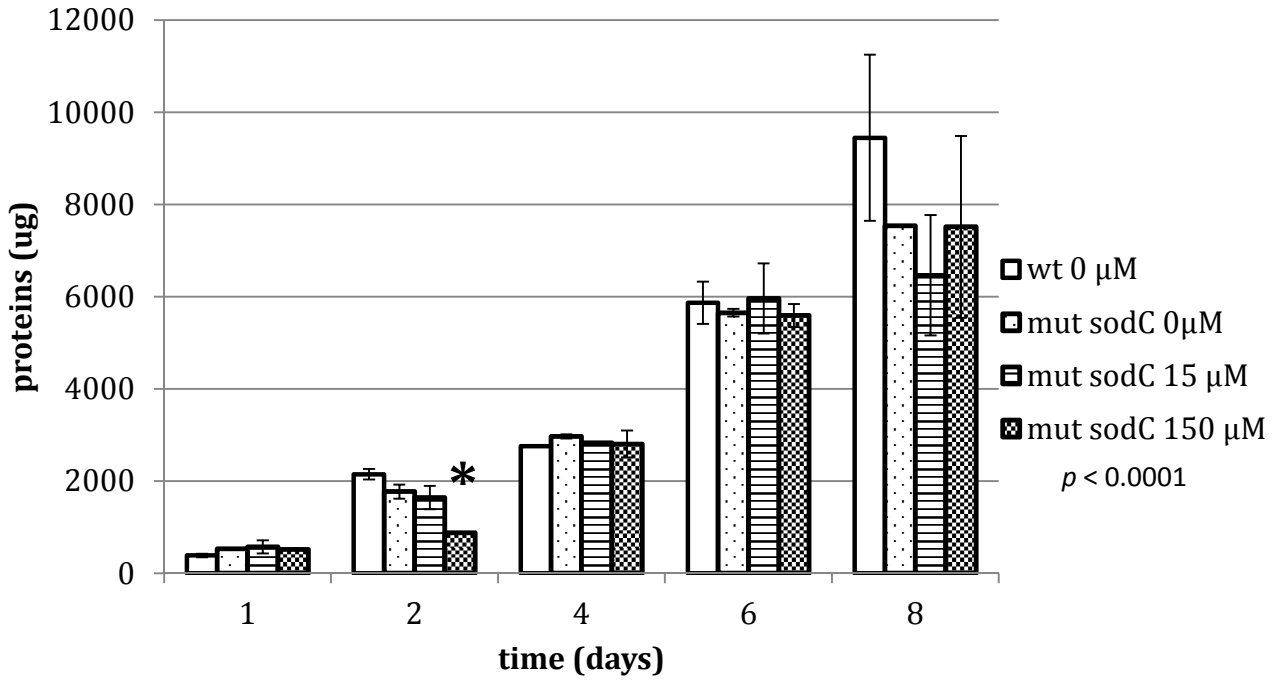

Figure 6. Total protein amounts from the biofilm of B. thailandensis sodC mutant in the presence of 0, 15 and 150 µM PMS over time. Data from the biofilm of B. thailandensis wt was added to facilitate the comparison of the results. Data represent the means ± the SD of three independent measurements of proteins for each membrane. The histograms provide the P-values obtained by ANOVA analysis. Post hoc comparisons results (Tukey's HSD, P < 0.05) are summarized with asterisks to underline the most relevant differences of PMS-treated samples with respect to control.

Levels of oxidative stress in planktonic cells and biofilm of *B. thailandensis sodC* mutant.

Oxidative stress levels in *sodC* planktonic cells (10.7 ± 4.4 fluorescence/ µg proteins) were similar to those measured in wt planktonic cells (14.9 ± 0.9 fluorescence/ µg proteins). Conversely to the wt, the exposure of *sodC* planktonic cells to PMS did not increase the oxidative stress levels (15 µM PMS: 12.6 ± 5.4 fluorescence/ µg proteins; 150 µM PMS: 17.9 ± 10.5 fluorescence/ µg proteins). Like the wt biofilm, in the *sodC* mutant we detected differences in the first 4 days of growth for the outer oxidative stress and just in the first day of growth for the inner oxidative stress. In addition, both outer and inner oxidative stress levels were lower than in wt biofilm (Fig. 7), being comparable to the levels that we measured in wt biofilms treated with PMS. Thus, the

deletion of *sodC* led to the same low oxidative stress levels measured with the exposure of planktonic and biofilm *B. thailandensis* wt to PMS.

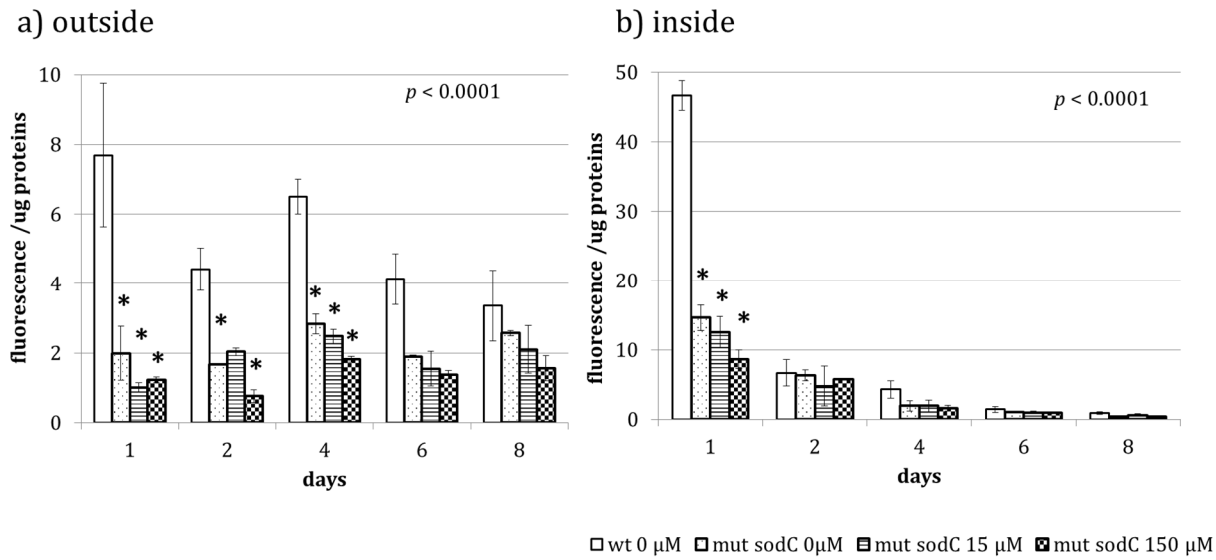

Figure 7. Reactive oxygen species detection outside (a) and inside (b) the cells of biofilm of Burkholderia thailandensis sodC mutant in the presence of 0, 15 and 150 µM PMS. Data from the biofilm of B. thailandensis wt was added to facilitate the comparison of the results. The histograms provide the P-values obtained by ANOVA analysis. Post hoc comparison results (Tukey's HSD, P < 0.05) are summarized with asterisks to underline the most relevant differences in PMS-treated samples with respect to the control.

Effect of PMS on matrix composition of biofilm of *B. thailandensis* wt and *sodC* mutant.

The presence of an extracellular matrix is one main element characterizing bacterial biofilms, where it provides protection against stresses, and promotes adhesion to surfaces and communication between cells (Hall-Stoodley et al., 2004; Davey et al., 2000). The matrix of mature biofilms (8 days) of *B. thailandensis* wt and *sodC* mutant strain, exposed to 0, 15 and 150 µM PMS, was extracted and characterized in its main components: proteins, polysaccharides and eDNA (Fig.8). Both PMS and *sodC* mutation had repercussions on the biofilm matrix composition. In wt biofilm, 150 µM PMS triggered the production of more matrix, as we calculated a higher production of proteins, polysaccharides and eDNA. Compared to the wt biofilm, the matrix of the *sodC* mutant was characterized by the same quantity of proteins and eDNA, but, interestingly, by a higher quantity of polysaccharides. This polysaccharides quantity was comparable

to the quantity accumulated in wt biofilm treated with 150 µM PMS. Challenging the *sodC* mutant biofilm with 15 and 150 µM PMS, this quantity did not increase. Instead, the treatment of *sodC* mutant biofilm with PMS (both concentrations) led also to a higher presence of eDNA in the matrix, though we cannot exclude that these values were caused by increased cellular lysis.

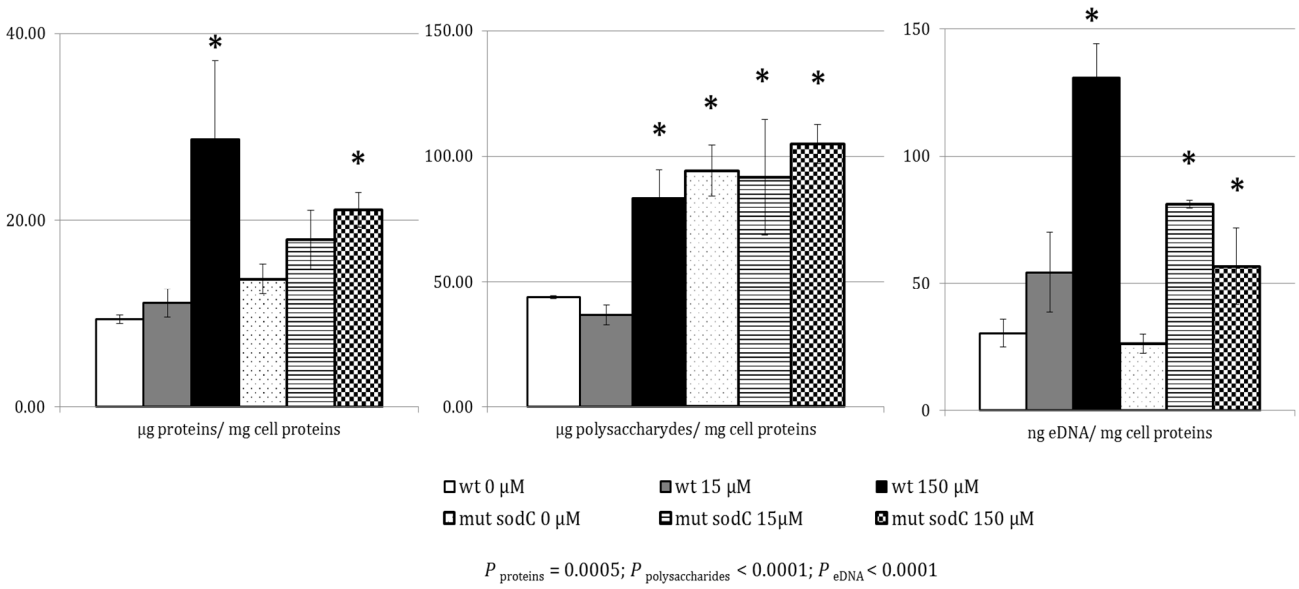

Figure 8. Biochemical composition of mature biofilm matrix of B. thailandensis wt and sodC mutant. Protein and polysaccharide values are expressed as mg/g of total cell proteins, while eDNA values are expressed as µg/g of total cell proteins. Data represent the means ± the SD of three independent measurements. The histograms provide the P-values obtained by ANOVA analysis. Post hoc comparison results (Tukey's HSD, P < 0.05) are summarized with asterisks to underline the most relevant differences in sodC mutant and/or PMS treated samples with respect to the control (wt 0 µM PMS).

Catalase assay.

The results of the experiments presented so far would suggest that the periplasmic enzyme encoded by *sodC* did not play a crucial role in PMS-induced oxidative stress. This compound is supposed to generate superoxide, but it can also increase the intracellular level of hydrogen peroxide (Hassett et al., 1999). Thus, we wondered whether induction of catalase activity might be involved in the apparently counterintuitive observation that ROS levels are reduced upon PMS treatment in B. *thailandensis* biofilms. Catalase is one of the most efficient scavenging enzyme, being able to promote the dismutation of hydrogen peroxide to water and oxygen (Imlay et al.,

2003). A catalase assay, performed on the total protein extract of the whole wild type biofilm, revealed a higher catalase activity in the biofilm treated with 150 μM PMS at the first day of growth (Fig. 9). The result concur to explain the lower level of inner oxidative stress of biofilm treated with 150 μM PMS, but not the same low oxidative stress in the biofilm treated with the 15 μM PMS. Similar catalase assays will now be performed in *sodC* mutant biofilms. We also plan to identify which of the two catalase encoding-genes in *B. thailandensis* might be responsible for the response to PMS-induced oxidative stress.

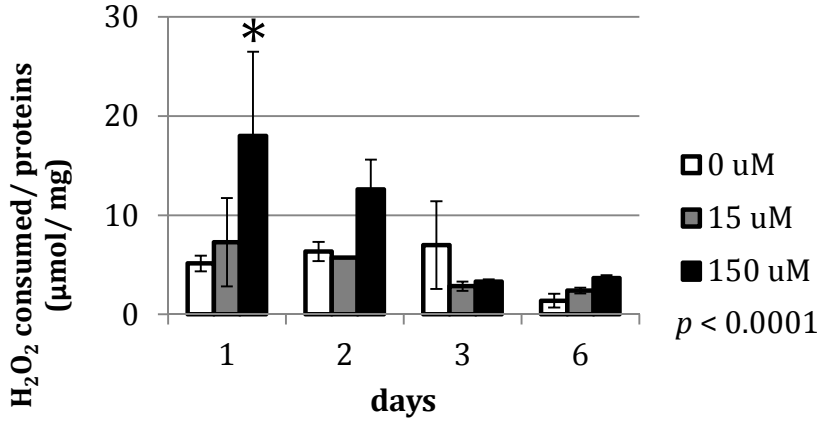

Figure 9. Catalase assay on total protein extract of B. thailandensis wt biofilm. The histograms provide the P-values obtained by ANOVA analysis. Post hoc comparison results (Tukey's HSD, P < 0.05) are summarized with asterisks to underline the most relevant differences in PMS-treated samples with respect to the control.

DISCUSSION

In both anthropic and natural systems, bacteria experience environmental stress factors leading to ROS formation and to oxidative stress (Dwyer et al., 2007; Kohanski et al., 2007). The soil bacterium *B. thailandensis*, can infect invertebrates and occasionally, humans with immunocompromised system. Host colonization, albeit not leading to infection, is likely in areas of the world where *B. thailandensis* is largely present (humid areas in the tropical and sub-tropical regions). Thus, *B. thailandensis* can experience oxidative stress both in the soil, upon exposure to toxic compounds and biocides (Fabrega et al., 2009; Villa et al., 2012), and in the host, attacked by immune system (Albesa et al., 2004). Phenazine methosulphate (PMS) is a well-known superoxide generator, widely used to mimic exogenous oxidative stress (Lee et al., 2004; Remelli et

al., 2010): we found that concentrations of 15 and 150 μM of PMS, albeit sub-lethal for planktonic cells of*B. thailandensis* CDC272, . had a range of effects on its growth, increasing its lag phase, reducing its growth rate and the adhesion to microtiters surface, thus forcing cells adapt to the stressful condition by activating specific mechanisms.

A clear effect of oxidative stress on biofilm was the drastic change in the colony morphology (Figure 3). *B. thailandensis* wt colony biofilm presented a series of smooth and rough ring structures, completely loss in biofilm exposed to 150 μM PMS. The presence of wrinkles confer various advantages, allowing the transport of water, nutrient, waste (Wilking et al., 2013) and oxygen, balancing the redox state (Okegbe et al., 2014). Morales et al. (2013) observed that the exposure of the yeast *Candida albicans* to phenazines (i.e. a class of redox-active antibiotics used by *Pseudomonas* spp. as electron shuttling that include PMS) causes the loss of wrinkle phenotype by perturbating cellular respiration. This could also be the case for the morphology change of *B. thailandensis* biofilm upon the exposure to PMS.

The exposure to 150 μM PMS caused higher inner oxidative stress in planktonic cells, but not in the biofilm. Conversely, lower levels of ROS were measured both in the matrix (the first 4 days of growth) and in the sessile cells (just the first day of growth), strengthening the idea of a scavenging mechanism activated to avoid deleterious oxidative stress.

Superoxide dismutase (SOD) is involved in scavenging ROS, converting the dangerous ROS superoxide to hydrogen peroxide and water. It has been hypothesized that the presence of periplasmic copper and zinc superoxide dismutases could be a defence from superoxide produced in the periplasm (Han and Cadenas, 2001) or exogenously (Hassan and Fridovich, 1979), for example by the host immune system (Sanjay et al., 2011). In *B. pseudomallei*, *sodC* encodes a periplasmic SOD, which plays a key role in its virulence and survival in the host cells (Vanaporn et al., 2011). Inactivation of the*sodC* gene caused a phenotype similar to the wt, except for the shorter lag phase in biofilms treated with 15 μM PMS. In addition, *sodC* planktonic cells did not experience higher oxidative stress in presence of 150 μM PMS and the level of oxidative stress in biofilm (both outside and inside cells, with or without PMS exposure) were lower than in the wt biofilm. According to these results, the deletion of periplasmic superoxide dismutase

lowered the level of oxidative stress, leading us to hypothesize that SodC is not the only enzyme involved in buffering oxidative stress caused by PMS.

Another candidate for the scavenging of ROS is catalase, which dismutates the hydrogen peroxide to water and oxygen. In many bacteria, such as *Escherichia coli* and *Azotobacter vinelandii*, at least two catalases are present, activated by the two regulator OxyR and RpoS, upon different stimuli (Gonzalez-Flecha et al., 1997; Sandercock et al., 2008). The increase in catalase activity in 150 μM PMS-treated wt biofilm during the first day of growth can only partially explain the lower levels of oxidative stress detected for stressed biofilm. The measurement of catalase activity in *sodC* biofilms will concur to clarify its role in the response to PMS and to the absence of the periplasmic superoxide.

Finally, we observed that both exposure to PMS and deletion of *sodC* triggered the production of polysaccharides in the *B. thailandensis* biofilm. Among matrix components, polysaccharides seem to be often involved in the oxidative stress response. For example, *P. aeruginosa* produces alginate in response to hydrogen peroxide (Mathee et al., 1999) and *E. coli* produces colanic acid under the regulation of the RpoS-controlled protein YddV, which promotes cell aggregation and EPS production via its diguanylate cyclase activity (Méndez-Ortiz et al., 2006). Increased EPS production might somehow shield bacterial cells from exogenous ROS; alternatively, polysaccharides accumulation might be the result of a reduced metabolic activity in order to limit the production of endogenous ROS. For example, in *B. pseudomallei*, RpoS, essential for the response to oxidative stress (Hengge-Aronis, 2002), directly down-regulates the succinyl-coA:3-ketoacid-coenzyme A transferase (SCOT) (Chutoam et al., 2013) to avoid the feeding with NADH and $FADH_2$ of the electron transport chain, one of the major source of intracellular ROS in bacteria (Messner and Imlay, 1999). This mechanism would lead to the accumulation of poly-β-hydroxybutyrate, a storage molecule (Chutoam et al., 2013). The activation of analogous strategies could be responsible for the observed accumulation of polysaccharides in biofilm matrix upon exposure to PMS and deletion of *sodC*.

Transcriptomic analysis on biofilms challenged with endogenous (*sodC* mutation) and exogenous (exposure to PMS) oxidative stress will allows us to unravel which scavenging mechanisms are activated and if the decrease of the metabolic activity is a strategy adopted also by *B. thailandensis*. Furthermore, we could have insight on the

460 molecular mechanisms connecting the regulators of oxidative stress response OxyR and
461 RpoS to the production of polysaccharides in the matrix. We are planning to perform
462 these experiments within the next months.
463
464 **REFERENCES**

465 Albesa, I., Becerra, M. C., Battán, P. C., Páez, P. L. (2004) Oxidative stress involved in the
466 antibacterial action of different antibiotics. Biochem Biophys Res Comm 317: 605-609.
467 Anderl, J.N., Franklin M.J. and Stewart, P.S. (2000) Role of antibiotic penetration
468 limitation in Klebsiella pneumoniae biofilm resistance to ampicillin and ciprofloxacin.
469 Antimicrob Agents Ch 44, 1818-1824.
470 Asally, M., Kittisopikul, M., Rué, P., Du, Y., Hu, Z., Çağatay, T., et al. (2012). Localized cell
471 death focuses mechanical forces during 3D patterning in a biofilm. Proc Nat Acad Sci
472 USA 109: 18891–18896.
473 Barrett, A. R., Kang, Y., Inamasu, K. S., Son, M. S., Vukovich, J. M., Hoang, T. T. (2008)
474 Genetic tools for allelic replacement in *Burkholderia* species. Appl Environ Microbiol 74:
475 4498-4508.
476 Bradford, M.M. (1976) A rapid and sensitive method for the quantitation of microgram
477 quantities of protein utilizing the principle of protein-dye binding. Anal Biochem 72:
478 248-254.
479 Cheng, A., Currie, B. (2005). Melioidosis: epidemiology, pathophysiology, and
480 management. Clin Microbiol Rev 18: 383–416.
481 Choi, K. H., Schweizer, H. P. (2005) An improved method for rapid generation of
482 unmarked *Pseudomonas aeruginosa* deletion mutants. BMC Microbiol 5: 30.
483 Corinaldesi, C., Danovaro, R. Dell Anno, A. (2005) Simultaneous recovery of extracellular
484 and intracellular DNA suitable for molecular studies from marine sediments. Appl
485 Environ Microbiol 71: 46-50.
486 Davey, M. E., O'toole, G. a. (2000). Microbial biofilms: from ecology to molecular
487 genetics. Microbiol Mol Biol Rev 64: 847–867.
488 Dwyer, D.J., Kohanski, M.A., Hayete, B., Collins, J.J. (2007) Gyrase inhibitors induce an
489 oxidative damage cellular death pathway in *Escherichia coli*. Mol Syst Biol 3: 91.
490 Espeso, D. R., Carpio, A., Einarsson, B. (2015) Differential growth of wrinkled biofilms.
491 Phys Rev E Stat Nonlin Soft Matter Phys 91.

492 Fabrega, J., Fawcett, S.R., Renshaw, J.C. and Lead, J.R. (2009) Silver nanoparticle impact
493 on bacterial growth: effect of pH, concentration, and organic matter. Environ Sci
494 Technol 43: 7285–7290.
495 Fang, F. C., DeGroote, M. a, Foster, J. W., Bäumler, a J., Ochsner, U., Testerman, T., et al.
496 (1999) Virulent *Salmonella* typhimurium has two periplasmic Cu, Zn-superoxide
497 dismutases. Proc Nat Acad Sci USA 96: 7502–7507.
498 Fazli M, O'Connell A, Nilsson M, Niehaus K, Dow JM, Givskov M, Ryan RP, Tolker-Nielsen
499 T. (2011) The CRP/FNR family protein Bcam1349 is a c-di-GMP effector that regulates
500 biofilm formation in the respiratory pathogen *Burkholderia cenocepacia*. Mol Microbiol
501 82: 327-341.
502 Fazli, M., McCarthy, Y., Givskov, M., Ryan, R. P., Tolker-Nielsen, T. (2013) The
503 exopolysaccharide gene cluster Bcam1330-Bcam1341 is involved in *Burkholderia*
504 *cenocepacia* biofilm formation, and its expression is regulated by c-di-GMP and
505 Bcam1349. Microbiology 2: 105–122.
506 Fazli, M., Harrison, J. J., Gambino, M., Givskov, M., Tolker-Nielsen, T. (2015) A Gateway-
507 compatible allelic exchange system for generation of in-frame and unmarked gene
508 deletions in *Burkholderia cenocepacia*. Appl Environ Microbiol
509 doi:10.1128/AEM.03909-14
510 Flemming, H.-C., Wingender, J. (2010) The biofilm matrix. Nat Rev Microbiol 8: 623–633.
511 Gambino, M., Marzano, V., Villa, F., Vitali, A., Vannini, C., Landini, P., Cappitelli, F. (2015)
512 Effects of sub-lethal doses of silver nanoparticles on *Bacillus subtilis* planktonic and
513 sessile cells. J Appl Microbiol 118: 1103–1115.
514 Gort, A. S., Ferber, D. M., James, A. (1999) The regulation and role of the periplasmic
515 Cu/Zn superoxide dismutase of *Escherichia coli*. Mol Microb Ecol Manual 32, 179–191.
516 Hall-Stoodley, L., Costerton, J. W. Stoodley, P. (2004) Bacterial biofilms: from the natural
517 environment to infectious diseases. Nature Rev Microbiol 2: 95–108.
518 Hamad, M., Austin, C. R., Stewart, L., Higgins, M., Vazquez-Torres, Voskuil, M. I. (2011)
519 Adaptation and antibiotic tolerance of anaerobic *Burkholderia pseudomallei*. Antimic
520 Agents Chemother 55: 3313–3323.
521 Han D,Williams E, Cadenas E. (2001) Mitochondrial respiratory chain-dependent
522 generation of superoxide anion and its release into the intermembrane space. Biochem J
523 353: 411–416.

524 Hassan, H. M., Fridovich, I. (1979) Paraquat and *Escherichia coli*. Mechanism of
525 production of extracellular superoxide radical. J Biol Chem 254: 10846–10852.
526 Hassett, D. J., Ma, J. F., Elkins, J. G., McDermott, T. R., Ochsner, U. a, et al. (1999) Quorum
527 sensing in *Pseudomonas aeruginosa* controls expression of catalase and superoxide
528 dismutase genes and mediates biofilm susceptibility to hydrogen peroxide. Mol
529 Microbiol 34: 1082-10893.
530 Hengge-Aronis, R., (2002) Signal transduction and regulatory mechanisms involved in
531 control of the sigma(S) (RpoS) subunit of RNA polymerase. Microbiol Mol Biol Rev 66:
532 373–395.
533 Herigstad, B., Hamilton, M. Heersink, J. (2001) How to optimize the drop plate method
534 for enumerating bacteria. J Microbiol Meth 44: 121-129.
535 Horton, R. M., Hunt, H. D., Ho, S. N., Pullen, J. K., Pease, L.R. (1989) Engineering hybrid
536 genes without the use of restriction enzymes: gene splicing by overlap extension. Gene
537 77: 61-68.
538 Imlay, J. (2003) Pathways of oxidative damage. Annual Rev Microbiol 57: 395–418.
539 Jakubowski, W., Bilinski, T. and Bartosz, G. (2000) Oxidative stress during aging of
540 stationary cultures of the yeast *Saccharomyces cerevisiae*. Free Radic Bio Med 28, 659-
541 664.
542 Jangiam, W., Loprasert, S., Smith, D. R., & Tungpradabkul, S. (2010) *Burkholderia*
543 *pseudomallei* Rpos regulates OxyR and the *katG-dpsA* operon under conditions of
544 oxidative stress. Microbiol Immunol 54: 389–397.
545 Kohanski, M. A., Dwyer, D. J., Hayete, B., Lawrence, C. A., Collins, J. J. (2007) A common
546 mechanism of cellular death induced by bactericidal antibiotics. Cell 130: 797-810.
547 Kroll, J., Langford, P., Wilkes, K., Keil, A. (1995) Bacterial [Cu,Zn] superoxide dismutase:
548 phylogenetically distinct from the eukaryotic enzyme, and not so rare after all!
549 Microbiology 141: 2271–2279.
550 Lee, J. H., Yeo, W. S., Roe, J. H. (2004) Induction of the *sufA* operon encoding Fe-S
551 assembly proteins by superoxide generators and hydrogen peroxide: Involvement of
552 OxyR, IHF and an unidentified oxidant-responsive factor. Mol Microbiol 51: 1745–1755.
553 Lushchak, V. I. (2011) Adaptive response to oxidative stress: Bacteria, fungi, plants and
554 animals. Comparative Biochem Physiol 153: 175–190.

555 Masuko, T., Minami, A., Iwasaki, N., Majima, T., Nishimura, S. Lee, Y.C. (2005)
556 Carbohydrate analysis by a phenolsulfuric acid method in microplate format. Anal
557 Biochem 339: 69-72.
558 Mathee K, Ciofu O, Sternberg C et al. (1999) Mucoid conversion of *Pseudomonas*
559 *aeruginosa* by hydrogen peroxide: a mechanism for virulence activation in the cystic
560 fibrosis lung. Microbiology 145: 1349–1357.
561 McDougald, D., Rice, S., Barraud, N., Steinberg, P. D., Kjelleberg, S. (2011). Should we stay
562 or should we go: mechanisms and ecological consequences for biofilm dispersal. Nat
563 Rev Microbiol 10: 39–50.
564 Méndez-Ortiz, M. M., Hyodo, M., Hayakawa, Y., Membrillo-Hernández, J. (2006) Genome-
565 wide transcriptional profile of *Escherichia coli* in response to high levels of the second
566 messenger 3′,5′-cyclic diguanylic acid. J Biol Chem 281: 8090–8099.
567 Messner K.R., Imlay J.A. (1999) The identification of primary sites of superoxide and
568 hydrogen peroxide formation in the aerobic respiratory chain and sulfite reductase
569 complex of *Escherichia coli*. J Biol Chem 274:119–128.
570 Okegbe, C., Price-Whelan, A., Dietrich, L. E. (2014) Redox-driven regulation of microbial
571 community morphogenesis. Curr Opin Microbiol 18: 39–45.
572 Peano, C., Chiaramonte, F., Motta, S., Pietrelli, A., Jaillon, S., Rossi, E., et al. (2014) Gene
573 and protein expression in response to different growth temperatures and oxygen
574 availability in *Burkholderia thailandensis*. PLOS One 9: e93009.
575 Remelli, W., Cereda, A., Papenbrock, J., Forlani, F., Pagani, S. (2010) The rhodanese RhdA
576 helps *Azotobacter vinelandii* in maintaining cellular redox balance. Biol Chem 391: 777–
577 784.
578 Sanjay, M. K., Srideshikan, S. M., Vanishree, V. L., Usha, M. S., Raj, a P. et al. (2011). Cu/Zn-
579 superoxide dismutase from clinically isolated *Escherichia coli*: cloning, analysis of *sodC*
580 and its possible role in pathogenicity. Indian J Microbiol 51: 326–331.
581 Sinha, K. (1972) Colorimetric assay of catalase. Analytical Biochem 47: 389–394.
582 Stevens, M. P., Galyov, E. E. (2004) Exploitation of host cells by *Burkholderia*
583 *pseudomallei*. Int J Medical Microbiol 293: 549–555.
584 Van Acker, H., Sass, A., Bazzini, S., De Roy, K., Udine, C., Messiaen, T., et al. (2013)
585 Biofilm-grown *Burkholderia cepacia* complex cells survive antibiotic treatment by
586 avoiding production of reactive oxygen species. PloS One 8: e58943.

587 Vanaporn, M., Wand, M., Michell, S. L., Sarkar-Tyson, M., Ireland, P., Goldman, S. et al.
588 (2011) Superoxide dismutase C is required for intracellular survival and virulence of
589 *Burkholderia pseudomallei*. Microbiology 157: 2392–400.
590 Villa, F., Remelli, W., Forlani, F., Gambino, M., Landini, P. Cappitelli, F. (2012) Effects of
591 chronic sub-lethal oxidative stress on biofilm formation by *Azotobacter vinelandii*.
592 Biofouling 28: 823-833.
593 Vlamakis, H., Chai, Y., Beauregard, P., Losick, R., Kolter, R. (2013) Sticking together:
594 building a biofilm the *Bacillus subtilis* way. Nat Rev Microbiol 11: 157–168.
595 Wiersinga, W. J., van der Poll, T., White, N. J., Day, N. P., Peacock, S. J. (2006) Melioidosis:
596 insights into the pathogenicity of *Burkholderia pseudomallei*. Nat Rev Microbiol 4: 272–
597 82.
598 Wilking, J. N., Zaburdaev, V., De Volder, M., Losick, R., Brenner, M. P., Weitz, D. (2013)
599 Liquid transport facilitated by channels in *Bacillus subtilis* biofilms. Proc Nat Acad Sci
600 USA 110: 848–852.
601 Zhao, X., Drlica, K. (2014) Reactive oxygen species and the bacterial response to lethal
602 stress. Curr Opin Microbiol 21: 1–6.
603 Zwietering, M. H., Jongenburger, I., Rombouts, F. M., van 't Riet, K. (1990) Modeling of
604 the bacterial growth curve. Appl Environ Microbiol 56: 1875–1881.